TOWARDS NEW TREATMENT STRATEGIES FOR INTERVERTEBRAL DISC DEGENERATION

Pathophysiology, histological and biochemical changes in IVD degeneration

Joost Rutges

Colofon

ISBN: 978 90 9028149 0
Design and lay-out: Punt Grafisch Ontwerp, Utrecht
Printing: DPP, Houten

Towards new treatment strategies for intervertebral disc degeneration

Pathophysiology, histological and biochemical changes in IVD degeneration

Op weg naar nieuwe behandelingsmogelijkheden voor tussenwervelschijfdegeneratie

Pathofysiologische, histologische en biochemische veranderingen in tussenwervelschijfdegeneratie (met een samenvatting in het Nederlands)

Proefschrift

ter verkrijging van de graad van doctor aan de Universiteit Utrecht op gezag van de rector magnificus, prof. dr. G.J. van der Zwaan, ingevolge het besluit van het college voor promoties in het openbaar te verdedigen op woensdag 28 mei 2014 des ochtends te 10.30 uur

door

Jozef Paulus Henricus Johannes Rutges
geboren op 23 september 1981 te Geertruidenberg

Promotoren

Prof. dr. W.J.A. Dhert

Prof. dr. F.C. Öner

Co-promotor

Dr. L.B. Creemers

This thesis was printed with financial support of Anna Fonds|NOREF, Nederlandse Vereniging voor Orthopedie, the Dutch Spine Society (DSS), InSpine, Het Rugcentrum Utrecht and DePuy Synthes Spine.

Voor Tas en Suze

Contents

This thesis is based upon the following publications

1 **Rutges JP**, Kummer JA, Oner FC, Verbout AJ, Castelein RJ, Roestenburg HJ, Dhert WJ, Creemers LB. Increased MMP-2 activity during intervertebral disc degeneration is correlated to MMP-14 levels. Journal of Pathology. 2008;214:523-30.

2 **Rutges JP**, Creemers LB, Dhert W, Milz S, Sakai D, Mochida J, Alini M, Grad S. Variations in gene and protein expression in human nucleus pulposus in comparison with annulus fibrosus and cartilage cells: potential associations with aging and degeneration. Osteoarthritis and Cartilage. 2010;18:416-23.

3 **Rutges JP**, Nikkels PG, Oner FC, Ottink KD, Verbout AJ, Castelein RJ, Creemers LB, Dhert WJ. The presence of extracellular matrix degrading metalloproteinases during fetal development of the intervertebral disc. European Spine journal. 2010;19:1340-6.

4 **Rutges JP**, Duit RA, Kummer JA, Oner FC, van Rijen MH, Verbout AJ, Castelein RM, Dhert WJ, Creemers LB. Hypertrophic differentiation and calcification during intervertebral disc degeneration. Osteoarthritis and Cartilage. 2010;18:1487-95.

5 **Rutges JP**, Jagt van der OP, Oner FC, Verbout AJ, Castelein RJ, Kummer JA, Weinans H, Creemers LB, Dhert WJ. Micro-CT quantification of subchondral endplate changes in intervertebral disc degeneration. Osteoarthritis and Cartilage. 2011;19:89-95.

6 Bergknut N, **Rutges JP**, Kranenburg HJ, Smolders LA, Hagman R, Smidt HJ, Lagerstedt AS, Penning LC, Voorhout G, Hazewinkel HA, Grinwis GC, Creemers LB, Meij BP, Dhert WJ. The dog as an animal model for intervertebral disc degeneration? Spine (Phila Pa 1976). 2012;37:351-8

7 **Rutges JP**, Duit RA, Kummer JA, Bekkers JE, Oner FC, Castelein RM, Dhert WJ, Creemers LB. A validated new histological classification for intervertebral disc degeneration. Osteoarthritis and Cartilage. 2013;21:2039-47

8 **Rutges JP**, Oner FC, Vincken KL, Bekkers JEJ, Dhert WJA, Creemers LB. Minor degenerative changes in rabbit model of compression-induced intervertebral disc degeneration. Submitted to European Spine Journal

9 **Rutges JP**, Bergknut N, van Tiel J, Meij BP, Waarsing E, Lagerstedt AS, Penning LC, Tryfonidou MA, Creemers LB and Dhert WJA. Intradiscal injections of BMP-7 and Marimastat in a rabbit model for IVD degeneration does not have a regenerative effect. Manuscript in preparation for submission.

CHAPTER 1
General introduction

Back pain

Low back pain is the most common musculoskeletal disease with an annual incidence of 22-65% and the life time risk to experience an episode of low back pain is estimated to be 70-85%[1-3.] The majority (80-90%) of the patients with low back pain fully recovers within 3 months[1,4]. However, from the remaining 10-20% of the patients, less than half of the patients will return to work[1,5]. When the symptoms persist for more than 2 years, the probability of returning to work declines to almost zero[1,5]. Although this is a minority of patients, they are responsible for more than 75% of the total costs related to this condition5.

The costs of chronic back pain are substantial. Total health care costs per patient, per year are known to be more than twice as high in patients with chronic low back pain when compared to age-matched controls without chronic low back pain[6,7]. Moreover, low back pain is the most common and most expensive cause of work related disability[1,6]. In the Netherlands, the total costs of low back pain were 3.5 billion euro in 2007, with 12% direct and 88% indirect costs respectively[8]. Although the exact cause of chronic low back pain remains largely unknown, intervertebral disc (IVD) degeneration has been associated with this condition and is often suggested to be one of the possible causes[9-12].

Anatomy of the intervertebral disc

The human vertebral column consists of 24 mobile vertebrae: 7 cervical, 12 thoracic, and 5 lumbar. With the exception of the first and second cervical vertebrae, all of the vertebral bodies are connected by a special structure, which is called the intervertebral disc (IVD). Thus, the human spine comprises of 23 IVDs: 6 cervical, 12 thoracic and 5 lumbar (figure 1.1).

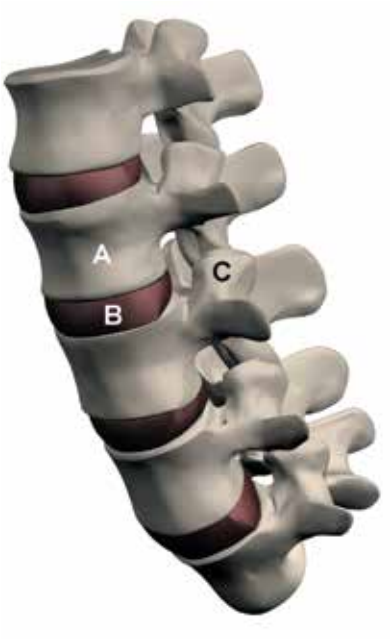

Figure 1.1. A schematic image of the human lumbar spine.

A: Vertebral body
B: Intervertebral disc
C: Facet joints

These IVDs are no synovial joints but rather a kind of syndesmosis forming a strong and flexible connection between the vertebrae, allowing flexion, extension, and rotation of the spinal column[13]. Moreover the IVDs distribute and dissipate the forces and axial loads over the vertebrae caused by the body weight and physical activity (e.g. running, jumping and bending), ensuring they are evenly spread over the endplates of the vertebral bodies[9,13]. The IVD is a fibro-cartilaginous structure that consist of three different anatomical areas, (figure 1.2)[13,14]. The nucleus pulposus (NP) forms the core of the IVD and is a gel-like structure responsible for the flexibility of the IVD. The NP consists of loosely organized collagen type II fibres and proteoglycans. Aggrecan is the most important proteoglycan in the NP and each aggrecan molecule contains 100-150 glycosaminoglycan chains capable to attract cations resulting in a high osmotic pressure which enables the NP to absorb water[9,15]. The highly hydrated elastic state of the healthy NP capacitates the IVD to withstand large compressive forces[9,13,15]. The annulus fibrosus (AF) is a fibrous structure surrounding the NP and consists of 15 - 25 rings or lamellae mainly containing collagen type I fibers[13,14,16]. These obliquely orientated concentric fibrous lamellae are firmly connected to the rims of the vertebrae[13,14]. Thereby, the AF enables the IVD to endure forces during compression, flexion or extension, while keeping the nucleus pulposus (NP), in place[9]. The endplate (EP) is the cartilage structure that forms the border between the IVD and its caudal and cranial vertebral bodies[14]. During childhood and adolescence, the EP functions also as a growth plate of the adjacent vertebrae in humans. The vertebral bodies of other mammals contain separate growth plates[14]. In adult IVDs, the endplates and the subchondral bone are thought to play a vital role in the nutrition of the IVD[17]. The majority of the IVD's nutrients diffuse from the capillary blood vessels in the subchondral bone through the cartilaginous endplate to the centre of the IVD[13]. In the healthy adult IVD, only a small number of capillaries is found in the outer layers of the annulus fibrosus , whereas the NP and cartilaginous endplate are completely avascular[14]. The intervertebral disc is the largest avascular structure in the human body[14;17].

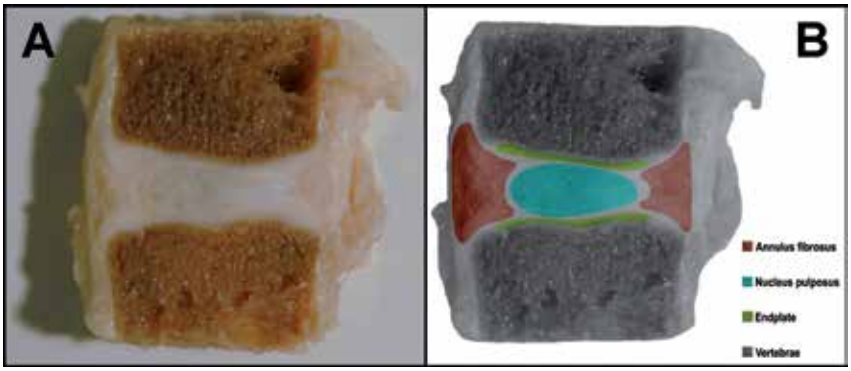

Figure 1.2. A mid-sagittal section of healthy IVD with adjacent bone (formalin fixation) (A). A schematic image of the 3 different anatomical structures of the IVD and the adjacent vertebral bodies (B).

Intervertebral disc and low back pain

Low back pain is a very common condition. It is not a disease entity or diagnosis, but is a mere symptom, which, can be caused by numerous pathologies. The differential diagnosis for low back pain comprises mechanical, non mechanical, and visceral causes and includes for example degenerative disc disease, spondylolysis, spondylolisthesis, spinal stenosis, spondylodiscitis and chronic pancreatitis[10]. The annual incidence of acute or sub-acute low back pain ranges form 22-65%[1-3]. Low back pain is qualified as chronic if the symptoms persist for more than 3 months, in approximately 10-20% of the patients with low back pain the condition becomes chronic[1,5,18]. In 85% of the patients with chronic low back pain the specific cause of the pain cannot be found[10]. Since the first half of the 20th century there is an ongoing debate regarding the role of IVD degeneration in the aetiology of chronic low back pain and currently the exact relation between disc degeneration and this condition remains still controversial.

Intervertebral disc degeneration

Intervertebral disc degeneration is a process which is radiologically and histologically characterized by a loss of disc height, subchondral sclerosis of the endplate, osteophyte formation and radial bulging[9]. This process starts with breakdown of extracellular matrix in the NP of the IVD, which results in reduced disc height, followed by increased lamellar disorganization in the AF, and eventually fissures and ingrowth of nerves and blood vessels (figure 1.3)[14,19]. In the early stages of IVD degeneration, proteoglycans (aggrecan) in the NP are broken down and in later stages, collagen type II is replaced by the more fibrous collagen type I[14,19]. As a result of the loss of proteoglycans, the swelling pressure of the NP is reduced, the tension on the AF fibers decreased, and the loading of the AF insertion at the rim of the vertebrae is increased[19]. Consequently, the ability of the IVD to dissipate compressive forces is diminished, and leading to more vulnerability to micro-trauma of the AF, NP, EP, but also indirectly of the facet joints[19]. These repetitive micro-traumas are thought to be responsible for a downwards spiral and further degeneration of the IVD by increasing levels of cytokines and degenerative enzymes, resulting in a decrease in proteoglycans, reduced swelling pressure and increased vulnerability to micro-trauma[19,20].

Histological and molecular characteristics of intervertebral disc degeneration.

At the cellular level, IVD degeneration is characterized by an increase of cell proliferation, formation of cell clusters and an increase of cell death[14]. At the molecular level, increased levels of cytokines and catabolic enzymes are associated with intervertebral disc degeneration[14]. The catabolic process in degenerative IVDs is thought to be mediated by several cytokines: IL1β, IL6, IL8, IL10, and TNFα[21,22]. Moreover, a large number of matrix metalloproteinases (MMPs) have been associated with IVD degeneration[14], and increased mRNA levels have been found in degenerating intervertebral discs for MMP-1, MMP-2, MMP-3 and MMP-13[23-25]. However, as these data relate to the gene expression at RNA level, and as most MMPs are known to be secreted as inactive pro forms, their actual participation in disc degeneration is still unclear. Additionally, disintegrins and metalloproteinases with thrombospondin motif (ADAMTSs) and cathepsins have also been associated with disc degeneration[9,19,26,27].

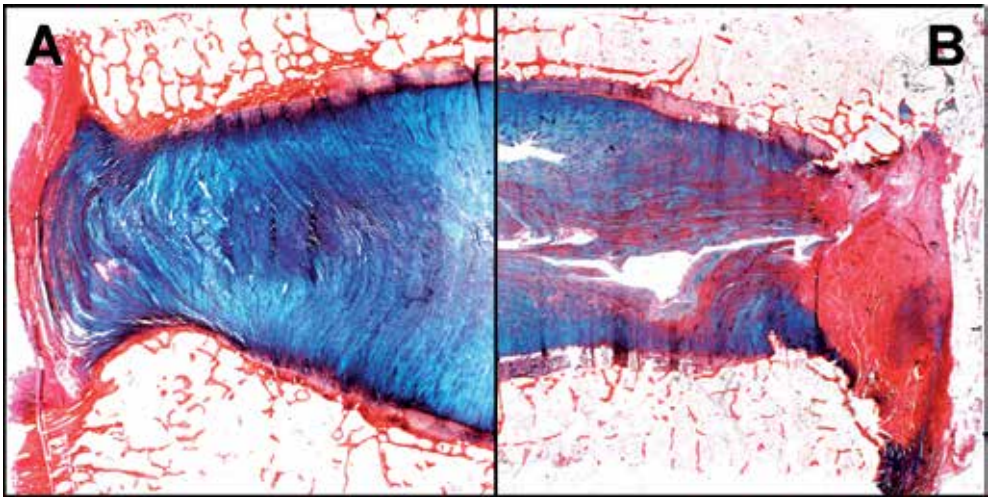

Figure 1.3. A healthy IVD with an intensely blue stained proteoglycan-rich NP (A). A severely degenerated IVD with reduced disc height, a fibrous NP (red instead of blue) and fissures in the NP and AF (B). IVDs sections are stained with alcian blue and picrosirius red.

Aetiology of intervertebral disc degeneration

Several mechanisms have been postulated to be involved in disc degeneration. Repetitive mechanical loading is probably an important cause of IVD degeneration, as mentioned earlier in this chapter[19]. While regular loading of the IVDs is assumed to be essential for maintaining a normal phenotype of IVD cells, excessive loading can lead to the biochemical and radiological changes that are associated with IVD degeneration[28,29]. Both occupational loading of the lumbar spine and obesity increase the risk of IVD degeneration, whereas moderate endurance sports reduce this risk[30-32].

While mechanical loading of the IVD is suggested to be an important factor in the development of disc degeneration, the role of IVD nutrition is still a matter of debate[9,19,29]. As mentioned earlier, the IVD is the largest avascular structure in the human body and for its nutrition the disc is almost solely dependent on diffusion through the endplates[14,17]. Sclerosis of the subchondral bone is a well known characteristic of IVD degeneration and is a radiological hallmark commonly seen on radiograms of patients with degenerative disc disease[33,34]. Permeability of the subchondral bone is decreased in degenerative IVDs, and fewer nutrients are supplied to the IVD by diffusion. The degenerative changes of the IVD might therefore be related to the decreased nutrition status in the degenerative IVD[17,33-35]. Although genetic factors by themselves are not a cause of disease, genes harbouring polymorphisms associated with a higher chance of disease can shed a light on the mechanisms involved. IVD degeneration seems to have a strong genetic background[13,19]. MRI twin studies have shown that the heritability of low back pain ranges between 52%-81%[36,37]. Only

a few polymorphisms have consistently been associated with IVD degeneration, among which are VDR and collagen IX polymorphisms[38,39]. Other variations in gene products which are possibly related to IVD degeneration include collagen type I, interleukin-6, aggrecan, MMP-3, thrombospondin, cyclooxygenase 2, TIMP-1, cartilage intermediate layer protein and interleukin-1[19]. These genes suggest a pivotal role of extracellular matrix molecules and hence biomechanical factors, but also inflammation is probably instrumental in the pathogenesis of IVD degeneration[21,40,41].

Currents treatment options for intervertebral disc degeneration

The optimal treatment regime of IVD degeneration still remains a subject of debate[42]. Conservative therapy of chronic low back pain consists of a vast group of treatment modalities, such as physiotherapy, analgesia, acupuncture and chiropractics. Approximately 75%-90% of all chronic low back pain patients obtain satisfactory results with conservative therapy[6,10,13,43]. Analgesia, such as non-steroidal anti-inflammatory drugs and muscle relaxants are very effective for both acute and chronic low back pain, especially when taken on regular schedule[10,44]. The effect of physiotherapy or chiropractics in the acute phase of low back pain is limited; however exercises and manipulations can be used to improve spinal muscle control and strength to prevent recurrence[10]. Since the natural history of low back pain is generally rather mild, with spontaneous recovery in 33% of the patients in the first week of symptoms and 66% after seven weeks, physiotherapy and chiropractics should not be started in the first weeks of symptoms[10]. The effectiveness of alternative therapies such as acupuncture remains largely unknown[10]. Although conservative therapy is effective in the vast majority of the patients, approximately 10 % of the patients remain symptomatic[10]. This relatively small group of patients with refractory chronic low back pain still represents a large number of patients and for them surgery becomes an option. Already 57.000 spinal fusions for degenerative conditions were performed in the USA in 1996. In the first decade of the 21st century this number increased considerably, 122.000 in 2001, 300.000 in 2004 and 413.000 in 2008[43,45,46,47].

Surgical therapy as treatment of IVD degeneration

Surgical therapy should only be used in the patients for whom conservative therapy is not effective[48]. The two main surgical treatment options for IVD degeneration are spinal fusion and the placement of an IVD prosthesis. Spinal fusion is the most commonly performed spinal operation and is considered the golden standard for surgical treatment of IVD degeneration[48,49]. Nonetheless, the results of spinal fusion are far from indisputable, and the three randomized controlled trials (RCTs) that have compared spinal fusion with conservative therapy showed substantial clinical improvement in only a limited number of patients[50-53]. Implantation of an IVD prosthesis (disc arthroplasty) has been introduced in the mid 80's of the previous century as the spinal equivalent of the thriving total hip and knee prosthesis and as a promising alternative to spinal fusion[48,54]. However, the total disc prosthesis failed to outperform spinal fusion when compared in RCTs, and comparable results were obtained with both techniques[49,55-58]. Recently, the disc prosthesis has been compared to conservative treatment in a RCT, and a statistically significant better clinical outcome was seen in the total disc prosthesis group[54]. Nevertheless, this improvement was too minor to be clinically

important, as suggested by the authors, and therefore, the peri-operative risks and possible complications do not out-weigh these limited benefits of total disc prosthesis placement[54].

Altogether, current surgical treatment strategies for chronic low back pain yield far from optimal results. Moreover, RCTs have failed to unquestionably prove the superiority of spinal fusion and total disc replacement over conservative treatment[48,50]. Furthermore, although still a matter of debate, spinal fusion could even accelerate the degenerative process in adjacent levels[59,60].

Towards novel treatments of IVD degeneration: regenerative medicine

Since the current surgical treatments of degenerative disc disease are only moderately effective, research on new treatment strategies have been strongly intensified during the past decades[48,61]. As an alternative to salvage procedures, such as spinal fusion and arthroplasty, new treatment strategies for IVD degeneration are focused on restoring the biomechanical function of the degenerative disc instead of replacing or removing the IVD. In particular, regenerative strategies in combination with the application of new biomaterials might be a promising approach for the treatment of IVD degeneration[62-65].

One of those promising new approaches is IVD regeneration by implantation of cells that are capable of the restoring the normal extracellular matrix of the IVD[65]. By implantation of cell-seeded scaffolds or injection of cells, the degenerative IVD may be regenerated by cultured healthy cells which are capable of producing normal NP matrix, collagen type II and proteoglycans[66]. Although these cell-based techniques for IVD degeneration are still in their infancy, two pilot studies already showed that autologous cell transplantation for IVD degeneration is technically possible[67,68]. The transplanted cells were cultured autologous IVD cells or IVD cells co-cultured with autologous mesenchymal stem cells[67,68]. Both pilot studies reported a significant reduction in clinical symptoms during the first months after surgery[67,68]. Although these preliminary results are promising, still extensive research is required before cell-based therapies for IVD degeneration can be implemented as treatment for chronic low back pain. For example, detailed identification of the IVD phenotype is required to culture NP-like cells instead of cartilage-like cells[69].

Also stimulation of the anabolic processes by the use of growth factors such as bone morphogenetic proteins (BMP's) is under investigation as potential treatment of degenerative disc disease[64]. Although the first preclinical results of this strategy were very promising, the approach has lost some of its popularity due to the recently reported side effects of BMP's, especially when high doses were used in spinal fusion procedures[64,70,71].

Next to the recent development of several new regenerative strategies, also the research regarding NP implants has intensified[72-74]. Injectable NP prostheses and even implants that are suitable as cell scaffold have become available[72-74]. However the ideal scaffold that combines both qualities is not yet available and would be an important breakthrough in NP replacements, especially if this approach could be combined with growth factors and inhibition of the degenerative process[75,76].

Finally, identification of patients that are eligible for IVD cell therapy is another great challenge for this kind of regenerative approaches. It is likely that the first regenerative strategies for IVD degeneration are not potent enough to cure patients with severely degenerated discs and, at first, can only be used to treat early

disc degeneration or to prevent progression of the degenerative process. It might even be possible that these new approaches are only effective in patients who are not symptomatic at the time of treatment, but may or may not develop back pain in the future. This may lead to serious medical-ethical dilemmas.
Successful development of regenerative treatments for IVD degeneration will require several issues to be dealt with. First of all, the environment of the degenerating IVD will be less amenable to regeneration. Secondly, cell-based approaches will depend on cell development to a properly functioning NP phenotype. Finally, the proof of principle of these therapies will need to be tested in appropriate and relevant animal models.

Targeting the degenerative process

A prerequisite for a successful regenerative approach is knowledge and targeting of the local conditions in the degenerating disc. The substantial increase in knowledge regarding the pathophysiology of osteoarthritis of synovial joints certainly helped IVD researchers in understanding the processes that are involved in IVD degeneration. Although articular cartilage and the IVD morphologically appear to be very different structures, they are remarkably similar at the biochemical level[77]. The main constituents of the extracellular matrix (ECM) of the NP are collagen type II and aggrecan, as in articular cartilage[9,13]. The ECM content of the outer AF more closely resembles meniscal cartilage, also containing collagen type I[14,78]. Additionally, both articular and meniscal cartilage and the IVD are in essence avascular tissues and nutrients mainly reach the cells by diffusion[79]. By the evaluation of the similarities and differences between osteoarthritis and IVD degeneration, knowledge on the pathophysiology of both diseases is increased, which can lead to a more efficient development of new treatment strategies.
Similar to subchondral bone changes in osteoarthritis, bony endplate sclerosis is also seen on radiographs of degenerative IVDs[80,81]. These subchondral changes can influence the diffusion of nutrients in the degenerative IVD[80,81]. Another phenomenon seen in osteoarthritis that might also be present in the degenerative disc is hypertrophic differentiation[82-84]. Determining the role of these phenomena in IVD degeneration could significantly increase our understanding of the degenerative process.
It is crucial to understand which factors are involved in IVD degeneration. Factors that are deemed instrumental in the extracellular matrix degeneration of the IVD are the matrix metalloproteinases (MMPs), a family of metallo-dependent proteases that are together capable of degrading all components of the extracellular matrix of connective tissues[14,24,85,86.] Detailed identification of enzymes involved in the consecutive stages of IVD degeneration is essential for further development of treatment strategies that aim at inhibition of these degenerative processes. Additionally, further elucidation of the regulation of enzyme production and activity could result in an even more potent strategy to stop or reverse IVD degeneration. Examples of these strategies could be inhibition of the action of inflammatory cytokines [40,41,87]. Moreover, enzymes involved in the degenerative process might also play a role in the foetal development of the IVD. Several enzymes known to be involved in osteoarthritis and IVD degeneration are also crucial in the development of limbs and joints and could also be involved in ECM remodelling during IVD regeneration[88-91]. Therefore, before targeting degenerative enzymes, their role in the foetal development of the IVD should also be illuminated.

Identifying the nucleus pulposus cell

For regenerative medicine approaches it is essential to elucidate the phenotype of the non-degenerative IVD cell. At this time, in most pilot and preclinical IVD studies, cartilage-like cells are used for regenerative strategies. These cell types could very well be adequate donor cells for IVD tissue engineering since they are capable of producing collagen type II and proteoglycans. However, optimal results are most likely only achieved with transplanted cells that produce adequate IVD matrix and display the NP phenotype. For example the ratio between proteoglycans and collagen type II in IVD cells and ECM is much higher than in articular cartilage[92]. The high proteoglycan content results in a hydrated and very elastic IVD with the capability to withstand large compressive forces[9,13]. If the transplanted cells do not have these specific characteristics, they are not likely to restore the hydration and elasticity of the healthy IVD. Unfortunately, there are still no reliable markers to distinguish NP cells from hyaline cartilage cells.

Animal models

To evaluate possible new regenerative treatments, appropriate animal models are required. There is an ongoing debate regarding the most appropriate animal model for IVD degeneration. Although many small and large animal models for IVD degeneration have been developed, the ideal model remains undetermined[93]. There are many differences in size, NP cell type, and biomechanical properties between human and animal IVDs[93]. Rodents, such as rabbits, are most commonly used in animal models for IVD degeneration for practical reasons. In these models, IVD degeneration is induced by a stab in the AF, which results in NP herniation. Major disadvantage of this model is that the pathophysiology of the degenerative process is completely different compared to the process in humans. Compression models are pathophysiologically more analogous to human disc disease and a rabbit model in which degeneration is induced by mechanical compression with an external fixator has already been developed[94]. However the level of disc degeneration achieved by this compression model is unfortunately rather mild and less suitable for translational research[94]. Spontaneously occurring IVD degeneration in animals would pathophysiologically be more comparable to human disc disease, and therefore, would be a more appropriate model for IVD degeneration. But, although for instance sand rats do develop spontaneous intervertebral disc degeneration, the IVD of small rodents differs biomechanically and biochemically substantially from the human IVD[88]. Moreover, the NP of adult rodents contains notochordal (NC) cells, which are thought not to be present in adult human IVDs[95]. Alternatively dog IVDs also contain NC cells till early adulthood and are biomechanically and histologically more comparable to human IVDs. Dogs do also develop spontaneous IVD degeneration resulting in back pain and neurological deficit[96,97]. For that reason, dogs with spontaneous IVD degeneration might be an interesting alternative to the rodent models.

Histological grading

The histological changes in the degenerative disc are well known and have been extensively described in literature[9,13,14,19]. However a well-validated histological grading system for IVD degeneration is currently lacking. Since many translational studies are using histological changes as the primary outcome variable,

a comprehensive and validated histological grading for IVD degeneration is essential to the field of IVD research.

Outline of this thesis

For successful development of a new regenerative treatment for IVD degeneration knowledge of the pathophysiology and targeting of the local conditions is essential. Therefore, our approach towards the development of a new therapy for IVD degeneration consisted of three phases.

In the first phase we further elucidated the pathophysiology of IVD degeneration and identified new therapeutic targets. In the second phase we evaluated several animal models for IVD degeneration and developed a new histological grading system. In the last phase we investigated the possibility to stop or reverse IVD degeneration by the injection of enzyme inhibitors or growth factors in an animal model. During the first phase we collected both healthy and degenerative IVDs of deceased patients. We analysed the pathophysiology of disc degeneration by comparing healthy and degenerative samples and determined the presence of degenerative enzymes in these samples. Since several matrix metalloproteinases (MMPs) are associated with IVD degeneration, we evaluated the presence and activity of these enzymes in degenerative IVDs (chapter 2). Since MMPs are also known to play a vital role in skeletal development, we also analysed which MMPs are involved in the foetal development of human IVDs (chapter 3).

Subchondral bone changes are a well-known characteristic of IVD degeneration and could influence the diffusion of nutrients in the degenerative IVD and thereby affect the feasibility of regenerative strategies[80,81]. However, these subchondral bone changes have never been quantified. Therefore, we evaluated the subchondral bone changes in healthy and degenerative IVDs with micro-CT (chapter 4).

The presence of small calcifications in the NP and AF is another known phenomenon seen in IVD degeneration. In osteoarthritis these calcifications are thought to be caused by hypertrophic differentiation[82-84]. Therefore, we have evaluated if hypertrophic differentiation is also present in IVD degeneration (chapter 5). For effective regenerative cell-based strategies it is essential to use appropriately differentiated cells. Since there are several known differences between chondrocytes, NP cells and the ECM produced by these cells, the potential of cell-based treatment strategies could be optimized by using cells with a NP phenotype. However, currently there are no reliable markers to distinguish NP cells from general hyaline cartilage cells. Therefore, we identified marker molecules for human NP cells (chapter 6).

The second phase of our approach consisted of the evaluation of various animal models for IVD degeneration and the development of a new histological grading for IVD degeneration. Many animal and human IVD studies use histology as an outcome variable, but a well-validated tool for histological classification of human IVD degeneration is still lacking. Hence, we have developed an easy to use well-validated histological classification system for human IVD degeneration (chapter 7).

There is an ongoing debate regarding the most appropriate animal model for IVD degeneration. Although many small and large animal models for IVD degeneration have been developed, the ideal model remains undetermined[93]. Many IVD degeneration models are based on a disruption of the AF and herniation of the NP, for example an anterior stab of the AF in one of the commonly used rabbit models for IVD degeneration[93].

However, IVD degeneration in humans is mainly caused by biomechanical loading, not by a sharp injury to the annulus fibrosus. Therefore, we examined if it is feasible and ethical to achieve an advance stage of IVD degeneration with compression in a rabbit model (chapter 8). Spontaneous IVD degeneration in animals is pathophysiologically more comparable to human disc disease, and therefore, could be a more appropriate model for IVD degeneration. Therefore, we evaluated if spontaneous occurring IVD disease in dogs can be used as a translational model for human IVD degeneration (chapter 9).
In the third phase of our strategy we evaluated if the degenerative changes in a rabbit model for IVD degeneration could be reversed by injection of hydrogels containing enzyme inhibitors or a growth factor (chapter 10). Based on the results of the previous phases of this thesis, we have chosen a broad spectrum MMP inhibitor and have used BMP-7 as growth factor since it was previously shown to be able to induce a regenerative response in a rabbit model of IVD degeneration[64].

Aims of this thesis

For the development of new treatment strategies for IVD degeneration, thorough understanding of the pathophysiology of the degenerative process is essential. Therefore, the main aim of this thesis is to contribute to a better understanding of the pathophysiology of IVD degeneration. The 10 specific aims addressed by the studies described in this thesis are stated below:

Aim 1: To determine the activity of MMP-2 in the nucleus pulposus of healthy and degenerated IVDs and to correlate its activity to the presence of MMP-14 and TIMP-2;

Aim 2: To evaluate the presence of MMP-1, 2, 3 and 14 and the activity of MMP-2 in human IVDs during consecutive stages of foetal development;

Aim 3: To quantify the subchondral bone changes occurring during IVD degeneration by micro-CT analysis;

Aim 4: To determine the extent to which markers of hypertrophic differentiation are present in degenerative intervertebral discs and whether extracellular matrix calcification is associated with the degenerative process;

Aim 5: To evaluate the presence and distribution of several molecules, which were found to be differently expressed in various animal IVD and cartilage cell populations, in human disc cells;

Aim 6: To develop an easily applicable histological classification for human IVD discs which can be used by both experienced and inexperienced observers;

Aim 7: To assess the extent of degeneration in the rabbit model of compression-induced IVD degeneration, after respectively 14, 28 and 56 days of compression of the L4-L5 discs;

Aim 8: To investigate whether spontaneous IVD degeneration occurring in dogs can be used as valid translational models for human IVD research;

Aim 9: To evaluate the degree of disc degeneration obtained with a rabbit stab model for IVD degeneration using a number of different diagnostic techniques;

Aim 10: To induce IVD degeneration in rabbit stab model and to regenerate the degenerated IVDs using a MMP inhibitor or BMP-7, with or without hydrogel carriers.

References

1. Anderson GBJ. Epidemiological features of chronic low-back pain. Lancet 354, 581-585. 1999.
2. Hoy D, Bain C, Williams G, March L, Brooks P, Blyth F et al. A systematic review of the global prevalence of low back pain. Arthritis Rheum 64, 2028-2037. 2012.
3. Walker BF. The prevalence of low back pain: a systematic review of the literature from 1966 to 1998. J Spinal Disord 13, 205-217. 2000.
4. Croft PR, Macfarlane GJ, Papageorgiou AC, Thomas E, Silman AJ. Outcome of low back pain in general practice: a prospective study. BMJ 316, 1356-1359. 1998.
5. Spitzer WO, LeBlanc FE, Dupuis M. Scientific approach to the assessment and management of activity-related spinal disorders: a monograph for clinicians. Report of the Quebec Task Force on Spinal Disorders. Spine (Phila Pa 1976) 12, S1-S59. 1987.
6. Core m, Sadosky A, Stacey BR, Tai KS, Leslie D. The burden of chronic low back pain: clinical comorbidities, treatment patterns, and health care costs in usual care settings. Spine (Phila Pa 1976) 37, E668-E677. 2012.
7. Hong J, Reed C, Novick D, Happich M. Costs Associated With Treatment of Chronic Low Back Pain: An Analysis of the UK General Practice Research Database. Spine (Phila Pa 1976) Oct 2. [Epub ahead of print]. 2012.
8. Lambeek L. “The Trend in Total Cost of Back Pain in the Netherlands in the Period 2002 to 2007.”. Spine (Phila Pa 1976) 13, 1050-1058. 2011.
9. Adams MA, Roughley PJ. What is intervertebral disc degeneration, and what causes it? Spine (Phila Pa 1976) 31, 2151-2161. 2006.
10. Deyo RA WJ. Low back pain. N Engl J Med 344, 363-370. 2001.
11. Hughes SPF, Freemont AJ, DWL Hukins, McGregor AH, Roberts S. The pathogenesis of degeneration of the intervertebral disc and emerging therapies in the management of back pain. J Bone Joint Surg Br 94-b, 1298-1304. 2012.
12. Nachemson AL. Back pain. Causes, diagnosis and treatment. SBU Stockholm: The Swedish Council of Technology Assessment in Health Care . 1991.
13. Raj PP. Intervertebral disc: anatomy-physiology-pathophysiology-treatment. Pain Pract. 8, 18-44. 2008.
14. Roberts S, Evans H, Trivedi J, Menage J. Histology and pathology of the human intervertebral disc. J Bone Joint Surg Am 88, S10-S14. 2006.
15. Eisenstein SM, Robberts S. The physiology of the disc and its clinical relevance. J Bone Joint Surg Br 2003; 85-B:633-636.
16. Marchand F, Ahmed AM. Investigation of the laminate structure of lumbar disc anulus fibrosus. Spine (Phila Pa 1976) 15, 402-410. 1990.
17. Urban JP, Smiths S, Fairbank JC. Nutrition of the intervertebral disc. Spine (Phila Pa 1976) 29, 2700-2709. 2004.
18. [No authors listed]. Non-drug management of chronic low back pain. Drug Ther Bull 47[102], 107. 2009.
19. Freemont AJ. The cellular pathobiology of the degenerate intervertebral disc and discogenic back pain. Rheumatology (Oxford) 48, 5-10. 2009.
20. Walter BA, Korecki CL, Purmessur D, Roughley PJ, Michalek AJ, Iatridis JC. Complex loading affects intervertebral disc mechanics and biology. Osteoarthritis Cartilage 2011; 19:1011-1018.
21. Hoyland JA, Le Maitre C, Freemont AJ. Investigation of the role of IL-1 and TNF in matrix degradation in the intervertebral disc. Rheumatology 47, 809-814. 2008.

22. Le Maitre C, Pockert A, Buttle DJ, Freemont AJ, Hoyland JA. Matrix synthesis and degradation in human intervertebral disc degeneration. Biochem Soc Trans 35, 652-655. 2007.
23. Crean JKG, Robberts S, Jaffray DC, Eisenstain SM, Duance VC. Matrix metalloproteinases in the human intervertebral disc: role in disc degeneration and scoliosis. Spine (Phila Pa 1976) 22, 2877-2884. 1997.
24. Goupile P, Jayson MI, Valat JP, Freemont AJ. Matrix metalloproteinases: the clue to intervertebral disc degeneration? Spine (Phila Pa 1976) 23, 1612-1626. 1998.
25. Weiler C, Nerlich AG, Zipperer J, Bachmeier BE, Boos N. 2002 SSE Award Competition in Basic Science: expression of major matrix metalloproteinases is associated with intervertebral disc degradation and resorption. Eur Spine J 11, 308-320. 2002.
26. Ariga K, Yonenobu K, Nakase T, Kaneko M, Okuda S, Uchiyama Y et al. Localization of cathepsins D, K, and L in degenerated human intervertebral discs. Spine (Phila Pa 1976) 26, 2666-2672. 2012.
27. Patel KP, Sandy JD, Akeda K, Miyamoto K, Chujo T, An HS et al. Aggrecanases and aggrecanase-generated fragments in the human intervertebral disc at early and advanced stages of disc degeneration. Spine (Phila Pa 1976) 32, 2596-2603. 2012.
28. Setton LA, Chen J. Mechanobiology of the intervertebral disc and relevance to disc degeneration. J Bone Joint Surg Am 88 Suppl 2, 52-57. 2006.
29. Wang DL, Jiang SD, Dai LY. Biologic response of the intervertebral disc to static and dynamic compression in vitro. Spine (Phila Pa 1976) 32, 2521-2528. 2007.
30. Pye SR, Reid DM, Adams JE, Silman AJ, O'Neill TW. Influence of weight, body mass index and lifestyle factors on radiographic features of lumbar disc degeneration. Ann rheum Dis 66, 426-427. 2007.
31. Schuman B, Bolm-Audorff U, Bergmann A, Ellegast R, Elsner G, Grifka J et al. Lifestyle factors and lumbar disc disease: results of a German multi-center case-control study (EPILIFT). Arthritis Res Ther 12, R139. 2010.
32. Seidler A, Bergmann A, Jäger M, Ellegast R, Ditchen D, Elsner G et al. Cumulative occupational lumbar load and lumbar disc disease--results of a German multi-center case-control study (EPILIFT). BMC Musculoskelet Disord. 10, 48. 2009.
33. Bell GR, Ross JS. Imaging of the spine. In: Frymoyer JW, Wiesel SW, editors. The adult & pediatric spine. 3rd ed. Philadelphia: Lippincott, Williams & Wilkins; 2004. 69-86.
34. Burkus JK, Zdeblick TA. Lumbar disc disease. In: Frymoyer JW, Wiesel SW, editors. The adult & pediatric spine. 3rd ed. Philadelphia: Lippincott, Williams & Wilkins; 2004. 899-944.
35. Haefeli M, Kalberer F, Saefesser D, Nerlich AG, Boos N, Paesolf G. The course of macroscopic degeneration in the human lumbar intervertebral disc. Spine (Phila Pa 1976) 31, 1522-1531. 2006.
36. MacGregor AJ, Andrew T, Sambrook PN, Spector TD. Structural, psychological, and genetic influences on low back and neck pain: a study of adult female twins. Arthritis Rheum 51, 160-167. 2004.
37. Sambrook PN, MacGregor AJ, Spector TD. Genetic influences on cervical and lumbar disc degeneration: a magnetic resonance imaging study in twins. Arthritis Rheum 42, 366-372. 1999.
38. Annunen S, Paassilta P, Lohiniva J, Perälä M, Pihlajamaa T, Karppinen J et al. An allele of COL9A2 associated with intervertebral disc disease. Science 285[409], 412. 1999.
39. Videman T, Leppävuori J, Kaprio J, Battié MC, Gibbons LE, Peltonen L et al. Intragenic polymorphisms of the vitamin D receptor gene associated with intervertebral disc degeneration. Spine (Phila Pa 1976) 23, 2477-2485. 1998.

40. Gorth DJ, Mauck RL, Chiaro JA, Mohanraj B, Hebela NM, Dodge GR et al. L-1ra delivered from poly(lactic-co-glycolic acid) microspheres attenuates IL-1?-mediated degradation of nucleus pulposus in vitro. Arthritis Res Ther 2012; 14:R179.
41. Goupille P, Mulleman D, Chevalier X. Is interleukin-1 a good target for therapeutic intervention in intervertebral disc degeneration: lessons from the osteoarthritic experience. Arthritis Res Ther 2007; 9:110.
42. Wood KB, Fritzell P, Dettori JR, Hashimoto R, Lund T, Shaffrey C. Effectiveness of Spinal Fusion Versus Structured Rehabilitation in Chronic Low Back Pain Patients With and Without Isthmic Spondylolisthesis. Spine (Phila Pa 1976) 36, S110-S119. 2011.
43. Deyo RA. Back Surgery — Who Needs It? N Engl J Med 2007; 356:2239-2243.
44. Fordyce WE, Brockway JA, Bergman JA, Spengler D. Acute back pain: a control-group comparison of behavioral vs traditional management methods. J Behav Med 1986; 9:127-140.
45. Deyo RA, Gray DT, Kreuter W, Mirza S, Martin BI. United States trends in lumbar fusion surgery for degenerative conditions. SPINE 2005; 30:1441-1445.
46. Rajaee SS, Bae HW, Kanim LE, Delamarter RB. Spinal fusion in the United States: analysis of trends from 1998 to 2008. Spine 2012; 37:67-76.
47. Deyo RA. Commentary: Managing patients with back pain: putting money where our mouths are not. Spine J 2011; 11:633-635.
48. Schizas C, Kulik G, Kosmopoulos V. Disc degeneration: current surgical options. Eur Cell Mater 20, 306-315. 2010.
49. van den Eerenbeemt KD, Ostelo RW, van Royen BJ, Peul WC, van Tulder MW. Total disc replacement surgery for symptomatic degenerative lumbar disc disease: a systematic review of the literature. Eur Spine J, 1262-1280. 2010.
50. Bogduk N, Andersson G. Is spinal surgery effective for back pain? F 1000 Med Rep 1, 60-62. 2009.
51. Brox JI, Sørensen R, Friis A, Nygaard Ø, Indahl A, Keller A et al. Randomized clinical trial of lumbar instrumented fusion and cognitive intervention and exercises in patients with chronic low back pain and disc degeneration. Spine (Phila Pa 1976) 28, 1913-1921. 2003.
52. Fairbank J, Frost H, Wilson-MacDonald J, Yu LM, Barker K, Collins R. Randomised controlled trial to compare surgical stabilisation of the lumbar spine with an intensive rehabilitation programme for patients with chronic low back pain: the MRC spine stabilisation trial. BMJ 330, 1233-1239. 2005.
53. Fritzell P, Hagg O, Wesseberg P, Nordwall A. 2001 Volvo Award Winner in Clinical Studies: Lumbar fusion versus nonsurgical treatment for chronic low back pain: a multicenter randomized controlled trial from the Swedish Lumbar Spine Study Group. Spine (Phila Pa 1976) 26, 2521-2532. 2001.
54. Hellum C, Johnsen LG, Storheim K, Nygaard OP, Brox JI, Rossvoll I et al. Surgery with disc prosthesis versus rehabilitation in patients with low back pain and degenerative disc: two year follow-up of randomised study. BMJ 342, 2786-2796. 2011.
55. Berg S, Tullberg T, Branth B, Olerud C, Tropp H. Total disc replacement compared to lumbar fusion: a randomised controlled trial with 2-year follow-up. Eur Spine J 18, 1512-1519. 2009.
56. Blumenthal S, McAfee PC, Guyer RD, Hochschuler SH, Geisler FH, Holt RT et al. A prospective, randomized, multicenter Food and Drug Administration investigational device exemptions study of lumbar total disc replacement with the CHARITE artificial disc versus lumbar fusion: part I: evaluation of clinical outcomes. Spine (Phila Pa 1976) 30, 1565-1575. 2013.

57. Guyer RD, McAfee PC. Prospective, randomized, multicenter Food and Drug Administration investigational device exemption study of lumbar total disc replacement with the CHARITE artificial disc versus lumbar fusion: five-year follow-up. Spine J 9, 374-386. 2009.
58. Zigler J, Delamarter R, Spivak JM, Linovitz RJ, Danielsin GO 3rd, Haider TT et al. Results of the prospective, randomized, multicenter Food and Drug Administration investigational device exemption study of the ProDisc-L total disc replacement versus circumferential fusion for the treatment of 1-level degenerative disc disease. Spine (Phila Pa 1976) 32, 1155-1162. 2007.
59. Harrop JS, Youssef JA, Maltenfort M, Vorwald P, Jabbour P, Bono CM et al. Lumbar adjacent segment degeneration and disease after arthrodesis and total disc arthroplasty. SPINE 2008; 33:1701-1707.
60. Lund T, Oxland TR. Adjacent level disk disease--is it really a fusion disease? Orthop Clin Nortn Am 2011; 42:529-541.
61. Smith LJ, Nerurjar NL, Choi KS, Harfe BD, Elliott DM. Degeneration and regeneration of the intervertebral disc: lessons from development. Dis Model Mech 4, 31-41. 2011.
62. Boyd LM, Carter AJ. Injectable biomaterials and vertebral endplate treatment for repair and regeneration of the intervertebral disc. Eur Spine J 2006; 15:S414-S421.
63. Kalson NS, Richardson S, Hoyland JA. Strategies for regeneration of the intervertebral disc. Regen Med 2008; 5:729.
64. Masuda K, An HS. Prevention of disc degeneration with growth factors. Eur Spine J 2006; 15:S422-S432.
65. O'Halloran DM, Pandit AS. Tissue-engineering approach to regenerating the intervertebral disc. Tissue Eng 2007; 13:1927-1954.
66. Richardson SM, Hoyland JA, Mobasheri R, Csaki C, Shakibaei M, Mobasher A. Mesenchymal stem cells in regenerative medicine: opportunities and challenges for articular cartilage and intervertebral disc tissue engineering. J Cell Physiol 222, 23-32. 2010.
67. Meisel HJ, Siodla V, Ganey T, Minkus Y, Hutton WC, Alasevic OJ. Clinical experience in cell-based therapeutics: disc chondrocyte transplantation A treatment for degenerated or damaged intervertebral disc. Biomol Eng 24, 5-21. 2007.
68. Orozco L, Soler R, Morera C, Alberca M, Sanchez A, Carcia-Sancho J. Intervertebral disc repair by autologous mesenchymal bone marrow cells: a pilot study. Transplantation 92, 822-828. 2011.
69. Rutges JPHJ, Creemers LB, Dhert W, Milz S, Sakai D, Mochida J et al. Variations in gene and protein expression in human nucleus pulposus in comparison with annulus fibrosus and cartilage cells: potential associations with aging and degeneration. Osteoarthritis Cartilage 2010; 18:416-423.
70. Epstein NE. Commentary on research of bone morphogenetic protein discussed in review article: Genetic advances in the regeneration of the intervertebral disc. Surg Neurol Int 2013; 4 (Suppl 2):S106-S108.
71. Maerz T, Herkowitz H, Baker K. Molecular and genetic advances in the regeneration of the intervertebral disc. Surg Neurol Int 2013; 4 (Suppl 2):S94-S105.
72. Feng G, Zhang Z, Jin X, Hu J, Gupte MJ, Holzwarth JM et al. Regenerating nucleus pulposus of the intervertebral disc using biodegradable nanofibrous polymer scaffolds. Tissue Eng Part A 2012; 18:2231-2238.
73. Kranenburg HJ, Meij BP, Onis D, van der Veen AJ, Saralidze K, Amolders LA et al. Design, synthesis, imaging, and biomechanics of a softness-gradient hydrogel nucleus pulposus prosthesis in a canine lumbar spine model. J Biomed Mater Res B Appl Biomater 2012; 100:2148-2155.

74. Malhotra NR, Han WM, Beckstein J, Cloyd J, Chen W, Elliott DM. An injectable nucleus pulposus implant restores compressive range of motion in the ovine disc. SPINE 2012; 37:1099-1105.
75. Chan SC, Gantenbein-Ritter B. Intervertebral disc regeneration or repair with biomaterials and stem cell therapy--feasible or fiction? Swiss Med Wkly 2013; 142:w13598.
76. Lewis G. Nucleus pulposus replacement and regeneration/repair technologies: present status and future prospects. J Biomed Mater Res B Appl Biomater 2012; 100:1702-1720.
77. Urban JP, Roberts S. Degeneration of the intervertebral disc. Arthritis Res Ther 2003; 5:120-130.
78. Eyre DR, Wu JJ. Collagen of fibrocartilage: a distinctive molecular phenotype in bovine meniscus. FEBS Lett 1983; 158:265-270.
79. Walsh DA. Angiogenesis in osteoarthritis and spondylosis: successful repair with undesirable outcomes. Curr Opin Rheumatol 2004; 16:609-615.
80. Blummenkrantz G, Lindsey CT, Dunn TC, Jin H, Ries MD, Link TM et al. A pilot, two-year longitudinal study of the interrelationship between trabecular bone and articular cartilage in the osteoarthritic knee. Osteoarthritis Cartilage 2004; 12:977-1005.
81. Radin EL, Rose RM. Role of subchondral bone in the initiation and progression of cartilage damage. Clin Orthop Relat Res 1986; 231:34-40.
82. Drissi H, Zuscik M, Rosier R, O'Keefe R. Transcriptional regulation of chondrocyte maturation: potential involvement of transcription factors in OA pathogenesis. Mol Aspects Med 2005; 26:169-179.
83. Wang H, Zhang J, Sub Q, Yang X. Altered gene expression in articular chondrocytes of Smad3ex8/ex8 mice, revealed by gene profiling using microarrays. J Genet Genomics 2007; 34:698-708.
84. Yang X, Chen L, Xu X, Li C, Huang C, Deng CX. TGF-beta/Smad3 signals repress chondrocyte hypertrophic differentiation and are required for maintaining articular cartilage. J Cell Biol 2001; 153:35-46.
85. Bramono DS, Richmond JC, Weitzel PP, Kaplan DL, Altman GH. Matrix metalloproteinases and their clinical applications in orthopaedics. Clin Orthop Relat Res 2004; 428:272-285.
86. Le Maitre CL, Freemont AJ, Hoyland JA. Localization of degradative enzymes and their inhibitors in the degenerate human intervertebral disc. J Pathol 2004; 204:47-54.
87. Genevay S, Finckh A, Mezin F, Tessitore E, Guerne PA. Influence of cytokine inhibitors on concentration and activity of MMP-1 and MMP-3 in disc herniation. Arthritis Res Ther 2009; 11:R169.
88. Brinckerhoff CE, Martrisian LM. Matrix metalloproteinases: a tail of a frog that became a prince. Nat Rev Mol Cell Biol 2002; 3:207-214.
89. Brama PA, TeKoppele JM, Beekman B, van Ei B, Barneveld A, van Weeren PR. Influence of development and joint pathology on stromelysin enzyme activity in equine synovial fluid. Ann rheum Dis 59, 155-157. 2000.
90. Edwards JC, Wilkinson LS, Soothill P, Hembry RM, Murphy G, Reynolds JJ. Matrix metalloproteinases in the formation of human synovial joint cavities. J Anat 188, 355-360. 1996.
91. Inoue K, Mikuni-Takagaki Y, Oikawa K, Itoh T, Inada M, Noguchi T et al. A crucial role for matrix metalloproteinase 2 in osteocytic canalicular formation and bone metabolism. J Biol Chem 281, 33814-33824. 2006.
92. Mwale F, Roughley P, Antoniou J. Distinction between the extracellular matrix of the nucleus pulposus and hyaline cartilage: a requisite for tissue engineering of intervertebral disc. Eur.Cell Mater 8, 58-63. 2004.

93. Alini M, Eisenstein SM, Ito K, Little C, Kettler AA, Masuda K et al. Are animal models useful for studying human disc disorders/degeneration? Eur Spine J 17, 2-19. 2008.
94. Kroeber MW, Unglaub F, Wang H, Schmid C, Thompsen M, Nerlich A et al. New in vivo animal model to create intervertebral disc degeneration and to investigate the effects of therapeutic strategies to stimulate disc regeneration. Spine (Phila Pa 1976) 27, 2684-2690. 2002.
95. Moskowitz RW, Ziv I, Denko CW, Boja B, Jones PK, Adler JH. Spondylosis in sand rats: a model of intervertebral disc degeneration and hyperostosis. J Orthop Res 8, 401-411. 1990.
96. Hansen HJ. A pathologic-anatomical interpretation of disc degeneration in dogs. Acta Orthop Scand 20, 280-293. 1951.
97. Webb A. Potential sources of neck and back pain in clinical conditions of dogs and cats: a review. Vet J 165[193], 213. 2003.

CHAPTER 2

Increased MMP-2 activity during intervertebral disc degeneration is correlated to MMP-14 levels

JPHJ Rutges, JA Kummer, FC Oner, AJ Verbout, RJM Castelein, HJA Roestenburg, WJA Dhert and LB Creemers

Journal of Pathology (2008) 214: 523–530

Abstract

Intervertebral disc (IVD) degeneration is associated with the increased expression of several matrix metalloproteinases (MMPs), in particular MMP-2. However, little is known about the actual activity of MMP-2 in healthy and degenerated discs, or what mechanisms are involved in its activation. A major activation pathway involves complex formation with MMP-14 and a tissue inhibitor of metalloproteinases-2 (TIMP-2). In a series of 56 human IVDs, obtained at autopsy and graded according to the Thompson score (I–V), we analysed whether MMP-2 activity was increased in different stages of IVD degeneration and to what extent activation was related to the production of MMP-14 and TIMP-2. MMP-2 activation and production were quantified by gelatin zymography. Immunohistochemical staining of MMP-14 and TIMP-2 was quantified with a video overlay-based system. A positive correlation was observed between the amount of active MMP-2 and pro-MMP-2 and degeneration grade ($p < 0.001$, correlation coefficient (CC) 0.557; and $p < 0.001$, CC 0.556, respectively). MMP-2 activity correlated positively with MMP-14 and less strongly with TIMP-2 ($p = 0.001$, CC 0.436; and $p = 0.03$, CC 0.288, respectively). Moreover, immunopositivity for MMP-14 correlated to degeneration grade ($p = 0.002$, CC 0.398). IVD degeneration was associated with the activity of MMP-2 and the correlation of its activation with MMP-14 production suggests MMP-14 activates MMP-2 during degeneration. As MMP-14 is capable of activating several other enzymes that are also thought to be involved in IVD degeneration, it may be a key mediator of the degenerative process.

Introduction

Back pain is a major health problem in Western industrialized countries, with a lifetime prevalence of up to 70%[1]. Intervertebral disc (IVD) degeneration is strongly associated with low back pain and is considered a major cause of chronic low back pain[2]. Causes of IVD degeneration are likely to be both genetic and environmental, but are probably also related to wear accumulating over a lifetime of normal daily use. Biochemically, degeneration is associated with loss of collagen type II and proteoglycans, the main extracellular matrix constituents of the healthy nucleus pulposus, which are replaced by collagen type I[3,4], leading to loss of function, secondary damage to the annulus and eventually horizontal clefts through the entire IVD[3–5].

Factors that are deemed instrumental in the extracellular matrix degeneration of the IVD are the matrix metalloproteinases (MMPs), a family of metallodependent proteases that are together capable of degrading all components of the extracellular matrix of connective tissues[4,6–8]. For a number of MMPs, including MMP-1, MMP-2, MMP-3 and MMP-13, high levels of mRNA have been found in the degenerating IVD[6,9,10]. Moreover, one of these enzymes, MMP-2, was also shown to be increased in the degenerative IVD at the protein level and levels of pro- MMP-2 were found to be negatively correlated with collagen type II content in the nucleus[11,12]. However, since almost all MMPs are produced as inactive pro enzymes and may reside in the tissue in their inactive conformation[13], it is important to measure the actual levels of activity rather than the presence of this enzyme. Only one study described the correlation of MMP-2 activity with degeneration grade in IVDs of patients with chronic low back pain by zymography[9]. However, a limited range of degeneration stages was included here and in particular no information was obtained on MMP-2 activation in non-degenerated (grade I) discs[5,9].

Despite the indications that MMP-2 is involved in IVD degeneration, nothing is known about the pathways involved in activation of MMP-2 in the IVD. Amongst several mechanisms known to lead to MMP-2 activation, the most common is considered its activation by MMP-14, also known as membrane type 1 MMP (MT1-MMP). MMP-14 is a membrane-bound MMP capable of MMP-2 activation through complex formation with pro-MMP-2 and tissue inhibitor of matrix metalloproteinases 2 (TIMP-2) [14]. MMP-14 plays an important role in normal development, but also in pathological processes such as tumour invasion[15,16]. Apart from its role in activating other MMPs such as MMP-2 and MMP-13, MMP-14 also has the capacity to degrade extracellular matrix components directly[16].

The aim of this study was to determine the activity of MMP-2 in the nucleus pulposus of healthy and degenerated IVDs and to correlate its activity to the presence of MMP-14 and TIMP-2, to verify whether MMP-2 is activated by MMP-14 in the IVD.

Materials and methods

Reagents and antibodies

Complete protease inhibitor cocktail was obtained from Roche (Mannheim, Germany) and porcine skin type A gelatin (B0149-25G) from Sigma (St. Louis, MO, USA). Mouse monoclonal antibody anti-human MMP-2 (MS-806-P) and polyclonal rabbit anti-human MMP-14 (RB-9254-P) and TIMP-2 (RB-1489-P) were obtained

from Neomarkers (Freemont, CA, USA). Mouse and rabbit isotype antibody controls were purchased from Dako (Glostrup, Denmark). Poly HRP-conjugated polyclonal goat anti-rabbit IgG and polyclonal goat anti-mouse (Powervision) were obtained from Labvision (Freemont, CA, USA). All other reagents were of analytical grade.

Sample acquisition

IVDs were obtained as part of the standard post-mortem procedure, in which a section of the lumbar and thoracic spine is always removed for diagnostic purposes. IVDs from fifty-six deceased patients [63.4 ± 17.6 (range 17–91) years; table 2.1] were included. In all patients the IVD between the fourth and fifth lumbar vertebra (L4–L5), including the adjacent endplates, were obtained within 24 h after death. The scientific committee from the Department of Pathology of UMC Utrecht approved the study and the material was stored in the tissue bank of the Department of Pathology/UMCU Biobank, UMC Utrecht, and used in line with the code Proper Secondary Use of Human Tissue, as installed by the Federation of Biomedical Scientific Societies[17]. The most common cause of death was cerebrovascular and myocardial pathology. After resection, the discs were sawn into sagittal samples. Of each IVD, a mid-sagittal sample was fixed and stored in 4% formalin and graded according to the Thompson degeneration score by three individual observers (FO, LC and JR)[5]. Scores of the three observers were averaged; outliers, i.e. more than 1 Thompson grade difference, were re-evaluated at a consensus meeting (table 2.1). The remaining sagittal slices were embedded in TissueTek (Sakura Finetek Europe Zoeterwoude, The Netherlands) for cryosectioning or protein extraction, or processed to paraffin histology.

Table 2.1. Number of samples and age characteristics for each group stratified according the Thompson score.

Thompson grade	N	Mean age (years)	Range
I	3	28.1	24.5 - 34.2
II	11	48.2	17.0 - 63.4
III	16	67.8	51.2 - 88.4
IV	17	73.1	23.8 - 88.4
V	9	73.7	57.4 - 90.8

Protein extraction

Protein extraction was performed at 4°C. Approximately 0.02 g nucleus pulposus tissue was minced, combined with zirconium beads of 0.7 mm diameter (Biospec, Bartlesville, OK, USA) and 800 µl MilliQ water was added. Vials were placed in a mini Beadbeater (Biospec) and samples were mechanically disrupted for 2 min. Concentrated lysis buffer was added to the disrupted tissue to a final concentration of 0.5% sodium deoxycholate, 0.1% Triton-X100, 0.1% SDS and Complete Protease Inhibitor Cocktail (Roche, Mannheim, Germany) according to the manufacturer's instructions. Samples were gently mixed for 20 h at 4°C and centrifuged for 15 min at 16 000 × g at 4°C. Protein content of the supernatant was assessed by BCA protein

analysis (Pierce, Rockford, IL, USA) and DNA content was determined using the PicoGreen assay (Invitrogen, Paisley, UK), according to the manufacturer's instructions.

Histology

IVD slices were decalcified in Kristensen's solution (50% formic acid, and 68 g/l sodium formate) in a microwave (Milestone Microwave Laboratory Systems, Italy) at 150 W and 50°C for 6 h[18]. The slices were dehydrated in a graded series of alcohols, rinsed in xylene, embedded in paraffin and cut to sections 5.0 µm thick. General morphology and proteoglycan and collagen distribution were analysed by Alcian blue/ Picrosirius red staining of paraffin sections[19], yielding blue staining of proteoglycans, while collagen type I and II in the annulus fibrosus and in the nucleus pulposus of the degenerative IVD show up red. Under polarized light, collagen I and II are seen as yellow/orange fibres on a black background.

Localization of MMP-2, MMP-14 and TIMP-2 by immunohistochemical staining was performed on paraffin sections of IVDs without (MMP-14 and TIMP-2) or with preceding microwave decalcification (MMP-2). Endogenous peroxidase was inactivated by incubation in 0.3% H_2O_2 in PBS for 15 min, followed by a 20 min block step with PBS/3% BSA. Sections were incubated with mouse anti-MMP-2 at 2 µg/ml, rabbit anti-MMP-14 at 10 µg/ml and rabbit anti-TIMP- 2 at 4 µg/ml in PBS/3% BSA for 1 h at room temperature (RT). Goat anti-mouse poly-HRP was used as secondary antibody for MMP-2 staining for 1 h at RT and goat anti-rabbit poly HRP for MMP-14 and TIMP-2 staining for 1 h at RT, followed by incubation with 0.06% DAB in PBS and haematoxylin counterstaining. Negative controls were incubated with isotype controls at the same IgG concentration.

Quantification of immunopositivity for MMP-14 and TIMP-2

Sections stained for MMP-14 and TIMP-2 were semiquantitatively analysed for the percentage of positive cells, using a video overlay-based measuring system (Q-PRODIT, Leica, Cambridge, UK), a system in accordance with the European Organization for Research and Treatment of Cancer (EORTC) immunoquantification guidelines[20]. The nucleus pulposus was selected as the region of interest. In this region, 250–500 fields were systematically analysed at ×400 magnification. Within these fields, the Q-prodit system randomly selected 50 nucleus pulposus cells which were analysed for immunopositivity.

MMP-2 activation and production by gelatin zymography

As quantitative analysis of immunopositivity for MMP-2 cannot be used for determining MMP-2, activation gelatin zymography was applied for quantification of MMP-2 activation and production. Protein of nucleus pulposus extract (5 µg) was separated on a 8% acrylamide/0.1% gelatin gel. After electrophoresis the gel was washed twice for 15 min in a buffer containing 2.5% Triton X-100, 50 mM Tris and 10 mM CaCl, pH 7.4, at RT and incubated for 18 h in 0.05% Brij 35, 50 mM Tris, 10 mM CaCl, pH 7.4, at 37°C. The gels were then stained with Coomassie brilliant blue and analysed by densitometry, using the Gel doc 2000 system (Bio-Rad, Hercules, CA, USA) and Quantity One software (Bio-Rad).

Statistical analysis

Statistical analysis was performed using SPSS 12.0.1 software. Spearman's non-parametric test was used for correlation analyses. Differences in enzyme and inhibitor content between separate degeneration grades were analysed by Kruskal–Wallis non-parametric one way analysis of variance (ANOVA), followed by nonparametric multiple comparison test and Bonferroni correction.

Results

Macro- and microscopical analysis of intervertebral disc degeneration

Macroscopical grading according to Thompson[5] resulted in three Grade I discs, 11 Grade II discs, 16 Grade III discs, 17 Grade IV discs and nine Grade V discs (table 2.1). Macroscopically, Grades I and II showed a distinct boundary between the nucleus pulposus and annulus fibrosus, while in Grades III, IV and V a distinction between these tissues was not possible. With increasing grade of degeneration, more fibrous tissue is seen in the nucleus pulposus. Fissures and clefts only appeared in Grade IV and V IVDs. Using Alcian blue/ Picrosirius red staining, clear microscopical differences between the different degeneration grades were observed. Endplate irregularities, chondrocyte clones, mucous degeneration and granular changes were seen to a higher extent in degenerated IVDs (figure 2.1).

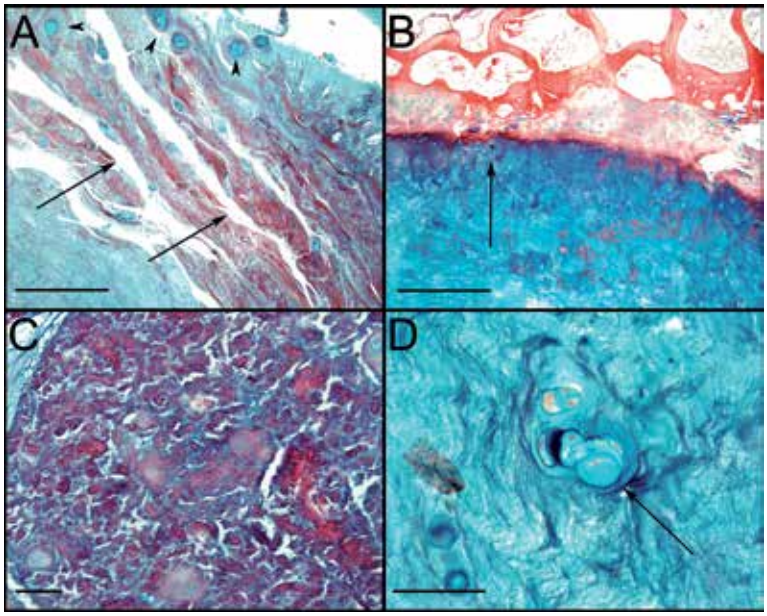

Figure 2.1. Alcian blue/Picrosirius red staining of degenerated intervertebral discs. (A) Cleft formation (arrows) and mucous degeneration (arrowheads). (B) Endplate irregularity (arrow). (C) Granular degeneration. (D) Chondrocyte cloning (arrow). Scale bars: A and B, 1 mm; C and D, 50 µm.

Localization of MMP-2, MMP-14 and TIMP-2 by immunohistochemistry

MMP-2 immunohistochemistry showed cytoplasmic staining of some nucleus pulposus cells in nondegenerative IVDs. A more frequent and more intense staining for MMP-2 of nucleus pulposus cells and chondrocyte clones was seen in degenerated IVDs (figure 2.2A). Also, limited MMP-2 staining of the annulus fibrosis cells was seen at the transition zone near the endplates in a small number of sections. No MMP-2-positive staining was seen at the endplates or in the other regions of the annulus fibrosus. Positive MMP-14 staining was seen in the cytoplasm of the nucleus pulposus cells and in chondrocyte clones (figure 2.2B). Annulus fibrosus and endplates showed no positive staining for MMP-14. TIMP-2-positive cells were located in the nucleus pulposus and showed staining of the cytoplasm of nucleus pulposus cells and chondrocyte clones (figure 2.2C). Positive staining was homogeneously distributed over the nucleus pulposus cells and no positive staining was observed in the annulus fibrosus and the endplates.

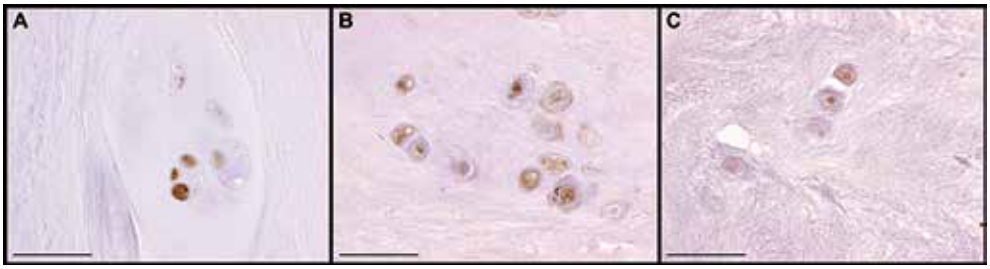

Figure 2.2. Immunohistochemical staining of MMP-2 (A), MMP-14 (B) and TIMP-2 (C) in degenerated intervertebral discs. Scale bars: 50 µm.

Quantification of immunopositivity for MMP-14 and TIMP-2

Semi-quantitative analysis of MMP-14 immunoreactivity with the Q-prodit system showed a statistically significant positive correlation with degeneration grade ($p = 0.002$, correlation coefficient (CC) 0.398). The percentage of MMP-14-positive cells was significantly lower in degeneration Grade II IVDs versus Grade IV and V IVDs ($p = 0.022$ and $p = 0.038$, respectively; figure 2.3). The percentage of MMP-14-positive cells correlated significantly with the amount of active and pro-MMP-2 as determined by zymography ($p = 0.001$, CC 0.436; and $p = 0.000$, CC 0.477, respectively). There was no statistically significant correlation between degeneration grade and TIMP-2 production, neither was there a significant difference in the percentage of positive nucleus pulposus cells between any of the degeneration grades (figure 2.4). However, a significant correlation was found between TIMP-2 and MMP-14 staining ($p = 0.000$, CC 0.623) and between TIMP-2 and MMP-2 activity ($p = 0.03$, CC 0.288).

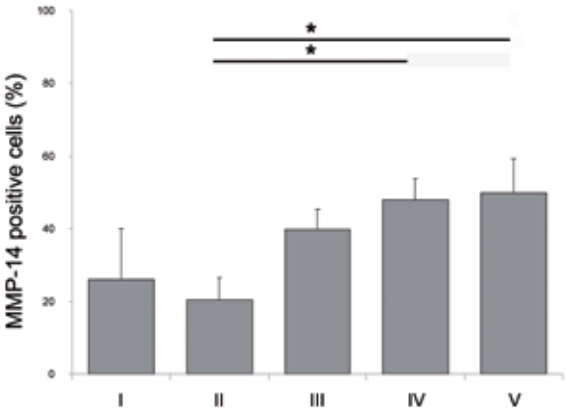

Figure 2.3. Percentage of nucleus pulposus cells staining positive by immunohistochemistry for MMP-14 during different stages of intervertebral disc degeneration. Error bars represent SEM. *p < 0.05

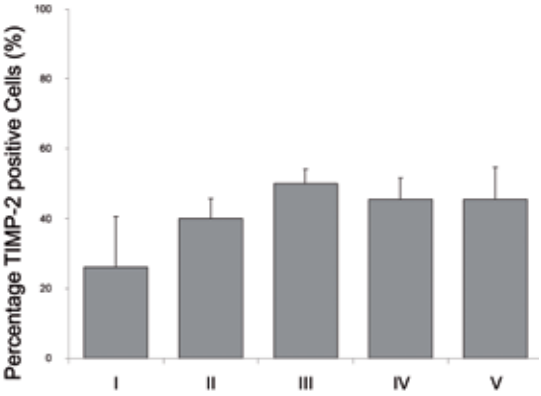

Figure 2.4. Percentage of positive stained nucleus pulposus cells by immunohistochemistry for TIMP-2 during different stages of intervertebral disc degeneration. Error bars represent SEM

MMP-2 activation and production as determined by gelatin zymography

Gelatin zymography showed distinct bands representing active MMP-2 at 68 kDa and pro-MMP-2 at 72 kDa. The amount of both active MMP-2 and pro-MMP-2 correlated significantly with degeneration grade (p = 0.000, CC 0.557; and p = 0.000, CC 0.556, respectively), although levels seemed to stabilize between Grades IV and V. Comparing separate grades of degeneration, the amount of active MMP-2 was significantly lower in Grade II compared with Grade IV and V discs (p = 0.001 and p = 0.023, respectively; figure 2.5). Comparing pro-MMP-2 levels, a significant difference was found between Grade I and Grades IV and V (p = 0.007 and p = 0.030, respectively), and between Grade II and Grades IV and V (p = 0.001 and p = 0.012, respectively;

figure 2.5). To check for a possible influence on enzyme production and activation induced by delay between time of death and time of tissue collection, the post mortem delay was correlated with MMP-2 levels and activity. No correlation was found for production (data not shown) or for MMP-2 activation (figure 2.6).

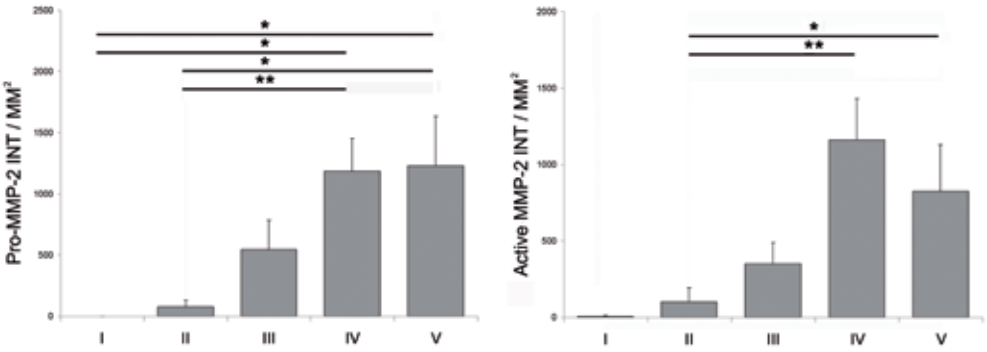

Figure 2.5. Active and Pro MMP-2 in nucleus pulposus extracts during different stages of intervertebral disc degeneration in intensity/mm2, as measured by densitometry. Error bars represent SEM. *p < 0.05; **p < 0.005.

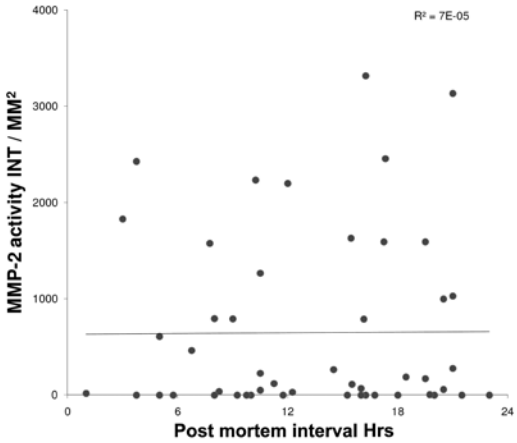

Figure 2.6. Verification of suitability of post mortem samples for MMP-2 activity studies. No significant correlation was found between post mortem delay and change in MMP-2 activity.

DNA content in different stages of IVD degeneration

To evaluate whether the differences in pro- and active MMP-2 levels found were related to cell content of the tissue extracts, the amount of DNA was assessed. DNA content/mg extracted protein showed a statistically significant positive correlation to degeneration grade (p = 0.006, CC 0.360). In particular, between grade

IV and grade V cell content seemed to have increased, although no statistically significant difference was found between any of the separate degeneration grades (figure 2.7). However, normalizing MMP levels to DNA content did not affect the correlation with degeneration grades. This indicates that the increase in pro-MMP-2 and active-MMP-2 is most likely caused by an increase of MMP-2 production per cell.

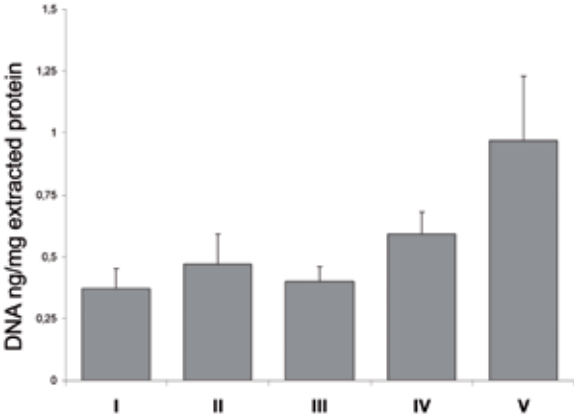

Figure 2.7. DNA content in different stages of intervertebral disc degeneration. Error bars represent SEM

Discussion

This study clearly shows an association between MMP-2 and IVD degeneration and that MMP-2 activation could be related to the increased levels of MMP-14, the presence of which is demonstrated for the first time in the human IVD. In L4–L5 IVDs of the 56 donors, encompassing all degeneration grades, as determined by macroscopic scoring according to Thompson et al[5], the levels of macroscopic degeneration were reflected by histological observations, including the gradual appearance of collagen I fibres in the nucleus, as described previously[10]. MMP-2, MMP-14 and TIMP-2 were mainly produced by the nucleus pulposus cells, with little staining in the annulus fibrosus or the endplates. MMP-2 activity correlated to the degeneration grade and to the percentage of MMP-14- and TIMP-2-immunopositive cells, suggesting that MMP-2, activated by MMP-14, may play an important role in IVD degeneration. A similar correlation of MMP-2 activity and disc degeneration was found previously in degenerated discs of patients undergoing surgery for low back pain pathology, where discs of Grades II–IV from 20 patients were analysed[9]. However, the disadvantage of using surgical samples is their limited size and the damage caused during their collection, often by punch forceps, which results in a complete loss of the normal architecture of the disc. In addition, healthy disc material will be unavailable, as grade I IVDs are not likely to be removed. The current study departs from a unique and large post-mortem dataset including both healthy and severely degenerated IVDs, thus precluding the risk of skewing data as a consequence of patient selection. The absence of any correlation between MMP-2 production and activation and post mortem delay until tissue collection further supports the use of post-mortem material for this kind of studies.

Given the apparent relationship of MMP-2 to IVD degeneration, the question arises as to which mechanism is involved in its activation. The concurrent increase of immunopositivity for MMP-14 and TIMP-2 with MMP-2 activity suggests that MMP-2 activation in the healthy, but also in the degenerating, human IVD is at least in part mediated by the MMP- 14/TIMP-2 complex. As TIMP-2 expression is likely to exert dual effects, with its role in MMP-2 activation being antagonistic to its function as inhibitor of MMPs, this may have somewhat obscured its association with degeneration and might explain the weak correlation between MMP-2 activity and TIMP-2. However, although MMP-14/TIMP-2-mediated activation is assumed to be most common and efficient, other pathways of activation cannot be excluded[21]. For example, MMP-2 can also be activated by MMP-15, with or without TIMP-2, and by MMP-24[22,23]. As yet, the presence of these enzymes in the IVD has not been studied.

Until now, the presence of MMP-14 has never been studied in the human IVD, let alone its possible involvement in IVD degeneration. Given the clear correlation between MMP-14 and IVD degeneration found in the current study, this enzyme may be involved in the degenerative changes occurring in the nucleus pulposus. However, the actual activity of MMP-14 could not be determined, as western blotting or activity assays were not sufficiently sensitive to detect active MMP-14 in IVD tissue extracts. Further support for a role of MMP-14 in IVD degeneration is provided by previous observations that TNFα-induced extracellular matrix degeneration by bovine IVD cells was mediated by MMP-14[24]. In addition to an increase in MMP-2 activity, an increase in the pro enzyme was also found, indicating that MMP-2 expression was upregulated. This could be due to an increase of MMP-2 production per cell or by an increase in the number of cells in the degenerative IVD. Increased nucleus pulposus cell proliferation and cell clustering have been reported in IVD degeneration[10,25], and also in the present study DNA content appeared to increase with degeneration. However, as no correlation was found between DNA content and active and pro-MMP-2, and normalization of MMP-2 production to DNA content did not affect its association with degeneration, it seems likely that the production of MMP-2 on a per-cell basis had increased. How MMP-2 production is regulated in the IVD is still unknown. The expression of MMP-2 is mainly constitutive and is only modestly inducible by cytokines and growth factors[26,27]. In chondral, meniscal and synovial cultures of human osteoarthritic knees, MMP-2 production was shown to be regulated by IL-1α and TNFα by as-yet unknown signalling pathways[28,29]. As IL-1 and TNFα both have been shown previously to be upregulated during IVD degeneration, the increase in MMP-2 expression in the current study may have been mediated through these cytokines[30,31].

The demonstration of the presence of MMP-14 in the IVD and its increased production during degeneration could have important implications. MMP-14 itself is capable of matrix degradation, and in addition is capable of activating not only MMP-2 but also MMP-13, another MMP related to IVD degeneration and MMP-8[4,8,32,33], enabling efficient and fast degradation of the resident matrix. Osteoarthritic degeneration of articular cartilage, a process that shares many similarities with IVD degeneration [34], is associated with an increase in production of these four MMPs[8,35–38], which possibly renders MMP-14 a key player in initiating and maintaining extracellular matrix destruction.

In conclusion, the production and activation of MMP-2 are clearly correlated with disc degeneration, with MMP-14 production reflecting MMP-2 activity. Together with the fact that MMP-14 is the main activator of MMP-2 in several other tissues, this correlation is suggestive of a role for MMP-14 in MMP-2 activation in IVD tissue. As MMP-14 is capable of degenerating essential extracellular matrix components of the intervertebral disc and activates other matrix-degrading proteases, further studies into the exact role of MMP-14 in intervertebral disc degeneration are of prime importance.

Acknowledgements

The authors acknowledge the Department of Pathology of the University Medical Centre, Utrecht, in particular F Bernhard and A de Ruiter for their help in obtaining the IVD specimens, PJ van Diest for his help with the Q-prodit system, and R Broekhuizen for his support with immunohistochemical staining. This study was supported by the Anna Foundation and the Dutch Arthritis Association.

References

1. Frymoyer JW, Cats-Baril WL. An overview of the incidences and costs of low back pain. Orthop Clin N Am 1991;22(2):263–271.
2. Brisby H. Pathology and possible mechanisms of nervous system response to disc degeneration. J Bone Joint Surg Am 2006;88:68–71.
3. Adams MA, Roughley PJ. What is intervertebral disc degeneration, and what causes it? Spine 2006;31(18):2151–2161.
4. Roberts S, Evans H, Trividi J, Menage J. Histology and pathology of the human intervertebral disc. J Bone Joint Surg Am 2006;88(suppl 2):S2 10–14.
5. Thompson JP, Pearce RH, Schechter MT, Adams ME, Tsang IKY, Bishop PB. Preliminary evaluation of a scheme for grading the gross morphology of the human intervertebral disc. Spine 1990;15(5):411–415.
6. Goupille P, Jayson MI, Valat JP, Freemont AJ. Matrix metalloproteinases: the clue to intervertebral disc degeneration? Spine 1998;23(14):1612–1626.
7. Le Maitre CL, Freemont AJ, Hoyland JA. Localization of degradative enzymes and their inhibitors in the degenerate human intervertebral disc. J Pathol 2004;204(1):47–54.
8. Bramono DS, Richmond JC, Weitzel PP, Kaplan DL, Altman GH. Matrix metalloproteinases and their clinical applications in orthopaedics. Clin Orthop Relat Res 2004;428:272–285.
9. Crean JKG, Robberts S, Jaffray DC, Eisenstein SM, Duance VC. Matrix metalloproteinases in the human intervertebral disc: role in disc degeneration and scoliosis. Spine 1997;22(24):2877–2884.
10. Weiler C, Nerlich AG, Zipperer J, Bachmeier BE, Boos N. 2002 SSE Award Competition in Basic Science: expression of major matrix metalloproteinases is associated with intervertebral disc degradation and resorption. Eur Spine J 2002;11(4):308–320.
11. Kozaci LD, Guner A, Oktay G, Guner G. Alterations in biochemical components of extracellular matrix in intervertebral disc herniation: role of MMP-2 and TIMP-2 in type II collagen loss. Cell Biochem Funct 2006;24(5):431–436.
12. Shen B, Melrose J, Ghosh P, Taylor F. Induction of matrix metalloproteinase-2 and -3 activity in ovine nucleus pulposus cells grown in three-dimensional agarose gel culture by interleukin- 1β: a potential pathway of disc degeneration. Eur Spine J 2003;12(1):66–75.
13. Matsui Y, Maeda M, Nakagami W, Iwata H. The involvement of matrix metalloproteinases and inflammation in lumbar disc herniation. Spine 1998;23(8):863–868.
14. Ruagngpanit N, Chan D, Holmbeck K, Birkedal-Hansen H, Polarek J, Yang C, et al. Gelatinase A (MMP-2) activation by skin fibroblasts: dependence on MT1-MMP expression and fibrillar collagen form. Matrix Biol 2001;20(3):193–203.
15. Holmbeck K, Bianco P, Caterina J, Yamada S, Kromer M, Kuznetsov SA, et al. MT1-MMP-deficient mice develop dwarfism, osteopenia, arthritis, and connective tissue disease due to inadequate collagen turnover. Cell 1999;99(1):81–92.
16. Holmbeck K, Bianco P, Birkedal-Hansen H. MT1-mmp: a collagenase essential for tumor cell invasive growth. Cancer Cell 2003;4(2):83-84.
17. Code for adequate secondary use of tissue. http://www.federa.org/?s=1&m=78.
18. Kristensen HK. An improved method of decalcification. Stain Technol 1948;23:151–154.
19. Gruber HE, Ingram J, Hanley EN Jr. An improved staining method for intervertebral disc tissue. Biotech Histochem 2002;77(2):81–83.

20. van Diest PJ, van Dam P, Hensen-Logmans SC, Berns E, van der Burg ME, Green J, et al. A scoring system for immunohistochemical staining: consensus report of the task force for basic research of the EORTC–GCCG (European Organization for Research and Treatment of Cancer — Gynaecological Cancer Cooperative Group). J Clin Pathol 1997;50:801–804.
21. Wang Z, Juttermann R, Soloway PD. TIMP-2 is required for efficient activation of proMMP-2 in vivo. J Biol Chem 2000;275(34):26411–26415.
22. Kolkenbrock H, Hecker-KIA A, Orgel D, Ulbrich N, Will H. Activation of progelatinase S and peogelatinase A/TIMP-2 complex by membrane type 2-matrix metalloproteinse. Biol Chem 1997;378(2):71–76.
23. Morrison CJ, Butler GS, Bigg HF, Roberts CR, Soloway PD, Overall CM. Cellular activation of MMP-2 occurs via a TIMP-2-independent pathway. J Biol Chem 2001;276(50):47402–47410.
24. Seguin CA, Bojarski M, Pilliar RM, Roughley PJ, Kandel RA. Differential regulation of matrix degrading enzymes in a TNFα-induced model of nucleus pulposus tissue degeneration. Matrix Biol 2007;25(7):409–418.
25. Johnson WE, Eisenstein SM, Roberts S. Cell cluster formation in degnerate lumbar intervertebral discs is associated with increased disc cell proliferation. Connect Tissue Res 2001;43(3):197–207.
26. Benbow U, Brinckerhoff CE. The AP-1 site and MMP gene regulation: what is all the fuss about? Matrix Biol 1997;15:519–526.
27. Yan C, Boyd DD. Regulation of matrix metalloproteinase gene expression. J Cell Physiol 2007;211(1):19–26.
28. Chu SC, Yang SF, Lue KH, Wu CL, Lu KH. Regulation of gelatinases expression by cytokines, endotoxin, and pharmacological agents in the human osteoarthritic knee. Connect Tissue Res 2004;45(3):142–150.
29. Mounain DJ, Singh M, Menon B, Singh K. Interleukin-1β increases expression and activity of matrix metalloproteinase-2 in cardiac microvascular endothelial cells: role of PKCα/β1 and MAPKs. Am J Physiol Cell Physiol 2007;292(2):C867–875.
30. Bachmeier BE, Nerlich AG, Weiler C, Paesold G, Jochum M, Boos N. Analysis of tissue distribution of TNF-α, TNF-α receptors, and the activating TNF-α-converting enzyme suggests activation of the TNF-α system in the aging intervertebral disc. Ann NY Acad Sci 2007;1096(44):54.
31. Le Maitre CL, Freemont AJ, Hoyland JA. The role of interleukin-1 in the pathogenesis of human intervertebral disc degeneration. Arthritis Res Ther 2005;7(4):R732–745.
32. Holopainen JM, Moilanen JA, Sorsa T, Kivela-Rajamaki M, Tervahartiala T, Vesaluoma MH, et al. Activation of matrix metalloproteinase-8 by membrane type 1-MMP and their expression in human tears after photorefractive keratectomy. Invest Ophthalmol Vis Sci 2003;44(6):2550–2556.
33. Murphy G, Knauper V, Atkinson S, Butler G, Hutton M, Starcke J, et al. Matrix metalloproteinases in arthritic disease. Arthritis Res 2002;4(suppl 3):S3 39–49.
34. Mwale F, Roughley PJ, Antoniou J. Distinction between the extracellular matrix of the nucleus pulposus and hyaline cartilage: a requisite for tissue engineering of intervertebral disc. Eur Cell Mater 2004;8:58–63.
35. Duerr S, Stremme S, Soeder S, Bau B, Aigner T. MMP-2/gelatinase A is a gene product of human adult articular chondrocytes and is increased in osteoarthritic cartilage. Clin Exp Rheumatol 2004;22(5):603–608.
36. Imai K, Ohta S, Matsumoto T, Fuijmoto N, Sato H, Seiki M, et al. Expression of membrane-type 1 matrix metalloproteinase and activation of progelatinase A in human osteoarthritic cartilage. Am J Pathol 1997;151(1):245–256.

37. Moldovan F, Pelletier JP, Hambor J, Cloutier JM, Martel-Pelletier J. Collagenase-3 (matrix metalloprotease 13) is preferentially localized in the deep layer of human arthritic cartilage in situ: in vitro mimicking effect by transforming growth factor beta. Arthritis Rheum 1997;40(9):1653–1661.
38. Tetlow LC, Adlam DJ, Woolley DE. Matrix metalloproteinase and proinflammatory cytokine production by chondrocytes of human osteoarthritic cartilage: associations with degenerative changes. Arthritis Rheum 2001;44(3):585–594.

CHAPTER 3

The presence of extracellular matrix degrading metalloproteinases during fetal development of the intervertebral disc

JPHJ Rutges, PGJ Nikkels, FC Oner, KD Ottink, AJ Verbout, RJM Castelein,
LB Creemers and WJA Dhert
European Spine Journal (2010) 19:1340–1346

Abstract

Matrix metalloproteinases (MMPs) regulate connective tissue architecture and cell migration through extracellular matrix (ECM) degradation and are associated with both physiological and pathological processes. Although they are known to play a role in skeletal development, little is known about the role of MMPs in intervertebral disc (IVD) development. Sixteen fetal human lumbar spine segments, obtained at autopsy, were compared with five normal, non-fetal L4–L5 IVDs. Intensity and/or localization of immunohistochemical staining for MMP-1, -2, -3 and -14 were evaluated by three independent observers. MMP-2 production and activation was quantified by gelatin zymography. MMP-1 and -14 were abundantly present in the nucleus pulposus (NP) and notochordal (NC) cells of the fetal IVDs. In non-fetal IVDs, MMP-1 and -14 staining was significantly less intense ($p=0.001$ and $p<0.001$, respectively). MMP-3 was found in almost the entire IVD with no significant difference from non-fetal IVDs. MMP-2 staining in the NC and NP cells of the fetal IVD was moderate, but weak in the non-fetal IVD. Gelatin zymography showed a negative correlation of age with MMP-2 activity ($p<0.001$).MMP-14 immunostaining correlated positively with MMP-2 activity ($p=0.001$). For the first time, the presence of MMP-1, -2, -3 and -14 in the fetal human IVD is shown and the high levels of MMP-1, -2 and -14 suggest a role in the development of the IVD. In particular, the gradual decrease in MMP-2 activation during gestation pinpoints this enzyme as key player in fetal development, possibly through activation by MMP-1 and -14.

Introduction

Since the identification of the first matrix metalloproteinase (MMPs) in 1962, MMPs have been shown to be associated with a large number of diseases, including vascular, renal, neurological, respiratory, oncological, rheumatic and orthopedic diseases[1,2]. However, the development of MMP knock-out mice with aberrant phenotypes and the severe side effects of MMP inhibitors in the late 1990s clearly indicated that MMPs are also crucial for normal tissue function[1,2]. MMPs are associated with complex regulatory processes such as cell migration, tissue architecture and development[2,3]. Fetal development of connective tissues has also been suggested to be dependent on this class of enzymes and various MMPs have been shown to play a role in skeletal development.

Various MMPs have been shown to be involved in the development of joints. MMP-1 was found in chondrocytes and synovium of fetal human joints[4.] Moreover, MMP-1 activity was found to be greatly increased in synovial fluid of fetal horses compared to juvenile and mature animals[5]. MMP-2 is associated with development of the osteocytic canalicular network, synovial tissue and articular surfaces[4,6]. In humans, a mutation in the gene encoding for MMP-2 results in a multicentre osteolysis and arthritis syndrome, which is characterized by short stature, facial anomalies, and arthropathy[7]. MMP-3 has been associated with the development of fetal joints and of joint cavities. An increase in MMP-3 activity was found in the synovial fluid of fetal equine joints compared to juvenile and mature horses[4,8]. The most severe phenotypical abnormalities of all MMP-deficient animals are seen in the MMP-14 knock-out mouse, characterized by dwarfism, osteopenia, arthritis, angiogenesis defects and death within 3–12 weeks after birth[9]. Remodeling of fetal unmineralized cartilage into joints and bone has been shown to be MMP-14-mediated[10].

However, nothing is known about the involvement of MMPs in fetal development of the intervertebral disc (IVD). As the extracellular matrix (ECM) of both articular cartilage and the nucleus pulposus (NP) of the IVD is mainly composed of aggrecan and collagen type II, and the respective degenerative processes have been shown to share many factors, it is likely that also during fetal development, cartilage and IVD tissue share the same mediators[11].

Given this clear association of MMP-1, -2, -3 and -14 with the fetal development of cartilage, the aim of this study was to evaluate their presence and in particular the activity of MMP-2 in human IVDs during consecutive stages of fetal development and compare these to normal non-fetal IVDs.

Materials and methods

Reagents, antibodies and tissue processing

Used reagents, antibodies, antibody concentrations, antigen retrieval and tissue processing are described in the supplement of this chapter.

Sample acquisition

Fetal IVDs were obtained during a standard post-mortem procedure in which the lumbar spine is partly removed for diagnostic purposes. IVDs from 16 deceased patients (spontaneous abortions, gestation age

15.5–40.3 weeks) were obtained within 24 h after death (table 3.1, supplement). Patients with skeletal pathology were excluded from this study. Several lumbar segments, including the vertebrae and adjacent endplates, were obtained. A control group of five non-fetal, non-degenerative, human L4–L5 IVDs (age 3.3–21.8 years) was collected in a similar manner as the fetal IVDs. This control group will be referred to as the non-fetal discs. The scientific committee from the Department of Pathology of the UMC Utrecht approved the study and the material was used in line with the code ''Proper Secondary Use of Human Tissue'' as installed by the Federation of Biomedical Scientific Societies. After resection, the discs were cut (fetal discs) or sawed (non-fetal discs) in sagittal samples. Of each IVD, a mid-sagittal sample was fixed and stored in 4% formalin for histology. The remaining sagittal slices were embedded in TissueTek (Sakura Finetek Europe, Zoeterwoude, The Netherlands), stored at -80°C and were used for protein extraction.

Immunolocalization of MMP-1, -2, -3, -14, collagen type II, endothelial membrane antigen (EMA) and pan cytokeratin (AE1/AE3)

Paraffin sections were rehydrated through xylene and graded ethanol series. Endogenous peroxidase was inactivated by incubation in 0.3% H_2O_2 in PBS for 15 min, followed by a 20-min block step with PBS/3% BSA. Sections were incubated with primary antibodies and the appropriate secondary antibody. DAB (0.06%) in PBS was used for antigen detection and sections were counterstained with Mayer's hematoxylin. Negative controls were incubated with isotype controls at the same IgG concentration.

Immunohistochemical staining for MMP-1, -2, -3 and -14 was graded by three independent observers according a semiquantitative four-point scoring scale[12]. An intense staining for the antigen in [50% of the cells was scored as ++, an intense staining in 10–50% of the cells was scored +, ± was scored if the staining was seen in less than 10% of the cells and - was scored when no staining was observed. In each section, the cartilage endplate (CE), NP, AF, and notochordal (NC) cells were analyzed. Scores of the three observers were averaged and outliers, i.e. more than 1 grade difference, were re-evaluated at a consensus meeting.

Collagen type II immunohistochemistry was used to demonstrate the cartilaginous nature of the ECM throughout the fetal and non-fetal IVDs (figure 3.6E and 3.6F, supplement). The EMA and pan cytokeratin (AE1/AE3) staining was used for identification of NC cells[13,14].

Gelatin zymography for MMP-2 activation and production

Five micrograms of protein of tissue extract was separated on an 8% acrylamide/0.1% gelatin gel. After electrophoresis, the gel was washed twice for 15 min in 2.5% Triton X-100, 50 mM Tris and 10 mM CaCl (pH 7.4) and incubated for 18 h in 0.05% Brij 35, 50 mM Tris, 10 mM CaCl (pH 7.4) at 37°C. Gels were stained with Coomassie Brilliant Blue, destained in deionized water and analyzed by densitometry using the Gel doc 2000 system (Bio-rad, Hercules, CA) and Quantity One software (Bio-rad). A degenerative IVD sample containing active and pro-MMP-2 was used as control sample. Densitometry data were corrected to the measurements of the control sample on each gel. Gelatin zymography of both fetal and non-fetal samples is shown in figure 3.7 (supplement). Casein zymography for MMP-1 and MMP-3 was also attempted; however, this technique was not sensitive enough to detect MMP-1 or MMP-3 activity in fetal and non-fetal IVDs.

Statistical analysis

Statistical analysis was performed with SPSS 12.0.1 software. Differences in enzyme content between fetal and non-fetal IVDs were determined by a Mann–Whitney U test. Differences between age groups were analyzed by Kruskal–Wallis' non-parametric test followed by non-parametric multiple comparison test and Bonferroni correction. Spearman's non-parametric test was used for correlation analyses. Categorical data obtained by grading of the immunochemical staining were analyzed with the 2 x C Fisher exact test[15].

Results

Immunohistochemistry

In the non-fetal IVDs, NC cells, identified by their morphology of large irregularly shaped cells containing vesicle-like structures predominantly laying in cell clusters (figure 3.1A)[16,17], were found to stain positive for EMA and pan cytokeratin (AE1/AE3), which did not stain any other cell type (figure 3.1B and 3.1C, respectively).

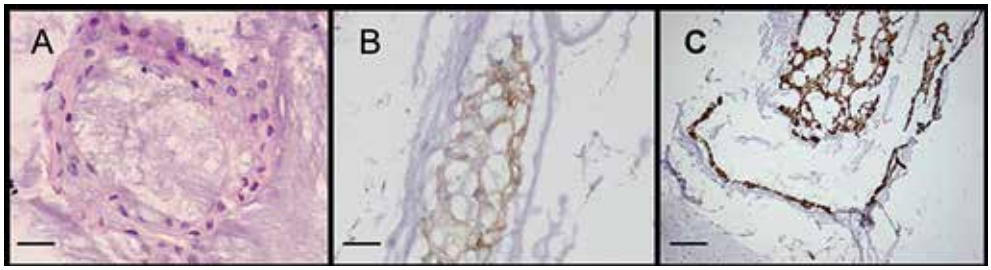

Figure 3.1. Hematoxylin–eosin staining of NC cells in the fetal intervertebral disc (A). Identification of NC cells by positive immunohistochemical staining for EMA (B) and CK AE1/AE3 (C). Scale bars represent 25µm (A,B) and 100µm (C).

Abundant staining for MMP-1 was seen in the NP of the fetal IVD, whereas staining of the AF and CE was less intense (figure 3.2A). In the fetal NP, both the chondrocyte-like NP cells and the NC cells stained positive for MMP-1 (figure 3.2A). In the non-fetal IVDs, MMP-1 staining was moderately positive in NP and AF, while no staining was seen in the CE (figure 3.2B). The positive staining in the NP was mainly localized in the NC cells (figure 3.2B). The intensity of the immunohistochemical staining in all three areas of the IVD (CE, AF and NP) combined was significantly higher in the fetal IVDs compared to the non-fetal IVDs, p=0.001 (figure 3.3). MMP-2 staining was moderate in the NP, in both chondrocyte-like NP and NC cells, of the fetal IVDs, whereas no staining was found in the CE and AF (figure 3.2C). MMP-2 staining in the non-fetal IVDs was variable throughout the IVD, with in general a moderate to weak staining in the entire IVD (figure 3.2D).
MMP-3 was clearly seen in the NP, AF and CE of fetal IVDs (figure 3.2E). Intense staining of the NC cells and a moderate staining of chondrocyte-like NP cells were seen in the NP (figure 3.2E). In the non-fetal IVDs, MMP-3 staining was seen in the NP and moderately in the CE and AF. In the NP the NC cells showed a clear staining and the chondrocyte-like NP cells showed a moderate staining for MMP-3 (figure 3.2F).

The intensity of MMP-14 staining in the fetal IVDs was strong in the NP and moderate in the AF and CE. In the NP, both the NC and chondrocyte-like NP cells stained positive for MMP-14 (figure 3.2G). In the non-fetal IVDs, the NP showed a moderate staining and the AF and CE were negative (figure 3.2H). In the NP, the NC cells were still clearly positive for MMP-14, but a few cartilage-like NP cells were also positive for MMP-14 (figure 3.2H). The intensity of the staining in all three areas of the non-fetal IVDs combined was significantly less than in the fetal IVDs, $p<0.001$ (figure 3.3).

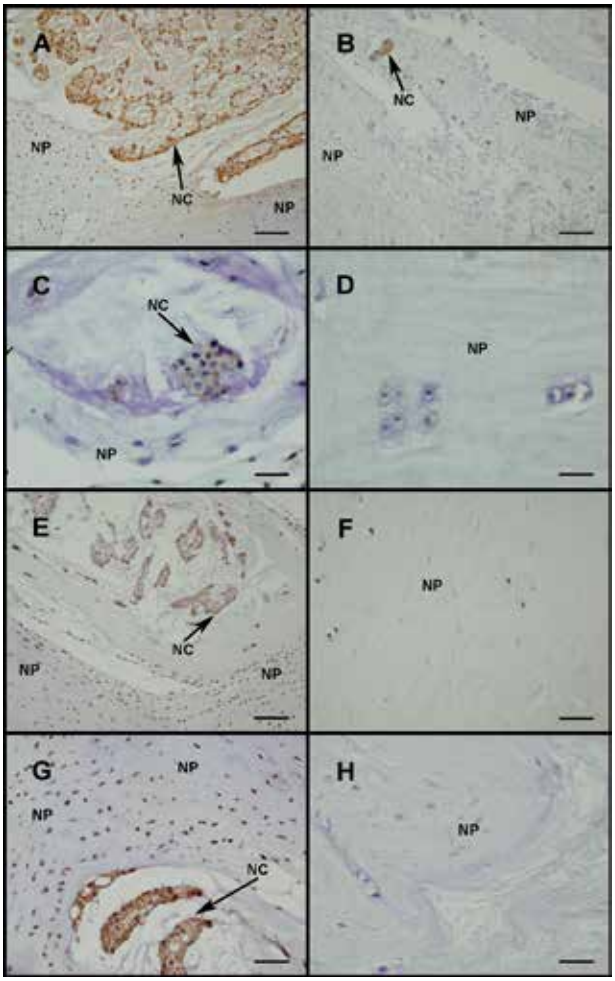

Figure 3.2. Immunohistochemical staining for MMP-1 (A,B). MMP-2 (C,D), MMP-3 (E,F) and MMP-14 (G,H) in the nucleus pulposus of fetal (A,C,E,G) and non-fetal IVDs (B,D,F,H). Arrows accompanied by ''NC'' indicate clusters of notochordal cells and within the nucleus pulposus and ''NP'' indicates the nucleus pulposus containing chondrocyte-like NP cells. Scale bars represent 100 µm (A,B,E,F), 50µm (G,H) and25µm (C,D).

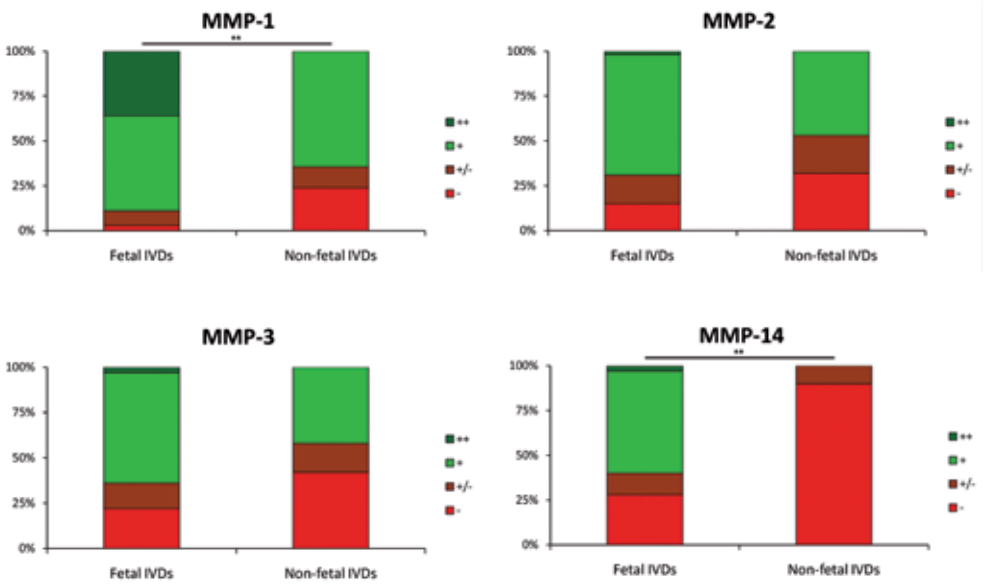

Figure 3.3. Intensity of immunohistochemical staining for MMP-1, -2, -3 and -14 in fetal and non-fetal IVDs. An intense staining for the antigen in >50% of the cells was scored as ++, an intense staining in 10–50% of the cells was scored +, ± was scored if the staining was seen in <10% of the cells and - was scored when no staining was observed, ** p< 0.005.

Gelatin zymography for MMP-2 activation and production

Gelatin zymography showed a statistically significant negative correlation between age in weeks and active MMP-2[p<0.001; correlation coefficient (CC)-0.80]. Also with respect to fetal development only (first 3 age groups), a negative correlation was found for MMP-2 activity and gestational age (p=0.013 CC=-0.61). No correlation was found between levels of pro-MMP-2 and age. The level of active MMP-2 in the fetal groups was higher in comparison to the non-fetal discs (p=0.004). Also the levels of pro-MMP-2 were significantly higher in fetal samples compared to non-fetal discs (p=0.008). A significant decrease in active MMP-2 was found between the 15–22 weeks after gestation group and the non-fetal group (0–22 years, p<0.001). The level of pro-MMP-2 was significantly higher in 30–41 weeks after gestation group, compared to the IVDs from the non-fetal group (0-22 years, p=0.044). Active MMP-2 levels in all IVD samples showed a strong positive correlation with the intensity of MMP-14 immunohistochemistry (p=0.001, CC= 0.673). Faint MMP-9 bands were found in most samples, no differences in active and pro-MMP-9 levels were seen between fetal and non-fetal IVDs (figure 3.4).

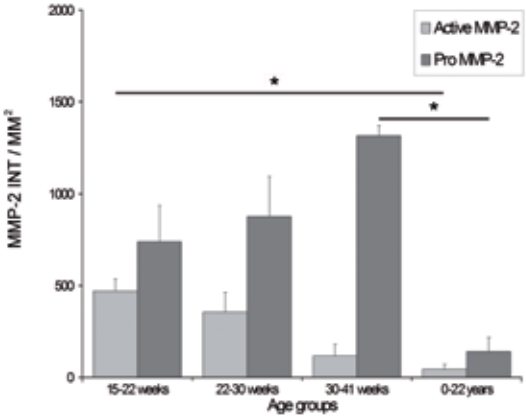

Figure 3.4. Amount of active and pro-MMP-2 in fetal and non-fetal IVDs.
Error bars represent standard error of the mean, * $p<0.05$.

Discussion

This study for the first time shows the presence of MMP-1, -2, -3 and -14 in fetal and non-fetal human IVDs. The enzymes were mainly localized in the NP and in the NC cells of the IVD. Significantly, more MMP-1 and -14 were seen in the fetal IVDs compared to the non-fetal IVDs. Moreover, MMP-2 activity during fetal development was high during the first 15–22 weeks of gestation and decreased with gestational age and even further in postnatal and young healthy IVDs.

Not much is known about the presence of MMPs in fetal and non-fetal IVDs. An immunohistochemical study describing the presence of MMP-1, -2, -3 and -9 in degenerative human IVDs included some data on an unknown number of fetal and non-fetal IVDs of donors of undefined age[18]. In contrast to the present data, these MMPs were not found in fetal IVDs and only an occasional staining for MMP-1, -2 and -3 was reported in non-degenerative IVDs[18]. The discrepancies with this study could be explained by various factors such as different and less sensitive immunohistochemistry protocols and the limited number of fetal and non-degenerative IVDs in the degenerative disc study.

In this study, it was shown that these enzymes are present in the fetal IVD and that their levels decreased during childhood and adolescence, suggesting a physiological function of these enzymes during development of the IVD. In support of this role is the available literature on MMP-1, -2, -3 and -14, clearly associating these enzymes with the development of connective tissues, including cartilaginous tissue. The function of these MMPs during the fetal development of the IVD could be: direct ECM degradation for cell migration or tissue remodeling, regulation of the activity of other proteases by removal of the pro-domain and modulation of biologically active molecules by direct cleavage or release from ECM store[19]. MMP-14 is the only MMP, which has specifically been studied in non-degenerative IVDs. A rat IVD organ culture

study describes the presence of MMP-14 in chondrocytes migrating from the CE to the NP and an extensive immunohistochemical positivity of the NC cells for MMP-14 is reported[20], in concordance with the current results. The authors suggest that MMP-14 enables the chondrocytes to migrate from the CE to the NP and replace the NC cells[20]. During growth of the IVD, the normal ECM has to be degraded to allow IVD cells to migrate through the tissue[21]. Additionally, existing ECM could undergo partial or complete degradation prior to new matrix synthesis[21]. MMP-1, -2, -3 and -14 are all capable of degrading one or both of the most important ECM components of the fetal IVD, collagen type II and aggrecan.

Besides their role in remodeling by ECM degradation, several MMPs also have regulatory functions by activating other proteases[2]. In the developing IVD, MMP-1 and -14 could have a regulatory function since both enzymes are capable of activating several MMPs including MMP-2[22]. Additionally, regulatory activity of MMP-1 could be regulated by MMP-3 which is capable of not only activating pro-MMP-1 but also pro-MMP-7, -8, -9 and -13[22]. The strongly abnormal phenotype of several MMP knock-out mice may well be caused by these important regulatory functions of the enzymes. In particular, MMP-14 knock-out mice display decreased proliferation of chondrocytes in growth plates and defective vascular invasion of cartilage ends of fetal long bones, which leads to shortening and skeletal malformation[9,23]. The decreased activation of MMP-2 in MMP-14-deficient mice suggests that the function of MMP-14 during development may not just be limited to ECM turnover and that MMP-14 also has a more regulatory function[23]. The statistically significant correlation between MMP-2 activity and the intensity of MMP-14 immunohistochemistry could be an indication that MMP-2 activity in fetal IVDs is regulated by MMP-14.

Strikingly, MMP-14 and -1 were clearly present in the NC cells of the fetal IVD, suggesting a possible role for these cells in the regulation of extracellular remodeling and cell migration. This theory is supported by the fact that the loss of these cells during late childhood or adolescence is associated with the onset of IVD degeneration[24]. Moreover, recently rat NC cells have been found to stimulate migration of rat CE chondrocytes in vitro[25]. NC cells are remnants of the embryonic notochord and are entrapped inside the IVD during embryonic formation of the vertebrae and IVDs[17]. There are two hypotheses on the role of NC cells during IVD development. The first postulates that NC cells regulate matrix synthesis and cell migration and undergo apoptosis once disc formation is complete. The second theory assumes that NC cells directly synthesize the ECM of the NP and then differentiate into chondrocyte-like NP cells[17]. Since the NC cells were found to stain less intense for proteoglycans than the chondrocyte-like NP cells and hardly any staining for collagen type II is seen in the ECM surrounding the NC cells, the first theory seems to be most likely.
Although this study clearly shows the presence of MMP-1, -2, -3 and -14 in the fetal IVD, it must be kept in mind that immunohistochemistry is seldom capable of distinguishing between active and inactive forms of enzymes. Only the actual activity of MMP-2 could be determined here, whereas casein zymography and ELISA-based activity assays were not sensitive enough to measure detectable levels of enzyme activity. Although PCR is a very sensitive technique, the presence mRNA levels do not always correlate to the protein levels and PCR is unable to detect the presence of active MMPs. More sensitive techniques determining

actual MMP activity are required to further elucidate the role of MMPs in IVD development. As to the clear association of IVD development with MMP-2 activity, it remains unknown how MMP-2 exactly is involved in IVD, or even cartilage or joint development. A role in ECM turnover and growth seems likely; however, no support for this hypothesis can be found in literature. It is remarkable that MMP-2 seems to have such a close association with the development of connective tissues and is also strongly associated with degenerative diseases as osteoarthritis and IVD degeneration[26]. MMP knock-out mice studies could further elucidate the role of MMPs in fetal IVD development; however, results of these studies should be analyzed with care since human and mice MMPs are not entirely comparable.

In addition to the MMPs studied, other proteases may be involved in fetal development of the IVD. However, the enzymes currently studied are the only MMPs shown to be involved in the development of cartilage and joints. ADAMTS-4 and -5 may provide good candidates for IVD development through ECM turnover. Nevertheless, neither of these enzymes have been shown to be required for normal cartilage and skeletal development as demonstrated in knock-out models[27].

Conclusion

This study clearly shows the presence of MMP-1, -2, -3 and -14 in the fetal human IVD. Their increased expression as compared to non-fetal healthy IVDs suggests their involvement in IVD development. In particular, MMP-2 activity was closely correlated to developmental stage. During IVD development, MMPs could be involved in cell migration, regulation of ECM turnover and activation of other MMPs.

Acknowledgments

The authors acknowledge F. Bernhard and A. de Ruiter from the Department of Pathology of the University Medical Center Utrecht for their help in obtaining the IVD specimens. This study was supported by the Dutch Arthritis Association and the Anna Foundation.

References

1. Le Maitre CL, Freemont AJ, Hoyland JA (2004) Localization of degradative enzymes and their inhibitors in the degenerate human intervertebral disc. J Pathol 204:47–54
2. Page-McCaw A, Ewald AJ, Werb Z (2007) Matrix metalloproteinases and the regulation of tissue remodelling. Nat Rev Mol Cell Biol 8:221–233
3. Lemaitre V, D'armiento J (2006) Matrix metalloproteinases in development, disease. Birth Defects Res C Embryo Today 78:1–10
4. Edwards JC, Wilkinson LS, Soothill P, Hembry RM, Murphy G, Reynolds JJ (1996) Matrix metalloproteinases in the formation of human synovial joint cavities. J Anat 188:355–360
5. Brama PA, van den Boom R, de Groot J, Kiers GH, van Weeren PR (2004) Collagenase-1 (MMP-1) activity in equine synovial fluid: influence of age, joint pathology, exercise and repeated arthrocentesis. Equine Vet J 36:34–40
6. Inoue K, Mikuni-Takagaki Y, Oikawa K, Itoh T, Inada M, Noguchi T et al (2006) A crucial role for matrix metalloproteinase 2 in osteocytic canalicular formation and bone metabolism. J Biol Chem 281:33814–33824
7. Martignetti JA, Al Aqeel A, Sewaira WA, Boumah CE, Kambouris M, Mayouf SA et al (2001) Mutation of the matrixmetalloproteinase 2 gene (MMP2) causes a multicentric osteolysis and arthritis syndrome. Nat Genet 28: 261–265
8. Brama PA, TeKoppele JM, Beekman B, van Ei B, Barneveld A, van Weeren PR (2000) Influence of development and joint pathology on stromelysin enzyme activity in equine synovial fluid. Ann Rheum Dis 59:155–157
9. Holmbeck K, Bianco P, Caterina J, Yamada S, Kromer M, Kuznetsov SA et al (1999) MT1-MMP-deficient mice develop dwarfism, osteopenia, arthritis, and connective tissue disease due to inadequate collagen turnover. Cell 99:81–92
10. Holmbeck K, Bianco P, Chrysovergis K, Yamada S, Birkedal- Hansen H (2003) MT1-MMP-dependent, apoptotic remodeling of unmineralized cartilage: a critical process in skeletal growth. J Cell Biol 163:661–671
11. Roberts S, Evans H, Trividi J, Menage J (2006) Histology and pathology of the human intervertebral disc. J Bone Joint Surg Am 88(S2):10–14
12. Zlobec I, Steele R, Michel RP, Compton CC, Lugli A, Jass JR (2006) Scoring of p53, VEGF, Bcl-2 and APAF-1 immunohistochemistry and interobserver reliability in colorectal cancer. Mod Pathol 19:1236–1242
13. Chordoma MM (1984) Antibodies to epithelial membrane antigen and carcinoembryonic antigen in differential diagnosis. Arch Pathol Lab Med 108:891–892
14. Naka T, Iwamoto Y, Shinohara N, Chuman H, Fukui M, Tsuneyoshi M (1997) Cytokeratin subtyping in chordomas and the fetal notochord: and immunohistochemical analysis of aberrant expression. Mod Pathol 10:545–551.15
15. Requena F, Ciudad NM (2006) A major improvement to the network algorithm for Fisher's Exact Test in 2xc contingency tables. Comput Stat Data Anal 51:490–498
16. Guehring T, Urban JP, Cui Z, Tirlapur UK (2008) Noninvasive 3D vital imaging and characterization of notochordal cells of the intervertebral disc by femtosecond near-infrared two-photon laser scanning microscopy and spatial-volume rendering. Microsc Res Technol 71:298–304
17. Hunter CJ, Matyas JR, Duncan NA (2003) The notochordal cell in the nucleus pulposus: a review in the context of tissue engineering. Tissue Eng 9:667–677

18. Weiler C, Nerlich A, Zipperer J, Bachmeier BE, Boos N (2002) 2002 SSE Award Competition in Basic Science: expression of major matrix metalloproteinases is associated with intervertebral disc degradation and resorption. Eur Spine J 11:308–320
19. Ortega N, Behonick D, Stickens D, Werb Z (2003) How proteases regulate bone morphogenesis. Ann N Y Acad Sci 995:109–116
20. Kim KW, Ha KY, Park JB, Woo YK, Chung HN, An HS (2005) Expression of membrane-type I matrix metalloproteinase, Ki-67 protein, and type II collagen by chondrocytes migrating from cartilage endplate into nucleus pulposus in rat intervertebral disc. Spine 30:1373–1378
21. Holmbeck K, Szabova L (2006) Aspects of extracellular matrix remodeling in development, disease. Birth Defects Res C Embryo Today 78:11–23
22. Murphy G, Knauper V, Atkinson S, Butler G, Hutton M, Starcke J et al (2002) Matrix metalloproteinases in arthritic disease. Arthritis Res 4(S3):39–49
23. Zhou Z, Apte SS, Soininen R, Cao R, Baaklini GY, Rause RW et al (2000) Impaired endochondral ossification and angiogenesis in mice deficient in membrane-type matrix metalloproteinase I. Proc Natl Acad Sci 97:4052–4057
24. Aguiar DJ, Johnson SL, Oegema TR (1999) Notochordal cells interact with nucleus pulposus cells: regulation of proteoglycan synthesis. Exp Cell Res 246:129–137
25. Kim KW, Ha KY, Lee JS, Nam SW, Woo YK, Lim TH et al (2009) Notochordal cells stimulate migration of cartilage endplate chondrocytes of the intervertebral disc in in vitro cell migration assays. Spine 9:323–329
26. Rutges J, Kummer J, Oner F, Verbout A, Castelein R, Roestenbrug H et al (2008) Increased MMP-2 activity during intervertebral disc degeneration is correlated to MMP-14 levels. J Pathol 214:523–530
27. Rogerson FM, Stanton H, East CJ, Golub SB, Tutolo L, Farmer PJ et al (2008) Evidence of a novel aggrecan-degrading activity in cartilage: studies of mice deficient in both ADAMTS-4 and ADAMTS-5. Arthritis Rheum 58:1664–1673

Supplement

Table 3.1: Characteristics of fetal and non-fetal IVD samples obtained at autopsy

Sample	Gender	Age of death	Diagnosis	Level
1	M	109 days after gestation	Prune belly sequence	Lumbar
2	F	112 days after gestation	Trisomy 21	Lumbar
3	M	133 days after gestation	Mosaic trisomy 9 and Pierre-Robin sequence	Lumbar
4	F	149 days after gestation	Trisomy 9	Lumbar
5	F	150 days after gestation	Tharacic-lumbar menigomyelocele	Lumbar
6	M	151 days after gestation	Bicuspid aorta valve	Lumbar
7	M	153 days after gestation	Unknown, no syndrome diagnosis.	Lumbar
Group 15-22 weeks (N=7)		137 days after gestation (mean)		
8	M	161 days after gestation	Hydrocephalus and possibly Vater syndrome	Lumbar
9	F	161 days after gestation	Bardet-Biedl syndrome	Lumbar
10	M	167 days after gestation	Deletion chromosome 15	Lumbar
11	F	170 days after gestation	Chorioamnionitis and funiculitis	Lumbar
12	M	189 days after gestation	Placental pathology	Lumbar
13	M	196 days after gestation	Unknown, no syndrome diagnosis	Lumbar
Group 22-30 weeks (N=6)		174 days after gestation (mean)		
14	F	214 days after gestation	Miller Dietz syndrome	Lumbar
15	M	280 days after gestation	Cerebral infarction, cause unknown	Lumbar
16	M	282 days after gestation	Hypoxia / Ischemia, cause unknown	Lumbar
Group 30-41 weeks (N=3)		259 days after gestation (mean)		
17	F	3.3 years	Aritmia, possible cause: myocarditis	Lumbar, L4-L5
18	F	6.4 years	Aritmia, possible cause: PTLD	Lumbar, L4-L5
19	F	14.2 years	Aritmia, AV node pathology	Lumbar, L4-L5
20	M	17.7 years	Neurological trauma	Lumbar, L4-L5
21	F	21.8 years	Aritmia, myocardial failure after infarction	Lumbar, L4-L5
Group 0-22 years (N=5)		12.7 years (mean)		

Materials & Methods:

Reagents and antibodies

Complete protease inhibitor cocktail was obtained from Roche (Mannheim, Germany), porcine skin type A gelatin (B0149-25G) was obtained from Sigma (St. Louis, MO). Antibodies used in this study and the applied immunhistochemical staining procedure are described in table 3.2. Mouse and rabbit isotype controls were purchased from Dako (Glostrup Denmark). Hyaluronidase (H2126) and pronase (10165921001) were obtained from respectively Sigma (St. Louis, MO) and Roche (Mannheim, Germany).

Table 3.2: Used antibodies and staining procedures.

Primary AB	Manufacturer	Concentration	Secondary AB	Manufacturer	Antigen retrieval
MMP-1 (RB-1536)	Neomarkers	5 µ/ml	Powervision Goat anti Rabbit	Labvision	None
MMP-2 (MS-806)	Neomarkers	2 µ/ml	Powervision Goat anti mouse	Labvision	None
MMP-3 (MS-810)	Neomarkers	2 µ/ml	Powervision Goat anti mouse	Labvision	None
MMP-14 (AB 815)	Chemicon	4 µ/ml	Powervision Goat anti Rabbit	Labvision	None
Collagen type II (II-II6B3)	DSHB	1:100*	Goat anti mouse HRP: P0-447	Dako	0.1% Pronasse and 1.0% Hyaluronidase
EMA (M 613)	Dako	0.22 µ/ml	Horse anti mouse biotin: BA2000	Vector	None
CK AE1/AE3 (MS-343)	Neomarkers	2 µ/ml	Horse anti mouse biotin: BA2000	Vector	95°C 10 mM Citrate buffer pH 6.0

* = Concentration of the antibody was not described by the manufacturer. AB = antibody

Protein extraction

Protein extraction was performed at 4°C. Approximately 0.02 g of IVD tissue, containing both annulus fibrosus (AF) and NP, combined with zirconium beads of 0.7 mm diameter (Biospec, Bartlesville, Oklahoma) and 0.80 ml Milli Q. Samples were mechanically disrupted for 2 minutes with a mini Beadbeater (Biospec, Bartlesville, Oklahoma, USA). Concentrated lysis buffer was added to a final concentration of 0.5% sodium deoxycholate, 0.1% Triton-X100, 0.1% SDS and Complete protease inhibitor cocktail (Roche, Mannheim Germany), according to the manufacturer's instructions. Samples were gently mixed for 20 hours at 4°C

and centrifuged for 15 minutes at 16000g at 4°C. Protein content of the supernatant was assessed by BCA protein analysis (Pierce Rockford, Illinois).

Histology

Non-fetal IVD slices were decalcified in 50% formic acid and 68 g/l sodium formiate in a microwave oven at 50°C for 6 hours[1]. Fetal IVD samples were sectioned without prior decalcification. Immunohistochemical staining of decalcified and non-decalcified samples were evaluated and showed no differences in immunohistochemical staining for the used antibodies . The samples were dehydrated in graded alcohol series, rinsed in xylene, embedded in paraffin and cut to five µm thin sections. General morphology, proteoglycan and collagen distribution were analyzed by alcian blue/ picrosirius red staining[2].

Results

Histology

Histology showed clear differences between fetal and non-fetal IVDs. Fetal IVDs showed more vascularisation (figure 3.5A, 3.5C, arrows) and staining for proteoglycans seemed more intense (blue staining figure 3.5C vs Figure 3.5D). Less notochordal cells (NC, arrows in Sup fig2) were seen in the non-fetal IVDs as compared to the fetal discs (figure 3.6A vs 3.6B). The IVDs from the 17.7 and 21.8 year old patient did not contain any NC cells at all. The NC cells in both the fetal and the non-fetal IVDs were arranged in clusters and were surrounded by ECM. Although the ECM surrounding the NC cells contained some proteoglycans, the ECM surrounding chondrocyte-like NP cells appeared to contain much more proteoglycans (figure 3.6C vs figure 3.6D). The NC cell clusters appeared to be separated from the chondrocyte-like nucleus pulposus cells by a fibrous sheet at least partially consisting of collagen type II (indicated by the asterisks in figure 3.6E, 3.6F). The ECM outside the territorial matrix of the NC cell clusters stained less intensive for collagen type II than the chondrocyte-like NP cells (figure 3.6E vs figure 3.6F).

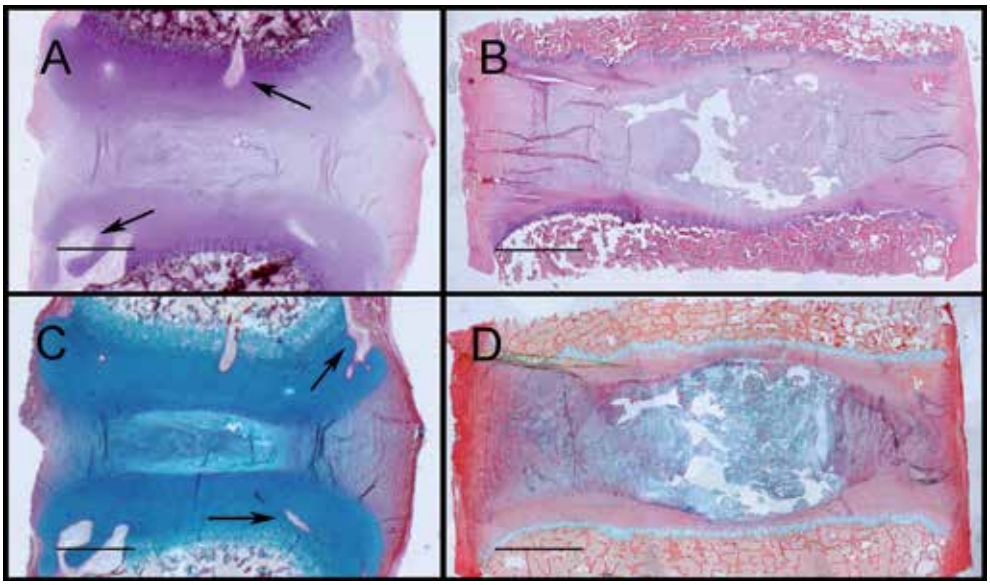

Figure 3.5. Fetal (A, C) and non-fetal IVDs (B, D) IVDs. Haematoxylin eosin (A, B) and alcian blue/picrosirius red staining (C, D). Tears in non-fetal IVDs (C,D) were caused by dehydration of the highly hydrated nucleus pulposus Scale bars represent: A, C: 1 mm and B, D: 5 mm. Arrows indicate blood vessels. Acian blue/ picrosirius red staining yields a blue staining of proteogycans, while collagen type I and II in the annulus fibrosus and in the nucleus pulposus show up red[2].

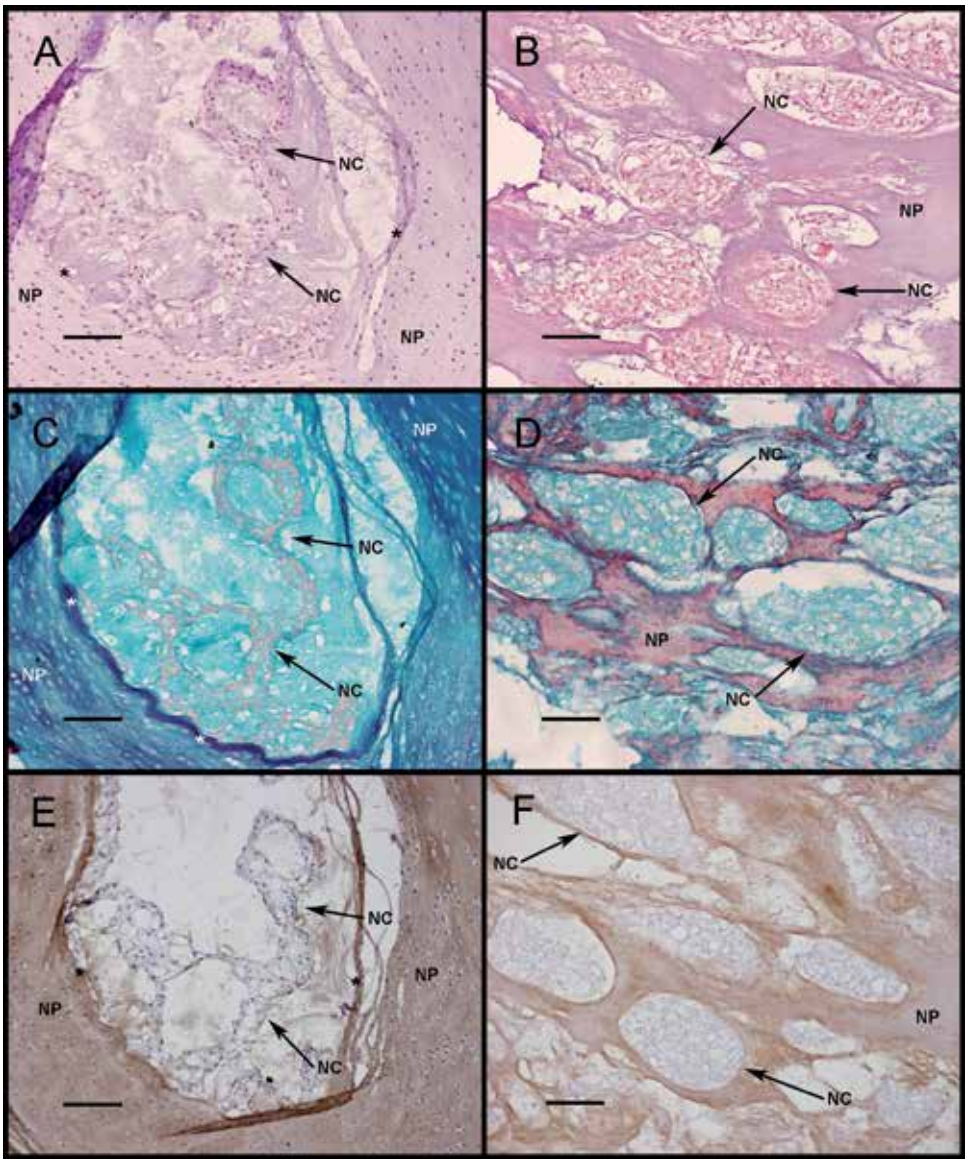

Figure 3.6. Notochordal cells in fetal (A, C, E) and non-fetal (B, D, F) IVDs. Haematoxylin eosin (A, B), alcian blue/picrosirius red staining (C, D) and immunohistochemical staining of collagen type II (E, F). Arrows accompanied by "NC" indicate clusters of notochordal cells and "NP" indicates the nucleus pulposus surrounding the NC cells. Asterisks indicate the fibrous sheet separating the NC cell clusters and the chondrocyte-like NP cells. Scale bars represent: 100 µm.

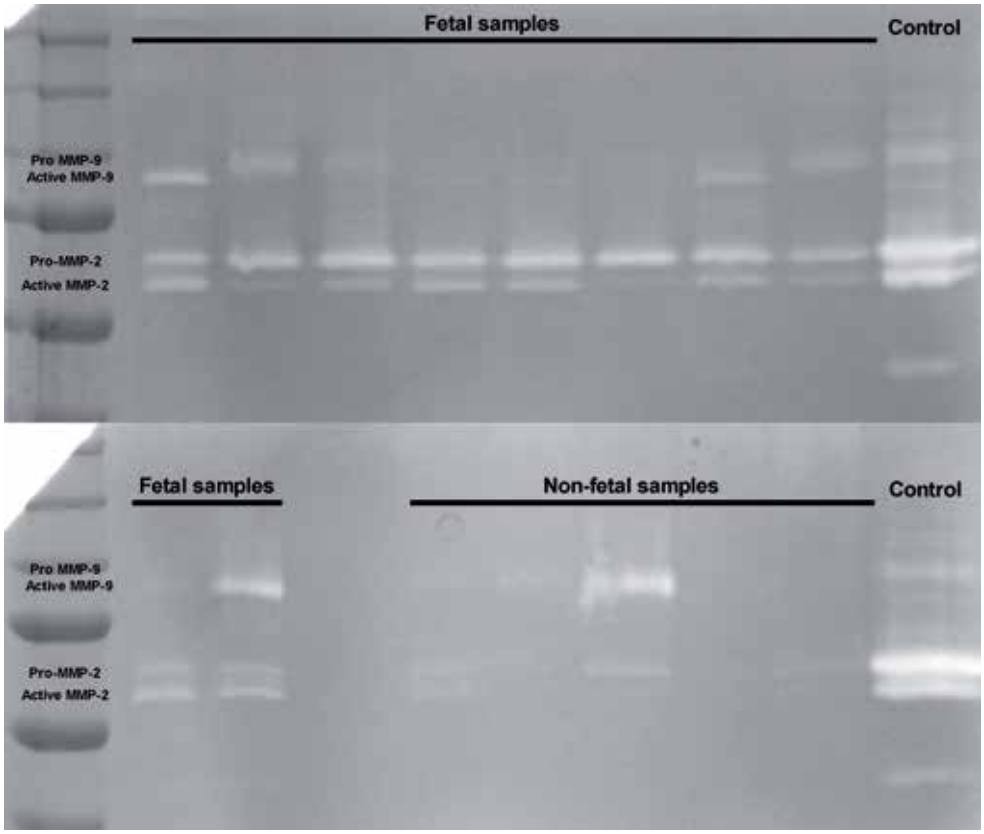

Figure 3.7. Gelatin zymgrams of both fetal and non-fetal samples showing the presence of active and pro-MMP-2. A degenerative IVD of a 88 year old patient, known to be positive for MMP-2, was used as control.

References

1 Kristensen HK. (1948) An improved method of decalcification. Stain Technol 23: 151-154

2 Gruber HE, Ingram J, Hanley EN Jr (2002) An improved staining method for intervertebral disc tissue. Biotech Histochem 77: 81-83.

CHAPTER 4

Micro-CT quantification of subchondral endplate changes in intervertebral disc degeneration

JPHJ Rutges, OP van der Jagt, FC Oner, AJ Verbout, RJM Castelein, JA Kummer, H Weinans, LB Creemers and WJA Dhert

Osteoarthritis and Cartilage (2011) 19:89–95

Abstract

The intervertebral disc (IVD) is dependent on nutrient provision through a cartilage layer with underlying subchondral bone, analogous to joint cartilage. In the joint, subchondral bone remodelling has been associated with osteoarthritis (OA) progression due to compromised nutrient and gas diffusion and reduced structural support of the overlaying cartilage. However, subchondral bone changes in IVD degeneration have never been quantified before.

The aim of this study is to determine the subchondral bone changes at different stages of IVD degeneration by micro-CT.

Twenty-seven IVDs including the adjacent vertebral endplates were obtained at autopsy. Mid-sagittal slices, graded according the Thompson score, were scanned. Per scan 12 standardized cylindrical volumes of interest (VOI) were selected. Six VOIs contained the bony endplate and trabeculae (endplate VOIs) and six accompanying VOIs only contained trabecular bone (vertebral VOIs). Bone volume as percentage of the total volume (BV/TV) of the VOI, trabecular thickness (TrTh) and connectivity density (CD) were determined. An increase in BV/TV and TrTh was found in endplate VOIs of IVDs with higher Thompson score whereas these values remained stable or decreased in the vertebral VOIs.

The increase in bone volume combined with the increase in TrTh in endplate VOIs strongly suggest that the subchondral endplate condenses to a more dense structure in degenerated IVDs. This may negatively influence the diffusion and nutrition of the IVD. The endplate differences between intact and mild degenerative IVDs (grade II) indicate an early association of subchondral endplate changes with IVD degeneration.

Introduction

Osteoarthritis (OA) and intervertebral disc (IVD) degeneration are the most common degenerative diseases of the musculoskeletal system. The extracellular matrix of both articular cartilage and the IVD mainly consists of collagen type II, and proteoglycans. Degeneration of their extracellular matrix is biochemically very similar and characterized by degradation through matrix metalloproteinases (MMPs) and ADAMTSs (a disintegrin and metalloproteinase with thrombospondin motifs)[1,2]. Similarity is also seen in clinical and radiological presentation of these diseases. Pain is the most imported clinical sign and radiological hallmarks are decreased joint space/disc height, osteophyte formation and subchondral sclerosis.

A particular hallmark of OA is the subchondral bone changes, including thickening of the subchondral plate, increased stiffness of subchondral bone and an increased bone turnover[3-6]. Thickening of the subchondral bone in OA is thought to negatively influence the nutrition of cartilage by limiting the diffusion of nutrients through the endplate[7,8]. Moreover, increased stiffness of the subchondral plate has been suggested to be an initiating factor in OA by increase of shear stresses in the overlaying cartilage and subsequent induction of degeneration[9,10].

Also in the IVD, calcification of the cartilage endplate and subchondral bone changes are frequently observed. Endplate sclerosis is a radiological hallmark of IVD degeneration and is commonly seen on Radiographs of degenerative IVDs[11,12]. Permeability of subchondral bone is decreased in degenerative IVDs and as nutrients are supplied to the IVD by diffusion, primarily from vessels in the subchondral bone and to a limited extent from peripheral blood vessels in the annulus fibrosus, the degenerative changes may be related to the decreased nutrition in the degenerative IVD[11-14].

However, little is known about the exact nature of the changes occurring in the subchondral endplate during IVD degeneration. Moreover, for a causative role in IVD degeneration, subchondral changes should already be present in IVDs at an early degeneration stage, which usually do not induce clinical symptoms and therefore have hitherto not been studied. Therefore the aim of this study is to quantify the subchondral bone changes occurring during IVD degeneration by micro-computed tomography (micro-CT) analysis of a set of IVDs spanning the full range of Thompson degeneration grades.

Materials and methods

Sample acquisition

IVDs were obtained during a standard post-mortem procedure in which the lumbar spine is partly removed for diagnostic purposes. IVDs were obtained within 48 h of death (average 18.6 h). During the post-mortem delay, bodies were kept at 4°C in the mortuary. Patients with skeletal disorders, e.g., evident scoliosis or metastatic disease affecting skeletal tissues, were excluded from this study. Cardiovascular disease was the most common cause of death. From all patients, the IVD between fourth and fifth lumbar vertebrae (L4-L5), including the vertebrae and adjacent endplates, was obtained. After resection, the discs were sawed in sagittal samples. Of each IVD a mid-sagittal sample was fixed and stored in 4% formalin and graded according to the Thompson degeneration score by three individual observers (FO, LC and JR)[15]. IVDs from 27 deceased patients (mean age 53.7 years, range 3.3-90.8 years) with an even distribution of the Thompson

degeneration grades were selected for this study (table 4.1). The formalin-fixed mid-sagittal samples were used for micro-CT analysis (figure 4.1).

The scientific committee from the Department of Pathology of our institution approved the study. IVDs were stored in the tissue bank of the Department of Pathology/Biobank, and were used in line with the code "Proper Secondary Use of Human Tissue" as installed by the Federation of Biomedical Scientific Societies[16].

Thompson grade	N	Male / Female	Mean age (yrs)	Range
I	5	20% / 80%	12.7	3.3 – 21.8
II	5	80% / 20%	41.7	17.0 – 60.0
III	7	86% / 14%	71.0	56.0 – 78.9
IV	6	67% / 33%	63.0	23.8 – 79.8
V	4	25% / 75%	75.9	57.4 – 90.8
Total	27	59% / 41%	53.7	3.3 – 90.8

Table 4.1. Number of samples and patient characteristics for each group, stratified according the Thompson score

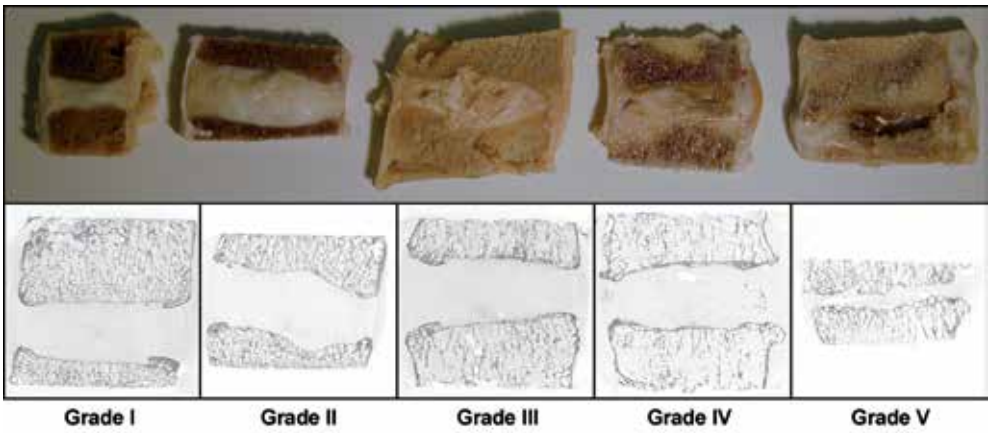

Figure 4.1. Example of macroscopical appearance and micro-CT images of IVDs for each degeneration grade according to the Thompson score.

Micro-CT

The mid-sagittal sections were scanned using a micro-CT scanner (Skyscan 1076, Skyscan, Kontich, Belgium). A scan of 180 degrees was made at a voltage of 60 kV and a current of 167 µA using a 0.5 aluminum filter and an exposure time of 4.4 s. Three-dimensional (3D) reconstructions were created using NRecon (NRecon software version 1.5, Skyscan, Belgium). The reconstructed datasets had a voxel size of 17.8 µm. In the reconstructed datasets, six pairs of cylindrical volume of interests (VOIs) were selected (figure 4.2).

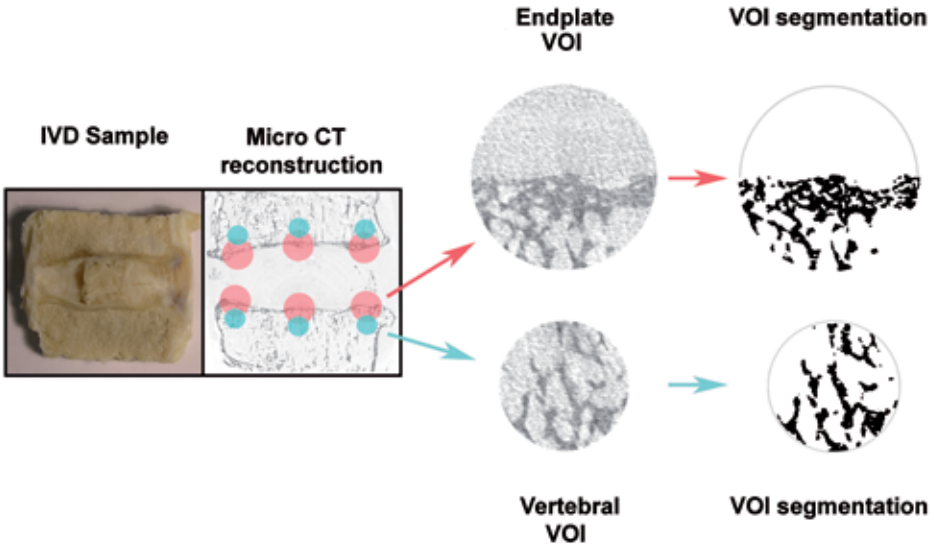

Figure 4.2. Schematic overview of study procedure: micro-CT, VOI selection, and segmentation.

First, six VOIs were placed at the anterior, the posterior and the center of the cranial and caudal endplate. Osteophytes and calcifications of the cartilaginous growth plate were not included in the VOIs. The cylinders were placed in such way that the center of circle was put exactly on top of the endplate and therefore only half of the VOI contains bony structures (21 mm^3 of 42 mm^3). The diameter of the cylinder was 5.4 mm and the length was 1.8 mm. The thinnest mid-sagittal sample of the analyzed IVDs was 1.8 mm thick and therefore a cylinder length of 1.8 mm was used for every sample. In thicker samples the cylinder is placed in the center of the sample. The VOIs at the endplate are referred to as 'endplate VOIs' and contain both the bony endplate and the subchondral trabeculae. To be able to assess the endplate specifically, a 'vertebral VOI' was selected in parallel to each endplate VOI. The center of the cylindrical VOI was placed in the trabecular bone 3.15 mm from the center of the cylinder of its subsequent endplate VOI. Although there was an overlap of 1.4 mm between the endplate and vertebral VOI, the vertebral VOI never contained endplate bone. To get the same volume of bony structures as in the endplate VOIs, a diameter of 3.9 mm was used for the vertebral VOI, resulting in a volume of 21 mm^3. In contrast to the endplate VOI, the vertebral VOI only contained trabecular bone, which enables the assessment of the endplate by comparing the morphometric parameters of both VOIs.

To analyze the bony structures, binary datasets of each VOI was made using a local threshold algorithm (3D Calculator software freely available at http://www.erasmusmc.nl/orthopaedie/research/klinres)[17]. In each VOI, the bone architecture was characterized by determining the bone volume fraction, bone volume over total volume (BV/TV). Since bone is present in only the half of the endplate plate VOIs the total volume was

divided by two. Furthermore the 3D trabecular thickness and connectivity density (CD) were determined. Although subchondral endplate microfractures have been described in degenerative IVDs, no endplate or spongy bone fractures were observed in the VOIs of the degenerative IVDs[14].

Statistics

Statistical differences between endplate and accompanying vertebral VOIs from the same degeneration grade were analyzed by paired T-tests. Differences between degeneration grades and the three regions of the IVD (anterior, central and posterior) were determined by analysis of variance (ANOVA) followed by Bonferroni correction. Mean BV/TV, TrTh and CD were calculated from the data from all the three regions of the IVD (anterior, central and posterior). Statistical analysis was performed with SPSS 16.0 software (SPSS Inc, Chicago United States of America).

Results

Bone volume fraction

Bone volume fractions (BV/TV) in the vertebral VOIs (not containing any endplate material) varied slightly between the samples (range 8-12%), without significant differences between the different degenerative grades. The BV/TV in the endplate VOI ranged from 20% to 30%. Grade II, III and V IVDs showed a significantly higher BV/TV in the endplate VOIs compared to the grade I VOIs (P=0.003, P=0.004 and P=0.019, respectively) (figure 4.3A). The difference in BV/TV between the endplate and vertebral VOIs was significantly increased in degeneration grade II-V in comparison to healthy grade I IVDs (P= 0.004, P< 0.0001, P= 0.008 and P= 0.013 respectively), indicating a relatively thick endplate (figure 4.3B).

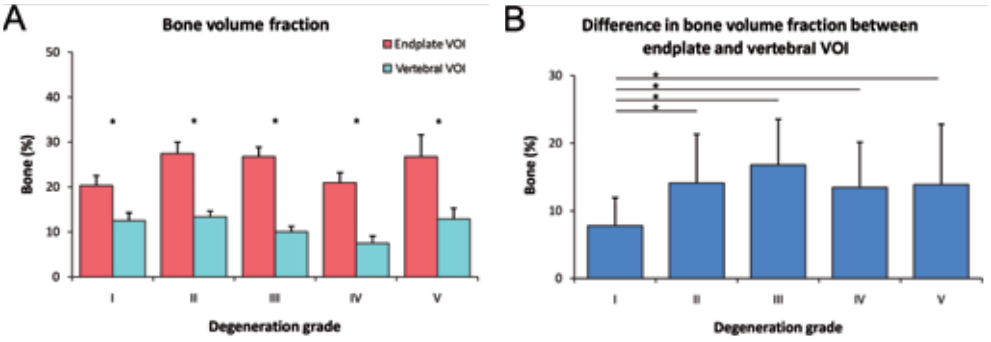

Figure 4.3. Bone volume fraction for endplate and vertebral VOIs for each degeneration grade (A). Difference in bone volume fraction between endplate and vertebral VOIs for each degeneration grade. Grade II, III and V IVDs showed a significantly higher BV/TV in the endplate VOIs compared to the grade I VOIs (B). Error bars represent 95% confidence intervals. Grade I: N = 5, II: N = 5, III: N = 7, IV: N = 6 and grade V: N = 4. * P < 0.05.

Bone volume fraction in endplate and vertebral VOIs per region

BV/TV in the vertebral VOIs ranged from 9.8% to 11.6% and no statistically significant differences were found between anterior, center or posterior regions of the endplate. In the endplate VOIs BV/TV ranged from 16.3% to 31.7%. A significantly higher BV/TV in the anterior VOIs in comparison to the center VOIs was found in grade III and IV IVDs (P= 0.023 and P= 0.013 respectively). A higher BV/TV in comparison to the center VOIs was also found in the posterior VOIs in grade IV and V (P= 0.030 and P= 0.039 respectively) (table 4.2). A statistically significantly higher BV/TV in the anterior endplate VOIs in comparison to the center VOIs was found in grade III and IV IVDs. A statistically significant higher BV/TV in comparison to the center VOIs was also found in the posterior endplate VOIs in grade IV and V. In the vertebral VOIs no statistically significant differences were found between anterior, center or posterior regions of the endplate. * P <0.05.

Table 4.2. Endplate VOI bone volume fraction (BV/TV) per endplate region (anterior, center and posterior) for each degeneration grade

Thompson grade	BV/TV					
Endplate VOI	**Anterior**	**95% CI**	**Center**	**95% CI**	**Posterior**	**95% CI**
I N = 5	21.2	15.4 - 27.0	20.7	16.4 - 25.0	18.9	16.1 - 21.7
II N = 5	27.9	21.7 - 34.2	26.1	22.4 - 29.8	28.3	23.8 - 32.8
III N = 7	30.1*	26.6 - 33.5	23.3*	20.8 - 25.8	26.7	22.2 - 31.2
IV N = 6	23.7*	19.7 - 27.4	16.3*	12.4 - 20.2	22.9*	19.3 - 26.4
V N = 4	30.5	18.9 - 42.0	18.0*	12.0 - 24.0	31.7*	25.1 - 38.4
	BV/TV					
Vertebral VOI	**Anterior**	**95% CI**	**Center**	**95% CI**	**Posterior**	**95% CI**
I N = 5	11.6	8.2 - 15.1	13.6	9.3 - 17.9	12.3	9.9 -14.7
II N = 5	14.5	12.5 - 16.4	11.9	8.9 - 14.9	13.6	11.5 - 15.8
III N = 7	10.3	8.5 - 12.1	8.2	7.0 - 9.5	11.4	8.3 - 14.4
IV N = 6	8.1	5.6 - 10.6	6.5	3.4 - 9.6	7.8	4.5 - 11.1
V N = 4	15.6	10.3 - 20.8	9.7	6.4 - 12.0	13.4	8.6 - 18.1

A significantly higher BV/TV in the anterior endplate VOIs in comparison to the center VOIs was found in grade III and IV IVDs (p = 0.023 and p = 0.013 respectively). A higher BV/TV in comparison to the center VOIs was also found in the posterior endplate VOIs in grade IV and V (p = 0.030 and p = 0.039 respectively). In the vertebral VOIs no statistically significant differences were found between anterior, center or posterior regions of the endplate. * = p < 0.05.

Trabecular thickness

The TrTh measured in the vertebral VOIs was not significantly different between the degeneration grades and was approximately 150 µm for all IVDs. Mean TrTh in the endplate VOI was in the range of 150 to 250 µm. The grade I endplate VOIs were 150 µm, indicating that the trabeculae in the endplate of these healthy discs are similar to the trabeculae in the vertebral body. Grade II-V endplate TrTh showed higher values, 200-250 µm, compared to grade I endplates (P= <0.0001, P <0.0001, P= 0.006 and P= 0.0001 respectively for grade II till V). Additionally, in grade II, III and IV IVDs, an increase in difference in TrTh between endplate en vertebral VOIs was found in comparison to grade I IVDs (P < 0.0001, P< 0.0001, and P= 0.002 respectively) (table 4.3).

Table 4. 3. Trabecular thickness (TrTh) and Connectivity density (CD) for endplate and vertebral VOIs for each degeneration grade.

Thompson grade	TrTh		CD	
Endplate VOI	**Endplate VOI**	**95% CI**	**Endplate VOI**	**95% CI**
I N = 5	150.7*	144.1 - 157.3	19.6*	16.8 - 22.4
II N = 5	235.4*	212.8 - 257.9	10.4*	8.2 -12.5
III N = 7	209.5*	194.2 - 224.7	12.2*	10.6 - 13.9
IV N = 6	193.7*	179.4 - 208.1	13.5*	10.4 - 16.5
V N = 4	206.8*	183.2 - 230.4	15.7	11.0 - 20.4
	TrTh		**CD**	
Vertebral VOI	**Vertebral VOI**	**95% CI**	**Vertebral VOI**	**95% CI**
I N = 5	147.0	137.1 - 157.0	6.8*	5.7 - 7.9
II N = 5	165.6	150.8 - 180.4	5.2	4.4 - 6.1
III N = 7	149.5	135.1 - 163.8	3.7*	3.0 - 4.3
IV N = 6	140.4	133.2 - 147.7	4.1*	2.5 - 5.7
V N = 4	164.3	148.3 - 180.4	5.4	4.1 - 6.6

In Grade II to V endplate VOIs TrTh was significantly higher when compared to grade I endplates , p = < 0.001, p < 0.001, p = 0.006 and p = 0.001 respectively for grade II till V. In the vertebral VOIs no statistically significant differences in TrTh were found. In the endplate VOIs a statistically significant lower CD was found in grade II, III and IV IVDs in comparison to grade I IVDs, p = < 0.001, p = 0.001 and p = 0.005 respectively. Statistically significant lower CD levels were found in grade III and IV vertebral VOIs compared to grade I VOIs, p < 0.001 and p = 0.006 respectively. * = p < 0.05

Connectivity density

Mean CD in the vertebral VOIs ranged from 3.5 to 7.0 Conn/mm3, and 10 to 20 CD in the endplate VOIs. CD in the vertebral VOIs appeared quite stable, although significantly lower CD levels were found in grade III and IV vertebral VOIs compared to grade I VOIs (P <0.0001 and P =0.006 respectively). In the endplate VOIs a significant lower CD was found in grade II, III and IV IVDs in comparison to healthy grade I IVDs (P =< 0.0001, P = 0.001 and P= 0.005 respectively) (table 4.3).

Discussion

This study shows that the architecture of the subchondral endplate differs at different stages of IVD degeneration. We suggest that these differences represent changes in time with subsequent stages of IVD degeneration and are initiated already at a relatively early stage in the disease process, since stage II IVDs already significantly differ from stage I IVDs. Quantification of these changes showed an increase in bone volume and TrTh in the endplate during degeneration. Moreover, the bone volume was found to be increased specifically in the anterior and posterior regions of the endplate of degenerative discs. Connectivity was relatively constant in the vertebral VOIs and was slightly decreased in the endplates of grade II, III and IV discs. Significantly higher bone volume, TrTh and CD were found in most of endplate VOIs compared to the matching vertebral VOIs. This is in line with calcification of the cartilage endplate and sclerosis in aging and degenerative discs reported before[18-21]. However the current study is the first to quantify the subchondral bone changes in a set of IVDs spanning the full range of Thompson degeneration grades.

The clear increase in bone volume and TrTh during IVD degeneration in the current study is similar to the subchondral changes observed in human OA[22-26]. However, micro-CT analysis of joints in animal models of OA showed a consistent decrease in bone volume and TrTh[27-30]. This possibly indicates that the changes found in animals are part of the early stages of OA, which cannot be observed in humans since patients are still asymptomatic at this stage.

However, in the current study the earliest stage of IVD degeneration (grade II) showed an increase rather than a decrease in bone volume or TrTh. This may suggest that OA does not in all aspects etiologically resemble IVD degeneration. Micro-CT techniques have been used in two animal models for IVD degeneration[31,32]. Unfortunately bone volume and TrTh were not determined and only roughening and pitting of the endplate surface was described[31,32].

Surprisingly, no osteoporotic changes in bone volume were found in the vertebral bodies adjacent to the grade V discs, despite the fact that these samples were mostly derived from older and mainly female patients. This phenomenon may be related to the changed mechanical loading in the degenerative IVD. In end stage IVD degeneration, the entire IVD is replaced by nonfunctional fibrous scar tissue. Compressive forces in grade V discs are mainly guided along the large osteophytes growing from the vertebral bodies, thereby indirectly increasing the load on the bone of the vertebral bodies and thereby enhancing bone formation[33]. In addition we have observed a gradual increase in osteoprotegerin (OPG) levels in the IVD during degeneration (Rutges et al, Osteoarthritis Cartilage 2010, chapter 5), which in grade V discs, in combination with the increased permeability of the endplate at this stage, may further have increased vertebral bone density, CD was decreased between grade I and II IVDs, but not at later stages of degeneration. In human proximal tibiae with early OA, CD of the subchondral plate was found to be decreased, most likely as a result of increased bone remodelling[26]. Connectivity in later stages of OA has not yet been evaluated.

It is not clear which mechanism underlies the observed subchondral bone changes in IVD degeneration nor whether subchondral bone changes cause degeneration of the extracellular matrix of the IVD or vice versa. The early onset of bone changes found in the endplate could indicate that these changes may be instrumental in the initiation or progression of IVD degeneration. In OA, subchondral bone changes have been found to coincide with or even precede cartilage destruction [10,34-36]. However, as the imaging methods used were not able to detect micro-damage to the cartilage, it cannot be excluded that degeneration had already started in the latter tissue. Alternatively, changes in the biomechanical environment of the joint, for example by a rupture of the anterior cruciate ligament may simultaneously affect both the articular cartilage and the subchondral bone[34,36].

One of the mechanisms postulated to be responsible for IVD degeneration is through diminished nutrition caused by endplate calcification and subchondral bone changes[14]. The plausibility of this hypothesis was recently shown in an animal model in which the permeability in the degenerative discs appeared to be correlated to a reduction in the bone marrow contact channel surface of the endplate in degenerated IVDs [32]. In humans the permeability of the cartilage endplate and the subchondral endplate is significantly lower in degenerative IVDs, which was shown by limited gadolinium diffusion as imaged by Magnetic Resonance Imaging (MRI), and high levels of lactic acid and concomitant low pH values in degenerative IVDs[14,37-40]. Additionally, in scoliotic spines, sclerosis of the endplate is found to be associated with limited diffusion in the IVDs[20,38,41]. In contrast, in end stage IVD degeneration, the endplate is thought to be more permeable due to loss of the endplate cartilage and an increased number of cracks and micro-fractures in the subchondral endplate. In the current study, a loss of bone volume, loss of TrTh and a more trabecular appearance were found in the more advanced stages of IVD degeneration, which is, however, not capable of restoring IVD tissue integrity.

In addition to diffusion and permeability of the IVD, vascularisation of the endplate is also essential for its nutrient supply. The blood supply of the IVD consists of capillaries penetrating the annulus fibrosus and more importantly a capillary bed which penetrates the subchondral endplate[14]. In degenerated IVDs, both the number and size of channels for the penetrating capillaries are reduced[14]. Changes in the vascularization of the degenerated IVD will most likely further enhance the effect of the limited diffusion and permeability. If bony alterations would really be at the basis of IVD degeneration, which cannot be proven by the cross-sectional design of this and other studies, it remains under debate whether biomechanical alterations or changes in nutrient diffusion are the major mechanism involved, as any change in trabecular morphology affecting diffusion is also likely to affect biomechanical properties. The notion that in particular moderate degeneration is accompanied by an increase in bone volume of the anterior and posterior regions rather than the central region, suggests a changed load distribution, with more load transfer in the outer zones of the degenerated disc and relative stress shielding in the center, as described before[33]. At least at this stage, degeneration of the nucleus pulposus reducing the force transmission in the central zone of the disc seems to be responsible for the observed changes and not vice versa. Moreover, assuming that the tissue

volume of the endplate that is not filled with bone is the portion of the endplate that capacitates diffusion, the changes found during degeneration were actually minor, with 80% of total volume taken up by tissue other than bone in healthy IVDs vs. 70% during degeneration. In contrast, biomechanical properties are determined by the bony portion of the endplate, for which more intense changes were found, up to 50% increase in bone volume, biomechanical changes may have played a more profound role than changes in diffusion. It would be interesting to investigate the biomechanical outcome in terms of endplate strength and elasticity of the combination of sharply increased TrTh and decreased connectivity in grade II discs. Of course, this cannot rule out as yet undetected changes in diffusivity of endplate cartilage which, rather than bony changes, may have played a role in inhibiting nutrient diffusion.

Conclusion

Subchondral bone changes are already observed as early as in grade II IVDs, indicating that subchondral endplate changes are associated with early development of IVD degeneration. The changed morphology of degenerative subchondral endplates could affect diffusion of nutrients, change biomechanical loading and enhance further degeneration of the IVD. However, from this data it cannot be concluded whether subchondral changes play an etiological role in the development of IVD degeneration or that these changes are due to biomechanical changes subsequent to the degeneration itself.

Acknowledgments

The authors acknowledge F. Bernhard and A. de Ruiter from the Department of Pathology from the UMCU Utrecht the Netherlands for their help in obtaining the IVD specimens. This study was supported by the Dutch Arthritis Association and the Anna Foundation. Statement of role of funding source in publication: The Dutch Arthritis Association and the Anna Foundation had no role in study design, collection, analysis and interpretation of data; in the writing of the manuscript; and in the decision to submit the manuscript for publication.

References

1. Bramono DS, Richmond JC, Weitzel PP, Kaplan DL, Altman GH. Matrix metalloproteinases and their clinical applications in orthopaedics. Clin Orthop Relat Res 2004;428:272-85.
2. Le Maitre CL, Pockert A, Buttle DJ, Freemont AJ, Hoyland JA. Matrix synthesis and degradation in human intervertebral disc degeneration. Biochem Soc Trans 2007;35:652-5.
3. Bailey AJ, Mansell JP, Sims TJ, Banse X. Biochemical and mechanical properties of subchondral bone in osteoarthritis. Biorheology 2004;41:349-58.
4. Grynpas MD, Alpert B, Katz I, Lieberman I, Pritzker KP. Subchondral bone in osteoarthritis. Calcif Tissue Int 1991;49: 20-6.
5. Day JS, Ding M, Van Der Linden JC, Hvid I, Sumner DR, Weinans H. A decreased subchondral trabecular bone tissue elastic modulus is associated with pre-arthritic cartilage damage. J Orthop Res 2001;19:914-8.
6. Karachalios T, KarantanasAH,Malizos K.Hip osteoarthritis:what the radiologist wants to know. Eur J Radiol 2007;63:36-48.
7. Malinin T, Ouellette EA. Articular cartilage nutrition is mediated by subchondral bone: a long-term autograft study in baboons. Osteoarthritis Cartilage 2000;8:483-91.
8. Zhou S, Cui Z, Urban JP. Factors influencing the oxygen concentration gradient from the synovial surface of articular cartilage to the cartilage-bone interface. Arthritis Rheum 2004;50:3915-24.
9. Radin EL, Paul IL, Rose RM. Role of mechanical factors in pathogenesis of primary osteoarthritis. Lancet 1972;1:519-22.
10. Radin EL, Rose RM. Role of subchondral bone in the initiation and progression of cartilage damage. Clin Orthop Relat Res 1986;213:34-40.
11. Bell GR, Ross JS. Imaging of the spine. In: Frymoyer JW, Wiesel SW, Eds. The adult & pediatric spine. 3rd edn. Philadelphia: Lippincott, Williams & Wilkins; 2004:69-86.
12. Burkus JK, Zdeblick TA. Lumbar disc disease. In: Frymoyer JW, Wiesel SW, Eds. The adult & pediatric spine. 3rd edn. Philadelphia: Lippincott, Williams & Wilkins; 2004:844-99.
13. Haefeli M, Kalberer F, Saefesser D, Nerlich AG, Boos N, Paesolf G. The course of macroscopic degeneration in the human lumbar intervertebral disc. Spine 2006;31:1522-31.
14. Urban JP, Smith S, Fairbank JC. Nutrition of the intervertebral disc. Spine 2004;29:2700-9.
15. Thompson JP, Pearce RH, Schechter MT, Adams ME, Tsang IKY, Bishop PB. Preliminary evaluation of a scheme for grading the gross morphology of the human intervertebral disc. Spine 1990;15:411-5.
16. Code for proper secondary use of humantissue in the Netherlands, http://www.federa.org/?s=1&m=82&p=0&v=4#827; 2002
17. Waarsing JH, Day JS, Weinans H. An improved segmentation method for in vivo microCT imaging. J Bone Miner Res 2004;19:1640-50.
18. Bernick S, Cailliet R. Vertebral end-plate changes with aging of human vertebrae. Spine 1982;7:97-102.
19. Resnick D. Degenerative diseases of the vertebral column. Radiology 1985;156:3-14.
20. Roberts S, Urban JP, Evans H, Eisenstein SM. Transport properties of the human cartilage endplate in relation to its composition and calcification. Spine 1996;21:415-20.
21. Roberts S, McCall IW, Menage J, Haddaway MJ, Eisenstein SM. Does the thickness of the vertebral subchondral bone reflect the composition of the intervertebral disc? Eur Spine J 1997;6:385-9.

22. Carlson CS, Loeser RF, Puser CB, Gardin JF, Jerome CP. Osteoarthritis in cynomolgus macaques. III: effects of age, gender, and subchondral bone thickness on the severity of disease. J Bone Miner Res 1996;11:1209-17.
23. Day JS, Van Der Linden JC, Bank RA, Ding M, Hvid I, Sumner DR, et al. Adaptation of subchondral bone in osteoarthritis. Biorheology 2004;41:359-68.
24. Dequeker J, Mokassa L, Aerssens J, Boonen S. Bone density and local growth factors in generalized osteoarthritis. Microsc Res Tech 1997;37:358-71.
25. Kamibayashi L, WySs UP, Cooke TD, Zee B. Trabecular microstructure in the medial condyle of the proximal tibia of patients with knee osteoarthritis. Bone 1995;17:27-35.
26. Ding M, Odgaard A, Hvid I. Changes in the three-dimensional microstructure of human tibial cancellous bone in early osteoarthritis. J Bone Joint Surg Br 2003;85:906-12.
27. Botter SM, van Osch GJ, Waarsing JH, Day JS, Verhaar JA, Pols HA, et al. Quantification of subchondral bone changes in a murine osteoarthritis model using micro-CT. Biorheology 2006;43:379-88.
28. Botter SM, van Osch GJ, Waarsing JH, van der Linden JC, Verhaar JA, Pols HA, et al. Cartilage damage pattern in relation to subchondral plate thickness in a collagenase-induced model of osteoarthritis. Osteoarthritis Cartilage 2008;16:506-14.
29. McErlain DD, Appletan CT, Litchfield RB, Pitelka V, Henry JL, Bernier SM, et al. Study of subchondral bone adaptations in a rodent surgical model of OA using in vivo micro-computed tomography. Osteoarthritis Cartilage 2008;16:458-69.
30. Sniekers YH, Intema F, Lafeber FP, van Osch GJ, van Leeuwen JP, Weinans H, et al. A role for subchondral bone changes in the process of osteoarthritis; a micro-CT study of two canine models. BMC Musculoskelet Disord 2008;9:1-11.
31. Gruber HE, Anshraf N, Kilburn J, Williams C, Norton HJ, Gordon BE, et al. Vertebral endplate architecture and vascularization: application of micro-computerized tomography, a vascular tracer, and immunocytochemistry in analyses of disc degeneration in the aging sand rat. Spine 2005;30: 2593-600.
32. Laffosse JM, Accadbled F, Molinier F, Bonnevialle N, de Gauzy JS, Swider P. Correlations between effective permeability and marrow contact channels surface of vertebral endplates. J Orthop Res 2010;28:1229-34.
33. Homminga J, Weinans H, Gowin W, Felsenberg D, Huiskes R. Osteoporosis changes the amount of vertebral trabecular bone at risk of fracture but not the vertebral load distribution. Spine 2001;26:1555-61.
34. Bailey AJ, Mansell JP. Do subchondral bone changes exacerbate or precede articular cartilage destruction in osteoarthritis of the elderly? Gerontology 1997;43:296-304.
35. Blummenkrantz G, Lindsey CT, Dunn TC, Jin H, RiesMD, Link TM, et al. A pilot, two-year longitudinal study of the interrelationship between trabecular bone and articular cartilage in the osteoarthritic knee. Osteoarthritis Cartilage 2004;12:977-1005.
36. Lindsey CT, Narasimhan A, Adolfo JM, Jin H, Steinbach LS, Link TM, et al. Magnetic resonance evaluation of the interrelationship between articular cartilage and trabecular bone of the osteoarthritic knee. Osteoarthritis Cartilage 2004;12:86-96.
37. Diamant B, Karlsson J, Nachemson A. Correlation between lactate levels and pH in discs of patients with lumbar rhizopathies. Experientia 1968;24:1159-96.
38. Kitano T, Zerwekh JE, Usui Y, Edwards ML, Flicker PL, Mooney V. Biochemical changes associated with the symptomatic human intervertebral disk. Clin Orthop Relat Res 1993;293:372-7.

39. Nachemson A, Lewin T,Marouda A, FreemanMA. In vitro diffusion of dye through the endplates and annulus fibrosus of human lumbar intervertebral discs. Acta Orthop Scand 1970;41:589-607.
40. Nguyen-minh C, Haughton VM, Papke RA, An H, Censky CS. Measuring diffusion of solutes into intervertebral disks with MR imaging and paramagnetic contrast medium. AJNR Am J Neuroradiol 1998;19:1781-4.
41. Urban MR, Fairbank JC, Etherington PJ, Loh L, Winclove CP, Urban JP. Electrochemical measurement of transport into scoliotic intervertebral discs in vivo using nitrous oxide as a tracer. Spine 2001;26:984-90.

CHAPTER 5

Hypertrophic differentiation and calcification during intervertebral disc degeneration

JPHJ Rutges, RA Duit, JA Kummer, FC Oner, MH van Rijen, AJ Verbout, RJM Castelein, WJA Dhert and LB Creemers

Osteoarthritis and Cartilage (2010) 18:1487–1495

Abstract

In degenerative intervertebral discs (IVDs) collagen type X expression and calcifications have been demonstrated, resembling advanced osteoarthritis (OA), which is associated with hypertrophic differentiation, characterized by the production of collagen type X, Runt-related transcription factor 2 (Runx2), osteoprotegerin (OPG), alkaline phosphatase (ALP) and calcifications.

The aim of this study was to determine if hypertrophic differentiation occurs during IVD degeneration. IVDs from all Thompson degeneration grades were prepared for histology, extraction of nucleus pulposus (NP) and annulus fibrosis (AF) tissue (N= 50) and micro-CT (N= 27). The presence of collagen type X, OPG and Runx2 was determined by immunohistochemistry, with OPG levels also determined by enzyme-linked immunosorbent assay (ELISA). The presence of calcification was determined by micro-CT, von Kossa and Alizarin Red staining.

Immunohistochemical staining for collagen type X, OPG, Runx2 appeared more intense in the NP of degenerative compared to healthy IVD samples. OPG levels correlated significantly with degeneration grade (NP: $P< 0.000$; AF: $P= 0.002$) and the number of microscopic calcifications (NP: $P= 0.002$; AF: $P= 0.008$). The extent of calcifications on micro-CT also correlated with degeneration grade (NP: $P< 0.001$, AF: $P= 0.001$) as did von Kossa staining (NP: $P= 0.015$, AF: $P= 0.016$). ALP staining was only incidentally seen in the transition zone of grades IV and V degenerated IVDs.

This study for the first time demonstrates that hypertrophic differentiation occurs during IVD degeneration, as shown by an increase in OPG levels, the presence of ALP activity, increased immunopositivity of Runx2 and collagen type X.

Introduction

Chronic low back pain is a common health problem in industrialized countries with high medical, insurance and disability costs[1]. Intervertebral disc (IVD) degeneration is considered to be a major cause of this disorder[2]. The IVD is a cartilaginous structure consisting of a gel-like core, the nucleus pulposus (NP), which is surrounded by a fibrous ring, the annulus fibrosis (AF)[2,3]. Although articular cartilage (AC) and the IVD morphologically appear to be very different structures, there are quite some similarities at the biochemical level3. The main constituents of the extracellular matrix (ECM) of the NP and AC are collagen type II and aggrecan. Additionally, both articular and meniscal cartilage and the IVD are essentially avascular tissues and nutrients mainly reach the cells by diffusion[4]. On the other hand, also clear differences are found, including a higher proteoglycan to collagen ratio in the NP compared to AC and differential expression levels of several proteins[2,5-7]. The similarities between AC and the IVD are not only limited to their physiology, but also include the pathological processes accompanying their degeneration. In both osteoarthritis (OA) and IVD degeneration, collagen II and aggrecan are degraded by several matrix degrading enzymes, including several matrix metalloproteinases (MMPs) and a disintegrin and metalloproteinase with thrombospondin motifs (ADAMTSs)[5,6,8-10]. Radiologically a narrowed joint/disc height, subchondral sclerosis and osteophytes are found. Moreover, the histological changes found in OA are similar to those found in the degenerating IVDs, with an increase in fibrous tissue, clefts and chondroid nests[5]. Advanced stages of OA are accompanied by hypertrophic differentiation, a process characterized by the induction of collagen type X, alkaline phosphatase (ALP) and eventually matrix calcification[11,12]. Runt-related transcription factor 2 (Runx2), a transcription factor essential in osteoblast differentiation and bone formation, is clearly upregulated during hypertrophic differentiation and is thought to be involved in the progression of OA[13,14]. Most of Runx2's downstream targets are found to be increased in OA, including collagen X, osteoprotegerin (OPG) and ALP. OPG is a glycoprotein that is secreted by osteoblastic cells and is a potent inhibitor of osteoclast differentiation and activation[15,16]. Increased levels of OPG have been found in osteoarthritic cartilage and more recently in synovial fluid and serum from patients with OA[17,18]. ALP is known to be involved in ECM mineralization during hypertrophic differentiation and endochondral ossification and is produced in OA chondrocytes[12,19,20]. Ultimately, hypertrophic differentiation in chondrocytes leads to matrix calcification, as seen in end stage OA and during endochondral ossification[12,21]. Despite the similarities found in the biochemistry of IVD degeneration and OA, only circumstantial data are available on the possible occurrence of hypertrophic differentiation in disc degeneration. Previous reports have described the presence of type X, MMP-13 and calcifications of the ECM in degenerative discs[22-26]. Also the presence of Runx2 and OPG has been found in degenerated or herniated human IVDs. However, these studies involved a small number of IVDs, without healthy grade I discs for comparison and thus could not definitively pinpoint a possible association between degeneration and the production of Runx2 and OPG[27,28]. ALP has until now only been described in a rabbit model of IVD degeneration[29].

Therefore the aim of this study is to determine the extent to which markers of hypertrophic differentiation are present in degenerative IVDs and whether calcification is associated with degeneration, by studying these processes in a collection of human IVDs of all degeneration stages.

Materials and methods

Reagents and antibodies

Rabbit polyclonal antibody anti-human Runx2 (SC-10758) was obtained from Santa Cruz biotechnology, (Santa Cruz, USA). Mouse monoclonal antibody anti-human OPG (MAB8051) was purchased from R&D systems (Minneapolis, USA). The mouse monoclonal antibody anti-human collagen type X, was a kind gift from Dr. Kwan (Cardiff University, Cardiff, Wales, United Kingdom)[26]. Mouse and rabbit isotype controls and polyclonal goat anti-rabbit/HRP (P0449) and polyclonal goat anti-mouse immunoglobulins/HRP (P0447) were purchased from Dako (Glostrup, Denmark). ALP activity was detected by a fuchsin substrate-chromogen system (K0624, DAKO, Glostrup Denmark). The recombinant protein, the capture and detection antibody for the OPG enzyme-linked immunosorbent assay (ELISA) were all obtained from R&D Systems (Minneapolis, USA, 185-OS, MAB8051 and BAF805 respectively).

Sample acquisition

The study was approved by the medical ethical committee of the University Medical Center Utrecht and the scientific committee from the Department of Pathology of the UMC Utrecht. Human IVD tissue was obtained as part of the standard post mortem procedure, inwhich a section of the lumbar and thoracic spine is removed for diagnostic purposes. Samples were obtained within 38 h after death of the patient (92% of the patients within 24 h). Between death and time of tissue collection, the deceased patients were kept at the mortuary at 4°C. In a previous study, it was shown that in tissue obtained by this procedure, activation of matrix degrading enzymes was not affected by a postmortem delay of up to 24 h[9]. From all patients, the IVD from the fourth and fifth lumbar vertebrae (L4-L5), including the adjacent endplates, was obtained. One grade I disc from a 25-year-old patient was not obtained at autopsy but from schwannoma resection. The grade of degeneration was macroscopically scored according Thompson et al. by three individual observers (JR, RD and LC)[30]. After individual scoring the score was averaged; outliers, i.e., more than one Thompson grade difference, were re-evaluated by the three observers at a consensus meeting (table 5.1).

Table 5.1. Patient characteristics.

A

Thompson grade	N	Gender		Mean age (years)	Range
		M	F		
I	10	4	**6**	17.7	3.3 – 34.2
II	10	7	**3**	45.7	17.0 – 69.3
III	10	6	**4**	62.3	46.9 – 76.4
IV	10	3	**7**	73.2	54.3 – 88.5
V	10	4	**6**	76.6	59.5 – 88.2
Total	50	24	**26**	55.1	3.3 – 88.5

B

Thompson grade	N	Gender		Mean age (years)	Range
		M	F		
I	5	1	**4**	12.7	3.3 – 21.8
II	5	4	**1**	41.7	17.0 – 60.0
III	7	6	**1**	71.0	56.0 – 78.9
IV	6	4	**2**	63.0	23.8 – 79.8
V	4	1	**3**	75.9	57.4 – 90.8
Total	27	16	11	53.7	3.3 – 90.8

Number of samples, gender and age for histology, immunohistochemistry and biochemistry per Thompson degeneration grade (A). Number of samples, gender and age for Micro-CT analysis per Thompson degeneration grade (B).

Localization of OPG, Runx2 and collagen type X by immunohistochemistry

Immunohistochemical staining was performed on decalcified paraffin sections. Peroxidase activity was blocked with 0.3% H_2O_2 in methanol for 10 min at room temperature (RT). Antigen retrieval was performed by pronase (0.1%, Roche) and hyaluronidase (1%, Sigma) in phosphate buffered saline (PBS) at 37°C for 30 min. A block step with PBS/bovine serum albumin (BSA) 5% was used for the OPG and collagen type X staining. In Runx2 staining blocking with 1% egg white in PBS for 15 min at RT was followed by incubation with 5% skim milk in phosphate buffered saline with 0.1% Tween (PBS-T) for 10 min at 4°C. Incubation with primary antibodies for OPG (5 µg/ml), Runx2 (0.2 µg/ml) and collagen type X (30 µg/ml) in PBS/BSA 5% was done overnight at 4°C. The secondary antibody in PBS/BSA 5% (5 µg/ml) was incubated for 1 h at RT followed by incubation with DAB. Sections were counterstained with Mayer's hematoxylin. Negative controls were incubated with isotype controls at the same IgG concentration as the primary antibody.

Protein extraction

Macroscopically, IVD tissue was divided into NP and AF. In one grade I (surgical sample) as well as in one grade V patient only NP tissue was acquired, since macroscopically no AF tissue could be identified. Tissues were embedded in Tissue Tek and from each NP or AF sample, 100 sections (7 µm) were cut with a cryomicrotome. Sections were collected, weighed after removal of the Tissue Tek and lysed in 0.5% sodium deoxycholate, 0.1% Triton X-100, 0.1% SDS and complete protease inhibitor cocktail (Roche, Mannheim Germany). Samples were gently mixed overnight at 4°C, followed by 15 min centrifugation at 16,000g at 4°C after which the supernatant was collected and stored at -20°C.

Quantification of OPG levels by ELISA

Human OPG levels were detected by multiplex ELISA. Recombinant OPG was reconstituted to a concentration of 5 mg/ml. Calibration curves from recombinant protein standards were prepared using two-fold dilution steps in serum diluents. 10 µl containing 1000 capture antibody-coupled microspheres (antibody coupling

concentration 200 µg/ml) was added to the standard, sample or blank, and incubated for 60 min. Next, 10 µl of biotinylated detection antibodies (0.5 µg/ul) was added to each well and incubated for an additional 60 min. Beads were washed with 1% BSA, 0.5% Tween 20 in PBS pH 7.4. After incubation for 10 min with 50 ng / well streptavidin R-phycoerythrin (BD Biosciences, San Diego CA, USA) and washing twice with 1% BSA, 0.5% Tween 20 in PBS pH 7.4, the fluorescence intensity of the beads was measured in a final volume of 100 ml High Performance ELISA-buffer (Sanquin, Amsterdam, the Netherlands). Measurements and data analysis were performed using the Bio-Plex system in combination with the Bio-Plex Manager software version 3.0 using five parametric curve fitting (Bio-Rad Laboratories, Hercules CA, USA). OPG levels were corrected to the wet weight lysed protein per sample.

Micro-CT experiments

Mid-sagittal IVD slices (2-4 mm thick) were scanned using a micro-computed tomography (micro-CT) scanner (Skyscan 1076, Skyscan, Kontich, Belgium). A scan of 180 degrees was made at a voltage of 60 kV and a current of 167 µA using a 0.5 aluminum filter and an exposure time of 4.4 seconds. Three-dimensional reconstructions were made using NRecon (NRecon software version 1.5, Skyscan, Belgium). Reconstructions were semi-quantitatively scored by two independent observers (JR and MR). In the endplate (EP), NP and AF multiple calcifications were graded ++, two clear calcifications +, one single calcification +/- and no calcifications were graded -. Scores were analyzed and differences between the observers were re-evaluated during a consensus meeting.

Histology: von Kossa, alizarin red, ALP and combined staining of NADH dehydrogenase, von Kossa and eosin

Von Kossa and alizarin red staining were performed on nondecalcified paraffin sections. For the von Kossa staining, the sections were placed in 1% silver nitrate under UV light for 20 min, washed in 5% sodium thiosulfate for 5 min and counterstained with Mayer's hematoxylin[31]. For alizarin red staining, sections were stained for 2 min in 2% alizarin red S, pH 4.0, and counterstained with Mayer's hematoxylin[32]. Blinded sections were graded by two independent observers (JR and RD). In the EP, NP and AF, intensive calcifications throughout the entire region were graded ++, two clear calcifications +, one single calcification +/- and no calcifications were graded -. The transition zone between the AF and the NP was scored as part of the NP, since the border between the transition zone and the AF was more easily determined than between the NP and the transition zone. Differences between the observers were re-evaluated during a consensus meeting. For 9% of the sections, more than one grade difference in calcification score between the observers was noted. For these sections an experienced pathologist (JK) independently scored the calcification grade. The ALP staining and the combined staining of nicotinamide adenine dinucleotide hydrogen (NADH) dehydrogenase with von Kossa and eosin were performed on frozen sections. The fuchsine substrate-chromogen system was used for staining of ALP activity according to the manufacturer's instructions. A combined NADH von Kossa staining was used to verify that calcifications occurred around viable cells as indicated by positive NADH staining, to exclude possible aspecific calcification by cell death. Sections were incubated in 0.1%

NADH in nitro blue tetrazolium solution, fixed in 10% formalin, followed by von Kossa staining and eosin staining.

Statistical analysis

Statistical analysis was performed with SPSS 16.0 software. Spearman's non-parametric test was used for correlation analyses. Differences between degeneration grades were analyzed by Kruskal-Wallis non-parametric one-way analysis of variance followed by non-parametric multiple comparison test and Bonferroni correction.

Results

Immunohistochemistry of Runx2, collagen type X and OPG

In non-degenerative discs, no staining for Runx2 was observed (figure 5.1C). A predominantly nuclear staining in both the NP and AF was seen in degenerative discs (figure 5.1A and 5.1B). Striking was the staining in the transition zone between the NP and the AF (figure 5.1B), as early as in grade III discs. In more degenerative IVDs, grades IV and V, Runx2 was also found in the NP and AF of the IVD. Collagen type X staining was found in the cytoplasm and the territorial matrix surrounding cells in the NP of degenerative discs from grades II to V. The matrix surrounding chondrocyte clusters in severely degenerated discs also showed a positive staining (figure 5.1D). This pattern, albeit apparently less intense, was also seen in the inner rim of the AF (figure 5.1E). In non-degenerative discs, some staining of NP cells was observed, however this seemed far less than in degenerative discs (figure 5.1F). Collagen type X staining of cells or matrix of the AF was not seen in non-degenerative discs. Immunohistochemical staining for OPG showed a cytoplasmic and ECM staining in the NP and transition zone between NP and AF in degenerative IVDs (figure 5.1G and 5.1H). This staining pattern seemed less intense in the AF. More ECM staining was observed near clefts and the transition zone between the AF and the vertebral body. In non-degenerative discs some positive cells were seen, however this seemed clearly less than in degenerative IVDs and no ECM staining was found (figure 5.1I).

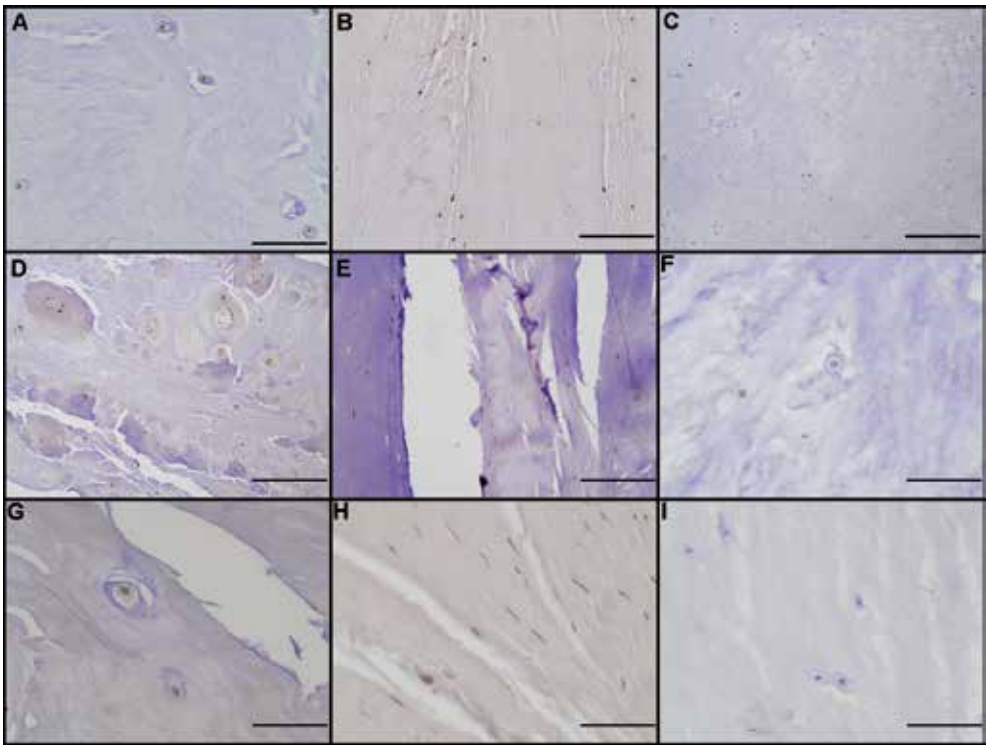

Figure 5.1. Immunohistochemical staining of Runx2 (A-C), collagen type X (D-F) and OPG (G-I). Runx2 staining in (A); the NP of a Thompson grade IV IVD, in (B); the transition zone from NP to AF of a Thompson grade IV IVD and (C); in a Thompson grade III non-degenerative IVD. Staining for collagen type X in (D); the NP of a Thompson grade V IVD, (E); the transition zone from NP to AF of a Thompson grade V IVD and (F); in a non-degenerative Thompson grade III IVD. Staining for OPG in (G); the NP of a Thompson grade IV IVD, (H); the transition zone from NP to AF of a Thompson grade V IVD and (I); in a non-degenerative grade I IVD. Scale bars indicate 100 µm in A and B, 500 µm in C and D, 200 µm in E and 50 µm in F-I.

OPG levels quantified by ELISA

Quantitative analysis of OPG showed a positive correlation between degeneration grade and OPG levels for both the NP and AF; (CC 0.563, P< 0.001 and CC 0.430, P= 0.002 respectively). Significant differences in NP OPG levels were found between several degeneration grades; (grades I vs III P= 0.02, grades I vs IV P= 0.03 and grades I vs V P = 0.002) (figure 5.2). A significant positive correlation between microscopic calcifications shown by the von Kossa staining and OPG levels was found both in the NP and AF, CC 0.420, P= 0.002 and CC 0.380, P= 0.008 respectively. No difference was found between OPG levels in NP and AF.

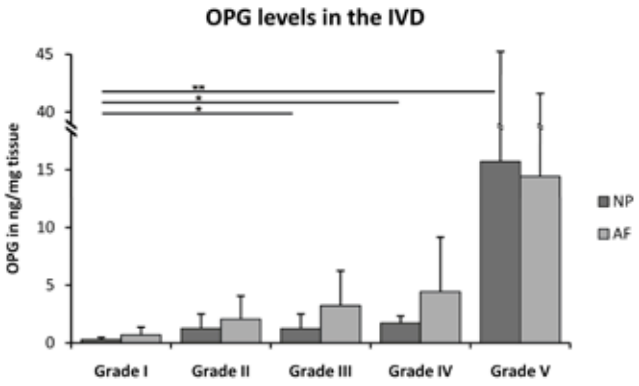

Figure 5.2. OPG levels for NP and AF per degeneration grade and age group. * = P < 0.05 and ** = P < 0.005. Error bars indicate the 95% confidence intervals.

Micro-CT analysis

Calcifications were found in both the AF and the NP of degenerative IVDs, especially near tears and clefts (figure 5.3). The extent of calcifications on micro-CT correlated significantly to degeneration grade for both the NP and the AF, (correlation coefficient (CC): 0.580, P = 0.002 and CC: 0.670, P < 0.001 respectively) (table 5.2). The youngest patient in which calcifications in the AF were observed was 17 years old (Thompson grade II). The youngest patient in which calcifications in the NP were found was 56 years old (Thompson grade III).

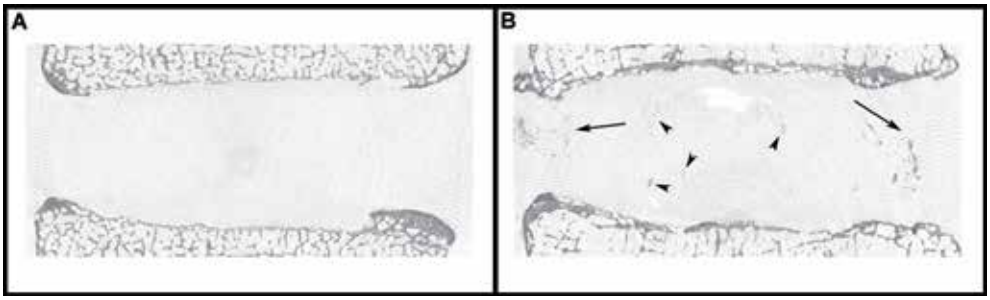

Figure 5.3. Micro-CT image of a Thompson grade I IVD (A) and of a grade IV IVD with calcification in both the AF (arrows) and NP (arrowheads) (B).

Table 5.2. Calcifications in the NP and AF per degeneration grade on micro-CT images

NP	Grade I (n=5)	Grade II (n=5)	Grade III (n=7)	Grade IV (n=6)	Grade V (n=4)
-	100%	100%	86%	67%	25%
+/-	0%	0%	14%	0%	0%
+	0%	0%	0%	33%	25%
++	0%	0%	0%	0%	50%
AF					
-	100%	60%	57%	17%	0%
+/-	0%	40%	29%	50%	50%
+	0%	0%	14%	0%	25%
++	0%	0%	0%	33%	25%

++: multiple intense calcifications, +: two or more clear calcifications, +/-: one single calcification, -: no calcifications.

Histology: von Kossa, alizarin red, ALP and combined staining of NADH dehydrogenase, von Kossa and eosin

Microscopic calcifications were demonstrated by alizarin red and von Kossa staining in the NP and AF of both non-degenerative and degenerative IVDs. No calcifications were found in the cartilage endplate of degenerative en non-degenerative discs. In non-degenerative discs, calcifications were found in the NP around remaining notochordal cells (age until 21 years) and the areas where these cells probably had been present earlier on (figure 5.4E and 5.4F); histologically, notochordal cells are easily recognized as large irregularly shaped cells containing vesicle-like structures, usually organized in cell clusters[33]. In a recent publication on fetal IVD development, these were further characterized by immunopositivity for endothelial membrane antigen (EMA) and pan cytokeratin (AE1/AE3)[34]. After the notochordal cells are gone, the remaining ECM is characterized by the presence of large cell remnants still containing some vesicle-like structures. In degenerative discs, the calcifications were mainly found near clefts in the discs and in the transition zone between NP and AF (figure 5.4A and 5.4B).

No significant correlation was found between alizarin red staining and degeneration grade. In contrast, a clear statistically significant positive correlation was found between the extent of calcification shown by von Kossa staining in the NP and AF and degeneration grade (CC: 0.342, P= 0.015 and CC: 0.344, P= 0.016 respectively) (tables 5.3 and 5.4). Staining of NADH dehydrogenase showed viable cells throughout the entire IVD of both non-degenerated and degenerated discs, and few non-viable cells were seen. In combination with the von Kossa staining, calcifications were found in the areas directly surrounding viable cells, indicating the calcifications were not a result of cell death[12,35], but most likely involved in an active process (figure 5.4D). However, ALP activity was incidentally seen in a limited number of cells and sections of severely degenerated (Thompson grades IV and V) discs in the transition zone from NP to AF (figure 5.4C).

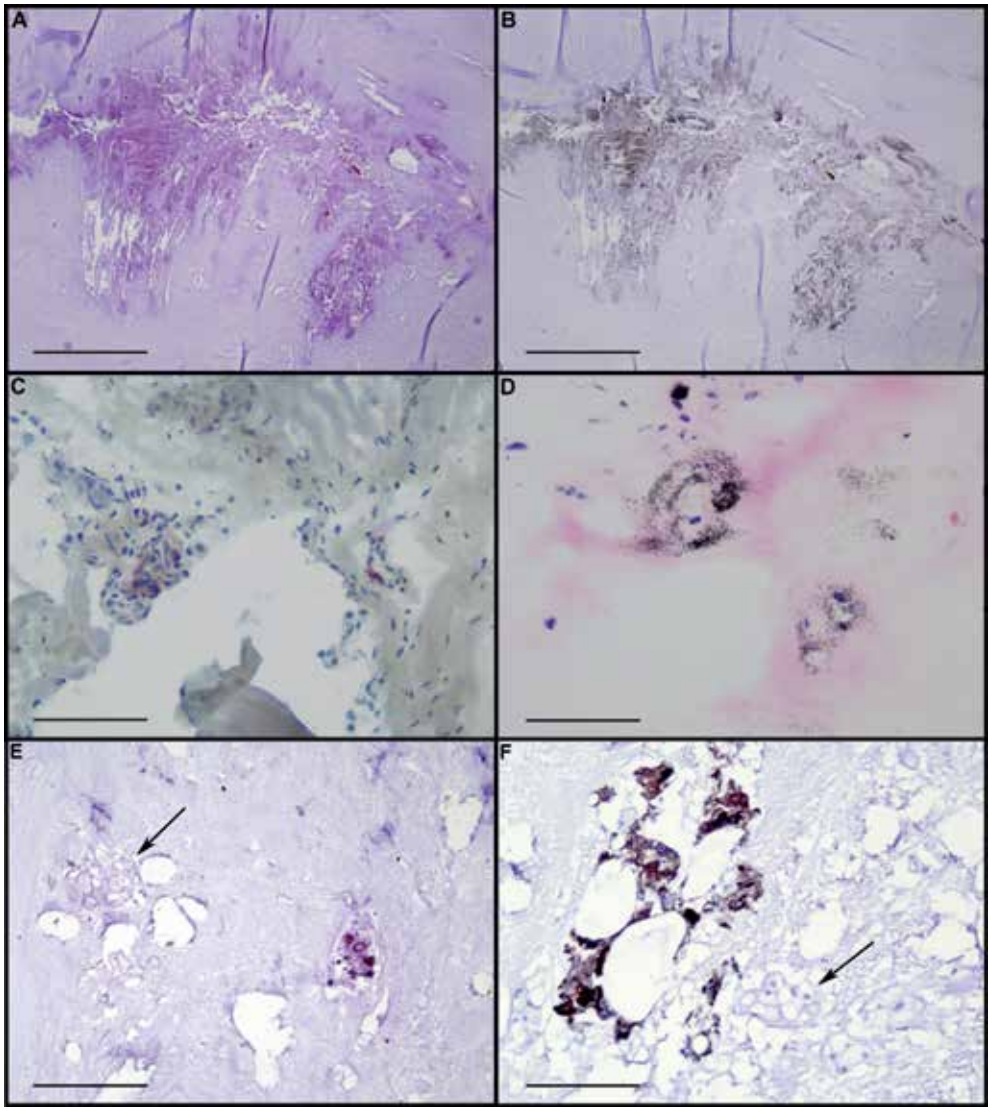

Figure 5.4. Large calcification in the AF from a Thompson grade IV IVD stained with alizarin red (A) and von Kossa (black/brown B). ALP activity (red staining) in the transition zone of the NP and AF of a Thompson grade IV IVD (C). Combined staining of NADH dehydrogenase (blue), von Kossa (black/brown) and eosin (pink) in Thompson grade V IVD (D). Calcification stained with alizarin red near notochordal cells (arrow) in the NP of a 3.3-year-old child (E). Calcification stained with von Kossa (black/brown) near notochordal cells (arrow) in the NP of a 3.3-year-old child (F). Scale bars indicate 500 µm (A, B), 100 µm (C, F) 50 µm (D) and 200 µm (E).

Table 5.3. Microscopic calcifications, stained with alizarin red, in the NP and AF per degeneration grade

NP	Grade I (n=9)	Grade II (n=10)	Grade III (n=10)	Grade IV (n=10)	Grade V (n=10)
-	44%	40%	40%	10%	20%
+/-	33%	30%	10%	30%	10%
+	22%	30%	50%	60%	50%
++	0%	0%	0%	0%	20%
AF					
-	88%	50%	50%	50%	40%
+/-	11%	20%	20%	20%	10%
+	0%	30%	30%	30%	50%
++	0%	0%	0%	0%	0%

++: multiple intense calcifications, +: two or more clear calcifications,

+/-: one single calcification, -: no calcifications.

Table 5.4. Microscopic calcifications, stained with von Kossa, in the NP and AF per degeneration grade

NP	Grade I (n=9)	Grade II (n=10)	Grade III (n=10)	Grade IV (n=10)	Grade V (n=10)
-	44%	30%	30%	0%	30%
+/-	33%	40%	10%	30%	0%
+	22%	30%	60%	60%	50%
++	0%	0%	0%	10%	20%
AF					
-	89%	40%	40%	50%	20%
+/-	0%	30%	30%	10%	10%
+	11%	30%	30%	40%	50%
++	0%	0%	0%	0%	20%

++: multiple intense calcifications, +: two or more clear calcifications,

+/-: one single calcification, -: no calcifications.

Discussion

This study clearly shows that hypertrophic differentiation occurs during IVD degeneration, with a concomitant increase in calcification. As the primary aim was to demonstrate hypertrophy in degenerated IVDs, extensive histological analysis was employed to yield mainly qualitative data on the presence of hypertrophic markers. Positive collagen type X staining was found both in the NP and AF of degenerative IVDs. Positive staining for OPG and Runx2 was found in the NP, AF and transition zone of degenerative IVDs and OPG levels correlated with degeneration grade in both the NP and AF. An increase in calcifications in the IVD was seen by micro-CT and histology in both the NP and AF of the degenerative IVD. Calcifications demonstrated by micro-CT were predominantly found in the transition zone and AF, while by von Kossa and alizarin red staining, calcifications were also seen in the NP. NADH staining showed that these calcifications were not a result of cell death. OPG levels also correlated with the extent of macroscopic calcifications in the NP and AF shown by the von Kossa staining. However, only a limited number of ALP-positive cells were found, restricted to the transition zone between the NP and AF of degenerative IVDs.

Recently the presence of Runx2 mRNA was reported in a murine model for IVD degeneration and in a limited number of IVD samples from patients with degenerative disc disease[27]. In the murine model Runx2 protein was demonstrated in the endplate of degenerated discs, but in human IVDs, Runx2 protein has not been analyzed before[27]. From the current study, it appears that Runx2 is clearly produced by the NP and AF cells of degenerated IVDs. How Runx2 expression is induced during the degeneration of cartilaginous tissues is currently unknown[14]. Runx2 expression could be induced by the loss of proteoglycans and hyaluronic acid, as Runx2 expression was recently found to be inhibited by hyaluronic acid[36]. Additionally the increase in Runx2 production could also be caused by altered mechanical loading in degenerative discs, since Runx2 is known to be a mechanoresponsive transcription factor[37].
As in OA, Runx2 during IVD degeneration may regulate the expression of genes that characterize the hypertrophic and osteoblastic phenotype, for example collagen type X. An increase in the production of collagen type X in degenerative discs compared to non-degenerative discs has been described previously, although some staining in the NP of non-degenerative discs was always observed[24-26].

The current study clearly shows increased OPG levels in degenerative IVDs compared to healthy discs. Similar findings are reported in a recent immunohistochemical study which describes the presence of OPG in a porcine model for IVD degeneration and one herniated human IVD[28]. The positive cytoplasmic staining of OPG in degenerative discs indicates that OPG is produced by NP and AF cells, however, the ECM staining near the clefts could indicate that OPG here was partially derived from diffusion into the degenerative disc from the adjacent vertebrae. Especially in grade V degenerative discs, the endplate is completely disrupted and therefore OPG produced by the osteoblasts in the vertebrae could easily have diffused through the clefts to the IVD. It is currently unknown how OPG expression is regulated in the IVD, but similarly to OPG expression by osteoblasts, it may be regulated by Runx2 produced by the NP and AF cells[38,39]. As to the role of OPG in IVD degeneration, as in OA, OPG may be chondroprotective[40].

A significant correlation between calcifications in the IVD and degeneration grade was found, largely in accordance with the results of other studies[22,23,41], although no difference in the extent of calcifications in the NP and AF was found, in contrast to a previous report[41]. This difference could be caused by the fact that we were able to detect smaller sized calcifications in the NP with micro-CT than is possible by X-ray analysis. Still, not all calcifications found by von Kossa and alizarin red staining in grades II and III discs were detected by micro-CT. This is most likely due to the resolution of micro-CT. Whereas small calcifications on a histological section can easily be visualized by increasing the magnification, small calcifications on a micro-CT image appear as 1 or 2 darker pixels, which are not recognizable as calcifications. Large calcifications were more easily detected by micro-CT since multiple slides per sample were analyzed for the micro-CT scoring and only one section per sample was analyzed for histological scoring.

Calcifications of the IVD have been described previously in degenerative discs from older patients, but also in young patients[22,23,42]. In the latter group (0-20 years), calcifications are rare, usually found in the cervical and thoracic spine and not related to degeneration[42,43]. In older patients, disc calcifications are mainly found in the cervical and lumbar spine[42]. In the current study, microscopic calcifications were also found both in degenerative and non-degenerative IVDs. Calcium salts stained by von Kossa were found around viable cells, indicating that at least some of the calcifications are produced by viable cells. The calcifications produced by these cells could be the result of end stage hypertrophic differentiation. In young, non-degenerative discs, microscopic calcifications were mainly found in the NP and were always associated with notochordal cells or the remnants of these cells, indicating a different underlying mechanism. Also the size of calcifications found in non-degenerative discs seemed smaller than in the degenerated discs. The absence of Runx2, OPG and ALP activity in non-degenerated IVDs with calcification indicate that these calcifications are most likely not caused by end stage hypertrophic differentiation. Hypertrophic differentiation is finally accompanied by an increase in ALP activity and mineralization. The ALP activity found in the current study was located in the transition zone between the NP and AF, in a limited number of cells in degenerative IVDs. Limited ALP activity was described in a rabbit model of IVD degeneration, although from this study a relation with degeneration could not be inferred[29]. Our findings suggest that ALP is also involved in ECM mineralization during IVD degeneration, especially since the localization of ALP activity coincided with the location where many of the calcifications were found, i.e., the transition zone. However, there is a clear discrepancy between the high extent of calcification found in the degenerative IVD and the relatively low number of ALP-positive cells. Moreover, the chondroid nests in the IVD sections were negative, in contrast to the ALP positivity characteristic for chondrocyte clones in OA. These discrepancies may be partly explained by the difference in detection methods, In the current study, active ALP was visualized with a substrate-chromogen system, whereas in other studies immunohistochemical staining was used to visualize ALP-positive chondrocytes[19,44]. As ALP is sensitive to fixation, this may have partially reduced ALP activity to below enzymatic detection levels in areas with relatively low activity compared to the transition zone[45]. As for articular chondrocytes[46]. ALP activity in the IVD may be regulated by Runx2.

Why hypertrophic differentiation is most prominent in the transition zone is not clear, but may be related to local biomechanical loading profiles. As hydrostatic pressure inhibits ossification, whereas tensile strains stimulate this, in the transition zone, which is relatively low in PGs and thus will experience less hydrostatic pressure, the balance may be tipped earlier towards ossification[47].

In contrast to the NP and AF, calcifications in the cartilage endplate were not observed. The endplate calcification reported in previous studies, measured by conventional radiology or micro-CT, usually denotes the thickening of the subchondral bone underlying the cartilaginous endplate, rather than calcification of the endplate proper. Until now, calcification in the human IVD endplate as local calcium deposits has never been shown, only variations in calcium concentration of endplate tissue digests26. Thinning of the endplate has also been termed calcification, but this parameter is difficult to quantify[48].

The apparently increased immunopositivity of Runx2, collagen type X, OPG and presence of ALP in the current study suggest that the process of hypertrophic differentiation also occurs in and is part of the process of IVD degeneration. Calcification in advanced stages of IVD degeneration could be a final result of the ongoing hypertrophic differentiation. Further empirical studies are needed to define the role of hypertrophy in IVD degeneration and the possibility to interfere with these processes in order to prevent or slow down degeneration.

Acknowledgements

The authors acknowledge the Department of Pathology of the University Medical Center, Utrecht, in particular F. Bernhard and A. de Ruiter for their support in obtaining the IVD specimens, A.P.L. Kwan (Cardiff University, Cardiff, Wales UK) for kindly providing the collagen type X antibody, M. Rutgers (dept. Orthopaedics, University Medical Center, Utrecht) for his help with the OPG ELISA and O van der Jagt (dept. Orthopaedics, Erasmus MC, University Medical Center, Rotterdam) for his help with the micro-CT analyses. This study was supported by the Anna Foundation and the Dutch Arthritis Association.

References

1. Wenig CM, Schmidt CO, Kohlmann T, Schweikert B. Costs of back pain in Germany. Eur J Pain 2008;13:280-6.
2. Raj PP. Intervertebral disc: anatomy-physiology-pathophysiology-treatment. Pain Pract 2008;8:18-44.
3. Urban JP, Roberts S. Degeneration of the intervertebral disc. Arthritis Res Ther 2003;5:120-30.
4. Walsh DA. Angiogenesis in osteoarthritis and spondylosis: successful repair with undesirable outcomes. Curr Opin Rheumatol 2004;16:609-15.
5. Adams MA, Roughley PJ. What is intervertebral disc degeneration, and what causes it? Spine 2006;31:2151-61.
6. Mwale F, Roughley P, Antoniou J. Distinction between the extracellular matrix of the nucleus pulposus and hyaline cartilage: a requisite for tissue engineering of intervertebral disc. Eur Cell Mater 2004;8:58-63.
7. Cui YYJ, Urban JP, Young DA. Differential gene expression profiling of metalloproteinases and their inhibitors: a comparison between bovine intervertebral disc nucleus pulposus cells and articular chondrocytes. Spine 2010;35:1101-8.
8. Roberts S, Evans H, Trivedi J, Menage J. Histology and pathology of the human intervertebral disc. J Bone Joint Surg Am 2006;88. S2-10-S2-14.
9. Rutges J, Kummer J, Oner F, Verbout A, Castelein R, Roestenburg H, et al. Increased MMP-2 activity during intervertebral disc degeneration is correlated to MMP-14 levels. J Pathol 2008;214:523-30.
10. Song RH, Tortorella MD, Malfait AM, Alston JT, Yang Z, Arner EC, et al. Aggrecan degradation in human articular cartilage explants is mediated by both ADAMTS-4 and ADAMTS-5. Arthritis Rheum 2007;56:575-85.
11. Yang X, Chen L, Xu X, Li C, Huang C, Deng CX. TGF-beta/Smad3 signals repress chondrocyte hypertrophic differentiation and are required for maintaining articular cartilage. J Cell Biol 2001;153:35-46.
12. Drissi H, Zuscik M, Rosier R, O'Keefe R. Transcriptional regulation of chondrocyte maturation: potential involvement of transcription factors in OA pathogenesis. Mol Aspects Med 2005;26:169-79.
13. Kamekura S, Kawasaki Y, Hoshi K, Shimoaka T, Chikuda H, Maruyama Z, et al. Contribution of runt-related transcription factor 2 to the pathogenesis of osteoarthritis in mice after induction of knee joint instability. Arthritis Rheum 2006;54:2462-70.
14. Wang X, Manner PA, Horner A, Shum L, Tuan RS, Nuckolls GH. Regulation of MMP-13 expression by RUNX2 and FGF2 in osteoarthritic cartilage. Osteoarthritis Cartilage 2004; 12:963-73.
15. Bucay N, Sarosi I, Morony S, Tarpley J, Capparelli C, Scully S, et al. Osteoprotegerin-deficient mice develop early onset osteoporosis and arterial calcification. Genes Dev 1998;12:1260-8.
16. Simonet WS, Lacey DL, Dunstan CR, Kelley M, Chang MS, Luthy R, et al. Osteoprotegerin: a novel secreted protein involved in the regulation of bone density. Cell 1997;89: 309-19.
17. Pilichou A, Papassotrriou I, Michalakakou K, Fessatou S, Fandridis E, Papachristou G, et al. High levels of synovial fluid osteoprotegerin (OPG) and increased serum ratio of receptor activator of nuclear factor-kappaB ligand (RANKL) to OPG correlate with disease severity in patients with primary knee osteoarthritis. Clin Biochem 2008;41:746-9.
18. Komuro H, Olee T, Kuhn K, Quach J, Brinson DC, Shikhman A, et al. The osteoprotegerin/receptor activator of nuclear factor kappaB/receptor activator of nuclear factor kappaB ligand system in cartilage. Arthritis Rheum 2001;44:2768-76.
19. Pfander D, Swoboda B, Kirsch T. Expression of early and late differentiation markers (proliferating cell nuclear antigen, syndecan-3, annexin VI, and alkaline phosphatase) by human osteoarthritic chondrocytes. Am J Pathol 2001;159: 1777-83.

20. Roach HI. Association of matrix acid and alkaline phosphatises with mineralization of cartilage and endochondral bone. Histochem J 1999;31:53-61.
21. Schmid TM, Bonen DK, Luchene L, Linsenmayer TF. Late events in chondrocyte differentiation: hypertrophy, type X collagen synthesis and matrix calcification. In Vivo 1991;5:533-40.
22. Feinberg J, Boachie-Adjei O, Bullough PG, Boskey AL. The distribution of calcific deposits in intervertebral discs of the lumbosacral spine. Clin Orthop Relat Res 1990;254:303-10.
23. Sandstrom C. Calcifications of the intervertebral discs and the relationship between various types of calcifications in the soft tissues of the body. Acta radiol 1951;36:217-33.
24. Boos N, Nerlich AG, Wiest I, von der MK, Aebi M. Immunolocalization of type X collagen in human lumbar intervertebral discs during ageing and degeneration. Histochem Cell Biol 1997;108:471-80.
25. Nerlich AG, Schleicher ED, Boos N. 1997 Volvo Award winner in basic science studies. Immunohistologic markers for agerelated changes of human lumbar intervertebral discs. Spine 1997;22:2781-95.
26. Roberts S, Bains MA, Kwan A, Menage J, Eisenstein SM. Type X collagen in the human invertebral disc: an indication of repair or remodelling? Histochem J 1998;30:89-95.
27. Sato S, Kimura A, Ozdemir J, Asou Y, Miyaki M, Jinno T, et al. The distinct role of the Runx proteins in chondrocyte differentiation and intervertebral disc degeneration: findings in murine models and in human disease. Arthritis Rheum 2008;58:2764-75.
28. Mackiewicz Z, Salo J, Konttinen YT, Kaigle Holm AIA, Pajarinen J, Holm S. Receptor activator of nuclear factor kappa B ligand in an experimental intervertebral disc degeneration. Clin Exp Rheumatol 2009;27:299-306.
29. Gan JC, Ducheyne P, Vresilovic EJ, Swaim W, Shapiro IM. Intervertebral disc tissue engineering I: characterization of the nucleus pulposus. Clin Orthop Relat Res 2003;411:305-14.
30. Thompson JP, Pearce RH, Schechter MT, Adams ME, Tsang IK, Bishop PB. Preliminary evaluation of a scheme for grading the gross morphology of the human intervertebral disc. Spine 1990;15:411-5.
31. Bonewald LF, Harris SE, Rosser J, Dallas MR, Dallas SL, Camacho NP, et al. Von Kossa staining alone is not sufficient to confirm that mineralization in vitro represents bone formation. Calcif Tissue Int 2003;72:537-47.
32. Lievremont M, Potus J, Guillou B. Use of alizarin red S for histochemical staining of Ca^{2+} in the mouse; some parameters of the chemical reaction in vitro. Acta Anat 1982;114:268-80.
33. Hunter CJ, Matyas JR, Duncan NA. The notochordal cell in the nucleus pulposus: a review in the context of tissue engineering. Tissue Eng 2003;9:667-77.
34. Rutges JP, Nikkels PG, Oner FC, Ottink KD, Verbout AJ, Castelein RM, et al. The presence of extracellular matrix degrading metalloproteinases during fetal development of the intervertebral disc. Eur Spine J 2010;19:1340-6.
35. Kim KM. Apoptosis and calcification. Scanning Microsc 1995;9:1137-75.
36. Tanne Y, Tanimoto K, Tanaka N, Ueki M, Linn YY, Onkuma S, et al. Expression and activity of Runx2 mediated by hyaluronan during chondrocyte differentiation. Arch Oral Biol 2008;53:478-87.
37. Ziros PG, Basdra EK, Papavassiliou AG. Runx2: of bone and stretch. Int J Biochem Cell Biol 2008;40:1659-63.
38. Komori T. Runx2, a multifunctional transcription factor in skeletal development. J Cell Biochem 2002;87:1-8.

39. Thirunavukkarasu K, Halladay DL, Miles RR, Yang X, Galvin RJ, Chandrasekhar S, et al. The osteoblast-specific transcription factor Cbfa1 contributes to the expression of osteoprotegerin, a potent inhibitor of osteoclast differentiation and function. J Biol Chem 2000;275:25163-72.
40. Haynes DR, Barg E, Crotti TN, Holding C, Weedon H, Atkins GJ, et al. Osteoprotegerin expression in synovial tissue frompatients with rheumatoid arthritis, spondyloarthropathies and osteoarthritis and normal controls. Rheumatology 2008;42:123-34.
41. Prescher A. Anatomy and pathology of the aging spine. Eur J Radiol 1998;27:181-95.
42. Templick JG. Degenerative disk disease. In: Templick GJ, Simeone FA, Eds. Lumbar spine CT and MRI. 2nd edn. Philadelphia: J.B. Lippincott Company; 1992:39-68.
43. Dai LY, Ye H, Qian QR. The natural history of cervical disc calcification in children. J Bone Joint Surg Am 2004;86:1467-72.
44. Pullig O, Weseloh G, Ronneberger DKS, Swoboda B. Chondrocyte differentiation in human osteoarthritis: expression of osteocalcin in normal and osteoarthritic cartilage and bone. Calcif Tissue Int 2000;67:230-40.
45. Doty SB. Problems inherent in obtaining the alkaline phosphatise reaction. J Histochem Cytochem 1980;28:66-8.
46. Enomoto-Iwamoto M, Enomoto H, Komori T, Iwamoto M. Participation of Cbfa1 in regulation of chondrocyte maturation. Osteoarthritis Cartilage 2001;9:S76-84.
47. Smith RL, Carter DR, Schurman DJ. Pressure and shear differentially alter human articular chondrocyte metabolism: a review. Clin Orthop Relat Res 2004;427(Suppl):S89-95.
48. Bernick S, Cailliet R. Vertebral end-plate changes with aging of human vertebrae. Spine 1982;7:97-102.

CHAPTER 6

Variations in gene and protein expression in human nucleus pulposus in comparison with annulus fibrosus and cartilage cells: potential associations with aging and degeneration

JPHJ Rutges, LB Creemers, WJA Dhert, S Milz, D Sakai, J Mochida, M Alini and S Grad
Osteoarthritis and Cartilage (2010) 18, 416-423

Abstract

Regardless of recent progress in the elucidation of intervertebral disc (IVD) degeneration, the basic molecular characteristics that define a healthy human IVD are largely unknown. Although work in different animal species revealed distinct molecules that might be used as characteristic markers for IVD or specifically nucleus pulposus (NP) cells, the validity of these markers for characterization of human IVD cells remains unknown.

Eleven potential marker molecules were characterized with respect to their occurrence in human IVD cells. Gene expression levels of NP were compared with annulus fibrosus (AF) and articular cartilage (AC) cells, and potential correlations with aging were assessed.

Higher mRNA levels of cytokeratin-19 (KRT19) and of neural cell adhesion molecule-1 were noted in NP compared to AF and AC cells. Compared to NP cytokeratin-18 expression was lower in AC, and alpha-2-macroglobulin and desmocollin-2 lower in AF. Cartilage oligomeric matrix protein (COMP) and glypican-3 expression was higher in AF, while COMP, matrix gla protein (MGP) and pleiotrophin expression was higher in AC cells. Furthermore, an age-related decrease in KRT19 and increase in MGP expression were observed in NP cells. The age-dependent expression pattern of KRT19 was confirmed by immunohistochemistry, showing the most prominent KRT19 immunoreaction in the notochordal-like cells in juvenile NP, whereas MGP immunoreactivity was not restricted to NP cells and was found in all age groups.

The gene expression of KRT19 has the potential to characterize human NP cells, whereas MGP cannot serve as a characteristic marker. KRT19 protein expression was only detected in NP cells of donors younger than 54 years.

Introduction

Degeneration of the intervertebral disc (IVD) and related spinal disorders are leading causes of morbidity, resulting in substantial pain, disability and increased health care costs[1]. The IVD comprises the highly hydrated nucleus pulposus (NP), the surrounding multilaminar annulus fibrosus (AF) and the cartilaginous endplates. Pathophysiological evidence indicates that IVD degeneration starts in the NP, where the concentration of proteoglycans and the synthesis of type II collagen decrease[2,3]. At the same time denaturation of type II collagen fibers and synthesis of type I collagen occurs[3]. As a consequence the NP loses its osmotic properties and becomes fibrotic; the disc loses its ability to transmit intervertebral forces and further degenerative processes may occur.

Regeneration of NP tissue in the early stages of degeneration may slow down or even reverse the degenerative processes and might possibly restore part of the degenerated disc. Thus, regenerative medicine and biological therapies hold great promise. In particular the therapeutic implications of stem cells have been highly anticipated by both the clinical and scientific communities[4,5]. The challenge in characterizing cellular degeneration and ultimately accomplishing cellular regeneration begins with the identification of the molecular phenotype of the cells that constitute the NP. The NP includes small cells commonly referred to as ''chondrocyte-like'', since they have a similar rounded morphology and synthesize similar extracellular matrix macromolecules as articular chondrocytes. Currently, no reliable markers exist to distinguish NP cells from the chondrocytes from hyaline cartilage. A cell population with the properties of articular cartilage (AC) would fail to restore the necessary function of the IVD because the requisite fluid properties unique to the IVD would not be recreated. While the ratio of proteoglycan to collagen shows a certain potential to separate disc cells, recent research has focused on the clarification of their molecular phenotype[6]. In a recent study, rat NP cells were compared with cells from the AF and AC tissues by means of large scale microarray gene expression screening. Subsequent quantitative gene expression and immunohistochemical analyses identified distinct molecules, namely glypican-3 (GPC3) and cytokeratin-19 (KRT19), as promising candidates for NP cell characterization[7]. Similar studies in the beagle dog revealed additional potential NP marker molecules, including alpha-2-macroglobulin (A2M), cytokeratin-18 (KRT18), desmocollin-2 (DSC2), and neural cell adhesion molecule-1 (NCAM1)[8].

However, considerable developmental, anatomical, and biochemical differences among species are likely to affect the phenotypical characteristics of the disc cells[9]. In particular the presence of notochordal cells, which are regarded to be remnants of the embryonic notochord, in the NP is the cause of substantial inter-species variation. Mice, rats, rabbits, and non-chondrodystrophoid dogs retain a predominantly notochordal NP until adulthood and often throughout life, whereas bovine, ovine and chondrodystrophoid dogs closer resemble humans in that the number of notochordal cells rapidly decreases after birth[10]. Moreover, differences in tissue size, oxygen and nutrient supply, and biomechanical requirements are also likely to affect the molecular features of the cells in the disc. As a consequence, observations from animal discs will not necessarily apply to human discs. Nevertheless, animal studies are indispensable for screening purposes,

since they allow investigation of normal healthy tissues with larger sample size and smaller inter-individual variability. Due to the limited availability of healthy and viable human IVD tissue, comprehensive screening is difficult in human individuals. The aim of this study therefore was to evaluate the presence and distribution of the molecules that were found to be differently expressed in disc and cartilage cell populations in various animal species in human disc cells. To account for potential variations related to aging and degeneration, cell and tissue samples from individuals of different age groups and disc degeneration grades were examined.

Materials and methods

Isolation of NP, AF, AND AC Cells

The study was approved by the medical ethical committee of the University Medical Center (UMC) Utrecht and the scientific committee from the Department of Pathology of the UMC Utrecht. Eleven patients with no known history of IVD disease were included in the study. Samples were obtained within an average of 17.5 h after death of the patient (range 6.25-23.0 h). The age of the individuals ranged from 22 to 81 years (average 46±20 years; median 43 years), and the average degree of disc degeneration, assessed according to the Thompson score[11], was 2.2± 1.0 (median 2) (table 6.1). IVD tissue was harvested from segments between L1 and L5 and was separated into NP and AF tissue. To exclude any contamination by AF tissue, only the innermost part of the disc was harvested to be assigned to NP tissue, whereas the transition zone, including part of the inner AF, was entirely excluded from analysis. This is of particular importance for aged discs, where it can be difficult to clearly distinguish NP and AF tissues. AC was harvested from the patellae of the same patients. Chondrocytes were extracted from full thickness cartilage which implies mixed populations of superficial, middle and deep zone cells. Gene expression data thus represent an average cellular expression of target mRNA. Tissue was cut into small pieces and cells were enzymatically isolated using sequential pronase (Roche) and type II collagenase (Worthington Biochemical) digestion with DNase II (Sigma) added to prevent cell clumping. AC and AF were treated with 0.2% pronase/0.004% DNase for 1 h, then with 200 U/mL collagenase/0.004% DNase over night. NP was treated with 0.2% pronase/0.004% DNase for 1 h, then with 100 U/mL collagenase/0.004% DNase for 8 h, stirring at 37°C in humidified atmosphere. After enzymatic isolation cell suspensions were filtered through a 70 µm cell strainer, washed twice with Dulbecco's Modified Eagles Medium, and lysed in TRI Reagent (Molecular Research Center, Cincinnati, OH). Samples were stored at -80°C until RNA isolation.

Table 6.1. Patients included for gene expression analysis of NP, AF, and AC cells.

Patient			Thompson
Number	Age	Gender	Grade
1	22	M	1
2	25	M	1
3	25	M	1
4	32	M	1-2
5	40	M	2
6	43	M	2
7	46	M	2-3
8	56	M	3
9	61	F	3
10	72	M	4
11	81	F	3

IVD tissue was harvested from discs between L1 and L5 and separated in NP and AF; AC was harvested from the patella joint surface. Cartilage quality was macroscopically assessed and was without detectable changes for patients 1-9. Slight degenerative changes were detected in patient 10, and signs of osteoarthritis in patient 11

RNA extraction and real time RT-PCR

RNA was isolated using a modified TriSpin method[7,12]. Briefly, bromochloro- propane (Sigma) was added to the lysate, phases were separated, and ethanol (Merck) added to the aqueous phase. Total RNA was extracted using the SV Total RNA Isolation System (Promega), which includes an oncolumn DNAse digestion, and eluted in 100 µl of RNase-free water. TaqMan reverse transcription reagents (Applied Biosystems, Foster City, CA) were used for cDNA synthesis. PCR was performed with an SDS 7500 real time PCR instrument using TaqMan Gene Expression Master Mix (all from Applied Biosystems) and standard thermal conditions (10 min 95°C for polymerase activation, followed by 45 cycles of 95°C for 15 s and 60°C for 60 s). Primer-probe systems, purchased as Gene Expression Assays, were from Applied Biosystems. Genes that were previously found to be differentially expressed in NP compared to AF and/or AC cells in the rat and/or chondrodystrophoid dog were chosen for analysis (table 6.2)[7,8,13]. Expression of target genes was normalized to the 18S ribosomal RNA as the endogenous control. Relative mRNA levels were calculated according to the 2^(delta Ct) method and presented as log(2) transformed values[14,15].

Table 6.2. Gene expression assays used for real time PCR (from Applied Biosystems)

Gene	Assay code
Alpha-2-macroglobulin (A2M)	Hs_00163474_m1
CD24	Hs_00273561_s1
Cartilage oligomeric matrix protein (COMP)	Hs_00164359_m1
Desmocollin-2 (DSC2)	Hs_00245200_m1
Glypican-3 (GPC3)	Hs_00170471_m1
Cytokeratin-18 (KRT18)	Hs_01920599_gH
Cytokeratin-19 (KRT19)	Hs_00761767_s1
Matrix-gla-protein (MGP)	Hs_00179899_m1
Neural cell adhesion molecule-1 (NCAM1)	Hs_00169851_m1
Pleiotrophin (PTN)	Hs_00383235_m1
Vimentin (VIM)	Hs_00185584_m1

Immunohistochemistry

For histological analysis human IVD tissue was obtained as part of a standard postmortem procedure, in which a section of the lumbar and thoracic spine is removed for diagnostic purposes. IVD samples were stored in the UMC Utrecht Biobank of the Department of Pathology. Collection and analysis of the IVDs was approved by the medical ethical committee of the UMC Utrecht and the scientific committee of the Department of Pathology of the UMC Utrecht. Samples were obtained within a mean of 17.7 h after death of the patient, 95% within 24 h after death. Between death and tissue collection the deceased patients were kept at the mortuary at 4°C. From all patients the IVD between the fourth and fifth lumbar vertebra (spinal motion segment L4-L5), including the adjacent endplates, was obtained. The grade of degeneration was scored by three individual observers using the classification of Thompson et al.[11]. After individual scoring the values were averaged; outliers, i.e., differences of more than 1 Thompson grade, were re-evaluated by the three observers at a consensus meeting. The expression and localization of KRT19 and matrix gla protein (MGP) in IVD tissue was evaluated in 41 human individuals aged between 3 and 86 years (average 47±25 years; median 51 years, table 6.3). Sagittal slices of the motion segments were fixed in formalin, decalcified with Kristensen's solution (50% formic acid and 68 g/L sodium formiate) in a microwave at 150 W and 50°C for 6 h, dehydrated in graded ethanol series, and embedded in paraffin[16]. Sections were deparaffinized, treated with 3% hydrogen peroxide in methanol for 30 min and then with heated (95°C) citrate buffer (10 mM sodium citrate, 0.05% Tween20, pH 6.0) for 20 min for antigen retrieval. Then they were blocked with 5% normal horse serum for 1 h, and were incubated with mouse monoclonal anti-KRT19 antibody (clone A53-B/A2; cat. no. EXB-11-120, Exbio, Praha, CZ) or mouse monoclonal anti-MGP antibody (clone 52.1C5D; cat. no. ALX-804-512, Alexis Biochemicals, Lausen, CH) at a concentration of 5 µg/ml over night at 4°C. Negative control sections were incubated without primary antibody. Biotinylated secondary anti-

mouse antibody (dilution 1:200; Vectastain ABC-kit Elite, cat. no. PK-6102, Vector Laboratories, Burlingame, USA) was applied, followed by ABC complex, and chromogen development using diaminobenzidine (DAB Kit, cat. no. SK-4100, Vector Laboratories, Burlingame, USA). Sections were counterstained with Mayer's haematoxylin.

Table 6.3. Immunohistochemical results obtained from IVD sections from the UMC Utrecht Biobank of the Dept. of Pathology. Only discs between the fourth and fifth human lumbar vertebra (L4-L5) were assessed. Cells were classified according to their topographical position within the disc tissue.

Patient	Age	Gender	Thompson	KRT19	MGP				
Number			Grade	NP	NP	IAF	OAF	EP	AOA
1	3	F	1	++	+++	-	-	-	++
2	3	F	1	+++	N/A	N/A	N/A	N/A	N/A
3	6	F	1	-	+++	++	++	-	N/A
4	14	M	1	+++	+++	++	+++	-	+++
5	14	F	1	++	+++	+++	+++	-	N/A
6	14	F	1	-	-	-	++	-	N/A
7	17	M	2	+++	+++	-	-	-	+++
8	18	M	1	+	-	-	-	N/A	N/A
9	19	F	1	-	+++	++	++	-	+++
10	21	M	1	++	+++	+	++	-	+++
11	22	F	1	+	++	-	N/A	-	N/A
12	25	M	1	-	++	-	-	-	++
13	35	F	2	+++	++	+++	+++	-	+++
14	35	M	N/A	-	+++	++	++	-	+++
15	36	M	2	-	++	+	+	-	N/A
16	38	M	2	-	+	-	-	-	+
17	41	M	2	(+)	+++	+	+++	-	+++
18	44	M	2	-	-	-	-	-	-
19	47	F	3	-	++	-	-	-	-
20	51	F	2	-	(+)	-	+	-	+++
21	51	F	2	(+)	++	-	-	-	+
22	54	F	4	(+)	+++	-	+++	-	N/A
23	57	M	4	-	++	++	+++	-	N/A
24	59	M	4	-	+++	++	N/A	-	N/A
25	60	M	5	-	+++	++	++	-	+++
26	62	F	2	-	-	-	-	-	+++

Patient	Age	Gender	Thompson	KRT19	MGP				
27	62	M	5	-	+++	+++	+++	-	+++
28	63	M	3	-	++	+	-	-	N/A
29	67	F	5	-	+	N/A	N/A	N/A	N/A
30	68	F	5	-	N/A	N/A	N/A	+	++

Grading scheme: (+) = 1-2 positive cells; +=3-4 positive cells; ++ = 5e10 positive cells; +++ = >10 positive cells per field of view. For analysis a Zeiss Axioplan2 microscope equipped with a 20x objective (Neofluar) and a 10x ocular was used. IAF: Inner annulus fibrosus; OAF: Outer annulus fibrosus; EP: Cartilaginous endplate; AOA: Attachment of outer annulus fibrosus; N/A: not available. KRT19 positive cells were only detected in the NP and in 2 cases of severe degenerative disc changes in the EP (*).

Statistical analysis

Differences in relative gene expression levels between paired NP and AF and paired NP and AC were assessed by the Wilcoxon Signed Ranks test. Correlations between relative gene expression and age or disc degeneration grade were determined using the Pearson correlation analysis. $P < 0.05$ was considered as significant.

Results

Gene expression

In both the NP vs AF and the NP vs AC comparisons, pronounced gene expression differences were observed for KRT19. Levels of KRT19 mRNA were constantly higher in the NP than in both AF and AC cells, although the extent of up-regulation varied between individuals. NCAM1 expression was also increased in NP compared to AF and AC cells, while the expression of A2M and DSC2 was higher in NP than in AF cells and KRT18 expression was higher in NP than in AC cells. On the other hand, mRNA expression levels of GPC3 and cartilage oligomeric matrix protein (COMP) were higher in the AF compared to the NP, whereas COMP, MGP, and pleiotrophin (PTN) were expressed more highly in the AC than in the NP cells. No differences in vimentin (VIM) and Cluster of Differentiation 24 antigen (CD24) expression were noted between NP and AF or AC cells (figure 6.1). While the KRT19 expression of AC and AF cells did not change throughout age groups, its expression in the NP cells showed a decrease with age ($P = 0.032$; figure 6.2). However, in spite of this decrease, KRT19 was still more highly expressed in the NP compared to the AF and AC cells even in older individuals. A correlation between age and gene expression in NP cells was also found for MGP mRNA, which increased with increasing age ($P = 0.003$; figure 6.3). In the AF cells, increasing levels of PTN mRNA were noted with aging ($P = 0.023$; data not shown). The expression of MGP in NP cells was also positively correlated with the degree of degeneration ($P = 0.007$). The relation between KRT19 level in the NP and degeneration grade was found to be almost significant ($P = 0.061$). No association between age or degeneration grade and the level of expression was detected with any of the other genes analysed. However, in agreement with previous reports, there was a strong relationship between age and degeneration grade of the disc ($P < 0.001$).

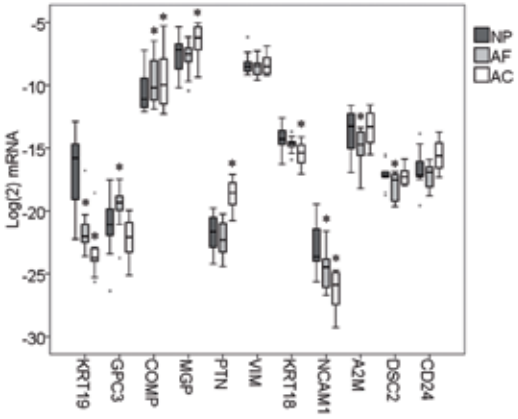

Figure 6.1. Relative mRNA expression in human NP, AF, and AC cells. Expression levels were normalized to 18S rRNA as the endogenous control. *P < 0.05 in pair-wise comparison of NP with corresponding AF or AC; N = 9-11.

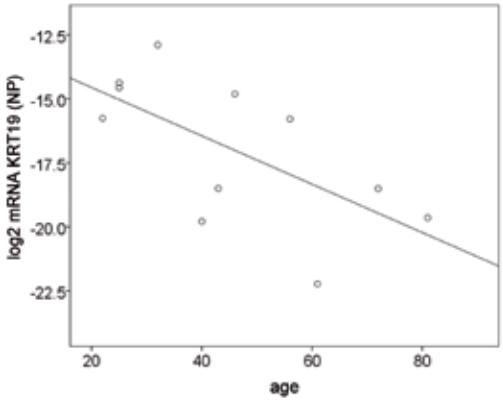

Figure 6.2. Relative mRNA expression for KRT19 in NP cells of 11 individuals between 22 and 81 years of age. Gene expression was normalized to the 18S ribosomal RNA. A decrease in the KRT19 expression level with increasing age is noted.

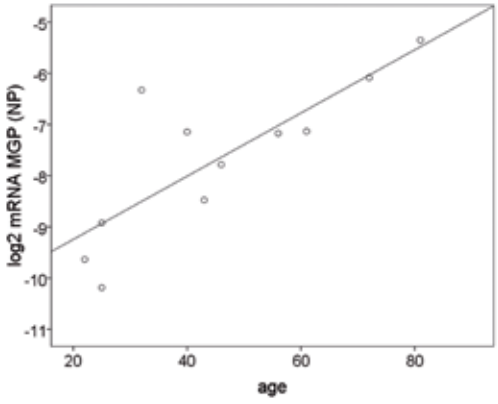

Figure 6.3. Relative mRNA expression for MGP in NP cells of 11 individuals between 22 and 81 years of age. Gene expression was normalized to the 18S ribosomal RNA. An increase in the MGP expression level with increasing age is noted.

Immunohistochemistry

KRT19 was chosen for immunohistochemical analysis, since this molecule showed most pronounced differences between NP and AF or AC with respect to mRNA expression, whereas MGP was selected for analysis at the protein level because of its apparent age- and degeneration-dependent increase in the NP cells, which are of main interest in this study.

In the NP of juvenile discs (<5 years of age), clusters of large cells with a notochordal morphology were identified. These cells were positive for KRT19 (figure 6.4A), while neither cells within the AF nor cells of the cartilaginous endplate revealed any positive labelling (figure. 6.4B, table 6.3). In the NP of young discs with Thompson score 1 but without apparent existence of notochordal cells (age range 6-25 years), KRT19 positive cells were observed in 60% (n = 6/10) of the individuals. Labelling was located predominantly intracellular and was limited to a small number of cells that had a somewhat chondrocytic appearance with no morphological evidence of a notochordal cell phenotype (figure 6.4C and D). On the other hand, the majority of healthy adult discs did not reveal any immunoreactivity for KRT19 (figure 6.4E). In two degenerate discs however (patients with sepsis), positive cells were detected adjacent to fissures associated with degenerative changes of the cartilaginous endplate (figure 6.4G). These cells exhibited a characteristic chondrocyte-like morphology, were located at the border between cartilaginous endplate and NP and were not regarded as NP cells.

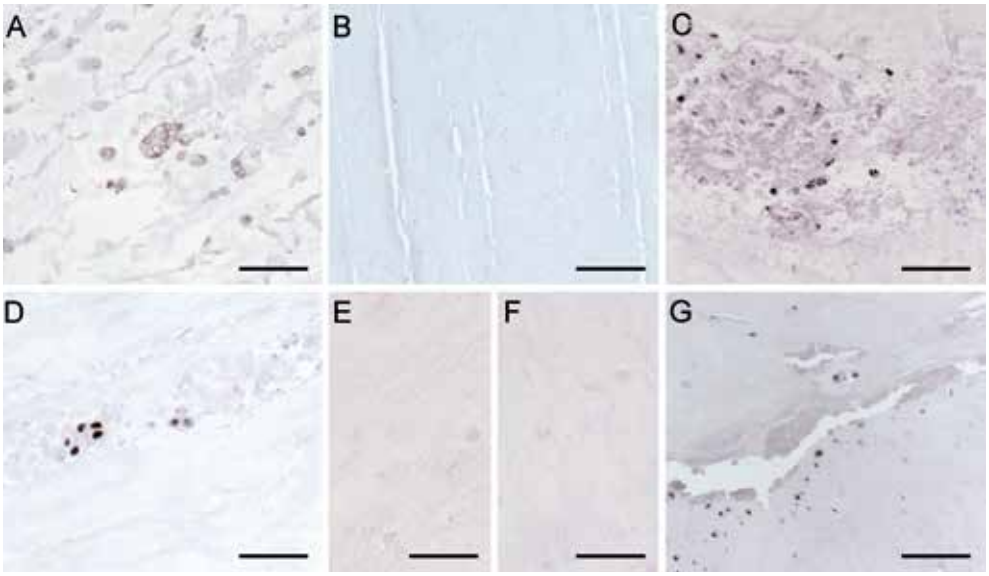

Figure 6.4. Immunolabelling characteristics for KRT19. Cells within the NP of a 3-year-old human female label positive for KRT19 (A). No KRT19 positive cells are detected in the inner annulus of a 21-year-old male individual (B). A group of KRT19 positive cells in the NP of a 14 year-old male (C). Small group of KRT19 positive cells from the NP of a 21-year-old male (D, same individual as in B). NP of a 47-year-old female with Thompson grade 3. No positive labelling can be detected (E). Control from same individual as in E (F). 72-year-old male donor with disc degeneration grade 4. (G) The image shows the edge of the NP region. The cartilaginous endplate is at the bottom of the image. Several KRT19 positive cells with a chondrocyte-like morphology can be detected. All scale bars = 100 µm.

The number of MGP positive cells in general was higher than the number of KRT19 positive cells, but non labelled cells clearly constitute the largest cell fraction. However, in juvenile and young adult discs positive cells could be detected in the NP (table 6.3). MGP positive cells were found in distinct clusters of NP cells in young individuals (figure 6.5A and B). In older more degenerated discs (grade 3 and higher) positive cells were found adjacent to clefts and cracks (figure 6.5D). Furthermore, the outer AF was often immunopositive (figure 6.5), with a decreasing intensity towards the inner AF (figure 6.5F). Labelling was limited to the cells and to a very small portion of the pericellular matrix in their immediate vicinity. The cells and extracellular matrix of the mineralized cartilage of the endplate often demonstrated a positive reaction for MGP, especially at the tidemark (figure 6.5G and H). The non-mineralized cartilage of the endplate was always negative (figure 6.5G and H). The fibrocartilaginous attachment of the outer AF frequently labelled positive (figure 6.5 I).

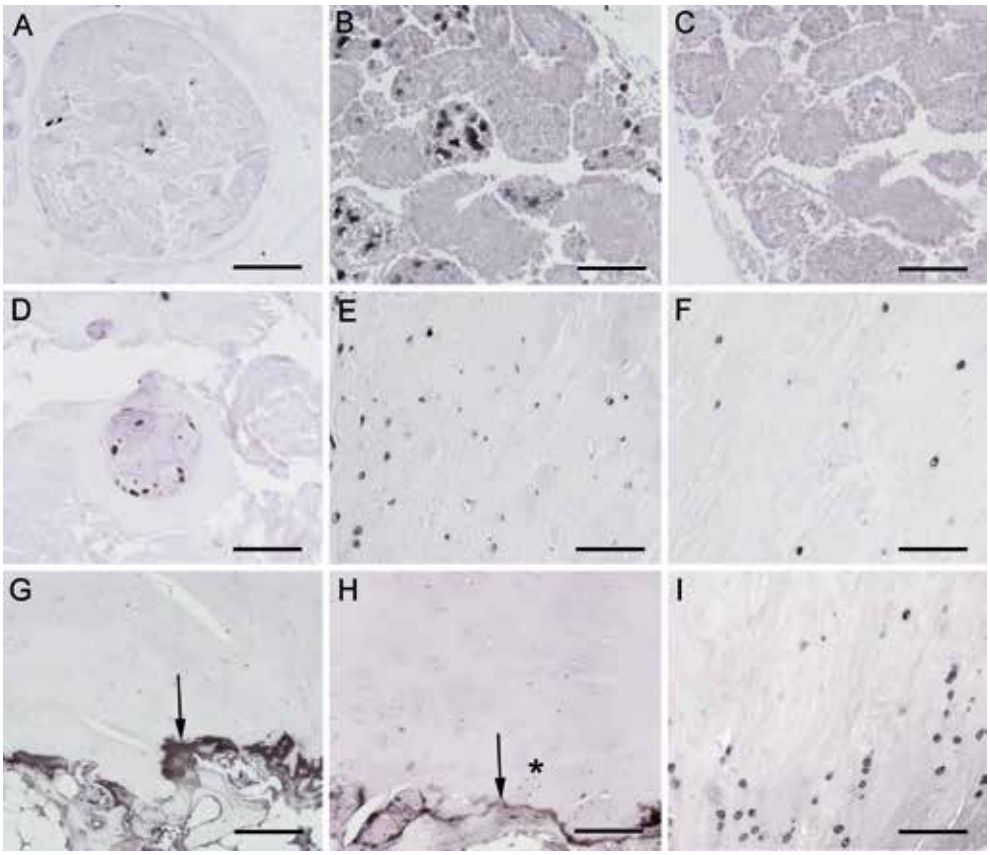

Figure 6.5. Immunolabelling characteristics for MGP. Cells within the NP of a 6-year-old human female label positive for MGP(A). Group of MGP positive cells in the NP of a 17-year-old male (B). Control from same individual and same region as shown in B (C). Small group of MGP positive cells from the NP of a 60-year-old male individual with disc degeneration Thompson grade 5 (D). Note that the cells are forming a cluster like structure in the neighbourhood of a fissure. Outer and inner annulus of a 35-year-old female with Thompson grade 2 (respectively E and F). Several positive cells can be detected. The surrounding extracellular matrix is negative. Endplate cartilage from a 72-year-old male with Thompson grade 5 (G). Note the strong positive labelling at the tidemark (arrow) and in the calcified cartilage. Cells in non-calcified cartilage are all negative. Endplate cartilage from a 35-year-old female individual with Thompson grade 2 (H). The positive labelling at the tidemark (arrow) is clearly visible. Cartilage cells form clusters (*) but are all negative. Fibrocartilaginous attachment of the outer annulus of a 35-year-old female individual, same as in H (I). The fibrocartilage cells are arranged in characteristic rows and label positive for MGP. Scale bar in G = 200 µm, all other scale bars = 100 µm.

Discussion

Degenerative changes occurring in the IVD have been extensively described and mechanisms, including genetic variations that may cause a predisposition to IVD degeneration are being elucidated. However, the molecular profile that characterizes the normal disc, and in particular the NP cell is still unknown. Previous investigations have suggested potential markers for IVD cells and more specifically for NP cells[7,8,13,17]. The present study is a further contribution to the identification of molecules expressed in human disc cells. It was undertaken to validate potential NP marker molecules identified by large scale gene expression screening in the rat and dog for their potential use with human cells.

Looking at genes previously identified as markers for the rat NP, the expression of KRT19 could be confirmed for human cells. However, a decrease in KRT19 expression with age was noted in the NP, while the expression in AF and AC remained constant. As KRT19 has also been associated with notochordal cells and chordoma, its expression in healthy adult human NP cells may be unexpected[18,19]. Indeed, immunohistochemical analysis confirmed its presence in cells with a notochordal phenotype and further supported the suggestion of an age-dependent expression pattern. At the protein level, KRT19 was barely detectable in the NP after the third decade, although mRNA expression was still clearly measurable. Possible explanations for this finding may include differences in the detection limit between mRNA and protein expression, instability of the mRNA, short protein half-life, or inhibition at the translational level.

In contrast to KRT19, the expression pattern of the other genes that had been found to be expressed more highly in the NP than in the AC in rat specimens, including CD24, was not confirmed in human samples[7,13]. However, GPC3 and PTN expression profiles were similar to observations in beagle dogs[8]. This might be related to the comparable development of the NP with respect to cell phenotype in human individuals and chondrodystrophoid dogs, which clearly differs from the development in rats. Looking at the genes evaluated for the beagle dog, the human samples generally showed a similar expression pattern, with higher levels of KRT18, A2M, and NCAM1 in NP vs AF and/or AC. Besides KRT19, only NCAM1 was expressed more highly in NP than both AF and AC cells in this study. NCAM1 is an integral membrane glycoprotein that can regulate both cell-cell and cell-substrate interactions, primarily through polysialic acid[20,21]. Although it is expressed primarily in the nervous system, NCAM1 has been identified in various tissues in the adult rat[22]. In development NCAM1 plays a significant role in cell differentiation, including diverse functions in osteogenesis and chondrogenesis[23.] However, the fact that NCAM1 was expressed at a low level in all cell types analysed depreciates this molecule as a useful marker for human NP cells.

The matrix protein COMP showed consistently lower expression in NP than in AF and AC cells in all species. This differential expression of COMP in cartilage and disc adds to earlier observations of variations in the relative amounts of distinct matrix molecules in these two tissues[6]. While COMP has been identified and localized in the IVD, its relatively lower expression may reflect differences in the mechanical properties between the NP and cartilage tissues[24]. The main molecular functions of COMP include binding other matrix

proteins and catalyzing polymerization of type II collagen fibrils. Furthermore, COMP is reported to prevent vascularization of cartilage and this could also be the case in the IVD tissues[25].
Commonly, work that addresses the disc cell profile leads to the conclusion that disc cells express a predominantly chondrocytic phenotype[26-28]. Investigations on mature bovine IVD cells agreed that NP cells produce more proteoglycans and less collagen than AF and cartilage cells, which is consistent with the higher hydration of the NP tissue[6,29]. In rat spinal units it was demonstrated that NP can be distinguished from adjacent tissues by the expression of proteins that are synthesized in response to restriction in oxygen and nutrient supply[17]. Additional studies in the rat revealed other potentially NP specific markers[7,13]. However, a major disadvantage of using rat NP is the presence of cells with a notochordal phenotype. In fact several studies have used rat cells to explore the notochordal molecular phenotype in the disc[30,31]. Therefore, results from the rat, as well as mouse or rabbit have to be extrapolated with care to the human situation. Apart from the different developmental pathways of the NP cell populations the large deviations in IVD size and thus nutrition and mechanical conditions are also likely to influence the molecular characteristics of NP cells. Nevertheless, the expression profile of KRT19 demonstrates that selected genes may be valuable as markers even in different species.

When comparing the present study with previous studies on beagles, it also has to be noted that the human samples in this study are very heterogeneous with respect to age, while the animals all had the same age. This may explain the less pronounced differences between NP, AF, and cartilage cells in human individuals compared to the dog species, while general trends were identical in both species. Consequently, the age of the animal always has to be taken into consideration for the interpretation of results from an animal model. Moreover, although a study in the rat did not reveal major differences in gene expression pattern between RNA extracted from isolated cells and RNA extracted directly from the tissues, enzymatic cell isolation might have contributed to the reduced tissue-related differences observed in human specimens[7]. Besides, it is sometimes difficult to clearly distinguish human NP from AF tissue, especially in aged discs, which can also result in lowered gene expression differences between NP and AF cells. In view of these difficulties and the observed age-related alterations, young individuals are clearly preferred for the study of the phenotype of the healthy human NP cell.
Age-related changes have been detected regarding matrix composition, expression of matrix degrading enzymes, and other processes[3,6,32-34]. Although differences between aging and (early) degeneration were recently described in rabbits, a strong correlation exists between age and degeneration grade in human patients[3,35,36], which is confirmed in this study. Thus, it is not possible to clearly separate the influence of aging from that of degeneration mechanisms. Accordingly, Adams and Roughly defined a degenerate disc as one with structural failure combined with accelerated or advanced signs of aging[37]. This has recently been demonstrated also for the cervical spine, where in a longitudinal study no other factor except for age was related to the progression of degeneration[38]. Although cases of early disc degeneration have been described and are of particular value for specific investigation of degenerative processes, the present study evaluated individuals with ‘‘natural’’ disc development, where aging is accompanied with a certain degree

of degeneration. This is particularly reflected in the mRNA expression of MGP in the NP, which strongly correlated with both aging and degree of degeneration. MGP is a Bone morphogenetic protein-2 (BMP-2) regulatory protein that is known as a calcification inhibitor in cartilage and in arteries[39,40]. Interestingly, MGP serum levels of community-based cohorts were also elevated with increasing age and were associated with individual risk factors for coronary heart disease[41]. It was suggested that induction of MGP expression may be a feedback mechanism to prevent mineralization of calcium deposits in the arteries[41]. Similarly, one could speculate that induction of MGP in the NP may be an attempt to prevent calcification processes that have been observed in the aging disc[42,43]. The presence of MGP in areas of mineralized cartilage in the endplate and in cells adjacent to sites of degeneration would support this hypothesis. The same is true for the expression at the fibrocartilaginous attachment of the outer AF where ectopic ossification (i.e., osteophyte growth) would be prevented. Interestingly MGP expression in non-calcified AC is restricted to the superficial regions in monkeys and is barely detectable in senile human cartilage tissue[44]. In chondrocytic cells, both over-expression of MGP in maturing chondrocytes and under-expression of MGP in proliferative and hypertrophic chondrocytes may induce apoptosis[45]. As it has been reported that some cells of the IVD may differentiate towards the hypertrophic chondrocyte phenotype with age, MGP might function to prevent apoptosis in these cells[46]. Further studies are required to clarify the role of MGP expressed in the disc.
The observed rise in PTN gene expression in the AF with aging may result from a cellular attempt to restore a slowly degrading tissue. PTN functions as a growth and differentiation factor in many cell types and has been shown to induce the synthesis of matrix molecules in articular chondrocytes[47]. In cartilage, elevated PTN levels have been related to both osteoarthritis and rheumatoid arthritis[48,49]. Interestingly, an increased amount of PTN-immunopositive cells was observed in degenerated and in prolapsed disc samples and was associated with vascularisation of diseased or damaged tissue[50]. Since blood vessels are mostly localized in the outer AF and rarely penetrate into deeper zones of the IVD, an increasing expression of PTN in the AF with aging would support the suggestion that PTN may function as an angiogenic factor in the degenerating IVD[50]. Age- or degeneration-associated changes might become clinically useful markers to determine the ‘‘juvenileness’’ or the regenerative capacity of IVD tissues sampled from discectomies or nucleotomies. More extended studies will be required to validate the potential of such markers to individually evaluate the most appropriate treatment of an IVD disorder.

In conclusion, from a selection of NP phenotype markers identified in animal studies, KRT19 and NCAM1 expression were found to be more pronounced in NP than AF and AC cells in human individuals. Whereas NCAM1 levels are relatively low even in NP cells, KRT19 may be regarded as a marker for human NP cells, being highly expressed in NP and at significantly lower levels in AF and AC cells. This observation on the subject of gene expression is at least partially reflected at the protein level, where KRT19 positive cells are almost exclusively identified in the NP of juvenile and young adult discs. This suggests that KRT19 transcripts are translated into detectable amounts of protein primarily in notochordal-like cells of juvenile NP and occasionally in young chondrocyte-like NP cells. MGP is found in a variety of human IVD tissues and thus cannot serve as a characteristic NP marker.

Acknowledgements

The authors acknowledge the Department of Pathology of the UMC Utrecht, in particular F. Bernhard and A. de Ruiter for their help in obtaining the IVD specimens. This study was supported by the SwissNational Science Foundation (Grant #3320000-116818).

References

1. Waddell G. Low back pain: a twentieth century health care enigma. Spine 1996;21:2820-5.
2. Phelip X. Why the back of the child? Eur Spine J 1999;8:426-8.
3. Antoniou J, Steffen T, Nelson F, Winterbottom N, Hollander AP, Poole RA, et al. The human lumbar intervertebral disc: evidence for changes in the biosynthesis and denaturation of the extracellular matrix with growth, maturation, ageing, and degeneration. J Clin Invest 1996;98:996-1003.
4. Leung VY, Chan D, Cheung KM. Regeneration of intervertebral disc by mesenchymal stem cells: potentials, limitations, and future direction. Eur Spine J 2006;15(Suppl 3):S406-13.
5. Hiyama A, Mochida J, Sakai D. Stem cell applications in intervertebral disc repair. Cell Mol Biol (Noisy-le-grand) 2008;54:24-32.
6. Mwale F, Roughley P, Antoniou J. Distinction between the extracellular matrix of the nucleus pulposus and hyaline cartilage: a requisite for tissue engineering of intervertebral disc. Eur Cell Mater 2004;8:58-63.
7. Lee CR, Sakai D, Nakai T, Toyama K, Mochida J, Alini M, et al. A phenotypic comparison of intervertebral disc and articular cartilage cells in the rat. Eur Spine J 2007;16:2174-85.
8. Sakai D, Nakai T, Mochida J, Alini M, Grad S. Differential phenotype of intervertebral disc cells: microarray and immunohistochemical analysis of canine nucleus pulposus and anulus fibrosus. Spine 2009;34:1448-56.
9. Alini M, Eisenstein SM, Ito K, Little C, Kettler AA, Masuda K, et al. Are animal models useful for studying human disc disorders/degeneration? Eur Spine J 2008;17:2-19.
10. Hunter CJ, Matyas JR, Duncan NA. Cytomorphology of notochordal and chondrocytic cells from the nucleus pulposus: a species comparison. J Anat 2004;205:357-62.
11. Thompson JP, Pearce RH, Schechter MT, Adams ME, Tsang IK, Bishop PB. Preliminary evaluation of a scheme for grading the gross morphology of the human intervertebral disc. Spine 1990;15:411-5.
12. Reno C, Marchuk L, Sciore P, Frank CB, Hart DA. Rapid isolation of total RNA from small samples of hypocellular, dense connective tissues. Biotechniques 1997;22:1082-6.
13. Fujita N, Miyamoto T, Imai J, Hosogane N, Suzuki T, Yagi M, et al. CD24 is expressed specifically in the nucleus pulposus of intervertebral discs. Biochem Biophys Res Commun 2005;338:1890-6.
14. Livak KJ, Schmittgen TD. Analysis of relative gene expression data using real-time quantitative PCR and the 2(-Delta Delta C(T)) method. Methods 2001;25:402-8.
15. Lee CR, Grad S, MacLean JJ, Iatridis JC, Alini M. Effect of mechanical loading on mRNA levels of common endogenous controls in articular chondrocytes and intervertebral disk. Anal Biochem 2005;341:372-5.
16. Kristensen HK. An improved method of decalcification. Stain Technol 1948;23:151-4.
17. Rajpurohit R, Risbud MV, Ducheyne P, Vresilovic EJ, Shapiro IM. Phenotypic characteristics of the nucleus pulposus: expression of hypoxia inducing factor-1, glucose transporter-1 and MMP-2. Cell Tissue Res 2002;308:401-7.
18. Stosiek P, Kasper M, Karsten U. Expression of cytokeratin and vimentin in nucleus pulposus cells. Differentiation 1988;39:78-81.
19. Gottschalk D, Fehn M, Patt S, Saeger W, Kirchner T, Aigner T. Matrix gene expression analysis and cellular phenotyping in chordoma reveals focal differentiation pattern of neoplastic cells mimicking nucleus pulposus development. Am J Pathol 2001;158:1571-8.

20. Rutishauser U, Acheson A, Hall AK, Mann DM, Sunshine J. The neural cell adhesion molecule (NCAM) as a regulator of cell-cell interactions. Science 1988;240:53-7.
21. Acheson A, Sunshine JL, Rutishauser U. NCAM polysialic acid can regulate both cellecell and cellesubstrate interactions. J Cell Biol 1991; 114:143-53.
22. Filiz S, Dalcik H, Yardimoglu M, Gonca S, Ceylan S. Localization of neural cell adhesion molecule (N-CAM) immunoreactivity in adult rat tissues. Biotech Histochem 2002;77:127-35.
23. Fang J, Hall BK. N-CAM is not required for initiation of secondary chondrogenesis: the role of N-CAM in skeletal condensation and differentiation. Int J Dev Biol 1999;43:335-42.
24. Ishii Y, Thomas AO, Guo XE, Hung CT, Chen FH. Localization and distribution of cartilage oligomeric matrix protein in the rat intervertebral disc. Spine 2006;31:1539-46.
25. Hyc A, Osiecka-Iwan A, Jozwiak J, Moskalewski S. The morphology and selected biological properties of articular cartilage. Ortop Traumatol Rehabil 2001;3:151-62.
26. Chelberg MK, Banks GM, Geiger DF, Oegema Jr TR. Identification of heterogeneous cell populations in normal human intervertebral disc. J Anat 1995;186(Pt 1):43-53.
27. Sive JI, Baird P, Jeziorsk M, Watkins A, Hoyland JA, Freemont AJ. Expression of chondrocyte markers by cells of normal and degenerate intervertebral discs. Mol Pathol 2002;55:91-7.
28. Poiraudeau S, Monteiro I, Anract P, Blanchard O, Revel M, Corvol MT. Phenotypic characteristics of rabbit intervertebral disc cells. Comparison with cartilage cells from the same animals. Spine 1999;24: 837-44.
29. Horner HA, Roberts S, Bielby RC, Menage J, Evans H, Urban JP. Cells from different regions of the intervertebral disc: effect of culture system on matrix expression and cell phenotype. Spine 2002;27: 1018-28.
30. Chen J, Yan W, Setton LA. Molecular phenotypes of notochordal cells purified from immature nucleus pulposus. Eur Spine J 2006;15(Suppl 3):S303-11.
31. Oguz E, Tsai TT, Di Martino A, Guttapalli A, Albert TJ, Shapiro IM, et al. Galectin-3 expression in the intervertebral disc: a useful marker of the notochord phenotype? Spine 2007;32:9-16.
32. Le Maitre CL, Freemont AJ, Hoyland JA. Localization of degradative enzymes and their inhibitors in the degenerate human intervertebral disc. J Pathol 2004;204:47-54.
33. Le Maitre CL, Freemont AJ, Hoyland JA. Human disc degeneration is associated with increased MMP 7 expression. Biotech Histochem 2006;81:125-31.
34. Nerlich AG, Schleicher ED, Boos N. 1997 Volvo award winner in basic science studies. Immunohistologic markers for age-related changes of human lumbar intervertebral discs. Spine 1997;22:2781-95.
35. Sowa G, Vadala G, Studer R, Kompel J, Iucu C, Georgescu H, et al. Characterization of intervertebral disc aging: longitudinal analysis of a rabbit model by magnetic resonance imaging, histology, and gene expression. Spine 2008;33:1821-8.
36. Miller JA, Schmatz C, Schultz AB. Lumbar disc degeneration: correlation with age, sex, and spine level in 600 autopsy specimens. Spine 1988; 13:173-8.
37. Adams MA, Roughley PJ. What is intervertebral disc degeneration, and what causes it? Spine 2006;31:2151-61.
38. Okada E, Matsumoto M, Ichihara D, Chiba K, Toyama J, Fujiwara H, et al. Aging of the cervical spine in healthy volunteers: a 10-year longitudinal magnetic resonance imaging study. Spine 2009;34:706-12.

39. Luo G, Ducy P, McKee MD, Pinero GJ, Loyer E, Behringer RR, et al. Spontaneous calcification of arteries and cartilage in mice lacking matrix gla protein. Nature 1997;386:78-81.
40. Zebboudj AF, Imura M, Bostrom K. Matrix gla protein, a regulatory protein for bone morphogenetic protein-2. J Biol Chem 2002;277: 4388-94.
41. O'Donnell CJ, Shea MK, Price PA, Gagnon DR, Wilson PW, Larson MG, et al. Matrix gla protein is associated with risk factors for atherosclerosis but not with coronary artery calcification. Arterioscler Thromb Vasc Biol 2006;26:2769-74.
42. Cheng XG, Brys P, Nijs J, Nicholson P, Jiang Y, Baert AL, et al. Radiological prevalence of lumbar intervertebral disc calcification in the elderly: an autopsy study. Skeletal Radiol 1996;25:231-5.
43. Oda J, Tanaka H, Tsuzuki N. Intervertebral disc changes with aging of human cervical vertebra. From the neonate to the eighties. Spine 1988;13:1205-11.
44. Loeser R, Carlson CS, Tulli H, Jerome WG, Miller L, Wallin R. Articular- cartilage matrix gamma-carboxyglutamic acid-containing protein. Characterization and immunolocalization. Biochem J 1992; 282(Pt 1):1-6.
45. Newman B, Gigout LI, Sudre L, Grant ME, Wallis GA. Coordinated expression of matrix gla protein is required during endochondral ossification for chondrocyte survival. J Cell Biol 2001;154:659-66.
46. Aigner T, Gresk-otter KR, Fairbank JC, Von der Mark K, Urban JP. Variation with age in the pattern of type X collagen expression in normal and scoliotic human intervertebral discs. Calcif Tissue Int 1998;63:263-8.
47. Tapp H, Hernandez DJ, Neame PJ, Koob TJ. Pleiotrophin inhibits chondrocyte proliferation and stimulates proteoglycan synthesis in mature bovine cartilage. Matrix Biol 1999;18:543-56.
48. Pufe T, Bartscher M, Petersen W, Tillmann B, Mentlein R. Pleiotrophin, an embryonic differentiation and growth factor, is expressed in osteoarthritis. Osteoarthritis Cartilage 2003;11:260-4.
49. Pufe T, Bartscher M, Petersen W, Tillmann B, Mentlein R. Expression of pleiotrophin, an embryonic growth and differentiation factor, in rheumatoid arthritis. Arthritis Rheum 2003;48:660-7.
50. Johnson WE, Patterson AM, Eisenstein SM, Roberts S. The presence of pleiotrophin in the human intervertebral disc is associated with increased vascularization: an immunohistologic study. Spine 2007;32:1295-302.

CHAPTER 7

A validated new histological classification for intervertebral disc degeneration

JPHJ Rutges, RA Duit, JA Kummer, JEJ Bekkers, FC Oner, RM Castelein, WJA Dhert and LB Creemers

Osteoarthritis and Cartilage (2013) 21:2039-47

Abstract

Histology is an important outcome variable in basic science and pre-clinical studies regarding intervertebral disc degeneration (IVD). Nevertheless, an adequately validated histological classification for IVD degeneration is still lacking and the existing classifications are difficult to use for inexperienced observers.

Therefore the aim of this study was to develop and to validate a new histological classification for IVD degeneration. Moreover, the new classification was compared to the frequently used nonvalidated classification.

The new classification was applied to human IVD sections. The sections were scored twice by two independent inexperienced observers, twice by two experienced IVD researchers and once by a pathologist. For comparison, the sections were also scored according to the classification described by Boos et al. by two experienced IVD researchers. Macroscopic grading according Thompson et al., glycosaminoglycan (GAG) content and age were used for validation.

The new classification had an excellent intra- and a good inter-observer reliability. Intraclass Correlation Coefficients (ICC) were 0.83 and 0.74, respectively. Intra- and inter-observer reliability were comparable for experienced and inexperienced observers. Statistically significant correlations were found between the new classification, macroscopic score, GAG content in the nucleus pulposus (NP) and age; Correlation coefficient (CC) 0.79, -0.62 and 0.68, respectively. The CCs of the Boos classification were all lower compared to the new classification.

The new histological classification for IVD degeneration is a valid instrument for evaluating IVD degeneration in human IVD sections and is suitable for inexperienced and experienced researchers.

Introduction

Low back pain is one of the major health problems in industrialized countries, with annual costs in European countries ranging from 0.6% to 2.3% of the gross national product (GNP)[1-3]. Intervertebral disc (IVD) degeneration is considered as one of the major causes of chronic low back pain[4-6]. Consequently, the IVD research intensified significantly during the past decade[6]. Fundamental biochemical studies have further elucidated the involvement of cytokines and degenerative enzymes in IVD degeneration and new tissue engineering and regenerative medicine-based treatment strategies have been developed[6]. In many of these studies, histology of human or animal IVDs has been used for stratification of the samples or as outcome variable. Although histology is very commonly used for this purpose, a well validated histological classification for human IVD degeneration is lacking. The most commonly used histological classification for human IVD degeneration is the score described by Boos et al.[7]. In this article aged-related changes of lumbar intervertebral discs are described in detail, and these characteristics were used to develop a grading system for IVD degeneration[7]. Although this score was developed after a very thoroughly conducted study on a large number of human IVD sections, the validation of the proposed classification could methodologically be improved[7]. Samples were scored once, by only 2 observers, therefore the intra-observer reliability could not be calculated[7]. Additionally the inter-observer reliability was not determined and only the grade of agreement between the observers was analysed by calculating the kappa value[7]. The ability of the classification to predict the age of the patients and the macroscopic degeneration grade according Thompson was analysed with a CHAID analysis[7,8]. However, correlation coefficients between the classification, extracellular proteoglycan content, age and Thompson grades were not described[7,8]. The degeneration score by Boos et al. is the only peer-reviewed published classification and is used by numerous IVD researchers including the authors of the current study[9-12]. Besides the possible methodological optimization of the Boos score there are also some practical aspects of the score that can be improved. For the complete score, the IVD needs to be graded on six different items and the endplate (EP) on another five items. Some of these items need to be graded on a 1-7 scale. Due to its complex design and large number of grading items, the Boos classification is often modified and mainly used by experienced IVD researchers[9-12]. Most modifications are simplifications of the classification, items that were difficult to score have been left out of the classification or the number of scoring options per item were limited[9-12]. The authors of this study also experienced some difficulties while using this system in their studies. Some items like mucoid degeneration and granular changes are inadequately described and are only displayed on small images in the original publication. Furthermore, tear and cleft formation results in the highest grade of degeneration in several of the items of the Boos score, whereas tears and clefts can also be caused by the extensive process of tissue preparation comprising decalcification, dehydration, embedding and sectioning. For inexperienced observers it is difficult distinguish between processing artifacts and degenerative characteristics, thus requiring extensive experience with IVD histology[7]. An easier to use and adequately validated histological classification for age-related- degenerative IVD changes would significantly contribute to the standardization of histology in fundamental and translational IVD research[13]. Therefore the aim of this study was to develop an easily applicable histological classification for human IVD discs which can be used by both experienced

and inexperienced observers. Both the new and the Boos classification were validated based on macroscopic degeneration according Thompson et al., age and glycosaminoglycan (GAG) content[8].

Materials and methods

Sample acquisition

Human IVDs were obtained at autopsy as part of the standard procedure, in which a section of the lumbar and thoracic spine is removed for diagnostic purposes. Samples were obtained within 48 h after death of the patient (93.4% of the patients within 24 h). Anonymous use of redundant tissue for research purposes is part of the standard treatment agreement with patients in our university hospital. In the time period between death and tissue collection, the deceased patients were kept at the mortuary at 4°C. From all patients, only the IVD between the fourth and fifth lumbar vertebra (L4-L5), including the adjacent EPs, was obtained. One grade I IVD from a 23-year-old patient was acquired at oncologic spine surgery, but the obtained IVD was not affected by a malignant process. Most common causes of death in adult patients were sepsis, metastatic disease and myocardial or brain infarction. In children and adolescents, the most common causes of death were cardiac arrhythmia and neurological trauma. After resection, the post-mortem samples were processed into mid-sagittal slices and stored in 4% formalin. The macroscopic grade of degeneration was scored by three individual observers (JR, RD and LC) according to Thompson et al[8]. After individual scoring, the score was averaged; outliers, i.e., more than one Thompson grade difference, were re-evaluated by the three observers at a consensus meeting. The remaining sagittal slices were macroscopically divided in nucleus pulposus (NP) and annulus fibrosis (AF) tissue and were embedded in TissueTek (Sakura Finetek Europe Zoeterwoude, The Netherlands) for cryosectioning and GAG analysis. In total sixty-one IVDs with an equal distribution over all five degeneration grades were processed for histological staining and a dimethylmethylene blue (DMMB) assay for the determination of proteoglycan content (table 7.1).

Table 7.1. Patients' characteristics for each Thompson degeneration grade

Thompson grade	N	Gender		Mean age (years)	Range (years)
		M	F		
I	12	4	8	16.5	3.3 – 34.2
II	12	8	4	46.4	17.0 – 69.3
III	13	8	5	65.0	46.9 – 77.4
IV	12	3	9	74.6	54.3 – 88.5
V	12	5	7	77.6	59.5 – 88.2
Total	61	28	33	56.2	3.3 – 88.5

Histology

Mid-sagittal IVD slices were decalcified in Kristensen's solution (50% formic acid and 68 g/l sodium formate) in a microwave (Milestone Microwave Laboratory Systems, Italy) at 150W and 50°C for 6 h[14].

After deparaffinization in xylene and a graded series of alcohols, hematoxylin and eosin (H&E), Alcian blue picrosirius red (ABPR) and safranin-O (Saf O) staining were performed on 5 µm thick sections. H&E and Saf O staining were performed according to the OARSI guidelines and the ABPR staining as described by Gruber et al[15,16].

Quantification of GAG

NP and AF tissue was cryosectioned before digestion, the approximately 100 sections per sample were weighted before digestion, with a mean weight of 53.7 mg per sample. IVD tissue was digested overnight at 56°C in PBS containing 250 µg/mL papain (Sigma, St. Louis, US). Hundred micro liters standard or 1:800 diluted tissue sample was added to 200 µL of filtered DMMB solution (Sigma, St. Louis, US) (pH 3.0) as prepared by Farndale et al[17.] Intensity of colour change was quantified immediately in a microplate reader (Bio-Rad model 3550, Hercules, US) by measuring absorbance at 540 and 595 nm. GAG per milligram digested IVD tissue was calculated using a standard of chondroitin sulfate C (Sigma, St Louis, US) and by calculating the ratio of absorbances.

Classification

Based on previous literature, experiences with histological grading of degenerative IVDs and macroscopic and radiological characteristics of degenerative IVDs, a new histological classification was developed [7,8,18-20]. All three major anatomical structures of the intervertebral disc, AF, NP and the EP were included in the new classification, resulting in six subcategories (table 7.1 and figure 7.1). Each item was graded 0, 1 or 2 on the HE sections; 0 representing no degenerative characteristics, 1 mild degenerative characteristics and 2 severe characteristics of degeneration (table 7.2 and figure 7.1). The total score of the new classification is the sum of the six different scorings item, resulting in a minimum score of zero points in a completely healthy IVD and a maximum of 12 points for an entirely degenerated IVD. A more detailed description of the grading process can be found in the supplement of this chapter.

GAG content based on NP matrix staining was classified on both Saf O and ABPR stained sections. The staining with the highest correlation to macroscopic degeneration and GAG content (DMMB assay) was selected as GAG staining for the new classification. Besides histological evaluation of GAG content in the NP, Saf O and ABPR sections can be used for evaluation of the transition zone between AF and NP tissue and AF morphology (figure 7.2). All separate items were correlated to the macroscopic grading according Thompson et al. (table 7.5)[8]. The matrix staining on Saf O and ABPR sections was additionally correlated to age and GAG content in the NP. The correlation coefficients (CCs) for the Saf O staining using Thompson score, GAG content and age were 0.58,-0.39, -054 respectively, $P < 0.001$ for Thompson score and age and $P = 0.002$ for GAG content. The CCs for the ABPR staining were 0.54, -0.45, -0.49 respectively, $P < 0.001$ for all three CCs. Due to the mean higher CC of the Saf O staining, this staining was chosen for assessment of the GAG content in the NP matrix in the new histological classification.

Table 7.2. Scoring items and grades from the new histological degeneration classification for IVD degeneration. Histological examples of each degeneration grade per scorings item can be found in figure 7.1 and figure 7.2. Saf. O.: safranin-O staining and ABPR: alcian blue picrosirius red staining.

A: Endplate		Figure 7.1
0	Homogeneous structure; regular thickness	A0
1	Slight irregularity with limited number of microfractures and locally decreased thickness	A1
2	Severe irregularity with multiple microfractures of the endplate and generalized decreased thickness	A2

B: Morphology AF		Figure 7.1/ Figure 7.2
0	Well-organized, half ring-shaped structure, collagen lamellae	B0 / B0
1	Partly ruptured AF; loss of half ring-shaped structure	B1 / B1
2	Completely ruptured AF; no intact half ring-shaped collagen lamellae	B2 / B2

C: Boundary AF and NP		Figure 7.1/ Figure 7.2
0	Clear boundary between AF and NP tissue	C0 / C0
1	Boundary less clear; loss of annular-nuclear demarcation	C1 / C1
2	No distinguishable boundary between AF and NP tissue	C2 / C2

D: Cellularity NP		Figure 7.1
0	Normal cellularity; no cell clusters	D0
1	Mixed cellularity; normal pattern with some cell clusters	D1
2	Mainly clustered cellularity, chondroid nests present	D2

E: Matrix NP		Figure 7.1
0	Well-organized structure of nucleus matrix	E0
1	Partly disorganised structure of nucleus matrix	E1
2	Complete disorganisation and loss of nucleus matrix	E2

F: NP matrix staining		Figure 7.1
0	Intense staining; red stain dominates	F0
1	Reduced staining; mixture of red and slight green staining	F1
2	Faint staining; increased green staining	F2

Maximum score 12	(ABPR staining of the NP matrix not included)	

G: NP matrix staining	(ABPR staining of the NP matrix was not included in the definitive classification of IVD degeneration)	Figure 7.1
0	Intense staining; blue staining dominates	G0
1	Reduced staining; mixture of blue and slight red staining	G1
2	Faint staining; increased red staining	G2

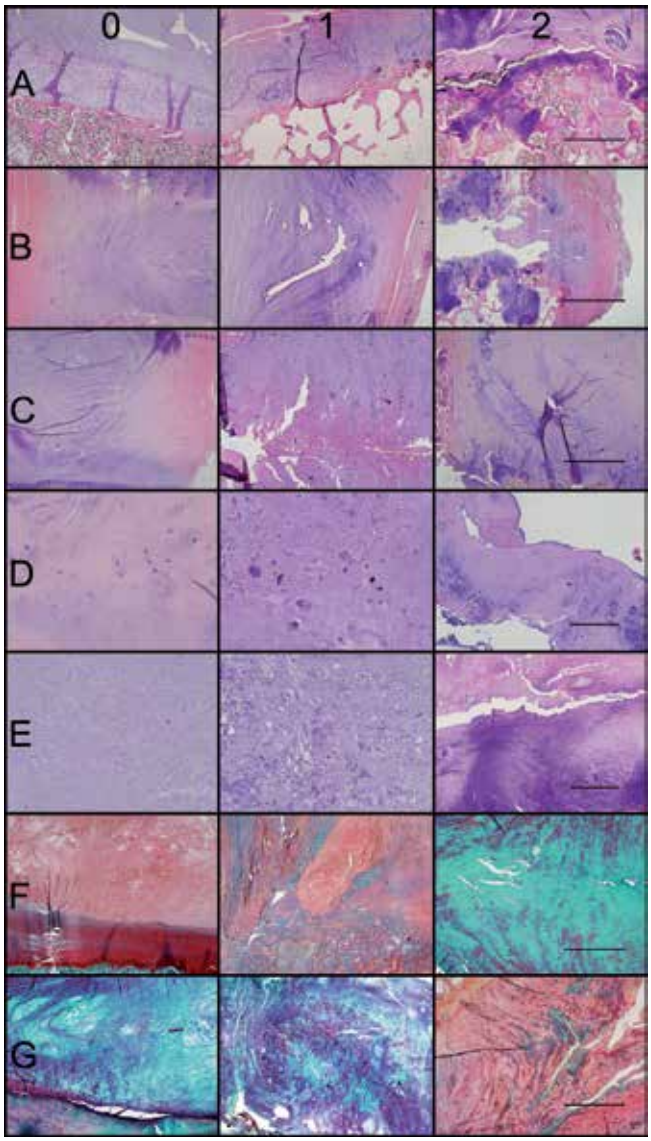

Figure 7.1 Histological examples of each degeneration grade per scorings item of the new histological IVD degeneration classification.
A: Endplate (HE), B: Morphology AF (HE), C: Boundary AF and NP (HE), D: Cellularity NP (HE), E: Matrix NP (HE), F: NP matrix staining (Saf O) and G: NP matrix staining (ABPR). The number 0 represents no degenerative characteristics, 1 mild degenerative characteristics and 2 severe characteristics of degeneration.
HE: hematoxylin and eosin staining. Saf O: safranin-O staining and ABPR: alcian blue and picrosirius red staining. Scale bars represent 2.0 mm in A, B, C, F, G, 200 µm in D and 500 µm in E. A description of each scoring item can be found in table 7.2.

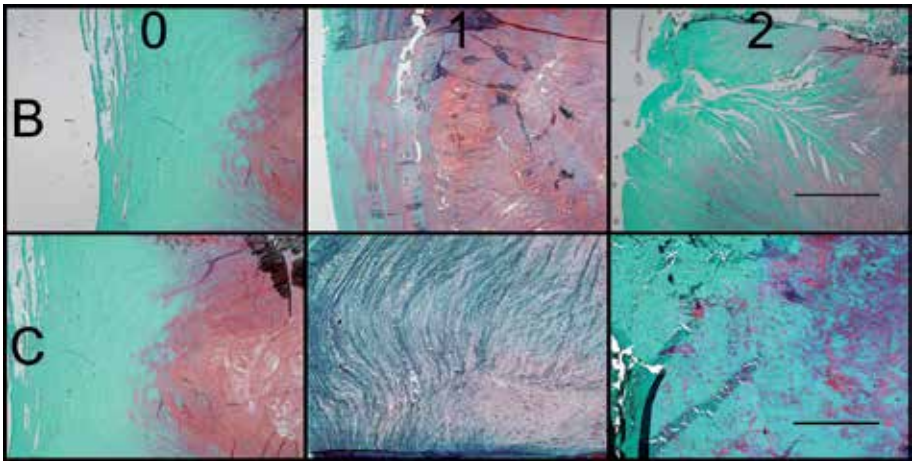

Figure 7.2. Additionally the Saf O sections can be used for evaluation of the morphology of the AF and to the boundary between AF and NP tissue. B: Morphology AF Saf O and C: Boundary AF and NP Saf O. The number 0 represents no degenerative characteristics, 1 mild degenerative characteristics and 2 severe characteristics of degeneration. Scale bars represent 2.0 mm in all images. A description of each scoring item can be found in table 7.2.

Scoring

Out of the sections of in total 61 IVDs, a test set of samples was composed and subsequently scored by three independent, inexperienced observers; a senior researcher, a PhD student and a research technician. The test set contained HE and Saf O sections of 10 IVDs, two from each Thompson degeneration grade[8]. None of the test observers was familiar with microscopic evaluation of IVD tissue. Based on the results and comments of the three observers, the description of the items and the example images were further adjusted. No evident problems or difficulties were encountered during evaluation of the test results. Four other observers scored all blinded 61 samples according to the adjusted new classification, of whom two, a laboratory technician and a PhD student (JB), were inexperienced with IVD histology. The other two observers have extensive experience with IVD histology, one is a pathologist with special interest in the IVD (AK) and the other a PhD student focusing on IVD degeneration (JR). The classification as described by Boos et al. was applied by two experienced observers, both PhD students focusing on IVD degeneration (JR and RD). All observers were trained how to perform the new histological grading. Scoring items were explanted (JR and RD) and typical examples were shown microscopically, approximately 5-10 slides were shown. Moreover 10 test slides were graded by the observers and evaluated (JR and RD) before grading the 61 samples described in the current study. For both the new classification and the Boos score the same sixty-one samples were used. All observers graded the sections twice, with an intermediary period of at least 4 weeks, except for the pathologist who graded the sections only once. For the IVD researcher who applied both the new and Boos classification (JR), the time passed between two evaluations was >1 year for the different classifications, and >4 weeks between the first and the second grading.

Statistical analysis

Statistical analyses were performed using the Statistical Package for the Social Sciences (SPSS) 16.0 software for Windows (SPSS Inc., Chicago, IL, USA). Spearman's non-parametric test was used for correlation analyses (CC) of both scoring systems, macroscopic degeneration according Thompson et al., GAG content and age[8]. Intra- and interobserver reliability were assessed by calculating the Intraclass Correlation Coefficient (ICC) for both scoring systems. A two-way mixed model was used based on consistency. The given ICCs in the manuscript were the "single measures" values. It is not possible with SPSS, statistical analysis system (SAS) or any other standard statistical program to determine if there are statistical differences between ICCs or CCs. Therefore we assessed ICCs and CC as described by Field, Fleiss, Westgard, Bland and Altman[21-24]. The concordance is considered good if the ICC is 0.4-0.75 and excellent if the ICC is >0.75[21-23]. The CC is considered low between 0.30 and 0.49, moderate between 0.50 and 0.69, high between 0.70 and 0.89 and very high between 0.89 and 1.00[24]. Agreement between the Boos and the new classification was analyzed as described by Bland and Altman[21]. For the Bland Altman plot, a transformation of both scores to a percentage of the maximum score was required.

Results

Inter- and intra-observer reliability

The intra-observer reliability for the new classification was excellent for both the inexperienced and experienced observers, with a mean ICC of 0.84, 0.79 for inexperienced and 0.93 for experienced observers, respectively. The mean inter-observer reliability of the new classification was good, with a mean ICC of 0.74. The mean inter-observer reliability between experienced and inexperience observers was also good, with a mean ICC of also 0.74, range 0.67-0.80. The intra-observer reliability for the Boos score was excellent for the two experienced observers, the mean ICC was 0.79. The interobserver reliability was also excellent with a mean ICC 0.79 (table 7.3).

Table 7.3. Intra- and inter-observer reliability, shown by the intraclass correlation coefficient (ICC), for the Boos and new classification

	Intra-observer reliability (ICC)	Inter-observer reliability (ICC)
New classification	**Mean (95% CI)**	**Mean (95% CI)**
All observers	0.84 (0.74-0.90)	0.74 (0.58-0.84)
Inexperienced observers	0.79 (0.67-0.87)	0.73 (0.59-0.83)
Experienced observers	0.93 (0.88-0.96)	0.72 (0.54-0.84)
Experienced vs inexperienced	-	0.84 (0.74-0.90)
Boos classification		
Experienced observers	0.79 (0.68-0.87)	0.79 (0.68-0.87)

Thompson score and age

The Boos and the new classification scores for each Thompson grade are shown in figure 7.3. Both scoring systems were correlated to the macroscopic degeneration grade. A high CC of 0.79 ($P < 0.001$) was found between the new classification and the macroscopic degeneration score according Thompson. The CC between the Boos classification and Thompson score was moderate 0.69 ($P < 0.001$) (table 7.4). Correlation coefficients for age and the two classifications were both moderate, 0.68 ($P < 0.001$) for the new classification and 0.65 ($P < 0.001$) for the Boos score (figure 7.4). Additionally all separate items of the new classification were correlated to the Thompson score and age (table 7.5).

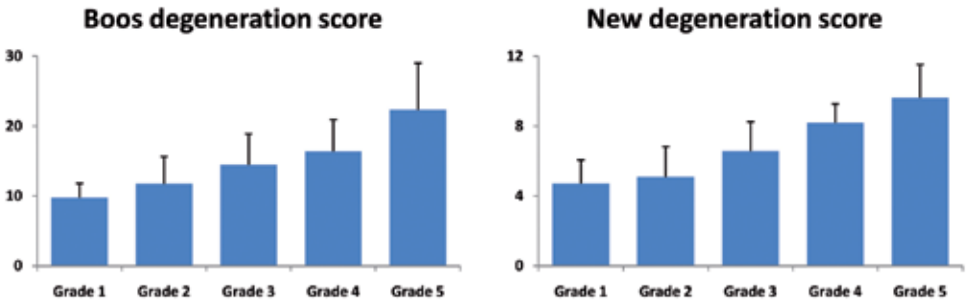

Figure 7.3. Boos and new IVD degeneration score in all five macroscopic degeneration grades according Thompson et al.

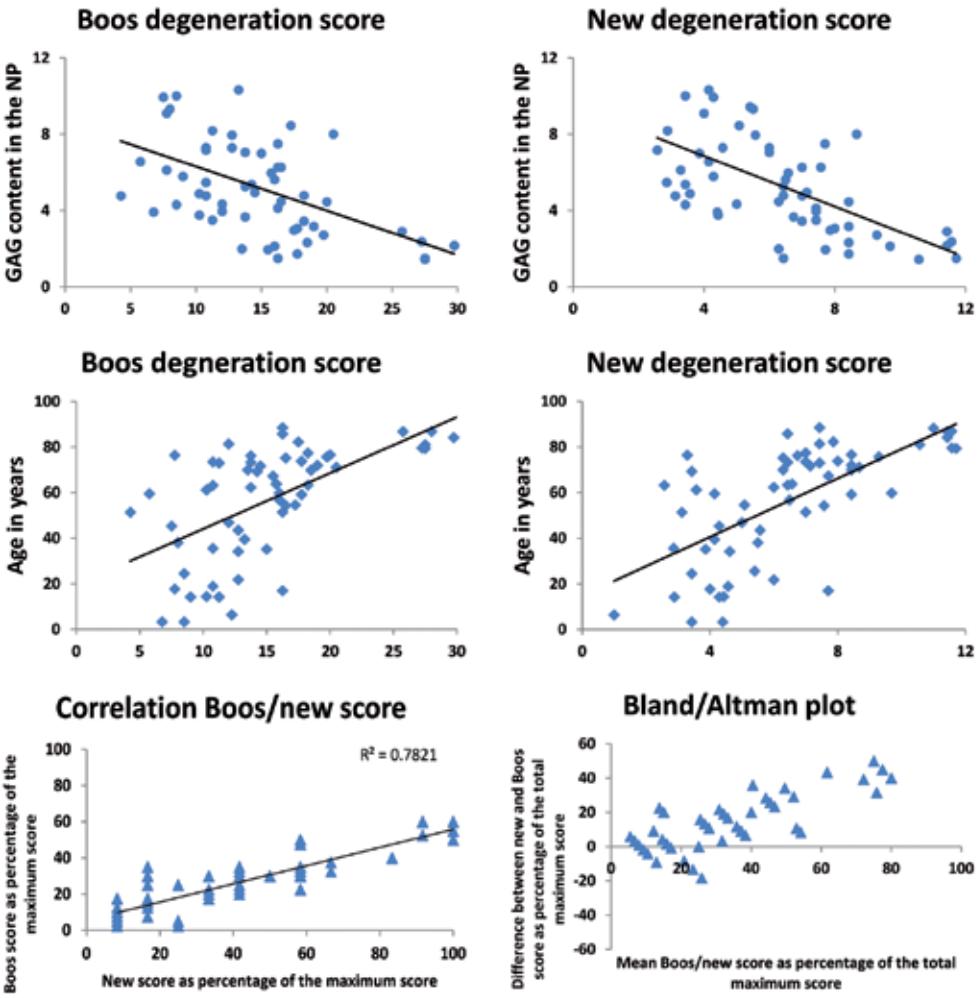

Figure 7.4. Scatter plot of GAG content in NP for the Boos and the new classification (dots). Scatter plot of age for the Boos and the new classification (squares). Scatter and Bland Altman plot of the Boos and the new classification (triangles).

Table7.4. Differences in correlation coefficient (CC) between the new and the Boos score for IVD degeneration.

	Boos classification (CC)	New classification (CC)
Thompson macroscopic score	0.69 (p <0.001)	0.79 (p <0.001)
Age	0.65 (p <0.001)	0.69 (p <0.001)
GAG content NP	- 0.50 (p <0.001)	- 0.62 (p <0.001)
GAG content AF	- 0.30 (p=0.020)	- 0.30 (p=0.023)

Correlation to GAG content

The new classification displayed a moderate negative correlation with the GAG content in the NP and a low correlation with GAG content in the AF (CC - 0.62 (P < 0.001) and CC - 0.30 (P = 0.0023), respectively). The Boos score also showed a moderate negative correlation to the GAG content of the NP (CC - 0.50 (P < 0.001)) and a low negative correlation to GAG content in the AF (CC - 0.30 (P = 0.020)). Correlations between the two classifications and the GAG content in the NP are shown by the scatter plots in figure 7.4. Additionally, all separate items of the new classification were correlated to the GAG content of the NP (table 7.5).

Table 7.5. Correlation coefficient (CC) with the macroscopic IVD degeneration score according Thompson score, age and GAG content per item of the new classification.

Scorings item	Thompson grade (CC) (p-value)	Age (CC) (p-value)	GAG content NP (CC) (p-value)
Morphology AF	0.70 (<0.001)	0.64 (<0.001)	-0.55 (<0.001)
Cellularity NP	0.68 (<0.001)	0.53 (<0.001)	-0.52 (<0.001)
Matrix	0.58 (<0.001)	0.54 (<0.001)	-0.53 (<0.001)
Endplate	0.72 (<0.001)	0.62 (<0.001)	-0.51 (<0.001)
Boundary NP/AF	0.72 (<0.001)	0.65 (<0.001)	-0.48 (<0.001)
Saf-O	0.58 (<0.001)	0.54 (<0.001)	-0.39 (0.002)
ABPR*	0.54 (<0.001)	0.49 (<0.001)	-0.45 (0.006)

Saf. O.: safranin-O staining and ABPR: alcian blue picrosirius red staining. * ABPR staining of the NP matrix was not included in the definitive classification of IVD degeneration.

Correlation of the Boos and the new classification

There was a high correlation, CC 0.78, between the Boos and the new degeneration score (figure 7.4). Agreement of the Boos and the new classification was analyzed with a Bland-Altman plot, as shown in figure 7.4. The Boos score was usually a lower percentage of the maximum score than the new classification, shown by the larger number of positive numbers when the differences between the new and the Boos score were calculated. Moreover the difference increased with higher degeneration grades, indicating that the correlation between the scores decreased with increase of the degeneration grade.

Discussion

The current study demonstrates that the new histological scoring system for the IVD is a valid instrument for grading various levels of age-related IVD degeneration and is the first biochemically validated histological IVD degeneration classification system. Intra and inter-observer reliability is comparable to the Boos classification, the only available peer-reviewed histological classification for IVD degeneration. Moreover the new classification showed a higher correlation coefficient with Thompson scores, age and GAG content in the NP when compared to the Boos classification.

Despite the fact that the Boos score is a valid classification of histological IVD degeneration, also proven in the current study, it is very extensive and difficult to use, especially for inexperienced IVD researchers. Therefore, the aim of the current study was to develop a classification that was easier to use and contained a reduced number of scorings items. When compared to the Boos classification, it is less elaborate with only six scoring items, whereas the former has 11 items. Moreover, these items only need to be graded at three levels: healthy, moderate en severe degeneration, while the Boos score has 3-7 different scorings options per item. To evaluate if the new scorings system was clear and easy to use for experienced and inexperienced observers the scorings forms were first tested in a small pilot set by three inexperienced observers.

Additionally the complete set of 61 samples was graded by two experienced and two inexperienced observers. Our reliability analysis showed an excellent intra- and a good inter-observer reliability for both groups. Therefore the new classification is suitable for both experience and inexperienced IVD researchers. As we developed the new classification, we made sure that all three different anatomical regions of the IVD were represented in the scoring system. In the Boos classification only the complete IVD, with emphasis on the NP, and EP were represented, the AF is not separately represented in the classification. Since the AF is involved in almost all forms of IVD degeneration, the AF should be separately evaluated in every macroscopic, radiological of histological classification for IVD degeneration[18,20,25]. In the new histological score, the AF is evaluated by two, the NP by three and the EP by one scoring item.

In addition to macroscopic degeneration, GAG loss in the NP is a well-known characteristic of IVD degeneration[18,20]. The new classification showed a moderate correlation with the GAG content in the NP, higher than the correlation with the Boos score, indicating that the new scoring system is a valid method to determine the level of histological IVD degeneration. This is further supported by the correlation of the new classification and the Thompson score and age. Strikingly the correlation between the Saf O staining of the NP matrix and the GAG content was, although statistically significant, the lowest of al scoring parameters. This finding could be explained by the fact that proteoglycans are still produced in the NP of degenerative IVDs[18,20]. For example large amounts of proteoglycans are found around chondrocyte nests[18,20]. These proteoglycans could be responsible for the low correlation between NP staining and GAG content[18,20]. Moreover, although considered a standard staining for GAG content several studies report that Saf O staining is not a sensitive method to determine the GAG content[26,27]. This could also be an explanation

for the low correlation between the GAG content and NP score. Boos et al. based their frequently used score for degenerative changes in the IVD on degenerative characteristic seen in IVDs of older patients and validated the scoring on age. Therefore, in the current study age was also chosen as validation parameter, enabling comparison of our results using the Boos score to the results in the original article. The increase of age-related changes as scored according Boos in this study were comparable to the results described in the manuscript by Boos et al[7]. Nevertheless, age is not an ideal validation parameter for a histological grading of IVD degeneration.

Although age is a well known and a major risk factor for IVD degeneration, the age distribution in the five macroscopic degeneration grades, table 7.1, show clearly why age must not be equated with degeneration [7,18,20,28,29]. A grade V disc was already found in a 59-year-old patient and a grade II disc was still found in a 69-year old patient.

Despite the thorough validation of the current scoring system, it has some minor limitations. The separation of NP and AF tissue for biochemical analysis was done macroscopically by separation of the tissue with a scalpel blade. This could theoretically have introduced some bias to our analysis, however in most samples the border between transition zone and the NP was clearly visible. In addition, the mid-sagittal IVD tissue was used for histology and tissue from the more lateral part was used for biochemistry. Even though the tissue for biochemical analysis and histology were situated only a few millimeters away from each other in the intact IVD, this could still induce some heterogeneity in our results. Although logistically it is very challenging to perform histology and biochemical analysis of the same tissue sample, this could have led to an even higher correlation between GAG content and histological grade.

The current study was limited to the L4-L5 level since this is often involved in IVD degeneration and also to reduce the heterogeneity within the study samples. However, in recent publications some histological differences between upper (L1-L2, L2-L3 and L3-L4) and lower (L4-L5 and L5-S1) lumbar disc degeneration [28,29] were demonstrated. It was hypothesized that upper lumber disc degeneration is more EP-driven and lumbar disc degeneration is more annulus-driven[28,29]. Although the current new scoring system is only validated on L4-L5 discs, most likely it can also be used for the L5-S1 level. However, despite the equal representation of the EP and annulus fibrosus (AF) in the scoring system, its applicability for the higher lumbar levels still needs to be evaluated.

The degenerative changes of the IVD are age-related and also the current scoring system will not be able to distinguish between patients with and without low back pain. Identification of why and how in some patients age-related IVD degeneration results in symptomatic degenerative disc disease is currently the largest hurdle in IVD research. Subchondral EP lesions and fissures of the AF have been suggested to be the most histological important risk factors for low back pain[28,30]. A correlation with specific histological changes would greatly enhance elucidation of the mechanisms involved.

In conclusion, we developed and validated a tool for histological evaluation of degenerated IVDs which can be used by both experienced and inexperienced observers. The use of well-validated scoring systems could make the analysis of histological results of fundamental studies more objective and less biased. Additionally, they allow for standardized analysis of basic and translational research and could hopefully increase the efficiency of the research in this field. This classification could significantly contribute to this standardization and hence research into mechanisms and treatment of IVD degeneration.

Acknowledgements

This study was supported by the Dutch Arthritis Association and the Anna Foundation. The Dutch Arthritis Association and the Anna Foundation had no role in study design, collection, analysis and interpretation of data; in the writing of the manuscript; and in the decision to submit the manuscript for publication.

References

1. Maniadakis N, Gray A. The economic burden of back pain in the UK. Pain 2000;84:95-103.
2. Lambeek LC, van Tulder MW, Swinkels IC, Koppes LL, Anema JR, van Mechelen W. The trend in total cost of back pain in The Netherlands in the period 2002 to 2007. Spine 2011;36:1050-8.
3. Wieser S, Horisberger B, Schmidhauser S, Eisenring C, Brugger U, Ruckstuhl A, et al. Cost of low back pain in Switzerland in 2005. Eur J Health Econ 2011;12:455-67.
4. Luoma K, Riihimaki H, Luukkonen R, Raininko R, Viikari-Juntura E, Lamminen A. Low back pain in relation to lumbar disc degeneration. Spine 2000;25:487-92.
5. Schwarzer AC, April CN, Derby R, Fortin J, Kine G, Bogduk N. The relative contributions of the disc and zygapophyseal joint in chronic low back pain. Spine 1994;19:801-6.
6. Smith LJ, NerurKar NL, Choi KS, Harfe BD, Elliott DM. Degeneration and regeneration of the intervertebral disc: lessons from development. Dis Model Mech 2011:31-41.
7. Boos N, Weissbach S, Rohrbach H, Weiler C, Spratt KF, Nerlich AG. Classification of age-related changes in lumbar intervertebral discs: 2002 Volvo award in basic science. Spine 2002;27:2631-44.
8. Thompson JP, Pearce RH, Schechter MT, Adams ME, Tsang IKY, Bishop PB. Preliminary evaluation of a scheme for grading the gross morphology of the human intervertebral disc. Spine 1990;15:411-5.
9. Bachmeier BE, Nerlich A, Mittermaier N, Weiler C, Lumenta C, Wuerts K, et al. Matrix metalloproteinase expression levels suggest distinct enzyme roles during lumbar disc herniation and degeneration. Eur Spine J 2009;18:1573-86.
10. Clouet J, Pot-Vaucel M, Grimandi G, Masson M, Lesoeur J, Fellah BH, et al. Characterization of the age-dependent intervertebral disc changes in rabbit by correlation between MRI, histology and gene expression. BMC Musculoskelet Disord 2011;12:147-55.
11. Kroeber M, Unglaub F, Guehring T, Nerlich A, Hadi T, Lotz J, et al. Effects of controlled dynamic disc distraction on degenerated intervertebral discs. Spine 2005;30:181-7.
12. Zhang Y, Drapeau S, An H, Markova D, Lenart B, Anderson DG. Histological features of the degenerating intervertebral disc in a Goat disc-injury model. Spine 2011;36:1519-27.
13. Masuda K, Lotz JC. New challenges for intervertebral disc treatment using regenerative medicine. Tissue Eng Part B Rev 2010;16:158.
14. Kristensen HK. An improved method of decalcification. Stain Technol 1948;23:151-4.
15. Gruber HE, Ingram J, Hanley Jr EN. An improved staining method for intervertebral disc tissue. Biotech Histochem 2002;77(2):81-3.
16. Pritzker KP, Gay S, Jimenez SA, Ostergaard K, Pelletier JP, Revell PA, et al. Osteoarthritis cartilage histopathology: grading and staging. Ostearthritis Cartilage 2006:13-29.
17. Farndale RW, Sayers CA, Barrett AJ. A direct spectrophotometric microassay for sulphated glycosaminoglycans in cartilage cultures. Connect Tissue Res 1982;9:247-8.
18. Freemont AJ. The cellular pathobiology of the degenerate intervertebral disc and discogenic back pain. Rheumatology 2009;48:5-10.
19. Pfirrmann CW, Metzdorf A, Zanetti M, Hodler J, Boos N. Magnetic resonance classification of lumbar intervertebral disc degeneration. Spine 2011;26:1873-8.

20. Roberts S, Evans H, Trividi J, Menage J. Histology and pathology of the human intervertebral disc. J Bone Joint Surg Am 2006;88(Suppl 2):10-4.
21. Bland JM, Altman DG. Statistical methods for assessing agreement between two methods of clinical measurement. Lancet 1986;327:307-10.
22. Reliability analysis. In: Field Andy, Ed. Discovering Statistics Using SPSS. 2nd edn. London: SAGE Publications Ltd; 2005: 666-72.
23. Fleiss JL. The Design and Analysis of Clinical Experiments. New York: Wiley; 1986.
24. Westgard JO. Basic Method Validation. Madison: Westgard QC; 1999.
25. Iatridis JC, Gwynn I. Mechanisms for mechanical damage in the intervertebral disc annulus fibrosus. J Biomech 2012;37: 1165-75.
26. Camplejohn KL, Allard SA. Limitations of safranin 'O' staining in proteoglycan-depleted cartilage demonstrated with monoclonal antibodies. Histochemistry 1988;89: 185-8.
27. Dickinson SC, Sims TJ, Pittarello L, Soranzo C, Pavesio A, Hollander AP. Quantitative outcome measures of cartilage repair in patients treated by tissue engineering. Tissue Eng 2005;11:277-87.
28. Adams MA, Dolan P. Intervertebral disc degeneration: evidence for two distinct phenotypes. J Anat 2012;221:497-506.
29. Wang Y, Videman T, Battie MC. Lumbar vertebral endplate lesions prevalence, classification, and association with age. Spine 2012;37:1432-9.
30. Wang Y, Videman T, Battie MC. Issls prize winner: lumbar vertebral endplate lesions associations with disc degeneration and back pain history. Spine 2012;37:1490-6.

Supplement

Grading guide for histological classification for intervertebral disc degeneration

Grading:

For histological grading of the intervertebral disc (IVD) all 6 scorings items, A - F, should be scored with 0, 1 or 2 points which are added. A complete grading will result in a score ranging from 0 – 12 points. A score of 0 points represents a healthy, nondegenerative IVD, whereas a score of 12 points represents a completely degenerative IVD.

A: Endplate

0: Homogeneous structure, regular thickness.

1: Slight irregularity with limited number of microfractures and locally decreased thickness.

2: Severe irregularity with multiple microfractures of the endplate and generalized decreased thickness.

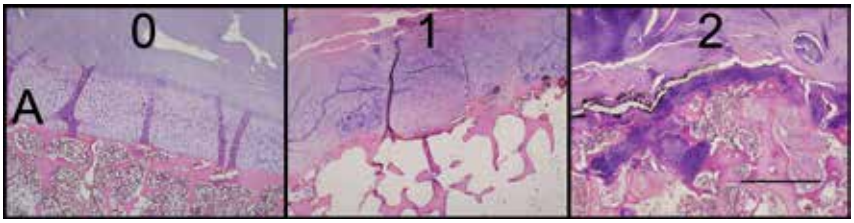

B: Morphology annulus fibrosus

0: Well-organized, half ring-shaped structure, collagen lamellae

1: Partly ruptured annulus fibrosus; loss of half ring-shaped structure

2: Completely ruptured annulus fibrosus; no intact half ring-shaped collagen lamellae

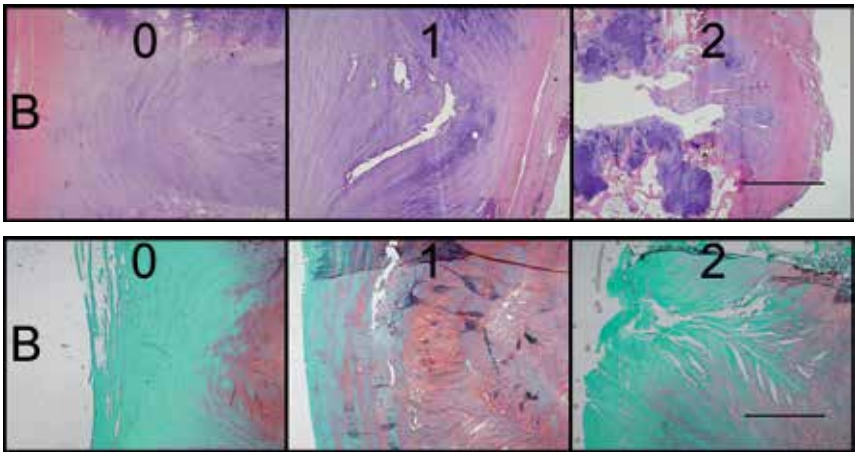

C: Boundary annulus fibrosus and nucleus pulposus

0: Clear boundary between annulus fibrosus and nucleus pulposus tissue

1: Boundary less clear; loss of annular-nuclear demarcation

2: No distinguishable boundary between annulus fibrosus and nucleus fibrosus tissue

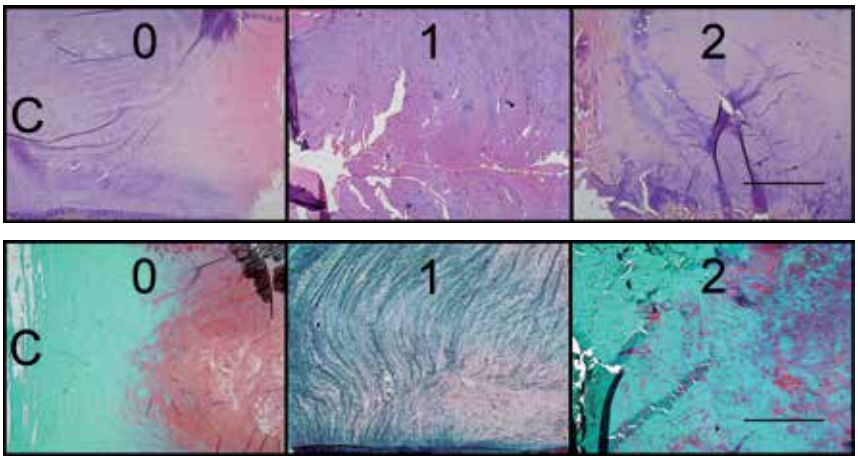

D: Cellularity nucleus pulposus

0: Normal cellularity; no cell clusters

1: Mixed cellularity; normal pattern with some cell clusters

2: Mainly clustered cellularity, chondroid nests present

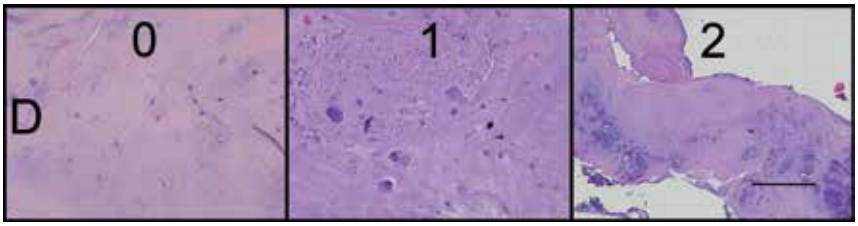

E: Matrix nucleus pulposus

0: Well-organized structure of nucleus matrix

1: Partly disorganised structure of nucleus matrix

2: Complete disorganisation and loss of nucleus matrix

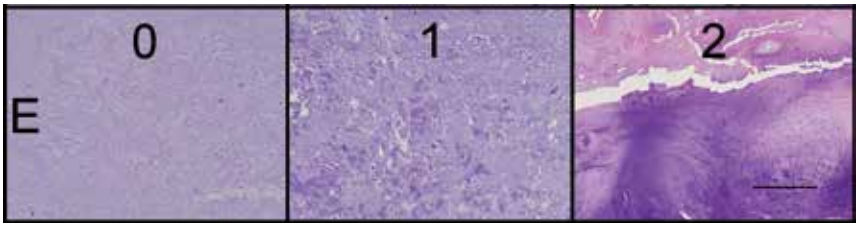

F: Nucleus pulposus matrix staining

0: Intense staining; red stain dominates

1: Reduced staining; mixture of red and slight green staining

2: Faint staining; increased green staining

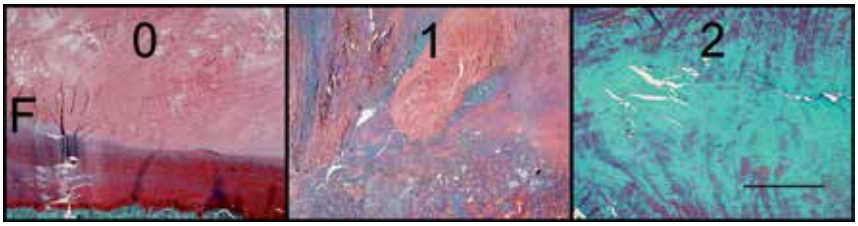

CHAPTER 8

Minor degenerative changes in a rabbit model of compression-induced intervertebral disc degeneration

JPHJ Rutges, FC Oner, KL Vincken, JEJ Bekkers, WJA Dhert and LB Creemers

Submitted to Eurpean Spine Journal

Abstract

The aim of this study was to further define the characteristics of disc degeneration in a rabbit model of mechanically induced IVD degeneration. Study design: L4-L5 discs of 24 NZW rabbits were compressed with an external loading device for 14, 18 and 56 days, including a sham group of 56 days follow-up.

Disc height was measured by radiography. Degeneration was histologically graded according to the Boos score. The presence and activity of MMP-2 was determined by gelatin zymography.

Significantly reduced disc height was found after 14 and 56 days in the compressed versus the non-compressed discs ($p = 0.029$ and $p = 0.009$ respectively), but recovery of disc height 1 hour after in vivo release of compression was found in both cases. No differences in histological score were observed between the compressed and non-compressed discs. Growth plate closure was induced in the compressed and sham compressed IVDs. Higher levels of active MMP-2 in the endplate region were found after 28 days of compression compared to the noncompressed and sham operated discs ($p = 0.005$ and $p = 0.011$ respectively).

Increased levels of active MMP-2 in the endplate region were found upon in vivo compression of rabbit IVDs. However, the limited degeneration in the current model suggests it may be more suitable for research into mechanisms of early disc degeneration than for the evaluation of new treatment strategies.

Introduction

Low back pain is a major health problem in urbanized countries with a lifetime prevalence up to 80%[1]. Although the exact relationship between intervertebral disc (IVD) degeneration and chronic low back pain remains controversial, several recent studies have shown a clear association between chronic low back pain and IVD degeneration[2]. Current surgical treatment strategies are still salvage procedures aiming at pain relief instead of restoring the degenerative segment[3]. New therapies aiming at regenerating the IVD are currently being developed[3]. For the translation of these new therapeutic strategies to low back pain patients, appropriate animal models for IVD degeneration are required.

To simulate human IVD degeneration many models in different species have been described[4]. Models in which IVD degeneration is induced by biomechanical loading appear to most closely resemble the pathophysiology of human IVD degeneration[4]. A rabbit compression model for IVD degeneration involving compression of load bearing IVDs was described by Kroeber et. al. in 2002[5]. After 28 days of compression, a decrease in disc height, increase in cell death and increased disorganization of the annulus fibrosus (AF) were reported, although the latter parameter was not quantified by any histological grading[5]. Intradiscal pressure of compressed discs was decreased and the number of BMP-2/4 and collagen type II-positive cells reduced6. Moreover, a decreased signal intensity on MRI and increased mRNA expression of multiple degenerative parameters including collagen type I and several matrix metalloproteinases (MMPs) were found[6]. However, protein nor enzymatic activity were measured[7]. MMP-2 is the only MMP of which its enzymatic activity has been shown to correlate to human disc degeneration and appears to be a good marker for degeneration[8].

The aim of this study was to more accurately and quantitatively assess the extent of degeneration in the rabbit model of compression-induced IVD degeneration, by measuring MMP-2 production and activity and by histological quantification, after respectively 14, 28 and 56 days of compression of L4-L5 discs.

Methods

Experimental design

This study was approved by the Animal Care Committee of the University Medical Center Utrecht (approval number 05.11.094). In 24 rabbits (Harlan, Horst the Netherlands) an external compression device was placed at the 4th and 5th lumbar vertebrae (L4-L5) as described previously[5]. A calibrated spring (Beste Veer, Utrecht the Netherlands) was used to apply continuous dynamic load of 200 N (approximately five times the body weight of the rabbits) on the L4-L5 discs (figure 8.1). The follow-up period was 14 (N = 6), 28 (N =6) and 56 days (N= 6). In the sham group (N=6) an unloaded compression device was placed for a follow-up period of 56 days. The unloaded compression device allows physiological axial compression and rotation of the IVD, though flexion and lateroflexion are not possible. The L3-L4 IVDs (adjacent discs) were used as control discs since these discs were previously shown not to be affected by the compression at L4-L5[9]. After termination, the lumbar spine was removed and the L3-L4 and the L4-L5 discs were processed for histological and biochemical analysis. More details regarding the surgical procedure, termination of the animals and collection of the IVDs can be found in the supplementary material.

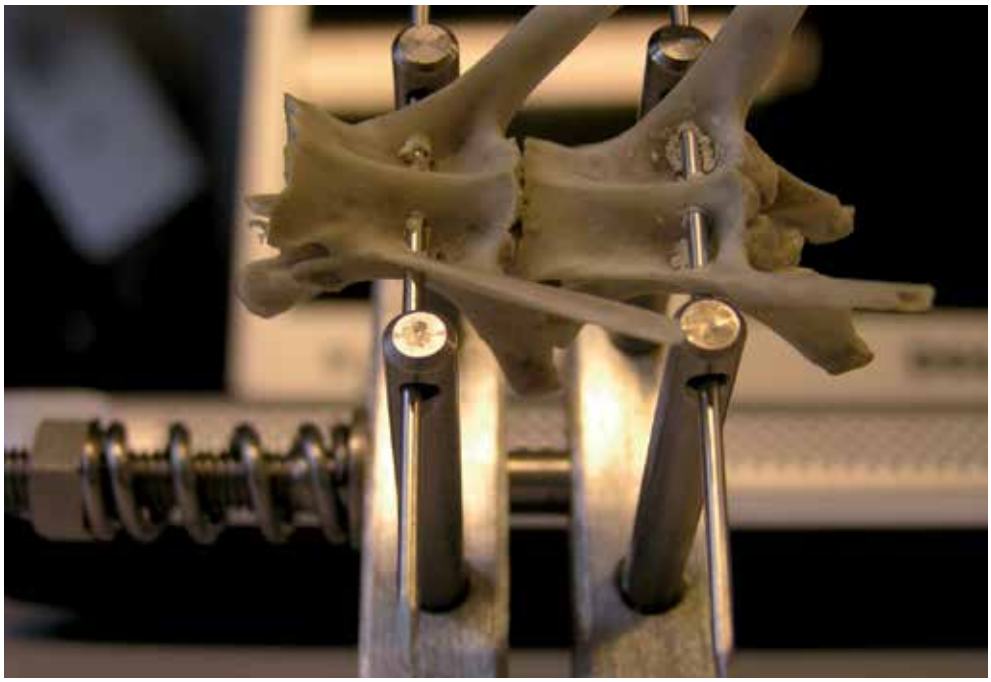

Figure 8.1. The external compression device which was used to load the L4-L5 disc

Animals

Twenty-four adult female New Zealand White rabbit (age 30 weeks) with a mean weight of 3.7 kg (sd 0.3 kg) were used. Nutritional behavior was monitored daily and weight of the animals was measured before surgery, before termination and weekly during the follow-up period.

Disc height determination by radiography

Lateral radiographs of the spine were made pre-operatively, post-operatively, and one hour before termination, using a Siremobile Iso-C fluoroscope (Siemens, Erlangen Germany). The 200 N compression load was relieved from the L4-L5 disc and at termination another radiograph was made. In the hour between unloading of the compression device and termination, animals were allowed to mobilize without restrictions. In the sham group, only at termination a radiograph was made. Disc height was measured on digital radiographs using ImageXplorer (Image Science Institute, Utrecht, the Netherlands) and a custom-made application made by KV (figure 8.2). Anterior, central and posterior disc height was measured perpendicularly to a line drawn parallel to the caudal endplate of the measured disc of the L3-L4 and L4-L5 vertebrae was measured. Mean disc height was calculated from the measurements of two observers and the L4-L5 disc height was calculated as ratio of the non-compressed L3-L4 disc and compressed/sham-compressed L4-L5 disc.

Figure 8.2. Anterior, center and posterior disc height measured at the L3-L4 disc with the IntervertebralIX application in ImageXplorer (Image Science Institute Utrecht the Netherlands). Disc height of the compressed L4-L5 disc is clearly decreased on this x-ray

Histology

IVD sections were scored according the histological grading scheme as described by Boos et. al. The L3-L4 and L4-L5 discs were decalcified in Kristensen's solution (50% formic acid and 68 g/l sodium formiate)[10] and embedded in paraffin. General morphology was analyzed by haematoxylin/eosin staining. Proteoglycan and collagen distribution were analyzed by alcian blue/ picrosirius red staining[11].

Sections were graded according to the Boos score[12] by two independent observers (JR, RD) blinded to the origin of the sections. Additionally the presence of open growth plates and bony bridges between the bony endplate and the vertebral body was assessed.

Gelatin zymography

Protein extraction was performed at 4°C by lysis of 100 5 µm cryosections from the IVD center in 0.5% sodium deoxycholate, 0.1% Triton X-100, 0.1% SDS and complete protease inhibitor cocktail (Roche, Mannheim Germany) Five µg protein of tissue extract was separated on an 8% acrylamide/0.1% gelatin gel and incubated for in 0.05% Brij 35, 50 mM Tris and 10 mM CaCl (pH 7.4) at 37°C. Gels were stained with Coomassie Brilliant Blue and pro- and active MMP-2 were analyzed by densitometry using the Geldoc 2000 system (Bio-rad, Hercules USA) and Quantity One software (Bio-rad).

A detailed description regarding gelatin zymography, protein extraction, and histological procedures can be found in the supplementary material.

Statistical analysis

Paired continuous variables were analyzed by paired T-tests followed by Bonferroni correction. Non-paired continuous variables were analyzed by a one-way ANOVA followed by a LSD post hoc test. Correlations between two continuous variables were analyzed by the Pearson correlation test. The Fisher's Exact test was used to determine differences between categorical variables, followed by Bonferroni correction. Single intra- and interclass correlations were determined to analyze the reliability of the disc height measurements. Intra- and interobserver reliability was determined. All calculations were performed with SPSS 16.0 software (SPSS Inc., Chicago USA).

Results

Surgery and animal health

Altogether 5 rabbits were excluded during the study. In two rabbits, the K-wires dislocated from the vertebral body and compression was lost. Three rabbits were terminated during the follow-up period. One animal appeared to be in unbearable pain for which no clear cause was found at autopsy. Two other rabbits had neurological deficits; one after misplacement of a K-wire and one rabbit an L4 fracture that occurred 1 week after placement of the compression device. Four rabbits completed the 14-days follow-up period and in the 28 ,56 and 56 days sham surgery group, 5 rabbits per group completed the follow-up period.

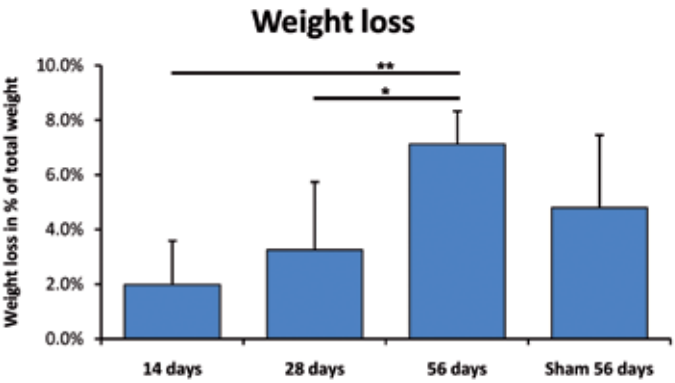

Figure 8.3. Mean weight loss as percentage of the preoperative body weight per study group. Error bars indicate the standard deviation. 56 days vs 14 and 28 days, $p = 0.002$ and $p = 0.011$ respectively, *: $p < 0.05$ and **: $p < 0.005$

These 19 rabbits recovered well after surgery, they showed no signs of illness and no wound or pin track infections were seen. Animals were able to move freely and showed normal behavior and a normal eating and drinking pattern. A statistically significant mean weight loss of 4.5% in all animals was seen during the follow-up period; 3.7± 0.2 kg before surgery and 3.5± 0.2 kg at the end of the follow-up period ($p < 0.001$). Significantly more weight loss was seen in the 56 days compression group when compared to the 14 and 28 days compression group, 7.1% vs 2.0% and 3.3% ($p = 0.002$ and $p = 0.011$ respectively, figure 8.3).

Disc height

In all compressed IVDs, a strong statistically significant negative correlation (CC -.710, $p = 0.004$) was found between compression time and L3/L4-L4/L5 disc height ratio one hour before, but not after, termination. Details for each study group and all time points are shown in figure 8.4. After 14 and 28 days of compression, a significant lower disc height ratio was found 1 hour before termination compared to the preoperative disc height ratio (0.68 ± 0.23 vs 0.95 ± 0.22, $p = 0.029$) which disappeared after 1 hour relief of the compression device (figure 8.4). Only in the IVDs compressed for 56 days, the disc height ratio remained statistically significantly lower after 1 hour relief of the compression device. However, also in the 56 days sham group, a statically significant decrease was found between the preoperative disc height ratio and height at termination (1.01 ± 0.09 vs 0.83 ± 0.07, $p = 0.032$, figure 8.4). There was no statistical significant correlation between disc height and the Boos score, CC -0.256, $p = 0.290$.

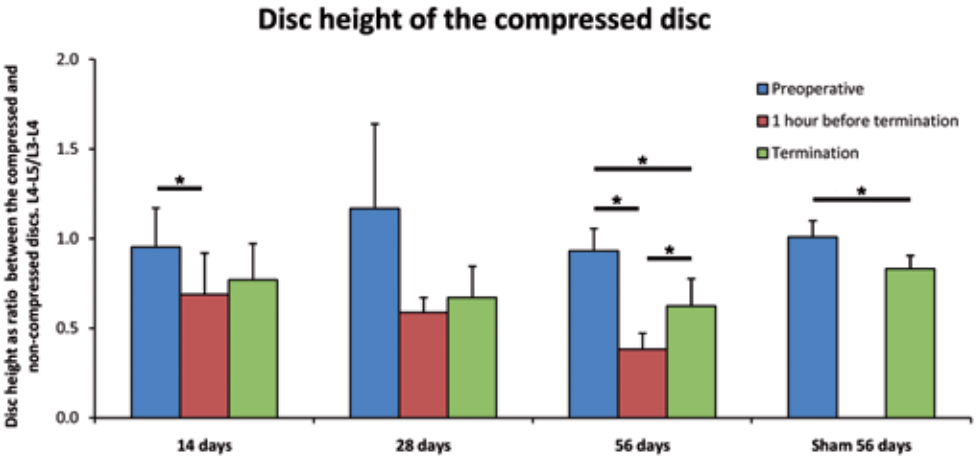

Figure 8.4. Disc height per study group as ratio between the compressed (L4-L5) and non-compressed discs (L3-L4). Error bars indicate the standard deviation. *: $p < 0.05$

Histology

The average Boos degeneration score was 3.3 (range 0.0 to 8.0). Forty percent of the points were related to changes in the NP and 60% to changes in the EP (figure 8.5).

No difference was found between the adjacent levels and the compressed discs at any time point (2.86 vs. 3.46, p = 0.17) except after 56 days, when the Boos score of sham compressed discs was statically significantly higher than their adjacent discs (figure 8.6; 4.2 vs 3.03, p = 0.042).

More discs with at least one closed growth plate in the adjacent vertebral body were found in the 56 days compressed group when compared to the adjacent discs (80% vs 5.3%, p = 0.020, figure 8.7). During histological evaluation no direct mechanical injuries of the growth plate were observed.

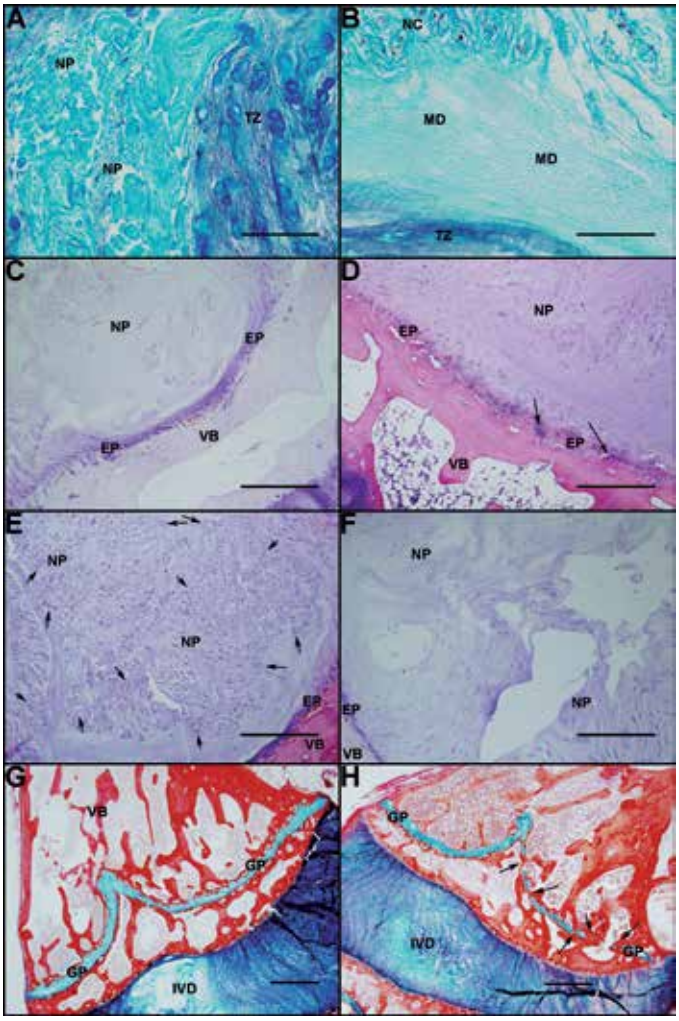

Figure 8.5. Photographs of sections showing the normal (A,C,E and F) and abnormal (B, D, F and H) findings. Normal nucleus pulposus (A). Nucleus pulposus with an area of mucous degeneration indicated with MD (B). Normal endplate with regular shaped cartilage endplate without cell proliferations (C). Disorganized irregular endplate with areas of cell proliferation indicated by the arrows (D). Normal nucleus pulposus with a large number of notochordal cells indicated by the arrows (E). A nucleus pulposus without any notochordal cells (F). Normal open growth plate (G). A growth plate which is partially closed as indicated by the arrows (H). Abbreviations; NP: nucleus pulposus, TZ: transition zone, NC: notochordal cells, MD: mucous degeneration, EP: endplate, VB: vertebral body, GP: growth plate and IVD: intervertebral disc. Scale bars indicate 100 µm in A and B, 500 µm in C, D, E and F, 1.0 mm in G and H

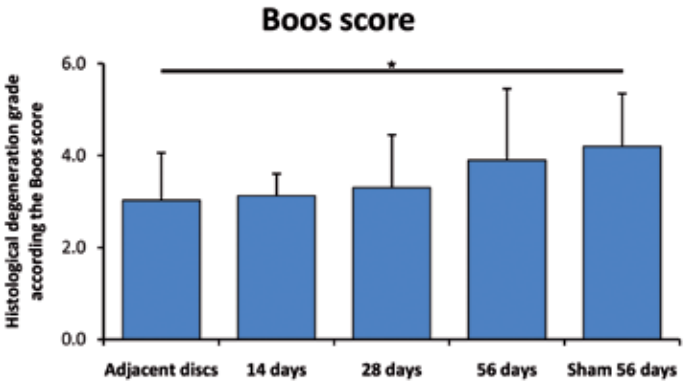

Figure 8.6. Points according the Boos histological IVD degeneration score per study group. 0 points indicates a healthy IVD without any signs of degeneration, 40 points is the maximum score and indicates a totally degenerated disc. Error bars indicate the standard deviation. Adjacent discs vs sham 56 days, $p = 0.042$, *: $p < 0.05$

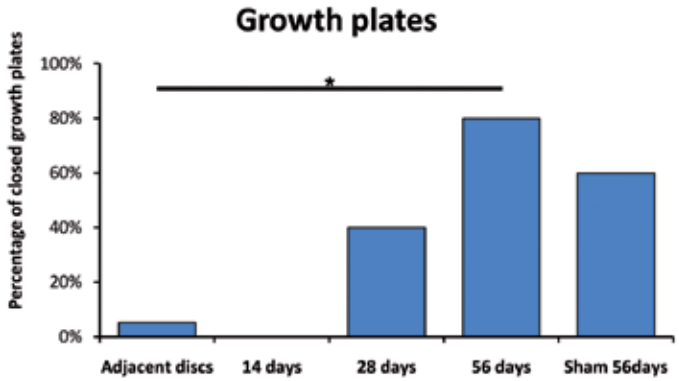

Figure 8.7. The percentage of discs in which one of the growth plates was closed at termination per study group. Adjacent discs vs 56 days, $p = 0.020$, *: $p < 0.05$

Gelatin zymography

Neither pro- nor active MMP-2 could be detected in the nucleus of the IVD. A significantly higher level of active MMP-2 was found in the endplate region of the discs compressed for 28 days in comparison to the adjacent discs and compared to the IVDs after 56 days compression and sham compression (figure 8.8; p = 0.005, p = 0.012 and p = 0.011 respectively).

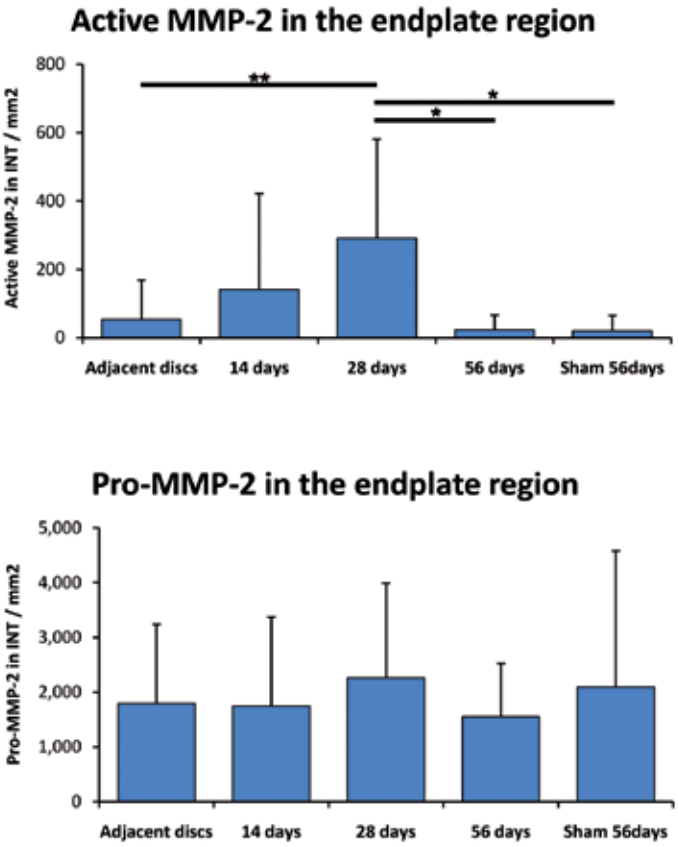

Figure 8.8. Levels of active and pro-MMP-2 per study group. Error bars indicate the standard deviation. Active MMP-2 28 days vs adjacent discs, 56 days, sham 56 days, p = 0.005, p = 0.012 and p = 0.011 respectively, *: $p < 0.05$ and **: p = 0.005

Discussion

The current study shows that long term intervertebral disc compression in rabbits leads to very mild IVD degeneration. Adequate compression of the L4-L5 levels was obtained after 14 and 56 days, as indicated by the reduced disc height by radiography, but disc height was partly regained by relief of the compression device after one hour. Histologically, no effects of compression were found, although a transient increase of MMP-2 activity in the endplate region was observed. Strikingly, the only effect at the histological level was found in the sham-compressed discs. Another striking feature noted in this study was growth plate closure, which occurred more frequently in discs compressed for 56 days in comparison to the adjacent discs.
Reduction in disc height is a frequently used parameter for disc degeneration. In the current study, immediately at termination this reduction was comparable with the effects described before in this in vivo model[5]. However, the compressed IVDs were found to increase their height up to twofold after relief of compression, suggesting immediate post-mortem measurement of disc height may not be a good indicator of degeneration and hence that degeneration in previous studies on compression models may have been overestimated[5,13].

The absence of a genuine effect on disc height corresponded with the absence of an effect at the histological level, together suggesting that the degeneration induced was at a very early stage. Previous studies using this model, described effects at a more detailed and cellular level, including a decrease of BMP-2, BMP-4 and collagen type II-positive cells, and an increase in mRNA expression of collagen type I, osteonectin, decorin, fibronectin, tissue inhibitor of MMP-1, BMP-2, and MMP-13[6,14]. In addition, an increase of fibrous tissue and mucoid degeneration in the NP and increased disorganization in the AF and EP were reported, however these results were not quantified[5,9]. Together these may indicate phenomena preceding or occurring very early in degeneration. Similar results were found in the rat tail compression model of IVD degeneration[15], including mild histological changes and upregulation of collagen type I, ADAMTS-4, MMP-3 and MMP-13 mRNA[16,17]. Although these findings indicate that a catabolic or degenerative response is stimulated by compression of the IVD, none of the studies reported histological degeneration to the extent found in humans with chronic lower back pain, which was further confirmed in the current study. Possibly the changes found at the mRNA level in these studies may not have resulted in a definitive tipping of the balance towards degeneration, either because the changes in mRNA levels did not result in an increased protein production, as has been reported frequently, or because the amount of protein formed was too low to have a significant impact[18].

MMP-2 activity has been shown to be clearly related to human disc degeneration[8]. In human Thompson grade II (minor degeneration) discs, MMP-2 was only found in the transition zone between the NP and AF near the endplates[8,19], compared to more extensive production throughout the entire disc at higher degeneration grades. Also in the current study, a transient increase in MMP-2 activity in the endplate region was found after 28 days of compression. An increase in MMP-2 mRNA levels and activity after compression have also been reported in mouse and rat tail models of IVD degeneration[20,21]. In the current study loading was applied for up to 56 days. Increased MMP-2 activity was seen until 28 days after start of the

compression, while after the 56 days of compression MMP-2 activity had returned to normal levels[20,21]. As such a combination of an increase in expression followed by a decrease at later time points has also been described for mRNA levels of extracellular matrix proteins like biglycan, decorin, collagen type I and type II in the same model as used in the current study[22]. It was suggested to point towards a remodeling or maintenance response to the initial loading event and returning to baseline levels after a certain period.

In the current study, striking effects of compression were seen in the growth plates. Although rabbits are considered skeletally mature at a age of 30 weeks, their growth plates remain open in nearly the entire life, as in nearly all small animals. In 80% of the discs compressed for 56 days, at least one of the two growth plates was closed, whereas nearly none of the growth plates in the vertebral bodies of the adjacent discs were closed. Compression is a plausible explanation for closure of the growth plates. In a recent porcine scoliosis model IVDs were unilaterally compressed for 8 weeks by custom made spine staples[23]. This study reported a clear decrease in growth plate height in the compressed IVDs, indicating that compression could lead to reduced height or even closure of the growth plate[23].

Alternatively, the increased number of closed growth plates could be induced by partial immobilization due to placement of the compression device, although the device allows compression and rotation, flexion and lateroflexion are not possible. Other possible explanations for the degenerative changes found in the IVDs in the sham animals could be a compromised vascularization of the adjacent vertebrae. The presence of a 1.6 mm K-wire rabbit vertebral body of ø 3.0-5.0 mm may have compromised the vascularization of the vertebrae, and thereby the diffusion of nutrients from the vertebral body to the growth plate and IVD. Additionally the compression applied in the loaded devices could further reduce the diffusion of nutrients. Reduced permeability of the endplate has been reported in a porcine scoliosis model in which the thoracic and lumbar spine were unilaterally compressed for 3 months[24].

Although no obvious changes in behavior and food and fluid intake were observed in the animals during the compression period, significant weight loss occurred while rabbits usually gain weight at 30 to 38 weeks of age. Next to weight loss, neurological deficits, infections, vertebral fractures, and even self mutilation were noted previously[5,9,14,25]. The proportion of excluded animals (21%) in the current study falls within the reported range for rabbit IVD degeneration models (from 0% till 27%)[5,9,14,25], however, together with the effect observed on weight, the model appears to impose a relatively high burden on the animals. In the current study we have shown that compression of the rabbit IVD with an external device caused disc height reduction, which recovered after 1 hour of compression release, stressing that caution must be taken when using disc height as a degeneration parameter in these models. The current model may be promising to study very early degenerative changes at the cellular level, as described previously. However, the burden for the animals and the limited histological grade of degeneration achieved are valid reasons not to use this model for the development of future treatment strategies for IVD degeneration. Other models like annular puncture models or animal ex vivo models may possibly be more suitable for this purpose.

Acknowledgements

The authors acknowledge the General Animal Laboratory of Utrecht University and their personnel for the help during surgery and for taking care of the rabbits. The authors would also like to acknowledge Robin Duit (RD) for histological grading of the samples. This study was supported by the Dutch Arthritis Association, the Anna Foundation and De Drie Lichten foundation.

References

1. Hoy D, Brooks P, Blyth F, and Buchbinder R (2012) The epidemiology of low back pain. Best Pract Res Clin Rheumatol 24: 769-781.
2. de Schepper EI, Damen J, van Meurs JB, Ginai AZ, Popham M, Hofman A, Koes BW, and Bierma-Zeinstra SM (2010) The association between lumbar disc degeneration and low back pain: the influence of age, gender, and individual radiographic features. Spine 35: 531-536.
3. Kalson NS, Richardson S, Hoyland JA (2008) Strategies for regeneration of the intervertebral disc. Regen Med 5:729.
4. Alini M, Eisenstein SM, Ito K et al (2008) Are animal models useful for studying human disc disorders/degeneration? Eur Spine J 17:2-19.
5. Kroeber MW, Unglaub F, Wang H et al (2002) New in vivo animal model to create intervertebral disc degeneration and to investigate the effects of therapeutic strategies to stimulate disc regeneration. Spine 27:2684-2690.
6. Guehring T, Omlor GW, Lorenz H et al (2005) Stimulation of gene expression and loss of anular architecture caused by experimental disc degeneration--an in vivo animal study. Spine 30:2510-2515.
7. Bramono DS, Richmond JC, Weitzel PP, Kaplan DL, Altman GH (2004) Matrix metalloproteinases and their clinical applications in orthopaedics. Clin Orthop Relat Res 428:272-285.
8. Rutges JPHJ, Kummer JA, Oner FC (2008) Increased MMP-2 activity during intervertebral disc degeneration is correlated to MMP-14 levels. J Pathol 214:523-530.
9. Unglaub F, Guehring T, Lorenz H, Carstens C, Kroeber M (2005) Effects of unisegmental disc compression on adjacent segments: an in vivo animal model. Eur Spine J 14:949-955.
10. Kristensen HK (1948) An improved method of decalcification. Stain Technol 23:151-154.
11. Gruber HE, Ingram J, and Hanley EN Jr (2002) An improved staining method for intervertebral disc tissue. Biotech Histochem 77:81-83.
12. Boos N, Weissbach S, Rohrbach H, Weiler C, Spratt KF, Nerlich AG (2002) Classification of age-related changes in lumbar intervertebral discs: 2002 Volvo Award in basic science. Spine 27:2631-2644.
13. Iatridis JC, Mente PL, Stokes IA, Aronsson DD, Alini M (1999) Compression-induced changes in intervertebral disc properties in a rat tail model. Spine 24:996-1002.
14. Guehring T, Omlor GW, Lorenz H et al (2006) Disc distraction shows evidence of regenerative potential in degenerated intervertebral discs as evaluated by protein expression, magnetic resonance imaging, and messenger ribonucleic acid expression analysis. Spine 31:1658-1665.
15. Lotz JC, Colliou OK, Chin JR, Duncan NA, Liebenberg E (1998) Compression-induced degeneration of the intervertebral disc: an in vivo mouse model and finite-element study. Spine 23:2493-2506.
16. Lai a, Chow DH, Siu SW et al (2008) Effects of static compression with different loading magnitudes and durations on the intervertebral disc: an in vivo rat-tail study. Spine 33:2721-2727.
17. Maclean JJ, Lee CR, Alini M, Iatridis JC (2005) The effects of short-term load duration on anabolic and catabolic gene expression in the rat tail intervertebral disc. J Orthop Res 23:1120-1127.
18. Ebrahimi M, Roudkenar MH, Imani Fooladi AA, Halabian R, Ghanei M, Kondo H, and Nourani MR (2010) Discrepancy between mRNA and Protein Expression of Neutrophil Gelatinase-Associated Lipocalin in Bronchial Epithelium Induced by Sulfur Mustard. Biotechnol 2010:823131.

19. Thompson JP, Pearce RH, Schechter MT, Adams ME, Tsang IKY, Bishop PB (1990)Preliminary evaluation of a scheme for grading the gross morphology of the human intervertebral disc. Spine 15:411-415.
20. Hsieh AH, Lotz JC (2003) Prolonged spinal loading induces matrix metalloproteinase-2 activation in intervertebral discs. Spine 28:1781-1788.
21. Maclean JJ, Roughley PJ, Monsey RD, Alini M, Iatridis JC (2008) In vivo intervertebral disc remodeling: kinetics of mRNA expression in response to a single loading event. J Orthop Res 26:579-588.
22. Omlor GW, Lorenz H, Engelleiter K et al (2006) Changes in gene expression and protein distribution at different stages of mechanically induced disc degeneration--an in vivo study on the New Zealand white rabbit. J Orthop Res 24:385-392.
23. Bylski-Austrow DI, Wall EJ, Glos DL, Ballard ET, Montgomery A, Crawford AH (2009) Spinal hemiepiphysiodesis decreases the size of vertebral growth plate hypertrophic zone and cells. J Bone Joint Surg Am 91:584-593.
24. Laffosse JM, Accadbled F, Odent T (2009) Influence of asymmetric tether on the macroscopic permeability of the vertebral end plate. Eur Spine J 18:1971-1977.
25. Guehring T, Unglaub F, Lorenz H, Omlor G, Wilke HJ, Kroeber MW (2006) Intradiscal pressure measurements in normal discs, compressed discs and compressed discs treated with axial posterior disc distraction: an experimental study on the rabbit lumbar spine model. Eur Spine J 15:597-604

Supplement

Supplementary methods

Surgery

Preoperatively and one day after surgery, the animals were injected with 2.5% enrofloxacin (0.2 ml/kg intramuscularly). Surgery was performed under general inhalation anaesthesia and aseptic conditions. Midazolam (1.0 mg/kg) and methadone (1.0 mg/kg) were administered intramuscularly as premedication. General anesthesia was induced by intravenous injection of etomidate (2.0 mg/kg). Anesthesia was sustained with sufentanil (3.0 ml/hour/kg) and isoflurane inhalation (2.0%). During surgery, pCO2, oxygen saturation, heart rate, blood pressure and temperature were monitored.

A posterior lumbar paraspinal incision was used to expose both lateral sides of the 4th and 5th vertebrae. During surgery, the level of the exposed vertebrae was verified by fluoroscopy. Two 1.6 mm K-wires were placed under direct visual inspection in the vertebral body by a percutaneous lateral approach. The connection rods were placed on the K-wires and the wound was closed in three layers. The external loading device was connected to the rods and a 200 N load was applied to the L4-L5 IVD, as described by Kroeber et al[5].

In the sham surgery treated animals, the surgical procedure was identical, however the calibrated spring was not placed on the external loading device and hence no load was applied. After surgery, the rabbits stayed at the intensive care unit for 24 hours and then were transferred to individual cages, where they were allowed to move freely. Buprenorphine (3 DD, 0.15ml/kg) was admitted for analgesia until day 3 after surgery. After the follow-up period animals were terminated using an overdose of Pentobarbital.

Collection of the IVDs

The same posterior approach as during surgery was used for collection of the IVDs. The entire lumbar spine was resected. Between the different processing steps, the specimens were stored on ice. After resection, the L3-L4 and L4-L5 discs, including cranial and caudal endplates, were removed from the lumbar spine using a water-cooled table saw (200111 CE, Adamas, Maasdijk, The Netherlands). Each IVD was sawed in a mid-sagittal direction in two halves. One half was fixed and stored in 4% formalin for histology, the remaining half was embedded in TissueTek (Sakura Finetek, Zoeterwoude, the Netherlands) and stored at – 80°C for protein extraction.

Histology

The L3-L4 and L4-L5 discs were decalcified in Kristensen's solution (50% formic acid and 68 g/l sodium formiate) in a microwave oven (Milestone microwave Laboratory systems, Bergamo Italy) at 150 W and 50ºC for 6 hours[10]. The samples were dehydrated in a graded alcohol series, rinsed in xylene, embedded in paraffin and cut to five µm thin sections. General morphology was analyzed by haematoxylin eosin staining. Proteoglycan and collagen distribution were analyzed by alcian blue/ picrosirius red staining, yielding a blue staining of proteoglycans, while collagen type I and II in the AF and in the NP show up red[11].

Hematoxylin-eosin and alcian blue/picrosirius red sections were graded according the Boos score by two independent observers (JR, RD) blinded to the origin of the sections[12]. As detailed description of the Boos score is shown in table 8.1. In each section also the presence of open growth plates and bony bridges between the bony endplate and the vertebral body was assessed.

Table 8.1. Boos histological degeneration score of the IVD.

Intervertebral Disc		**Endplate**	
Cells (chondrocyte proliferation)		**Cells**	
0 =	no proliferation	0 =	normal cellularity
1 =	increased cell density	1 =	localized cell proliferation
2 =	connection of two chondrocytes	2 =	diffuse cell proliferation
3 =	small-size clones (i.e., several chondrocytes group together, i.e., 2–7 cells)	3 =	extensive cell proliferation
4 =	moderate size clones (i.e., _8 cells)	4 =	scar/tissue defects
5 =	huge clones (i.e., 15 cells)		
6 =	scar/tissue defects		
Mucous degeneration		**Cartilage disorganization**	
0 =	absent	0 =	well-structured hyaline cartilage
1 =	rarely present	1 =	cartilage irregularities (obliterated vessels?)
2 =	present in intermediate amounts	2 =	disorganized matrix with thinning
3 =	abundantly present	3 =	complete cartilage disorganization with defects
4 =	scar/tissue defects	4 =	scar/tissue defects
Cell death		**Cartilage cracks**	
0 =	absent	0 =	absent
1 =	rarely present	1 =	rarely present
2 =	present in intermediate amounts	2 =	present in intermediate amounts
3 =	abundantly present	3 =	abundantly present
4 =	scar/tissue defects	4 =	scar/tissue defects
Tear and cleft formation		**Microfracture**	
0 =	absent	0 =	absent
1 =	rarely present	1 =	present
2 =	present in intermediate amounts	2 =	scar/tissue defects
3 =	abundantly present		
4 =	scar/tissue defects		

Granular changes		New bone formation	
0 =	absent	0 =	absent
1 =	rarely present	1 =	present
2 =	present in intermediate amounts	2 =	scar/tissue defects
3 =	abundantly present		
4 =	scar/tissue defects		
		Bony sclerosis	
		0 =	absent
		1 =	present
		2 =	scar/tissue defects
Maximum: 22 points		**Maximum: 18 points**	

Histological degeneration score of the IVD according Boos et. al.[12].

Protein extraction

Protein extraction was performed at 4°C. The center region could easily be cut out from the frozen IVD, embedded in TissueTek with a nr 15 scalpel blade, since the IVD including adjacent vertebrae was sawed in a sagittal plane and the NP and AF could clearly be identified. From each half IVD, 100 5 µm sections from the IVD center and the endplate region were cut with a cryomicrotome. The endplate region was directly cut from the vertebrae with the microtome. Approximately 100 sections of 5 µm were lysed in 0.5% sodium deoxycholate, 0.1% Triton X-100, 0.1% SDS and complete protease inhibitor cocktail (Roche, Mannheim Germany) according to the manufacturer's instructions. Samples were gently mixed overnight at 4°C, followed by 15 minutes centrifugation at 16000x g where after the supernatant was collected. Protein content of the supernatant was assessed by BCA protein analysis (Pierce Rockford, Illinois USA).

Supplementary results

Intra- and interobserver reliability of disc height determination by radiography

Intra-observer reliability for the anterior, center and posterior disc height measurements was 0.822, 0.814 and 0.746 for JR and 0.806, 0.897 and 0.772 for JB. Inter-observer reliability was 0.490, 0.680 and 0.540 for the anterior, center and posterior disc height. An average intra- and interclass correlation is considered good if the ICC is 0.4 – 0.75 and excellent if the ICC is > 0.75. Based on these results, central disc height appeared to be the most reliable region for disc height measurement since it had the highest intra- and interobserver reliability.

CHAPTER 9

The Dog as an Animal Model for Intervertebral Disc Degeneration?

N Bergknut, JPHJ Rutges, HJC Kranenburg, LA Smolders, R Hagman, HJ Smidt, AS Lagerstedt, LC Penning, G Voorhout, HAW Hazewinkel, GCM Grinwis, LB Creemers, BP Meij and WJA Dhert

Spine (2012) 37: 351–358

Abstract

To investigate whether spontaneous intervertebral disc degeneration (IVDD) occurring in both chondrodystrophic (CD) and nonchondrodystrophic dogs (NCD) can be used as a valid translational model for human IVDD research.

Different animal models are used in IVDD research, but in most of these models IVDD is induced manually or chemically rather than occurring spontaneously.

A total of 184 intervertebral discs (IVDs) from 19 dogs of different breeds were used. The extent of IVDD was evaluated by macroscopic grading, histopathology, glycosaminoglycan content, and matrix metalloproteinase 2 activity. Canine data were compared with human IVD data acquired in this study or from the literature.

Gross pathology of IVDD in both dog types (CD and NCD) and humans showed many similarities, but the cartilaginous endplates were significantly thicker and the subchondral cortices significantly thinner in humans than in dogs. Notochordal cells were still present in the IVDs of adult NCD but were not seen in the CD breeds or in humans. Signs of degeneration were seen in young dogs of CD breeds (< 1 year of age), whereas this was only seen in older dogs of NCD breeds (5–7 years of age). The relative glycosaminoglycan content and metalloproteinase 2 activity in canine IVDD were similar to those in humans: metalloproteinase 2 activity increased and glycosaminoglycan content decreased with increasing severity of IVDD.

IVDD is similar in humans and dogs. Both CD and NCD breeds may therefore serve as models of spontaneous IVDD for human research. However, as with all animal models, it is important to recognize interspecies differences and, indeed, the intraspecies differences between CD and NCD breeds (early vs. late onset of IVDD, respectively) to develop an optimal canine model of human IVDD.

Introduction

Low back pain is a common disorder with a lifetime prevalence over 70% in the global population[1]. It is the main cause of lost workdays in the United States, with estimated direct medical costs of $12 billion to $25 billion annually[2,3]. Intervertebral disc degeneration (IVDD) and herniation are considered the main causes of acute and chronic low back pain[4-8]. Before new treatments for IVDD are tested in clinical trials, their safety and functionality should be extensively tested in ex vivo and in vivo animal studies. Different animal models have been used in IVDD research[9–12], but in most of these models IVDD is induced manually or chemically rather than occurring spontaneously. Animal models of spontaneous IVDD are the sand rat[13–15], pintail mouse[16], baboon[17], and dog[18–20]. Unlike mice and baboons, dogs commonly suffer from back pain due to IVDD and are diagnosed and treated for this. Moreover, the clinical presentation, macroscopic and microscopic appearance, diagnostics, and treatment of IVDD are similar in humans and dogs[8,21–23]. Decompressive surgery and spinal fusion are common treatments for IVDD in both humans and dogs.

In the dog, herniation of the intervertebral disc (IVD) is the most common cause of neurological deficits [24], and IVDD-related diseases are common reasons for euthanasia in dogs younger than 10 years[25]. The dog has frequently been used as a translational model for surgical procedures and biomechanical studies of the spine[26–31]. In most of these studies, purpose-bred, research dogs have been used. However, the availability of veterinary IVDD patients as a study population for preclinical trials has not yet been utilized, although it is likely to be beneficial not only for humans but also for dogs as veterinary patients.

Dogs can be divided into chondrodystrophic (CD) and nonchondrodystrophic (NCD) breeds based on their physical appearance. In CD breeds, endochondral ossification of the long bones is disrupted, resulting in short, bow-shaped extremities. This trait is strongly linked with IVDD and has in the past been favored in selective breeding for some breeds[24,32], such as dachshunds, with short legs and a high prevalence of IVDD. The disease is reported to develop by 1 year of age in CD breeds[32]. However, NCD breeds, and especially large-breed dogs, also often develop IVDD-related diseases, but mostly later in life[24]. The main factors responsible for IVDD are considered to be trauma or “wear and tear” in NCD breeds, but genetic in CD breeds[24,32].

Aim of the study

To investigate whether spontaneous IVDD occurring in CD and NCD breeds can be used as valid translational models for human lumbar IVDD research, by comparing the morphological appearance, histological structure, and biochemical characteristics in different stages of IVDD in dogs and humans.

Materials and methods

Study population and processing of the spines

Lower spine segments from 19 dogs (of different breeds, ages, and sex) older than 1 year, without a history of IVDD-related diseases, that died or were euthanized for reasons unrelated to this study, were dissected within 24 hours postmortem. The spinal units (endplate-disc-endplate) of the lower spines were isolated, resulting in 184 intervertebral segments (137 from NCD and 47 from CD) and cut through the sagittal midline.

The mid-sagittal plane of each spinal unit was subsequently photographed with a high-resolution digital camera (10 megapixels, Nikon, Tokyo, Japan) for gross morphological grading according to Thompson et al [33, 34]. Thereafter, 3- to 4-mm-thick mid-sagittal slices were cut and stored in 4% neutral-buffered formalin for histopathological examination. The remaining nucleus pulposus (NP) material was snap frozen (in 123 of the 184 IVDs) for glycosaminoglycan (GAG) analysis and matrix metalloproteinase 2 (MMP-2) zymography. Twenty-five histological sections (5 per Thompson grade) and 20 photographs (randomly selected) of adult human lumbar IVDs, collected with the permission of the Medical Ethics Committee, were obtained from the Biobank, Department of Pathology, University Medical Centre Utrecht. The age of the human specimens ranged between 3.3 and 88.5 years with a mean age of 56.2 years and a standard deviation of 24.9 years.

Normal anatomy and gross pathology

All photographs were assessed by 3 independent observers (N.B., J.R., and B.M.) and graded I to V using the criteria of Thompson et al[34], which have been validated for use in dogs[33]. The results were compared between human and canine IVDs as well as between CD and NCD.

The mid-sagittal photographs of all Thompson Grade I canine and human lumbar IVDs were used to measure the width (anterior-posterior), height (superior-inferior), and area of the mid-sagittal surface of the IVD and NP. All measurements were obtained using the software Image J (National Institutes of Health, Bethesda, MD). In the photographs of the canine IVDs, but not in those of the human IVDs, a transparent ruler was included to enable calculation of the dimensions. The dimensions (mm) of human lumbar IVDs were obtained from the literature[35–37]. Ratios were calculated for IVD height/width, mid-sagittal NP area/IVD area, and NP width/IVD width for all Thompson Grade I IVDs.

Histopathology

The mid-sagittal, intervertebral segments were fixed in 4% neutral-buffered formalin and decalcified in ethylenediamine-tetraacetic acid. After decalcification, all discs were embedded in paraffin. With a microtome, 5-µm sections were cut, deparaffinized, and stained with hematoxylin/eosin or Alcian blue/Picrosirius red[38].

Thirty-five canine samples were used for histological evaluation: 7 samples of each Thompson grade were randomly selected (from CD and NCD pooled) and evaluated by 3 independent observers (N.B., J.R., and G.G.), using the modified Boos grading scheme recently described for use in dogs[39]. The 3 observers also examined 25 human IVD sections (5 per Thompson grade) for comparison. The height of the entire IVD (superior-inferior) including endplates and the thickness and number of cell layers of each endplate were measured on histological sections of canine and human IVDs graded Thompson I.

Glycosaminoglycan assay

The sulfated GAG content of 123 canine NP samples was measured using the Farndale (dimethylmethylene blue) assay[40]. The relationship between GAG content and severity of degeneration in dogs was compared with that previously reported for humans[41, 42].

MMP-2 zymography

MMP-2 activity was assayed by gelatin zymography, as described previously[43]. The protein content of the NP samples was measured[44] to standardize the amount of tissue extract loaded onto precast gels (Bio-rad Laboratories, Hercules, CA) for the measurement of MMP-2 activity. High-resolution pictures were taken of the gels, in which the activity of the MMP-2 enzyme was shown as a clear band against a darker background. Enzyme activity was assessed by evaluating the amount of gel degraded by each individual NP sample[45]. The background staining of each gel was used as baseline, and the relative destaining of the individual bands was calculated using Quantity One software (Bio-rad Laboratories Hercules, CA). MMP-2 activity was calculated and grouped per Thompson grade in the same way as for human IVD samples in a previous study[43].

Statistical analysis

Differences between dogs and humans in the ratios of IVD height/width, NP area/IVD area, and NP width/IVD width of Thompson Grade I IVDs were analyzed by means of an independent sample t test. Normal distribution was verified through Q–Q plots. Pearson correlation test was used to evaluate the correlation between IVD dimensions and the weight/size of the dogs and between GAG content and Thompson grades. A Mann-Whitney U test was used to test for the association between the type of dog and Thompson grades. Differences in GAG concentrations and MMP-2 activity between the 5 Thompson grades were analyzed by Kruskal–Wallis nonparametric 1-way analysis of variance with Bonferroni correction. Statistical significance was set at $P < 0.05$.

Results

Normal anatomy and gross pathology

The overall appearance of the IVDs from humans and dogs was similar, with healthy IVDs from both species consisting of an annulus fibrosus (AF) with a clear lamellar structure and a gelatinous central NP. All 5 grades of IVDD described in humans by Thompson et al[34] were also seen in dogs (figure 9.1). However, growth plates were found in the intervertebral segments of the growing dogs (1 year old), which is not the case in growing humans[46]. Dogs normally have 7 lumbar vertebrae in comparison with 5 in humans. The cartilaginous endplates were thicker in human IVDs, and, subsequently, more pronounced endplate irregularities were found in humans with increasing severity of IVDD. In both dogs and humans, radial clefts and fissures in the NP parallel to the endplate were first detected in Thompson Grade III IVDD, whereas more extensive clefts and fissures, transecting the AF, were seen first in Thompson Grade IV IVDs in both humans and dogs.

Although the canine IVDs were smaller than the human IVDs, the ratio of NP area/IVD area was similar in the 2 species ($P = 0.18$; figure 9.1, table 9.1); however, the ratios of IVD height/width, NP/IVD width, and endplate thickness/IVD height were significantly different in healthy humans and dogs. As in humans, the height of the canine lumbosacral IVDs (5.4 ± 1.1 mm) was greater than that of the lumbar IVDs (3.5 ± 0.6 mm).

IVD height at all spinal levels was significantly correlated with weight in dogs (r = 0.8, P = 0.01), as were IVD width and weight (r = 0.6, P = 0.01). The CD and NCD breed dogs were of comparable age (5.2 years for CD dogs and 5.5 years for NCD dogs). Higher Thompson grades (more degenerated IVDs) were seen more often in CD dogs than in NCD dogs (Z = − 3.6, P = 0.0001; table 9.2). There were too few human samples to allow analysis; however, the distribution of Thompson grades in the human IVDs was more similar to that of NCD dogs than to that of CD dogs (table 9.2).

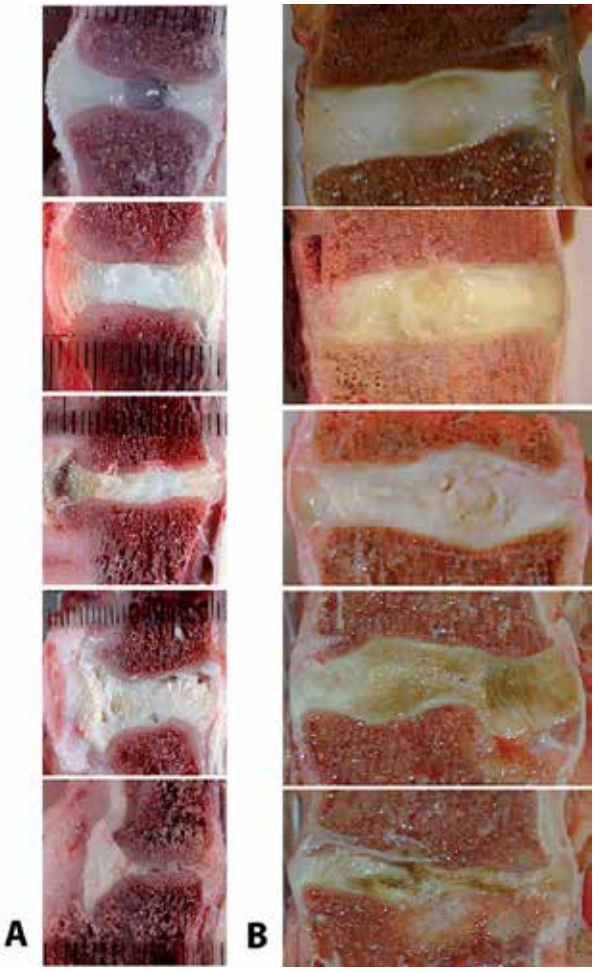

Figure 9.1. Mid-sagittal images of (A) canine intervertebral discs and (B) human intervertebral discs depicting, from top to bottom, Thompson Grades I, II, III, IV, and V

Table 9.1. Measurements and Dimensions of the Midsagittal Surface of Canine and Human Lumbar Intervertebral Discs as Determined by Gross- and Histopathological Examinations

Measurement	Dog		Human		
	Mean ± SD	Range	Mean ± SD	Range	P-value
Gross pathology					
Height IVD (mm)	3.5 ± 0.6	2.4-4.7	10 §	6-14 §	**N/A**
Width IVD (mm)	15.9 ± 2.0	11.0-18.9	35 §	27-45 §	**N/A**
Ratio IVD height/width	0.22 ± 0.03	0.14-0.28	0.29 ± 0.05	0.23-0.34	<0.01**
Ratio NP/ IVD width	0.30 ± 0.05	0.21-0.41	0.38 ± 0.05	0.31-0.44	<0.01**
Ratio NP/ IVD area	0.25 ± 0.05	0.17-0.34	0.28 ± 0.02	0.24-0.31	0.18
Histology					
Thickness EP (mm)	0.22 ± 0.06	0.1-0.42	1.58 ± 0.35	1.25-2.51	<0.01**
EP thickness/ IVD height (%)	6%	3-11%	13%	9-19%	<0.01**
Number of cell layers in EP	5	3-8	21	18-23	<0.01**
Thickness cortex (mm)	0.90 ± 0.36	0.27-1.78	0.66 ± 0.33	0.25-1.59	0.06

The P-values reflect significant differences between the values obtained in dogs and humans. NP = Nucleus pulposus, EP = Endplate, SD = Standard Deviation. N/A = Not available. § Measurements obtained from the literature[35-37]. ** Statistically significant at P < 0.01.

Table 9.2. Distribution of Thompson Grades in the Intervertebral Discs From Humans and Chondrodystrophic (CD) and Nonchondrodystrophic (NCD) Dogs

Thompson grade	CD	NCD	Humans
I	1 (2.1%)	62 (45.3 %)	7 (35 %)
II	28 (59.6%)	31 (22.6%)	3 (15 %)
III	10 (21.3%)	28 (20.4%)	3 (15 %)
IV	4 (8.5%)	12 (8.8%)	4 (20 %)
V	4 (8.5%)	4 (2.9%)	3 (15 %)

Histopathology

The overall histological appearance of the IVDs in different stages of degeneration was similar in humans and dogs (figure 9.2): the AF and NP had a similar appearance, and the cell populations and density were comparable, with fibrocyte like cells in the AF and chondrocyte-like cells in the endplate and NP. Notochordal cells were present in the NP of 7/7 canine Grade I IVDs and in 2/7 Grade II IVDs. All IVDs containing notochordal cells were from NCD. Notochordal cells were not found in any IVDs from CD dogs or humans.

In both humans and dogs, increasing Thompson grade was accompanied by degeneration of the NP with increasing cell cluster size, increasing disorganization of the AF lamellae, and increasing appearance of

clefts and cracks in the IVD. However, the endplates had more chondrocyte layers in human IVDs than in canine IVDs, whereas subchondral bony cortices were found to be thicker relative to the total IVD height and endplate thickness in dogs than in humans. The absolute thickness of the subchondral bony cortices was comparable in the 2 species (table 9.1).

The pattern of Alcian blue/Picrosirius red staining (staining GAG blue and collagen I red) was similar in human and canine IVDs: Thompson Grade I and II IVDs showed predominantly blue staining of the NP, whereas the NP of IVDs of Grade III or higher IVDs was stained red and blue or predominantly red.

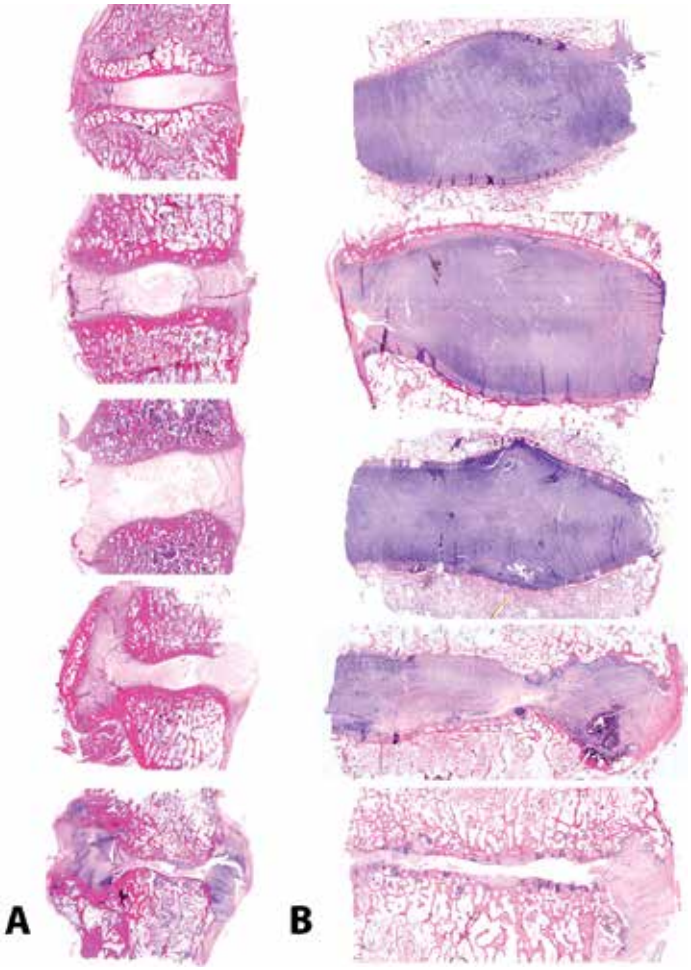

Figure 9.2. Mid-sagittal, hematoxylin/eosin stained histological sections of (A) canine intervertebral discs and (B) human intervertebral discs, depicting the histological appearance of, from top to bottom, Thompson Grades I, II, III, IV, and V

Glycosaminoglycan assay

Because only 1 of the 123 canine IVD samples used for the GAG and MMP-2 analyses was Thompson grade V, it was grouped with the Thompson Grade IV IVDs for statistical analysis (Thompson IV + V). In dogs, the mean GAG concentrations in the NP (wet weight) were negatively correlated with increasing Thompson grades ($r = -0.84$, $P = 0.0001$; figure 9.3), as has been reported in humans[41, 42].

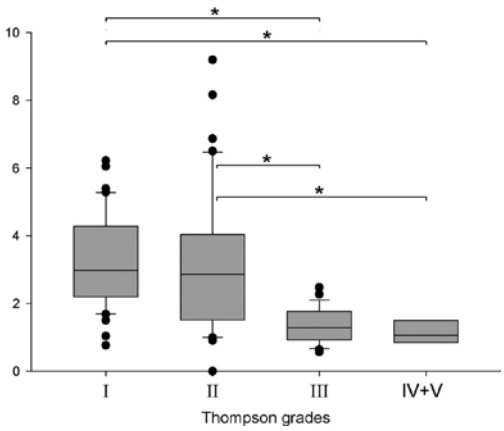

Figure 9.3. Box-plot displaying the glycosaminoglycan (GAG) concentration in the nucleus pulposus of canine intervertebral discs in relation to the Thompson Grade. * $P < 0.05$;•, outliers.

MMP-2 zymography

The mean relative activity of MMP-2 in canine IVDs increased significantly with increasing Thompson grade over Grades I to III, but decreased in the group Thompson IV + V (figure 9.4). A similar pattern has been reported in humans[43].

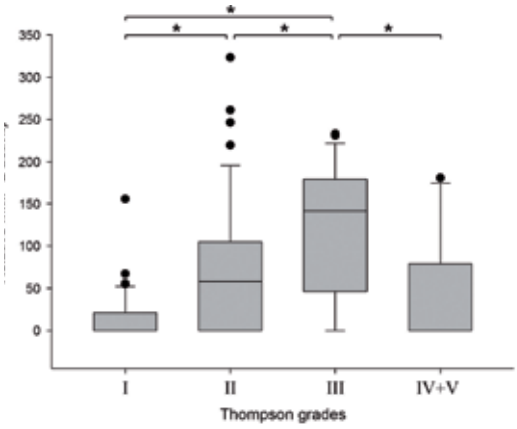

Figure 9.4. Box-plot displaying the matrix metalloproteinase2 (MMP-2) activity in the nucleus pulposus of canine intervertebral discs in relation to the Thompson Grade. * $P < 0.05$; •, outliers.

Discussion

We found that the gross pathology, histopathology, GAG content, and MMP-2 activity of human and canine IVDs were similar in all different stages of IVDD. In addition, dogs are the only animals that develop IVDD-related diseases that are diagnosed and treated, both medically and surgically, in the same way as in humans. Combined, these facts indicate that canine IVDD could prove a suitable model of spontaneously occurring IVDD for human research.

This study also shows the common occurrence of asymptomatic degenerated IVDs in dogs, just as in humans[47], and, in general, similar pathological changes were seen in degenerated IVDs from humans and dogs. Even the ratios of the different dimensions of the IVDs were similar in dogs and humans, although the canine IVDs were generally smaller relative to weight. Some differences were, however, found, such as the absence of growth plates in growing human vertebrae and the thicker cartilaginous endplates in humans. Whereas in dogs most vertebral growth takes place in the growth plates, in humans vertebral growth takes place in the junction between the vertebrae and the endplates[46], which may explain the thicker endplates found in humans.

Also at the histological level, comparisons between dogs and humans revealed similar pathological changes due to degeneration. The hallmarks of IVDD, including chondroid cell clusters, disorganization of the AF, and increasing appearance of clefts and cracks, were found in dogs and humans with increasing severity of IVDD. Notochordal cells were found in the healthy IVDs of adult NCD dogs but not in the IVDs of adult humans or CD dogs; notochordal cells are present in the NP in children and CD dogs younger than 1 year[32,48]. Apart from this discrepancy, the histological changes within each Thompson grade were similar in NCD and CD dog breeds and in humans, suggesting similar pathological processes. Also at the biochemical level, the changes occurring during IVDD were similar. In humans, MMP-2 activity is positively correlated with increasing Thompson grade up to Grade IV and decreases slightly in Grade V[43]. We found a similar trend in dogs, with the exception that MMP-2 activity was already reduced in Grade IV + V degeneration. The GAG content in canine IVDs was negatively correlated with increasing Thompson grades, as previously described for human IVDD[41, 42]. Previous studies have shown that the GAG content of IVDs from CD dogs is lower than that of IVDs from NCD dogs of similar age[49, 50]. This is consistent with IVDD occurring at a lower age in CD than in NCD dogs.

A previous study has also demonstrated the striking similarities between the magnetic resonance imaging appearance of IVDD in the different stages of degeneration in humans and dogs, even enabling the use of the human magnetic resonance imaging grading system for lumbar in veterinary practice[51,52]. Pfirrmann grading of canine lumbar IVDD is strongly correlated with Thompson grades [33,51]. In humans, degeneration of the IVD on T2-weighted magnetic resonance imaging is negatively correlated with the GAG content[53]. Our results and those of previous canine studies[33,52,54] indicate a similar trend in dogs, supporting the use of the dog as a translational model for studies of IVDD in humans.

The fact that dogs walk on 4 legs and humans on 2 is often raised as a reason to not use dogs as models for human IVDD because it is believed that humans have higher axial loading on the spinal segments due to gravity. However, the axial loading patterns of human and canine IVDs have been shown to be comparable or even higher in dogs[30,55,56]. The effect of IVDD on the biomechanical function of the canine spine has, however, not yet been investigated, and it would be of considerable interest to evaluate whether IVDD in dogs has similar effects on the functional spinal unit biomechanics as it does in humans.

The gross morphological and histological appearances of IVDs in different stages of degeneration were similar in CD and NCD dogs, but IVDD manifested much earlier in CD dogs, as reported previously[24,32,57]. All IVDs from adult CD dogs showed histological signs of degeneration, regardless of the dog's age, whereas similar signs were found in only 54.7% of the NCD dogs and most often in older dogs. These findings support the theory that the etiology of IVDD is different in the 2 groups of dogs, which could thus make 2 different IVDD models: early (CD dogs) and late (NCD dogs) onset of IVDD. The IVDD commonly seen in CD dogs is believed to be of genetic origin, as all IVDs show signs of degeneration from an early age. In contrast, the IVDD seen in NCD dogs is more likely to be caused by "wear and tear," as in most humans[22,24], although a genetic influence has also been suggested in some NCD breeds. This is supported by the higher correlation of age with IVDD in older NCD dogs and by the higher prevalence of IVDD in working dogs, and in the lumbosacral IVD, which is subjected to higher mechanical loads[58,59]. Although IVDD in CD and NCD breeds appears to have different etiologies, the pathology is similar.

When using the dog as a model for human IVDD research, it is important to recognize the differences between CD and NCD breeds (early vs. late onset, respectively). The fact that these 2 dog types spontaneously develop IVDD at vastly different ages makes them suitable as models for different types of studies. CD breeds, which develop degeneration in most of their IVDs early in life, are best suited for longitudinal studies investigating the process of IVDD, or for preclinical studies of interventional treatments aiming to prevent, stop, or slow the course of degeneration. NCD breeds, especially the German shepherd dog, are thought to have a similar disease process as humans with lumbosacral IVDD; that is, the degeneration of the lumbosacral disc in the German shepherd dog develops over a longer period (years) of chronic IVD stress, or "wear and tear." These dogs would thus make suitable models for investigating the development of IVDD of the human lumbosacral disc, and here veterinary patients could also be used for preclinical studies of new treatments for IVD degenerative diseases.

Relevant animal models are needed to improve the treatment of IVDD. As no animal model can perfectly mimic the complex processes of IVDD in humans[60], the similarities and differences between humans and animals should be considered when using animal models. Animal models of induced IVDD can result in substantial and reproducible IVDD in a short time, but it is likely that the pathological pathways differ from those involved in spontaneous IVDD, and thus the extrapolation of data from induced animal models to humans could lead to erroneous conclusions.

This study has shown that the many similarities between canine and human IVDD could make the dog a suitable animal model of human IVDD. In addition, canine IVD material for research (ex vivo) is substantially easier to obtain than human. Another advantage with using dogs as an animal model is the potential of using veterinary IVDD patients as a study population for the investigation of mechanisms of degeneration and potential new treatments. This would reduce the use of laboratory animals as models of human disease and may also lead to better treatments for canine patients. These facts, together with our findings, suggest that the dog is one of the most appropriate animal models for spontaneous IVDD.

Conclusions

There are many similarities between IVDD in humans and in CD and NCD breeds, and both types of dog breeds could serve as animal models of spontaneous IVDD for human research. However, when employing the dog as a model for human IVDD research, it is important to recognize the specific interspecies differences as well as the difference of IVDD between CD and NCD dogs (early vs. late onset, respectively).

Acknowledgments

The authors thank Joop Fama for photographs, Jane Sykes for language corrections, and Hans Vernooij (Utrecht University) for statistical analysis.

References

1. Andersson GB. Epidemiological features of chronic low-back pain. Lancet 1999; 354: 581 – 5.
2. Frymoyer JW, Cats-Baril WL . An overview of the incidences and costs of low back pain. Orthop Clin North Am 1991; 22: 263 – 71.
3. Druss BG, Marcus SC, Olfson M, et al. The most expensive medical conditions in America. Health Aff (Millwood) 2002; 21: 105 – 11.
4. Cappello R, Bird JL, Pfeiffer D, et al. Notochordal cell produce and assemble extracellular matrix in a distinct manner, which may be responsible for the maintenance of healthy nucleus pulposus. Spine 2006; 31: 873 – 82; discussion 883.
5. Mooney V. Presidential address. International Society for the Study of the Lumbar Spine. Dallas, 1986. Where is the pain coming from? Spine 1987; 12 : 754 – 9.
6. Vanharanta H, Guyer RD, Ohnmeiss DD, et al. Disc deterioration in low-back syndromes. A prospective, multi-center CT/discography study. Spine 1988; 13: 1349 – 51.
7. Luoma K, Riihimaki H, Luukkonen R, et al. Low back pain in relation to lumbar disc degeneration. Spine 2000; 25: 487 – 92.
8. Webb A. Potential sources of neck and back pain in clinical conditions of dogs and cats: a review. Vet J 2003; 165: 193 – 213.
9. Lotz J, Colliou O, Chin J, et al. Compression-induced degeneration of the intervertebral disc: an in vivo mouse model and finite-element study. Spine 1998; 23: 2493 – 506.
10. Iatridis J, Mente P, Stokes I, et al. Compression-induced changes in intervertebral disc properties in a rat tail model. Spine 1999; 24: 996 –1002.
11. Kroeber MW, Unglaub F, Wang H, et al. New in vivo animal model to create intervertebral disc degeneration and to investigate the effects of therapeutic strategies to stimulate disc regeneration. Spine 2002; 27: 2684 – 90 .
12. Omlor G, Nerlich A, Wilke H, et al. A new porcine in vivo animal model of disc degeneration: response of anulus fi brosus cells, chondrocyte-like nucleus pulposus cells, and notochordal nucleus pulposus cells to partial nucleotomy. Spine 2009; 34: 2730 – 9.
13. Silberberg R. Histologic and morphometric observations on vertebral bone of aging sand rats. Spine 1988; 13: 202 – 8.
14. Gruber HE, Johnson T, Norton HJ, et al. The sand rat model for disc degeneration: radiologic characterization of age-related changes: cross-sectional and prospective analyses. Spine 2002; 27: 230 – 4.
15. Moskowitz R, Ziv I, Denko C, et al. Spondylosis in sand rats: a model of intervertebral disc degeneration and hyperostosis. J Orthop Res 1990; 8: 401 – 11.
16. Berry RJ. Genetically controlled degeneration of the nucleus pulposus in the mouse. J Bone Joint Surg 1961; 43B: 387 – 93.
17. Lauerman W, Platenberg R, Cain J, et al. Age-related disk degeneration: preliminary report of a naturally occurring baboon model. J Spinal Disord 1992; 5: 170 – 4.
18. Ghosh P, Taylor T, Braund K, et al. A comparative chemical and histochemical study of the chondrodystrophoid and nonchondrodystrophoid canine intervertebral disc. Vet Pathol 1976; 13: 414 – 27.
19. Ghosh P, Taylor T, Braund K, et al. The collagenous and non-collagenous protein of the canine intervertebral disc and their variation with age, spinal level and breed. Gerontology 1976; 22: 124 – 34.

20. Goggin JE, Li AS, Franti CE. Canine intervertebral disk disease: characterization by age, sex, breed, and anatomic site of involvement. Am J Vet Res 1970; 31: 1687 – 92.
21. Lotz JC. Animal models of intervertebral disc degeneration: lessons learned. Spine 2004; 29: 2742 – 50 .
22. Hansen HJ. A pathologic-anatomical interpretation of disc degeneration in dogs. Acta Orthop Scand 1951; 20: 280 – 93.
23. Viñuela-Fernández I, Jones E, Welsh E, et al. Pain mechanisms and their implication for the management of pain in farm and companion animals. Vet J 2007; 174: 227 – 39.
24. Bray JP, Burbidge HM. The canine intervertebral disk. Part two: degenerative changes nonchondrodystrophoid versus chondrodystrophoid disks. J Am Anim Hosp Assoc 1998; 34: 135 – 44.
25. Agria I . Five Year Statistical Report. Stockholm, Sweden: Agria Animal Insurances; 2000: 33 – 8.
26. Cole T, Burkhardt D, Ghosh P, et al. Effects of spinal fusion on the proteoglycans of the canine intervertebral disc. J Orthop Res 1985; 3: 277 – 91.
27. Holm S, Nachemson A. Variations in the nutrition of the canine intervertebral disc induced by motion. Spine 1983; 8: 866 – 74 .
28. Cole TC, Ghosh P, Hannan NJ, et al. The response of the canine intervertebral disc to immobilization produced by spinal arthrodesis is dependent on constitutional factors. J Orthop Res 1987; 5: 337 – 47.
29. Smith K, Hunt T, Asher M, et al. The effect of a stiff spinal implant on the bone-mineral content of the lumbar spine in dogs. J Bone Joint Surg Am 1991; 73: 115 – 23.
30. Zimmerman MC, Vuono-Hawkins M, Parsons JR, et al. The mechanical properties of the canine lumbar disc and motion segment. Spine 1992; 17: 213 – 20 .
31. Bushell GR, Ghosh DP, Taylor TK, et al. The effect of spinal fusion on the collagen and proteoglycans of the canine intervertebral disc. J Surg Res 1978; 25: 61 – 9.
32. Hansen HJ. A pathologic-anatomical study on disc degeneration in dog, with special reference to the so-called enchondrosis intervertebralis. Acta Orthop Scand Suppl 1952; 11: 1 – 117.
33. Bergknut N, Grinwis G, Pickee E, et al. Validation of macroscopic grading of canine intervertebral disc degeneration according to Thompson and correlation with low field magnetic resonance imaging Am J Vet Res 2010 ; In press.
34. Thompson JP, Pearce RH, Schechter MT, et al. Preliminary evaluation of a scheme for grading the gross morphology of the human intervertebral disc. Spine 1990; 15: 411 – 5.
35. Amonoo-Kuofi HS. Morphometric changes in the heights and anteroposterior diameters of the lumbar intervertebral discs with age. J Anat 1991; 175: 159 – 68 .
36. Aharinejad S, Bertagnoli R, Wicke K, et al. Morphometric analysis of vertebrae and intervertebral discs as a basis of disc replacement. Am J Anat 1990; 189: 69 – 76.
37. Eijkelkamp MF, et al. On the development of an artificial intervertebral disc. Faculty of Medical Sciences, Thesis. Groningen, The Netherlands: University of Groningen; 2002: 106.
38. Gruber HE, Ingram J, Hanley EN Jr. An improved staining method for intervertebral disc tissue. Biotech Histochem 2002; 77: 81 – 3.
39. De Nies K, Bergknut N, Meij BP, et al. Introduction and validation of a new histological scoring scheme for classification of intervertebral disc degeneration in dogs. Proceedings of European Veterinary Congress, Amsterdam, The Netherlands; 2010: 248 – 9 .

40. Farndale RW, Buttle DJ, Barrett AJ. Improved quantitation and discrimination of sulphated glycosaminoglycans by use of dimethylmethylene blue. Biochim Biophys Acta 1986; 883: 173 – 7.
41. Antoniou J, Steffen T, Nelson F, et al. The human lumbar intervertebral disc: evidence for changes in the biosynthesis and denaturation of the extracellular matrix with growth, maturation, ageing, and degeneration. J Clin Invest 1996; 98: 996 – 1003.
42. Lyons G, Eisenstein SM, Sweet MB. Biochemical changes in intervertebral disc degeneration. Biochim Biophys Acta 1981; 673:443 – 53.
43. Rutges J, Kummer J, Oner F, et al. Increased MMP-2 activity during intervertebral disc degeneration is correlated to MMP-14 levels. J Pathol 2008; 214: 523 – 30.
44. Lowry OH, Rosebrough NJ, Farr AL, et al. Protein measurement with the Folin phenol reagent. J Biol Chem 1951; 193: 265 – 75.
45. Snoek-van Beurden PA, Von den Hoff JW. Zymographic techniques for the analysis of matrix metalloproteinases and their inhibitors. Biotechniques 2005; 38: 73 – 83.
46. Taylor JR. Growth of human intervertebral discs and vertebral bodies. J Anat 1975; 120: 49 – 68.
47. Boden SD, Davis DO, Dina TS, et al. Abnormal magnetic-resonance scans of the lumbar spine in asymptomatic subjects. A prospective investigation. J Bone Joint Surg Am 1990; 72: 403 – 8.
48. Hunter CJ, Matyas JR, Duncan NA. The notochordal cell in the nucleus pulposus: a review in the context of tissue engineering. Tissue Eng 2003; 9: 667 – 77.
49. Ghosh P, Taylor TK, Braund KG. Variation of the glycosaminoglycans of the intervertebral disc with ageing. II. Non-chondrodystrophoid breed. Gerontology 1977; 23: 99 – 109.
50. Ghosh P, Taylor TK, Braund KG. The variation of the glycosaminoglycans of the canine intervertebral disc with ageing. I. Chondrodystrophoid breed. Gerontology 1977; 23: 87 – 98.
51. Pfirrmann CW, Metzdorf A, Zanetti M, et al. Magnetic resonance classification of lumbar intervertebral disc degeneration. Spine 2001; 26: 1873 – 78.
52. Bergknut N, Auriemma E, Wijsman S, et al. Pfirrmann grading of intervertebral disc degeneration in chondrodystrophic and nonchondrodystrophic dogs with low field magnetic resonance imaging. Am J Vet Res 2010; In press.
53. Pearce RH, Thompson JP, Bebault GM, et al. Magnetic resonance imaging reflects the chemical changes of aging degeneration in the human intervertebral disk. J Rheumatol Suppl 1991; 27: 42– 3.
54. Smidt H-J, Bergknut N, Hagman R, et al. A comparative study on MMP-2 activity and GAG concentration in different stages of degenerated canine intervertebral discs. In: Proceedings of European Veterinary Congress. Amsterdam, The Netherlands; 2010: 266 – 7.
55. Bray JP, Burbidge HM. The canine intervertebral disk: part one: structure and function. J Am Anim Hosp Assoc 1998; 34: 55 – 63.
56. Smit TH. The use of a quadruped as an in vivo model for the study of the spine—biomechanical considerations. Eur Spine J 2002; 11: 137 – 44.
57. Hoerlein BF. Intervertebral disc protrusions in the dog. I. Incidence and pathological lesions. Am J Vet Res 1953; 14: 260 – 9.

58. Danielsson F, Sjostrom L. Surgical treatment of degenerative lumbosacral stenosis in dogs. Vet Surg 1999; 28: 91 – 8.
59. Meij BP, Bergknut N. Degenerative lumbosacral stenosis. Vet Clin North Am Small Anim Pract 2010; 40: 983 – 1009.
60. Alini M, Eisenstein SM, Ito K, et al. Are animal models useful for studying human disc disorders/degeneration? Eur Spine J 2008; 17: 2 – 19.

CHAPTER 10

Intradiscal injections of BMP-7 and Marimastat in a rabbit model for IVD degeneration does not have a regenerative effect

JPHJ Rutges, N Bergknut, J van Tiel, BP Meij, E Waarsing, AS Lagerstedt, LC Penning, MA Tryfonidou, LB Creemers and WJA Dhert

Manuscript in preparation for submission

Abstract

Low back pain, caused by IVD degeneration, is one of the most common health problems in the world. Since current therapies yield far from optimal results, new treatments strategies aiming at inhibition of IVD degeneration and regeneration of the disc are being developed.

Aim of this study is to evaluate the effect of local injection with Marimastat on intervertebral disc (IVD) degeneration in a rabbit annular puncture model with BMP-7 as positive control.

In 51 lumbar IVDs of 17 new Zeeland White rabbits degeneration was induced by stabbing with a 16 G needle. After 6 weeks, IVDs were injected with placebo, BMP-7 alone, BMP-7 or Marimastat in combination with a hyaluronic acid (HA)-based carrier, HA carrier alone. A non stabbed group was included as control. Animals were terminated at week 18 and the progression of IVD degeneration and/or regeneration was evaluated using radiography, MRI, micro-CT, histology, morphologic appearance and by measuring GAG/DNA of the nucleus pulposus.

Mild to moderate degeneration was seen in all IVDs, apart from the non-stabbed control group. No signs of regeneration could be detected in any of the treated IVDs.

BMP-7 and Marimastat did not regenerate the degenerated IV, nor did they halt the process of degeneration. This could be attributed to a number of different confounding factors such as: the low number of IVDs per treatment group, to low biologic activity of the active substances injected to achieve therapeutic effects or the severe periosteal reactions secondary to the surgical approach.

Introduction

Low back pain is one of the leading causes of disability in the world and is significantly associated with intervertebral disc (IVD) degeneration[1-4]. Most patients suffering from low back pain are treated conservatively with anti-inflammatory medication and physical therapy. Surgical treatment is reserved for patients not responding to conservative treatment or those suffering from more severe symptoms. The most common surgical treatments of end stage disc disease are spinal fusion or total disc replacement. These surgical procedures are considered salvage techniques and are primarily aimed at reducing pain. In addition, complications such as implant migration after total disc replacement and adjacent segment degeneration after spinal fusion may occur[5-8].

New treatments aim at restoring spinal function by biological repair of the degenerated intervertebral disc (IVD)[9-11]. Within the cascade of degeneration, the extracellular matrix is further degraded due to an imbalance between catabolism and anabolism. Regenerative strategies aim at restoring the homeostasis of the degenerated IVD by employing anabolic factors and by suppressing catabolic stimuli[12,13]. In this respect, intradiscal administration of the growth factor bone morphogenetic protein 7 (BMP-7) has been reported to have a regenerative effect in vivo in various experimental animal models with induced IVD degeneration[11,14-15]. It is also known that matrix metalloproteinases (MMPs) play an important role in the process of IVD degeneration[16]. MMPs can be inhibited by the enzyme inhibitor Marimastat[17,18]. Marimastat has also been shown to inhibit MMP activity in a rat arthritis model, evident by reduction of hindpaw swelling and local bone destruction[19]. Therefore, Marimastat may also be used to halt the process of IVD degeneration. The aim of this study was to evaluate the regenerative effects of Marimastat in an induced degeneration animal model. In order to do so, we studied the effects of a single injection of Marimastat in combination with a hydrogel carrier containing hyaluronic acid facilitating the prolonged release of Marimastat locally. A single injection of BMP-7 alone or in combination with the hydrogel carrier served as a positive control.

Material and Methods

Materials

Lyophilized BMP-7, containing sucrose, mannitol, glycine and tween, was obtained from Prospec Bio (Rehovot, Israel). The two component hyaluronic acid (HA) hydrogel was a gift from Dr. T. Bowden Uppsala University, Sweden. Marimastat was a gift from Dr. R. Hanemaaijer TNO Leiden, the Netherlands. The control sucrose solution was prepared before surgery, the BMP-7 solution and the control, BMP-7, and Marimastat HA gel were prepared during surgery.

The placebo solution consisted of 1% sucrose, 1.2% mannitol, 20mM glycine, and 0.005% tween 20. For the BMP-7 solution 125 µg BMP-7 was dissolved in 25 µl MQ resulting in 125 ug BMP-7 1% sucrose, 1.2% mannitol, 20 mM glycine, and 0.005% tween 20 in 25 µl solution. The HA gel was made of two components; the first component consisted of 0.24% polyvinylalcohol 2.4% mannitol, 40mM glycine, and 0.010% tween 20. The second component consisted of 2.75% hyaluronic acid. Equal volumes (12.5 µl) of each

component were mixed. The BMP-7 and Marimastat HA gel were prepared in a similar way as the control gel; the first contained 125 µg BMP-7 or 150 ng Marimastat. A total of 20 µl was injected with a 25 µl syringe (7654-01, Hamilton Reno USA) and a 26 gauge needle (7758-04, Hamilton Reno USA).

Experimental animals

A total of 17 skeletally mature female New Zealand White rabbits (age 15 months, weight 3.2-4.6 kg) were used after approval by the animal ethics commission at Utrecht University, the Netherlands (DEC 2007. III.08.108/vervolg4). The rabbits were housed in three groups (5, 6, and 6) in large cages and permitted free activity throughout the study. They were fed hay and pellets at maintenance level and had free access to fresh water.

Study design

Three lumbar discs, L2-L3, L3-L4, and L4-L5, were used in each rabbit, resulting in a total number of 51 IVDs. All IVDs were randomly divided into one control group (untreated IVDs) and five different treatment groups, i.e. the placebo solution, the HA hydrogel carrier alone, Marimastat in combination with the HA hydrogel carrier and BMP-7 alone or in combination with the HA hydrogel carrier (table 10.1). Disc degeneration was induced in all IVDs by means of annular puncture at week 0, apart from the 8 IVDs in the control group. At week 6 the IVDs in the five treatment groups were injected intradiscally in order to stop the process of degeneration by Marimastat or to initiate regeneration by BMP-7 and followed up for 12 weeks. Briefly, at 12 weeks radiographic evaluation of the lumbar spine was performed at week 18, all rabbits were terminated. Post-mortem, the lumbar spines were subjected to MRI and subsequently transected mid-sagittal using a water-cooled diamond saw. The dorsal vertebral arch was removed and after macroscopic evaluation, one half of the Intervertebral segment (IVD with adjacent vertebral end-plates) was stored in 4% formalin for micro-CT and histology. The other half was snap frozen in liquid nitrogen for analysis of the glycosaminoglycan (GAG) and DNA content of the nucleus pulposus (NP).

Table 10.1. The different treatment groups, the specific treatments given to each group and the number of IVDs per group.

Group	Treatment	Number of IVDs injected
1. Control	Non stabbed IVDs	7
2. Placebo solution	1% sucrose, 1.2% mannitol, 20mM glycine and 0.005% tween 20	7
3. HA hydrogel	First component (12.5 µl): 0.24% polyvinylalcohol, 2.4% mannitol, 40mM glycine and 0.010% tween 20. Second component (12.5 µl): 2.75% hyaluronic acid (HA)	8
4. BMP-7 solution	125 µg BMP-7 dissolved in 25 µl MQ resulting in 125 ug BMP-7 1% sucrose, 1.2% mannitol, 20mM glycine and 0.005% tween 20 in 25 µl solution	8
5. BMP-7 in HA hydrogel	First component (12.5 µl): of 125 µg lyophilized BMP-7), 0.24% polyvinylalcohol 2.4% mannitol, 40mM glycine and 0.010% tween 20. Second component (12.5 µl): 2.75% hyaluronic acid (HA)	9
6. Marimastat in HA hydrogel	First component (12.5 µl): 150 ng Marimastat, 0.24% polyvinylalcohol 2.4% mannitol, 40mM glycine and 0.010% tween 20. The second component consisted of 2.75% hyaluroninc acid (HA)	8

Anesthesia, analgesia and medical treatment

Premedication was given by intramuscular injections of midazolam 2 mg/kg, 5 mg/ml solution, Dormicum (Roche, Basel, Switzerland), and intravenous injection of methadone 0.5 mg/kg (Eurovet animal health, Bladel, The Netherlands). Preemptive antibiotic treatment was administered subcutaneously with 5 mg/kg, 2.5% solution, Baytril (Bayer, Leverkusen, Germany) and twenty-four hours after the intradiscal injection of the different treatments

Anesthesia was induced using intravenous injection of etomidate until effect, 1.5-2 ml/rabbit Etomidaat-Lipuro, 2 mg/ml, (Braun, Melsungen, Germany). Anesthesia was maintained with 2-2.5% isoflourane with a carrier of 50% oxygen mixed with air (Abbott animal health, IL, USA). Anesthesia was monitored with pulse-oximitry, arterial blood pressure, core temperature, and capnography. Post-operative analgesia was administered subcutaneously with buprenorphine twice daily for three days with 0,15 ml/kg, (Temgesic, Schering-Plough, NJ, USA).

Surgical procedure

The annular stab disc degeneration model according to Masuda was used[20]. Briefly, the rabbits were placed in right lateral recumbence and a posterolateral retroperitoneal approach was used to gain access to the anterolateral aspect of the vertebral column of the L2-3, L3-4, and L4-5 IVDs in the 5 treatment groups. Intra operative fluoroscopy was used to verify the correct IVDs to be punctured using a 16-gauge, 1.5 inches long needle (Microlance, BD, Drogheda, Ireland). The puncture was made 5 mm deep and the needle rotated 180º before withdrawal. The correct depth was controlled by use of a custom made stainless steel sleeve for

the needle and confirmation of NP material on the tip of the needle was used as verification that the IVD was stabbed correctly.
The intradiscal injections were administered six week after induction of IVD degeneration and the disc was approached from the contralateral side for the injections in order to avoid complications such as adhesions from the previous surgery. The same surgical technique as described above was used in order to gain access to the anterolateral aspect of the IVDs for the injections.

Radiographic evaluation of disc height

Lateral radiographs of the lumbar spines were obtained at week 0 (preoperatively), week 6 (before intradiscal injection) and at week 12 and 18 using Siemens fluoroscopy (Siremobile Iso-C, Siemens AG, Erlangen, Germany). All radiographs were obtained at a standardized distance with the rabbits under general anesthesia, apart from week 18 when radiography was performed postmortem. A radiopaque ruler was placed parallel to the spines during radiography as a size marker. The disc height was measured blinded, on lateral radiographs. One single horizontal measurement in the centre of the IVD of each radiograph was performed on enlarged, digitally enhanced images. The relative change in disc height relative to the pre-operative disc height of the healthy discs was calculated for further analysis.

MRI imaging and analysis

MR imaging of the IVDs were all performed within 4 hours post mortem. The caudal (lower) spines (T13 to L6) were surgically removed and wrapped in gauze moistened with saline before being subjected to MRI. A quadrature volume coil (ID 2 cm) was used in a 9.4 T, 12 cm bore animal magnet (Varian Inc., Paolo Alto, CA). T2 and ADC maps were obtained with a slice thickness of 500 µm or 300 µm in both the transverse and sagittal plane. T1-weighted 3D gradient echo images (TR/TE 10/1.98 ms, flip angle 5,20,50 or 90 degrees) had isotropic resolution (235 µm in all directions) and therefore transverse images through the middle of the IVD obtained from this set were used for the image analysis. MR images were analyzed using the software Image J (National Institutes of Health, Bethesda, MD). The average relative intensity of the entire IVD (1.00 = white and 0.0 = black) was determined.

Macroscopic grading

All intervertebral segments were macroscopically graded on degree of degeneration using the Thompson score[21]. The mid-sagittal surfaces of the intervertebral segments were photographed, blinded, and graded by three independent observers (NB, JR JvT). When the three observers did not agree on the grade of an IVD, the photograph was reviewed and a consensus decision made.

Glycosaminoglycan content of the NP

Half of each snap frozen NP sample was analyzed spectrophotometricly using the Farndale (dimethylmethylene blue) assay to determine the glycosaminoglycan (GAG) content corrected for the mg wet weight of each samples[22]. Protein digestion was performed overnight at 56°C in a Proteinase K digestion buffer. After

incubation the samples were heated to 100°C for 10 minutes to inactivate the proteinases K. Thereafter a series of 6 dilutions in PBS/EDTA, ranging from 1:500 to 1:2000, were prepared from each sample. 100µl of each sample dilution was pipetted into a 96 well, flat bottom, microtitre plate (microplate, 96w, PS, flat, 656191, Greiner bio-one, Frickenhausen, Germany). The standard line was based on Chondroitin Sulphate C (CSC) (shark cartilage sodium salt, C-4384, SIGMA-ALDRICH, St. Louis, MO, USA). Just before the spectrophotometric analysis at wavelengths of 530nm and 590nm, 200µl of filtered dimethylmethylene blue (DMB) solution was added to each well.

Micro-computed tomography (Micro-CT)

All IVDs were scanned with a micro-CT scanner (Skyscan 1076, Skyscan, Kontich, Belgium). A scan of 180 degrees was performed at a voltage of 55 Kv and a current of 181 µA using a 0.5 aluminum filter and an exposure time of 1180 ms. Thereafter three dimensional reconstructions of the micro-CT scans were made using NRecon (NRecon software version 1.5.1.4, Skyscan, Kontich, Belgium). The reconstructed datasets had a voxel size of 18 µm.

The amount of periosteal reaction and osteophyte formation per intervertebral segment was evaluated using DataViewer. Before evaluation, all intervertebral segments were viewed to give an idea of the range of new bone formation in the samples and a scoring system for periosteal reactions and osteophyte formation at the anterior side of the IVD was designed (table 10.2). The scoring was subsequently performed in unison by two of the researchers (JvT and NB).

Table 10.2. Scoring system for periosteal reaction and osteophyte formation.

Extent of osteophyte formation	Score
No periosteal reaction or osteophyte formation	0
Mild periosteal reaction and/or osteophyte formation	1
Moderate periosteal reaction and/or osteophyte formation	2
Severe periosteal reaction and/or osteophyte formation with tendency of bridging the effected segment (ankylosing spondylitis).	3

Histological evaluation

After micro-CT evaluation, the intervertebral segments were decalcified (0.5M EDTA) and embedded in paraffin. Three consecutive 5 µm thick sections per intervertebral segment were stained with: Hematoxylin - Eosine (HE), Alcian Blue - Picrosirius Red (AB/PR), and Safranin O (Saf-O) staining. Histological grading was performed as described before Rutges et. al[23]. Scoring was performed by three independent observers (JvT, NB, and JR) and interobserver deviations of more than two points were discussed in a consensus meeting.

Statistical analysis

Statistical analyses were performed using the Statistical Package for the Social Sciences (SPSS) 20.0 software for Windows (SPSS Inc., Chicago, IL, USA). The outcome variables were analyzed in a general linear model followed by a Benjamini Hoogberg correction for multiple comparisons. Treatment type was the fixed factor of the model and treatment level (L2-L3, L3-L4 or L4-L5) as random factor. P-values < 0.05 were considered significant. Normal distribution of all read out parameters were ensured through Q-Q plots.

Results

Four IVDs were excluded from the study, two IVDs due to an error in the stabbing procedure during surgery and another two IVDs due to damage sustained while transecting the spines post mortem. The exclusion resulted in a loss of one IVD in four different treatment groups. The final number of IVDs per treatment is shown in table 10.1.

Animal welfare and surgical complications

All animals were weighed weekly and although most animals lost weight in the week following surgery, all rabbits weighed more at the conclusion of the study than at the start. All rabbits where stable during both surgical procedures and recovered quickly post operatively. Only minor complications such as small seromas, delayed wound healing, and minor irritations around the surgical sites were noticed.

Radiographic evaluation of disc height

The mean disc height was not significantly restored compared with the pre-operative disc height in any of the treatment groups. The relative change in disc height at 6, 12 and 18 weeks did not significantly differ between the treatment groups, except for the Marimastat-HA group which showed a significantly smaller relative change in disc height at 6 (prior to intra-discal injection) and 12 weeks of the study (i.e., 6 weeks after intradiscal injection) (figure 10.1).

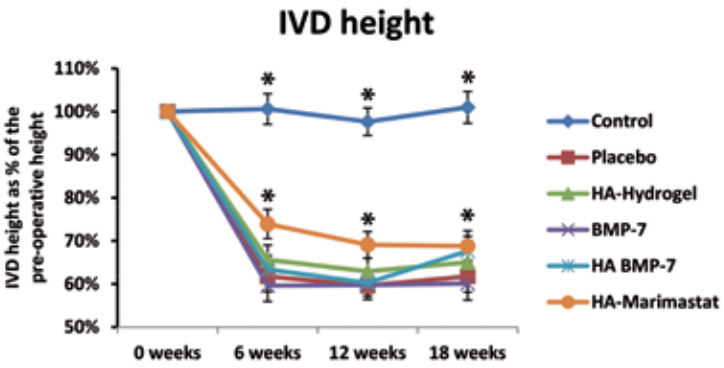

Figure 10.1. Disc height as percentage of pre-operative height at 6, 12 and 18 weeks follow-up. * = p < 0.05. HA=hyaluronic acid hydrogel

MRI assessment

Due to an error in the MR imaging, the scans of the first three rabbits could not be used rendering 9 IVDs lost to MRI evaluation. From the 38 IVDs that could be evaluated, there was however a significant lower average intensity of the entire IVD in the non stabbed control discs as compared to all treatment groups. There were no significant differences between the treatment groups (figure 10.2).

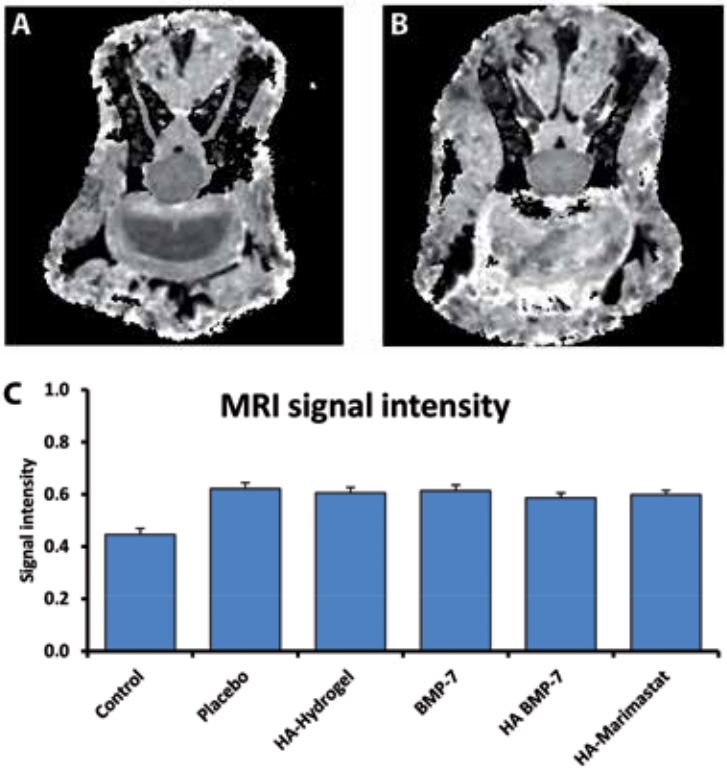

Figure 10.2. MRI images showing a healthy, non-degenerative IVD (A) and a degenerative IVD (B), in which the needle tract is still visible. MRI signal intensity for the control group and all treatment groups (C). HA= hyaluronic acid hydrogel

Macroscopic grading

The distribution of the Thompson score ranged from grade I (healthy IVD) to grade IV (moderate/severe degeneration)(figure 10.3)[21]. All non stabbed controls were grade I and most of the stabbed IVDs were graded II or III, only one IVD was given a Thompson grade IV. The non stabbed control discs had a significantly lower Thompson score compared to the treated IVDs, whereas there were no differences between the treatment groups.

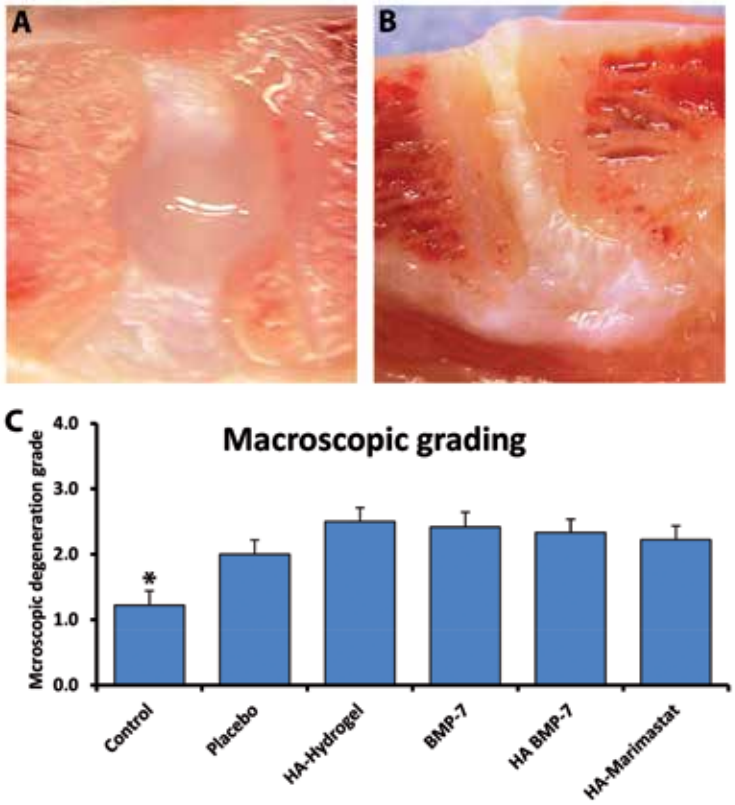

Figure 10.3. Mid sagittal photographs used for the macroscopic grading. Healthy, non-degenerative IVD (A) and moderately degenerated IVD from a rabbit. Macroscopic degeneration grade for each treatment (C). * = $p < 0.05$. HA= hyaluronic acid hydrogel

Glycosaminoglycan content of the NP

It was evident that the three treatment groups where hyaluronic acid was included showed a significantly lower GAG content of the NP than the other treatment groups, indicating that hyaluronic acid interfered with the GAG analysis.

The GAG content/mg tissue was significantly higher in the non stabbed control discs compared to HA alone, HA-BMP-7, and HA-Marimastat. The GAG content corrected for DNA was significantly higher in the on stabbed control discs compared to all treatment groups (figure 10.4).

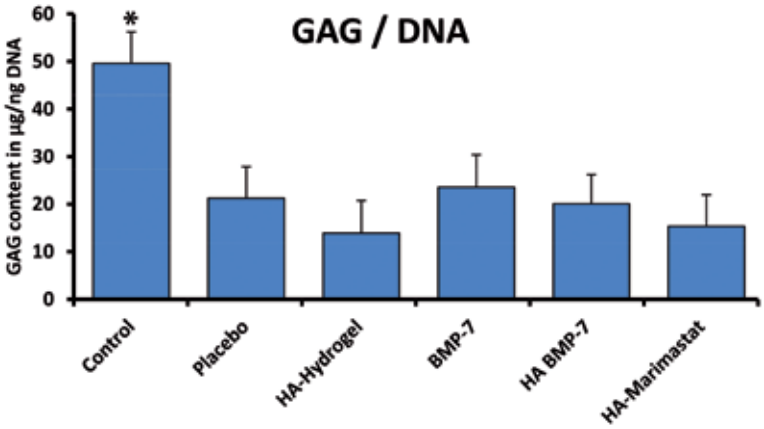

Figure 10.4. Glycosaminoglycan per ng DNA for the nucleus pulposus of each treatment group. * = $p < 0.05$. HA= hyaluronic acid hydrogel

Micro-CT

There was an unexpectedly high frequency of osteophyte and new bone formation on the ventral aspect of most IVDs in all treatment groups. ($p \leq 0.05$). There was no significant difference between the individual treatment groups (figure 10.5).

Histology

The mean outcomes of the histological degeneration score of the intervertebral segments varied in the treatment groups from (lowest) 5.5 points in group 5, to (highest) 7.0 points in groups 3 and 6. The mean score of the control non stabbed group was significantly lower than all treatment groups. The differences between the individual treatment groups were not significant (figure 10.6 and 10.7)

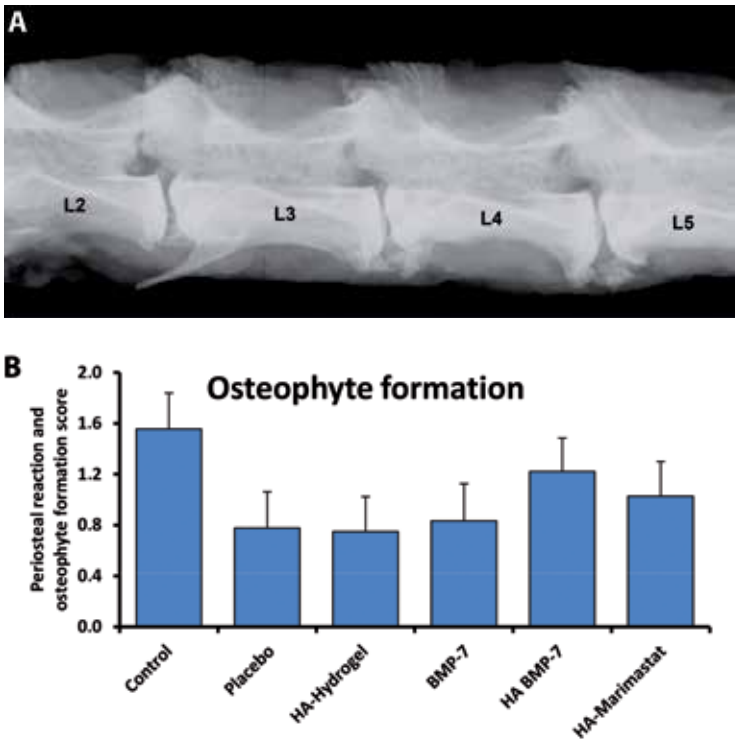

Figure 10.5. Lateral radiograph of spinal segment L2-L5 with a non stabbed control disc at L2-L3 with no ventral osteophyte formation. Moderate to severe osteophyte formation is seen at L3-L4 and L4-L5 (A). Extent of osteophyte formation for each treatment group (B). HA= hyaluronic acid hydrogel

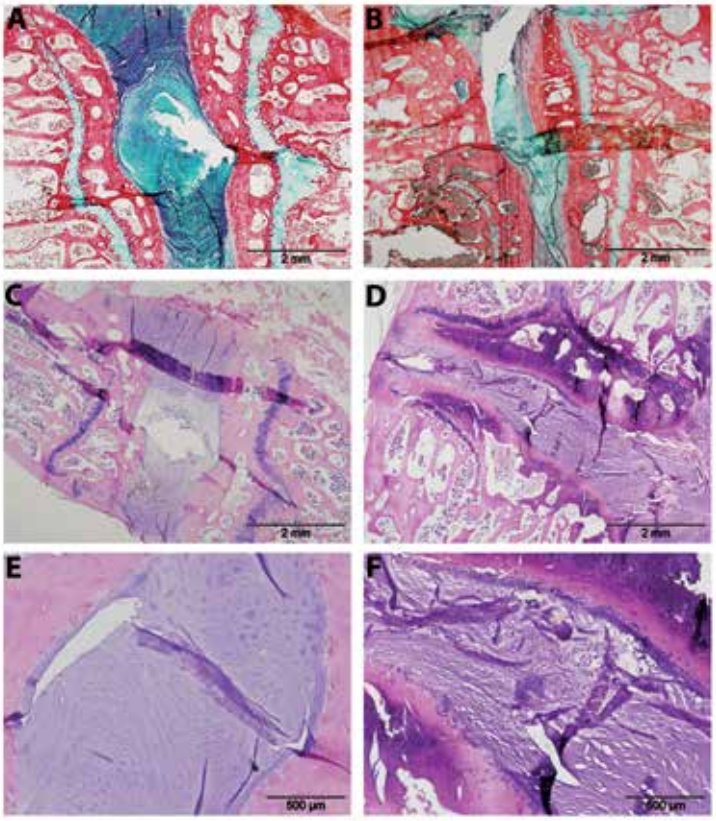

Figure 10.6. Histological images of lumbar rabbit IVDs. Alcian Blue - Picrosirius Red (AB/PR) staining of a healthy IVD depicting the proteoglycan matrix which is stained intensely blue (A), (the missing matrix in the center of the healthy IVD sections A and C is a result of the dehydration required for embedding in paraffin). AB/PR staining of a degenerated IVD where the intensity of the blue staining of the proteoglycan matrix is more faint (B). Hematoxylin - Eosine (HE) staining of a healthy IVD where there is a clear border between the annulus fibrosis (AF) and the nucleus pulposis (NP) (C). HE staining of a degenerated IVD where there is no clear border between the AF and NP (C). HE staining of a healthy IVD where the matrix structure of the NP is well organized (apart from the fold of the section which is an artifact) (E). HE staining of a degenerated IVD where the matrix structure of the NP is severely disorganized (F).

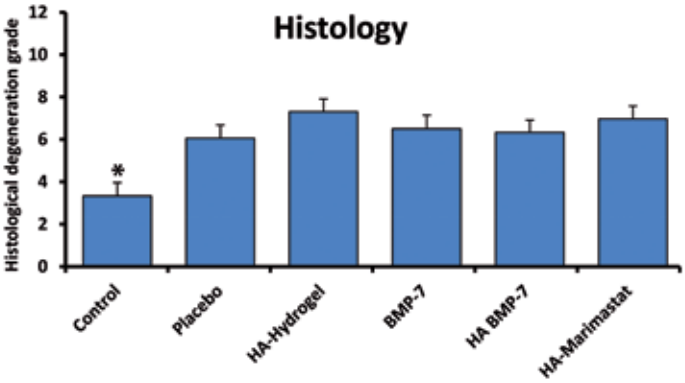

Figure 10.7. Histological degeneration grade for each treatment group. * = $p < 0.05$. HA= hyaluronic acid hydrogel

Discussion

The overall aim of this study was to investigate whether Marimastat could significant halt or even reverse the course of IVD degeneration in a rabbit stab model. An injection BMP-7 alone or in combination with a HA based hydrogel carrier was employed as a positive control. However, no significant improvement of any of the treatments was found, indicating that the different treatments had similar/or no effect on the degree of IVD degeneration.

It was however expected that the degree of degeneration would be lower in IVDs treated with Marimastat and BMP-7 compared to the placebo group. Especially BMP-7 injections were expected to have a positive effect on the IVDs since they have been previously reported in at least two different animal models with induced degeneration[11-15, 24-25].

The fact that no positive treatment effects could be seen in our study could indicate that the injected substances do not cause IVD regeneration but it could also be due to a number of different confounding factors such as: the low number of IVDs per treatment group, to low biological activity of the active substances injected to achieve therapeutic effects, or the severe periosteal reactions secondary to the surgical approach. In terms of relative loss of disc height and histological grading we found similar results to the previous studies in which disc degeneration was also induced by stabbing the annulus with a needle[11, 20, 23, 24, 26-27]. However, it has previously been described that care must be taken while surgically approaching the IVD as to prevent periosteal reactions. Nevertheless our surgical approach caused moderate to severe periosteal reactions in most IVDs which may have been detrimental for the study results[20].

Conclusion

The rabbit annular puncture model is effective in producing moderate IVD degeneration. However, we were not able to halt IVD degeneration or to induce regeneration by injection of Marimastat and BMP-7. The results for BMP-7 are in contrast with previous results described in literature and could be caused by difference in biological activity and extensive osteophyte formation in the current study. Further studies are needed to evaluate the effectiveness of BMP 7 and Marimastat in the treatment of IVD degeneration.

References

1. Manchikanti, L., et al., Comprehensive review of epidemiology, scope, and impact of spinal pain. Pain Physician, 2009. 12(4): p. E35-70.
2. Frymoyer, J.W. and W.L. Cats-Baril, An overview of the incidences and costs of low back pain. Orthop Clin North Am, 1991. 22(2): p. 263-71.
3. Cheung, K.M., et al., Prevalence and pattern of lumbar magnetic resonance imaging changes in a population study of one thousand forty-three individuals. Spine (Phila Pa 1976), 2009. 34(9): p. 934-40.
4. Adams, M.A., Biomechanics of back pain. Acupunct Med, 2004. 22(4): p. 178-88.
5. Resnick, D.K. and W.C. Watters, Lumbar disc arthroplasty: a critical review. Clin Neurosurg, 2007. 54: p. 83-7.
6. Jacobs, W., et al., Total disc replacement for chronic back pain in the presence of disc degeneration. Cochrane Database Syst Rev, 2012. 9: p. CD008326.
7. Min, J.H., et al., The clinical characteristics and risk factors for the adjacent segment degeneration in instrumented lumbar fusion. J Spinal Disord Tech, 2008. 21(5): p. 305-9.
8. Yang, J.Y., J.K. Lee, and H.S. Song, The impact of adjacent segment degeneration on the clinical outcome after lumbar spinal fusion. Spine, 2008. 33(5): p. 503-7.
9. Hiyama, A., et al., Transplantation of mesenchymal stem cells in a canine disc degeneration model. J Orthop Res, 2008. 26(5): p. 589-600.
10. Ganey, T., et al., Disc chondrocyte transplantation in a canine model: a treatment for degenerated or damaged intervertebral disc. Spine, 2003. 28(23): p. 2609-2260.
11. Masuda, K., et al., Osteogenic protein-1 injection into a degenerated disc induces the restoration of disc height and structural changes in the rabbit anular puncture model. Spine, 2006. 31(7): p. 742-54.
12. Masuda, K. and H.S. An, Prevention of disc degeneration with growth factors. Eur Spine J, 2006. 15 Suppl 3: p. S422-32.
13. Kalson, N.S., S. Richardson, and J.A. Hoyland, Strategies for regeneration of the intervertebral disc. Regen Med, 2008. 3(5): p. 717-29.
14. Kawakami, M., et al., Osteogenic protein-1 (osteogenic protein-1/bone morphogenetic protein-7) inhibits degeneration and pain-related behavior induced by chronically compressed nucleus pulposus in the rat. Spine (Phila Pa 1976), 2005. 30(17): p. 1933-9.
15. Masuda, K., Biological repair of the degenerated intervertebral disc by the injection of growth factors. Eur Spine J, 2008. 17 Suppl 4: p. 441-51.
16. Rutges, J., et al., Increased MMP-2 activity during intervertebral disc degeneration is correlated to MMP-14 levels. J Pathol, 2008. 214(4): p. 523-30.
17. French, J.J., et al., A matrix metalloproteinase inhibitor to treat unresectable cholangiocarcinoma. HPB (Oxford), 2005. 7(4): p. 289-91.
18. Jezierska, A. and T. Motyl, Matrix metalloproteinase-2 involvement in breast cancer progression: a mini-review. Med Sci Monit, 2009. 15(2): p. RA32-40.
19. Fujisawa, T., et al., Highly water-soluble matrix metalloproteinases inhibitors and their effects in a rat adjuvant-induced arthritis model. Bioorg Med Chem, 2002. 10(8): p. 2569-81.

20. Masuda, K., et al., A novel rabbit model of mild, reproducible disc degeneration by an anulus needle puncture: correlation between the degree of disc injury and radiological and histological appearances of disc degeneration. Spine (Phila Pa 1976), 2005. 30(1): p. 5-14.
21. Thompson, J.P., et al., Preliminary evaluation of a scheme for grading the gross morphology of the human intervertebral disc. Spine, 1990. 15(5): p. 411-5.
22. Farndale, R.W., D.J. Buttle, and A.J. Barrett, Improved quantitation and discrimination of sulphated glycosaminoglycans by use of dimethylmethylene blue. Biochim Biophys Acta, 1986. 883(2): p. 173-7.
23. Rutges, J.P., et al., A validated new histological classification for intervertebral disc degeneration. Osteoarthritis Cartilage, 2013. 21(12): p. 2039-47.
24. An, H.S., et al., Intradiscal administration of osteogenic protein-1 increases intervertebral disc height and proteoglycan content in the nucleus pulposus in normal adolescent rabbits. Spine, 2005. 30(1): p. 25-31; discussion 31-2.
25. Masuda, K., et al., Recombinant osteogenic protein-1 upregulates extracellular matrix metabolism by rabbit annulus fibrosus and nucleus pulposus cells cultured in alginate beads. J Orthop Res, 2003. 21(5): p. 922-30.
26. Sobajima, S., et al., A slowly progressive and reproducible animal model of intervertebral disc degeneration characterized by MRI, X-ray, and histology. Spine (Phila Pa 1976), 2005. 30(1): p. 15-24.
27. Chan, D.D., et al., Mechanical deformation and glycosaminoglycan content changes in a rabbit annular puncture disc degeneration model. Spine (Phila Pa 1976). 36(18): p. 1438-45.

CHAPTER 11

General discussion

Towards new treatments for IVD degeneration

The clinical outcome of surgical treatment for intervertebral disc (IVD) degeneration has been widely discussed ever since the introduction of spinal fusion and the IVD prosthesis in the past century[1-5]. Surgical therapy failed to establish unquestionably superior results in comparison to conservative treatment and therefore, the interest in new less invasive treatment modalities significantly increased in the past two decades[1-6]. Several new treatment strategies for IVD degeneration have been introduced at the beginning of this century, amongst which are growth factors, injectable nucleus pulposus prosthesis, inhibitors of degenerative enzymes and tissue engineering[6-11]. However, to date there is still no adequate regenerative medicine-based therapy available for IVD degeneration[12]. Thorough understanding of the pathophysiology of the degenerative process is essential for the further development of these new treatment strategies. Therefore, the main aim of this thesis is to contribute to a better understanding of the pathophysiology of IVD degeneration.

One of the most important explanations for limited success of RM approaches may be the ongoing process of degeneration[11,13]. Inhibiting this degenerative process most likely will be a prerequisite for successful regeneration and hence, discovery of the pathways involved in the degenerative process is required. Through interference with key enzymes or key cytokines involved in IVD degeneration, normal tissue homeostasis could be restored and further IVD degeneration might be prevented or will potentially pave the way for other regenerative approaches. To this end, we divided this thesis in three phases. In the first phase we further elucidated the pathophysiology of IVD degeneration and searched for new therapeutic targets, with special interest in matrix metalloproteinases (MMPs). The second phase consists of several studies to determine which animal model is most appropriate for the evaluation of new treatment strategies for IVD degeneration. Moreover, we developed a new histological grading of IVD degeneration to standardize the histological outcome. In the third phase we attempted to halt or reverse IVD degeneration by injection of a MMP inhibitor and a growth factor in a rabbit model for IVD degeneration.

MMPs as target in the treatment of IVD degeneration

IVD degeneration is a complex process with a clear genetic disposition and several contributing factors. Mechanical loading, poor vascularisation and nutrition, ageing and senescence are such factors that influence the balance between anabolism en catabolism, resulting in IVD degeneration[12-15]. Large numbers of enzymes, enzyme inhibitors and soluble mediators, including pro- and anti-inflammatory cytokines, take part in this process and lead to an increase in extracellular matrix degeneration which cannot be compensated for by an increased production of matrix proteins by the nucleus pulposus cells[12-15]. Amongst the degenerative enzymes reported to be present in the degenerated IVD are matrix metalloproteinases (MMPs), a disintegrin and metalloproteinase with thrombospondin motif (ADAMTS') and to a lesser extent cathepsins. MMP-1, MMP-2, MMP-3, MMP-9, MMP-13 and MMP-14 have been associated with IVD degeneration[14-18]. Moreover ADAMTSs, in particular ADAMTS 1, 4, 5 and 15, have been found in degenerative IVDs[17,19-21]. Apart from the metalloproteinases and ADAMTSs mentioned, also the cathepsins D, K and L are associated with disc degeneration[22-24].

MMP-13 is well known for its ability to degrade collagen type II, which potentially makes it an instrumental factor in the degradation of collagen type II in the degenerating disc[25]. Furthermore, ADAMTS-4, ADAMTS-5 and MMP-2 and MMP-3 are capable of degrading proteoglycans, which also suggest an important role in de degeneration of the NP in the early stages of IVD degeneration[8]. Cathepsins D, K, L are theoretically even capable of degrading both essential extracellular matrix (ECM) components, aggrecan and collagen type II. However, these enzymes have been associated with endplate separation and annulus fibrosus (AF) disorganisation rather than nucleus pulposus (NP) degeneration[8,26].

Whether the abovementioned enzymes are truly instrumental in IVD degeneration, is largely unknown. Many studies have focussed on mRNA levels, while mRNA levels do not necessarily reflect protein levels. Moreover, in particular MMPs are produced as inactive pro-enzymes. Higher levels of active MMP-2 were found in degenerate IVDs compared to healthy adult IVDs, rendering its role in IVD disease more likely (this thesis, chapter 2). The concomitant increase of MMP-14 points towards a role of this enzyme in activation of the MMP-2 (this thesis, chapter 2). MMP-14 may well be a key enzyme in IVD degeneration because of its ability to also activate other MMPs such as MMP-13, in addition to directly degrading extracellular matrix components[25,27]. Relatively little research is done on this enzyme until now.

Although targeting of specific proteases could be a promising strategy for reversing or delaying IVD degeneration, there also are some challenges. First of all, the role of specific degenerative enzymes should be further elucidated. Although in this thesis MMP-2 and MMP-14 are clearly associated with disc degeneration, it could be possible that inhibition of only MMP-14 and MMP-2 is not sufficient to halt the degeneration process and also inhibition of other enzymes, for example ADAMTS's, is required. Additionally, how and how long should these enzymes be inhibited? Is short-term inhibition with broad-spectrum inhibitors MMP such as Marimastat (this thesis, chapter 10) sufficient, or is a long-term release combined with a more advanced inhibition strategy such as RNA interference necessary?

Moreover, inhibition of degenerative enzymes should be done with caution. Namely, MMPs have also extensively been shown to be involved in the development of synovial joints, including MMP-1, 2, 3 and 14[8,17,26]. Indeed, high MMP-2 activity and MMP-14 production was found during human foetal disc development (this thesis, chapter 3). During IVD development, MMPs are most likely involved in cell migration, regulation of ECM turnover, and activation of other MMPs[28-31]. MMP-14 could also be one of the most important enzymes in this process, since MMP-14 knock-out mice have a very severe phenotype characterized by dwarfism, osteopenia, osteoarthritis, angiogenesis defects and death within 3-12 weeks after birth[32-34]. Therefore, successful regenerative strategies for IVD degeneration by enzyme inhibition should specific enough to purely inhibit the degenerative process without interference of the required matrix remodelling for tissue regeneration.

Other targets for inhibition of the degenerative process in IVD degeneration

The catabolic process in degenerative IVDs is assumed to be mediated by several cytokines that have been found to be associated with disc degeneration[7,14,15,35,36]. Increased TNFα and IL1β mRNA levels have been demonstrated in chondrocyte nests of degenerative IVDs[7,14,15,36,37]. TNFα positive cells have been clearly demonstrated by immunohistochemistry in degenerative areas of human IVDs[36]. The exact role of most up-regulated cytokines in IVD degeneration and herniation is still unknown. However, IL1β has been shown to increase the production of several MMPs and ADAMTSs in IVD cells in vitro and to mediate matrix degeneration on IVD sections as measured by in situ zymography. Moreover, TNFα and IL1β were able increase ADAMTS-5 expression and activity via syndecan-4 expression in vitro[38,39]. Another indication that IL-1β is instrumental in IVD degeneration is the fact that IL1 receptor antagonist deficient mice have IVDs with characteristics of IVD degeneration and their IVD cells show an increased expression of MMP-3, MMP-7 and ADAMTS-4[26]. Blocking the IL-1 receptor in vitro by IL-1 receptor antagonist reduced the production of MMP-1, MMP-3, MMP-7, MMP-13 and ADMTS-4 by NP cells[40].

Since cytokines appear to have such an important role in regulating extra cellular matrix (ECM) degradation in IVD degeneration, they could be interesting targets to halt this process. Decreasing cytokine mediated ECM degeneration could be a more potent approach than inhibition of specific enzymes, since it interferes with an earlier phase in the pathway of IVD degeneration. Nevertheless, the same limitations as mentioned earlier for enzyme inhibition therapy also apply to cytokine interference based IVD therapies; interference with which cytokine is most effective, how should this therapy be applied to the degenerative IVD and for how long? It is clear that for both enzyme en cytokine interference based therapies more knowledge regarding exact role of these proteins in the pathophysiology of IVD degeneration is required.

Subchondral bone changes in IVD degeneration

Sclerosis of the subchondral bone is a well known radiological hallmark of advanced IVD degeneration and it is commonly seen on radiographs of degenerative IVDs[41]. Confusingly, subchondral sclerosis in IVD degeneration is also described as endplate sclerosis or endplate calcification by several authors[42,43]. However, we have shown that there are no indications that the cartilaginous endplate calcifies during IVD degeneration, either histologically or radiologically (this thesis, chapter 4 and 5)[44,45].

In IVD degeneration the subchondral bone volume and trabecular thickness are already increased in grade II disc degeneration, as also shown in chapter 5 of this thesis[46,47]. The early onset of bone changes found in the endplate could indicate that these changes may be involved in the initiation of IVD degeneration. In humans the permeability of the cartilage endplate together with the subchondral bone is significantly lower in degenerative IVDs, which was shown by limited gadolinium diffusion as imaged by MRI, high levels of lactic acid and concomitant low pH values in degenerative IVDs[48,49]. Since the permeability of subchondral bone is decreased in degenerative IVDs and as nutrients are supplied to the IVD by diffusion, primarily from vessels in the subchondral bone and to limited extent from peripheral blood vessels in the annulus fibrosus, the

degenerative changes are commonly assumed to lead to the decreased nutrition in the degenerative IVD[50-52]. The observed increase in subchondral bone in degenerative IVDs is relatively large, approximately 30% more subchondral bone was found in grade II disc when compared to grade I IVDs. However, the absolute increase is limited, only 7% more subchondral bone was found in grade II discs when compared to grade I discs. It remains unclear if such small changes in bone volume alone could be responsible for a biochemically relevant reduction in subchondral endplate permeability.

Moreover, the nutrition and diffusion of waste products may not be solely dependent on diffusion and subchondral bone permeability. Transport of nutrients within the centre of the IVD may also be dependent on mechanical loading[42,43,45,53]. Due to the high osmotic pressure of compressed proteoglycans in loaded IVDs nutrient transport may be partly dependent on fluid flow through the IVD[54]. Since in degenerative IVDs the concentration of proteoglycans is reduced, diffusion of nutrients may not only be decreased due to subchondral bone sclerosis, but also by less efficient diffusion during loading caused by the lower osmotic pressure in the degenerative IVD.

The poor nutrition and accumulation of waste products is an important factor that should be taken into account when developing a new regenerative treatment for intervertebral disc degeneration. For example, are cells that are transplanted into a degenerative IVD able to survive in that environment and are there enough nutrients available for these cells to produce the appropriate ECM for IVD regeneration. Currently, there are no strategies under development that solely aim at restoring endplate permeability of the degenerative IVD. Moreover, it is unlikely that simple restoration of the endplate permeability would be sufficient to initiate IVD regeneration since also the degenerative process has to be stopped, the NP cells should be stimulated to produce new ECM, and the biomechanical properties of the degenerative IVD should be restored to prevent reoccurrence of endplate sclerosis. Therefore, a regenerative medicine strategy that combines cell transplantation with improvement of nutrient diffusion might be a logical new approach to halt IVD degeneration. For example, increasing of the local proteoglycan concentration would increase the osmotic pressure, improve the diffusion of nutrients, and possibly the regenerative potential of transplanted cells.

Hypertrophic differentiation in IVD degeneration

Besides endplate sclerosis, also ECM calcification is present in the NP and AF of degenerative IVDs and has been suggested to be the result of hypertrophic differentiation (this thesis, chapter 4)[54,55-57]. Hypertrophic differentiation is characterized by the induction of collagen type X, alkaline phosphatase (ALP) and, eventually, matrix calcification[58-61]. How hypertrophic differentiation is regulated in IVD degeneration is still unknown. In osteoarthritis (OA), several indications are present that hypertrophic differentiation is regulated by runt-related transcription factor 2 (RUNX-2), which is also known as core-binding factor subunit alpha-1 (CBFa-1)[58-61]. RUNX-2, a transcription factor that is essential in osteoblast differentiation and bone formation, is clearly up-regulated during hypertrophic differentiation and is thought to be involved in the progression of

OA[60,62,63]. The expression of the transcription factor RUNX-2 in degenerative IVDs, as described in chapter 4 of this thesis, indicate that that hypertrophic differentiation in IVD degeneration could also be RUNX-2-mediated[59,60,62,63]. This hypothesis is further support by the finding that mice that overexpress RUNX-2 have degenerative IVDs in which increased collagen type X expression and hypertrophic chondrocytes were found[59]. How RUNX-2 expression is induced during the degeneration of cartilaginous tissues is currently unknown[64].

However, preventing calcification is not considered as a new treatment strategy for IVD degeneration since there is no indication that local calcifications are responsible for any of the symptoms associated with degenerative disc disease. Nevertheless, calcification, as frequently observed at X-rays, CT or MRI scans, could be useful as cut off point for regenerative treatment strategies as hypertrophic differentiation may be a clear sign of advanced stages of IVD degeneration[65-67]. Moreover, another completely different treatment for IVD degeneration based on hypertrophic differentiation should be developed if regenerative treatment strategies turn out to be not successful. Spinal interbody fusion by stimulating hypertrophic differentiation and IVD calcification could be an interesting new minimally invasive treatment that potentially might replace traditional surgical spinal fusion or as adjuvant therapy to enhance the results of instrumented spinal fusion.

The importance of characterization of the nucleus pulposus cells

An essential step to be taken in regenerative medicine research, especially cell- based approaches, is the ability to identify NP cells. Although NP cells show many similarities with chondrocytes from articular cartilage there are some crucial differences[59]. For example, the ratio between proteoglycans and collagen mRNA is much higher in NP cells, compared to articular chondrocytes[68]. The high proteoglycan content results in a hydrated and very elastic IVD with the capability to withstand large compressive forces[69]. Imitation of these unique characteristics of NP cells is most likely essential for the restoration of the biomechanical properties of the IVD and consequently the success of regenerative medicine strategies.

Nevertheless, characterizing NP cells and identification of their specific markers is a true challenge. First of all, there are many differences in IVD morphology and NP cell phenotype between rodents, small and large mammals, and these differences limit the possibility to translate the results from animal studies to humans[14,70]. Secondly, healthy human IVD tissue from young donors without disc degeneration is only sparsely available and early stages of degeneration is difficult to identify and easily be mistaken for healthy IVDs[71]. Based on earlier results of rat and beagle dog studies we identified cytokeratin-19 as possible marker for NP cells in human samples (this thesis, chapter 6). At the protein level cytokeratin-19 was mainly observed in NP cells of non-degenerative IVDs and was barely detectable in IVDs from donors older than 30 years (this thesis, chapter 6). Interestingly, immunohistochemistry also showed clearly positive staining of the notochordal (NC) cells present in non-degenerative IVDs. This finding raises the following question: is cytokeratin-19 a marker for both the NP and NC phenotype cells? Does this finding indicate that both cell types originate from the same progenitor cell?

The potential of NC cells in regenerative treatment strategies

Historically NC cells are thought to be the remaining cells from the embryonic notochord that gets entrapped in the center of the NP during the embryological development of the IVD and that undergoes apoptosis during adulthood[15,72]. However, more recent theories suggest that NC cells differentiate to NP cell type instead of becoming apoptotic[73]. Fate mapping studies in mice have shown that all NP cells are of notochordal origin[15,72]. Moreover, it has been shown by labeling studies that NC cells remain present in adult non-degenerative IVDs[74]. This results in the current hypothesis that all NP cells are derived from NC progenitor cells and that both the chondrocyte-like NP cells and the NC cells originate from the notochordal lineage, but represent different stages of maturation[74,75]. Currently, little is known about the NC progenitor cells, however, they appear to remain present in human IVDs, also during adulthood, and are capable of differentiating along the mesenchymal pathway to replace apoptotic cells in the IVD[75,76].

NC cells are nowadays thought to play an important role in the development and normal homeostasis of the IVD and therefore, they are a very interesting cell type for new regenerative strategies[77,78]. However, it is not likely that NC cells will used for direct transplantation into degenerative IVDs since they produce less proteoglycans than the condrocyte like NP cells[79]. Currently, it is investigated how NC cells can be used to enhance the potential of other cells that might be used for IVD regeneration[31]. Moreover, NC cells could also be used to differentiate mesenchymal stem cells or chondrocytes towards a more NP phenotype[77,80,81]. Notochordal conditioned medium has been shown to stimulate the production of aggrecan, an collagen type II, to down-regulate MMP-3 expression, and decrease the production of collagen type I, III and X[77,80,81]. Although the results of the NC cell based regenerative medicine approaches that are currently under investigation are encouraging, the next big challenge in cell based therapy for IVD degeneration is the identification of the NC progenitor cell. If NC progenitor cells can be harvested and cultured, it would become possible to investigate how these progenitor cells can be stimulated to proliferate and differentiate towards NP and NC cells. This could be a first step towards a regenerative treatment strategy that is based on in vivo stimulation of NC progenitor cells.

Limitations of animal models for IVD degeneration

To date, more than fifty animals models for IVD degeneration have been described[77,80,81]. The fact that there are this many different animals models to simulate a single condition indicates that it is difficult to develop an ideal model for IVD degeneration. Like all animal models, the models for IVD degeneration have several limitations. The first hurdle is how to induce IVD degeneration. Stabbing and compression are the most commonly used methods to induce IVD degeneration[71]. Stab models rely on the puncture or disruption of the AF, which leads to herniation of the NP and subsequently, to IVD degeneration. However, the pathogenesis of disc herniation and degeneration has been shown to be biochemically and histologically different[71]. Therefore, stab models may not be the method of choice for animal studies on the pathogenesis of IVD degeneration (this thesis, chapter 10).

Compression models for IVD degeneration are much more suitable for elucidating the pathogenesis of IVD degeneration, because they resemble the aetiology of IVD degeneration much better than the stab models. Compression models induce degeneration by static or dynamic loading, which is assumed to be an important factor in the pathogenesis of human IVD degeneration[12,15]. Downsides of these models are that they can be a huge burden for the animals, for example shown by the weight loss during the experiments of chapter 7, and they are less practical since more time is needed to induce IVD degeneration. Furthermore, the level of degeneration achieved with these models is rather mild (this thesis, chapter 7). Consequently, in contrast to the stab models, compression models may be more suitable for evaluating the pathogenesis of early disc degeneration, but seem to be less appropriate for testing new treatment options since the achieved level of degeneration appears to be too mild to represent a clinically relevant level of degeneration.

Spontaneous degeneration caused by loading of the IVD would best resemble human the pathogenesis of human disc degeneration. Dogs develop spontaneous IVD degeneration and are commonly presented to the veterinarian with symptoms caused by IVD degeneration[82]. IVD degeneration is found in chondrodystrophic dogs such as Beagles and for some breeds of nonchondrodystrophic animals such as Labradors and German Shepherds[83]. Chondrodystrophic dogs show an early onset of IVD degeneration and most likely this has a strong genetic component[83]. This may imply a different etiology for disc degeneration in these breeds of dogs compared to disc degeneration seen in humans. Hence, nonchondrodystrophic dogs may be more suitable for research on pathology and treatment of IVD degeneration (this thesis, chapter 8). Even then, it must be kept in mind that larger mammals such as goats, pigs and dogs, due to their closeness to humans, are less often used for experiments due to ethical and emotional reasons. Furthermore, these studies are also far more expensive than rodent experiments.

In the end, the relevance of a model will largely depend on the aim of the study. Elucidation of the mechanisms of disc degeneration will preclude the use of stab, but rather be based on spontaneous disc degeneration models, such as the dog models, or models that show only slight degeneration, as in the rabbit model of compression (this thesis; chapter 7). However, damage-induced IVD degeneration may be suitable for the evaluation of the effectiveness of new treatment strategies for IVD degeneration. For example, stab models are still appropriate for evaluation of the efficacy of injectable hydrogels in degenerative IVDs.

The role of ex-vivo models in the translation from in-vitro results towards animal models

Ex vivo culturing models using goat, sheep and bovine motion segments could play a crucial role in the translation from in vitro results towards the first animal experiments. These ex-vivo cultures hold great potential and enable us to mimic different loading schemes, nutrition levels and test new treatment strategies in complete IVDs without the necessity of an animal model[83]. Although ex vivo IVD cultures provide us with many new research options that are not possible in animal models, it is unlikely that animals won't be needed anymore for IVD research. Apart from the notion that until now the IVDs cannot be kept in culture for much longer than four weeks, it is yet not possible to completely simulate the complex in vivo

environment of the human IVD in an ex vivo model and animal models will remain obligatory before starting a phase I clinical trial in humans[84-86].

Ethical aspects of IVD regeneration

Although the research on intervertebral disc degeneration has considerably intensified during the past decade and the in vivo results of new treatment strategies are promising, a clinical available regenerative therapy still seems far away[87]. It will be at least 10 to 20 years before such a therapy will become clinically available. To achieve this, enormous scientific and financial efforts are required.

Although recent MRI studies have shown a clear correlation between chronic low back pain and MRI characteristics of intervertebral disc degeneration, the exact relation between pain and radiologically observed degeneration is still unkown[88-91]. Therefore, it is questionable if the focus of our current research is ethically appropriate. We strive for completely regenerated degenerative discs, but it would be an undesirable situation if a “successfully treated” patient remains painful, despite an entirely regenerated IVD. For that reason, the investments in new degenerative therapies should be accompanied by an increased effort to further elucidate the exact mechanism how IVD degeneration can lead to chronic low back pain. Additionally, more insight into this mechanism could also improve the selection of patients who are eligible for such a regenerative treatment.

Another ethical aspect of regenerative therapies for IVD degeneration is the treatment of non-symptomatic patients. Most likely the first patients that can successfully be treated with a regenerative approach are patients with an early stage of degeneration. However, the question is if these patients are already symptomatic, and if not, how can we determine whether they will enter the next stage of degeneration? If degeneration has not yet led to back pain in this patient group, will screening and prevention for IVD degeneration be feasible? Moreover, is screening on degeneration of intervertebral discs ethical when there is still controversy about the relation between disc degeneration and chronic low back pain? Will such screening prevent the development of chronic low back pain? Therefore, from an ethical point of view thorough understanding of the pathophysiology of disc degeneration and insight into the pathway by which disc degeneration leads to pain is needed and should be integrated in the development of regenerative treatment strategies.

Future treatment strategies

The concept of intervertebral disc (IVD) regeneration as an alternative for spinal fusion or IVD prosthesis is based on the suboptimal results of these surgical treatment options[88-92]. The first articles that describe the potential of regenerative medicine strategies as treatment of IVD degeneration have been published more than 15 years ago[93,94].

Over the past decades, several interesting new treatment strategies for IVD degeneration have been developed. Amongst these therapies are injectable NP replacements, growth factors, and tissue engineering strategies

(cell transplantation). Since IVD degeneration is characterised by a combination of loss of extracellular matrix (ECM), loss of biomechanical function, loss of nucleus pulposus (NP) cells, and disturbance of the balance between anabolism and catabolism, it is unlikely that one of the proposed new treatment strategies alone would be able to achieve IVD regeneration. It is more likely that a combination of different therapies is needed to initiate IVD regeneration or to halt degeneration, for example a injectable hydrogel seeded with NP-like cells, supported by growth factors. Moreover, to be successful a new therapy should also take care of the degenerative process. Without inhibition of the degenerative process the effect of all regenerative strategies will most likely be temporary and the best possible results of these therapies will be a short-term improvement or slowing of the degenerative process. Therefore, the proposed growth factor and cell containing gel should also include bioactive factors that inhibit the degenerative process. Examples of such bioactive factors are cytokine receptor antagonist, inhibitors of degenerative enzymes, or modified extracellular matrix molecules that are biocompatible to the normal matrix, but cannot be degraded by human enzymes[9].

However, the question remains which cells should be used in the hydrogel NP replacements; NP cells, NC cells, notochordal progenitor cells, or no cells at all? Is a gel with growth factors and enzyme inhibitors sufficient to regenerate the degenerative IVD? In any case, we need to determine how and for how long growth factors and inhibitors of the degenerative process need to be released. An interesting option would be plasmid DNA-based gene therapy in an alginate hydrogel to provide a long-term release of growth factors. Recently, release of a BMP-2 plasmid DNA from an alginate hydrogel has been shown to successfully induce bone formation in an in vivo model[95]. A similar sustained release of SiRNA's could be used to inhibit the production of degenerative enzymes.

Nevertheless, if a cell seeded gel or construct appears to be more effective, it needs to be investigated how these cells should be transplanted into the degenerative disc. Can these cells simply be seeded in an injectable hydrogel? Or is a more sophisticated approach required? Although not injectable, a printable construct will offer the unique possibility to print AF cells, NP cells and NP progenitors at their appropriate anatomic location surrounded by suitable extracellular matrix[96].

Besides identifying the most effective combination of regenerative therapies and how these therapies should be delivered to the intervertebral disc, there are also numerous practical challenges that need to be addressed. Some of these challenges are the identification of growth factors that are safe for application in the IVD, the prevention of leakage of the injected hydrogels especially if multiple injections are required.
Most likely, on the long-term, regenerative medicine strategies for IVD degeneration will follow the path of autologous chondrocyte transplantation. However, since potential promising regenerative strategies for disc degeneration are no mono therapies, in contrast to autologous chondrocyte transplantation, these strategies will be more complex. The development of lasting regenerative IVD treatment modalities requires more extensive research before they can become clinically available. When the complete pathophysiology of IVD degeneration is known, we will be able to more effectively develop new treatment strategies.

These treatments can be used as independent treatment or as adjuvant therapy for adjacent segments in combination with spinal fusion or a IVD prosthesis. If these regenerative medicine strategies can be administered minimally invasive, they could hold great promise for treatment of multiple segments without the drawbacks of extended multi level surgery.

References

1. Arts MP, Kols NI, Onderwater SM, Peul WC. Clinical outcome of instrumented fusion for the treatment of failed back surgery syndrome: a case series of 100 patients. Acta Neurochir (Wien) 154[1213], 1217. 2012.
2. Bogduk N, Andersson G. Is spinal surgery effective for back pain? F 1000 Med Rep 1, 60-62. 2009.
3. Christensen FB. Lumbar spinal fusion. Outcome in relation to surgical methods, choice of implant and postoperative rehabilitation. Acta Orthop Scand 75, S2-S43. 2004.
4. Martin BI, Mirza SK, Comstock BA, Gray DT, Kreuter W, Deyo RA. Reoperation rates following lumbar spine surgery and the influence of spinal fusion procedures. Spine 32, 382-387. 2007.
5. Schizas C, Kulik G, Kosmopoulos V. Disc degeneration: current surgical options. Eur Cell Mater 20, 306-315. 2010.
6. Smith LJ, Nerurjar NL, Choi KS, Harfe BD, Elliott DM. Degeneration and regeneration of the intervertebral disc: lessons from development. Dis Model Mech 4, 31-41. 2011.
7. Alini M, Roughley PJ, Antoniou J, Stoll T, Aebi M. A biological approach to treating disc degeneration: not for today, but maybe for tomorrow. Eur Spine J. 11 Suppl 2, S215-S220. 2002.
8. Bramono DS, Richmond JC, Weitzel PP, Kaplan DL, Altman GH. Matrix metalloproteinases and their clinical applications in orthopaedics. Clin Orthop Relat Res 272[285]. 2004.
9. Le Maitre CL, Hoyland JA, Freemont AJ. Inlerleukin-1 receptor antogonist delivered directly and by gene therapy inhibtis matrix degradation in the intact degenerate human intervertrbral disc: an in situ zymographic and genen therapy study. Arthritis Research & Therapy 9, R83. 2007.
10. Ludwinski FE, Gnanalingham K, Richardson SM, Hoyland JA. Understanding the native nucleus pulposus cell phenotype has important implications for intervertebral disc regeneration strategies. Regen Med [1], 75-87. 2013.
11. Zhang Y, Chee A, Thonar EJ, An HS. Intervertebral disk repair by protein, gene, or cell injection: a framework for rehabilitation-focused biologics in the spine. PM R 3, S88-S94. 2013.
12. Freemont AJ. The cellular pathobiology of the degenerate intervertebral disc and discogenic back pain. Rheumatology 48, 5-10. 2009.
13. Hughes SPF, Freemont AJ, DWL Hukins, McGregor AH, Roberts S. The pathogenesis of degeneration of the intervertebral disc and emerging therapies in the management of back pain. J Bone Joint Surg Br 94-b, 1298-1304. 2012.
14. Adams MA, Roughley PJ. What is intervertebral disc degeneration, and what causes it? Spine (Phila Pa 1976) 31, 2151-2161. 2006.
15. Roberts S, Evans H, Trivedi J, Menage J. Histology and pathology of the human intervertebral disc. J Bone Joint Surg Am 88, S10-S14. 2006.
16. Mwale F, Roughley P, Antoniou J. Distinction between the extracellular matrix of the nucleus pulposus and hyaline cartilage: a requisite for tissue engineering of intervertebral disc. Eur.Cell Mater 8, 58-63. 2004.
17. Rutges JPHJ, Kummer JA, Oner FC, Verbout AJ, Castelein RJM, Roestenburg HJA, Dhert WJA, Creemers LB. Increased MMP-2 activity during intervertebral disc degeneration is correlated to MMP-14 levels. J Pathol 214, 523-530. 2008.
18. Song RH, Tortorella MD, Malfait AM, Alston JT, Yang Z, Arner EC et al. Aggrecan degradation in human articular cartilage explants is mediated by both ADAMTS-4 and ADAMTS-5. Arthritis Rheum. 56, 575-585. 2007.
19. Crean JKG, Robberts S, Jaffray DC, Eisenstein SM, Duance VC. Matrix metalloproteinases in the human intervertebral disc: role in disc degeneration and scoliosis. Spine 22, 2877-2884. 1997.

20. Goupille P, Jayson MI, Valat JP, Freemont AJ. Matrix metalloproteinases: the clue to intervertebral disc degeneration? Spine 23, 1612-1626. 1998.
21. Weiler C, Nerlich AG, Zipperer J, Bachmeier BE, Boos N. 2002 SSE Award Competition in Basic Science: expression of major matrix metalloproteinases is associated with intervertebral disc degradation and resorption. Eur Spine J. 11, 308-320. 2002.
22. Le Maitre CL, Freemont AJ, Hoyland JA. Localization of degradative enzymes and their inhibitors in the degenerate human intervertebral disc. J.Pathol 204, 47-54. 2004.
23. Zhao CQ, Zhang YH, Jiang SD, Li H, Jiang LS, Dai LY. ADAMTS-5 and intervertebral disc degeneration: the results of tissue immunohistochemistry and in vitro cell culture. J Orthop Res 29, 718-725. 2011.
24. Pockert AJ, Richardson SM, Le Maitre CL, Lyon M, Deakin JA, Buttle DJ et al. Modified expression of the ADAMTS enzymes and tissue inhibitor of metalloproteinases 3 during human intervertebral disc degeneration. Arthritis Rheum 60, 482-491. 2009.
25. Ariga K, Yonenobu K, Nakase T, Kaneko M, Okuda S, Uchiyama Y et al. Localization of cathepsins D, K, and L in degenerated human intervertebral discs. Spine , 2666-2672. 2001.
26. Wang J, Markova D, Anderson DG, Zheng Z, Shapiro IM, Risbud MV. TNF-a and IL-1ß promote a disintegrin-like and metalloprotease with thrombospondin type I motif-5-mediated aggrecan degradation through syndecan-4 in intervertebral disc. J Biol Chem. 286, 39738-39749. 2011.
27. Gruber HE, Ingram JA, Hoelscher GL, Zinchenko N, Norton HJ, Hanley EN Jr. Constitutive expression of cathepsin K in the human intervertebral disc: new insight into disc extracellular matrix remodeling via cathepsin K and receptor activator of nuclear factor-kB ligand. Arthritis Res Ther 13, R140. 2011.
28. Brama PA, TeKoppele JM, Beekman B, van Ei B, Barneveld A, van Weeren PR. Influence of development and joint pathology on stromelysin enzyme activity in equine synovial fluid. Ann Rheum Dis 59, 155-157. 2000.
29. Edwards JC, Wilkinson LS, Soothill P, Hembry RM, Murphy G, Reynolds JJ. Matrix metalloproteinases in the formation of human synovial joint cavities. J Anat 188, 355-360. 1996.
30. Inoue K, Mikuni-Takagaki Y, Oikawa K, Itoh T, Inada M, Noguchi T et al. A crucial role for matrix metalloproteinase 2 in osteocytic canalicular formation and bone metabolism. J Biol Chem 281, 33814-33824. 2006.
31. Rutges JP, Nikkels PG, Oner FC, Ottink KD, Verbout AJ, Castelein RJ et al. The presence of extracellular matrix degrading metalloproteinases during fetal development of the intervertebral disc. Eur Spine J. 19, 1340-1346. 2010.
32. Brinckerhoff CE, Martrisian LM. Matrix metalloproteinases: a tail of a frog that became a prince. Nat Rev Mol Cell Biol 3, 207-214. 2002.
33. Lemaitre V, D'armiento J. Matrix metalloprotienases in development and disease. Birth Defects Re C Embryo Today 78, 1-10. 2006.
34. Page-Mc Caw A, Ewald Werb AJ. Matrix metalloproteinases and the regulation of tissue remodelling. Nat Rev Mol Cell Biol 8, 221-233. 2007.
35. Mwale F, Roughley P, Antoniou J. Distinction between the extracellular matrix of the nucleus pulposus and hyaline cartilage: a requisite for tissue engineering of intervertebral disc. Eur.Cell Mater 8, 58-63. 2004.
36. Le Maitre CL, Hoyland JA, Freemont AJ. Catabolic cytokine expression in degenerate and herniated human intervertebral discs: IL-1beta and TNFalpha expression profile. Arthritis Res Ther 9, R77. 2007.

37. Mwale F, Roughley P, Antoniou J. Distinction between the extracellular matrix of the nucleus pulposus and hyaline cartilage: a requisite for tissue engineering of intervertebral disc. Eur.Cell Mater 8, 58-63. 2004.
38. Hoyland JA, Le Maitre C, Freemont AJ. Investigation of the role of IL-1 and TNF in matrix degradation in the intervertebral disc. Rheumatology 47, 809-814. 2008.
39. Le Maitre C, Pockert A, Buttle DJ, Freemont AJ, Hoyland JA. Matrix synthesis and degradation in human intervertebral disc degeneration. Biochem Soc Trans 35, 652-655. 2007.
40. Philips KL, Jordan-Mahy N, Nicklin MJ, Le Maitre CL. Interleukin-1 receptor antagonist deficient mice provide insights into pathogenesis of human intervertebral disc degeneration. Ann Rheum Dis 72, 1860-7. 2013.
41. Genevay S, Finckh A, Menzub F, Tessitore E, Guerne PA. Influence of cytokine inhibitors on concentration and activity of MMP-1 and MMP-3 in disc herniation. Arthritis Res Ther 11, R169. 2009.
42. Bell GR, Ross JS. Imaging of the spine. Frymoyer JW, Wiesel SW, editors. The adult & pediatric spine. 3rd ed, 69-86. 2004. Philadelphia, Lippincott, Williams & Wilkins.
43. Burkus JK, Zdeblick TA. Lumbar disc disease. Frymoyer JW, Wiesel SW, editors. The adult & pediatric spine. 844-899. 2004. Philadelphia, Lippincott, Williams & Wilkins.
44. Pye SR, Reid DM, Smith R, Adams JE, Nelson K, Silman AJ et al. Radiographic features of lumbar disc degeneration and self-reported back pain. J Rheumatol 31, 753-758. 2004.
45. Urban JP, Smith S, Fairbank JC. Nutrition of the intervertebral disc. Spine 29, 2700-2709. 2004.
46. Roberts S, Menage J, Eisensteim SM. The cartilage end-plate and intervertebral disc in scoliosis: calcification and other sequelae. J Orthop Res 11, 747-757. 1993.
47. Roberts S, Urban JP, Evans H, Eisenstein SM. Transport properties of the human cartilage endplate in relation to its composition and calcification. Spine 15, 415-420. 1996.
48. Blummenkrantz G, Lindsey CT, Dunn TC, Jin H, Ries MD, Link TM et al. A pilot, two-year longitudinal study of the interrelationship between trabecular bone and articular cartilage in the osteoarthritic knee. Osteoarthritis Cartilage 12, 977-1005. 2004.
49. Radin EL, Rose RM. Role of subchondral bone in the initiation and progression of cartilage damage. Clin Orthop Relat Res 231, 34-40. 1986.
50. Diamant B, Karlsson, Nachemson A. Correlation between lactate levels and pH in discs of patients with lumbar rhizopathies. Experientia 24, 1159-1196. 1986.
51. Nguyen-minh C, Haughton VM, Papke RA, An H, Censky CS. Measuring diffusion of solutes into intervertebral disks with MR imaging and paramagnetic contrast medium. AJNR Am J Neuroradiol 19, 1781-1784. 1998.
52. Thompson JP, Pearce RH, Schechter MT, Adams ME, Tsang IKY, Bishop PB. Preliminary evaluation of a scheme for grading the gross morphology of the human intervertebral disc. Spine 15, 411-415. 1990.
53. Haefeli M, Kalberer F, Saefesser D, Nerlich AG, Boos N, Paesolf G. The course of macroscopic degeneration in the human lumbar intervertebral disc. Spine 31, 1522-1531. 2006.
54. Huang CY, Gu WY. Effects of mechanical compression on metabolism and distribution of oxygen and lactate in intervertebral disc. J Biomech 41, 1184-1196. 2008.
55. Feinberg J, Boachie-Adjei O, Bullough PG, Boskey AL. The distribution of calcific deposits in intervertebral discs of the lumbosacral spine. Clin Orthop Relat Res 254, 303-310. 1990.

56. Prescher A. Anatomy and pathology of the aging spine. Eur J Radiol 27, 181-195. 1998.
57. Sandstrom C. Calcifications of the intervertebral discs and the relationship between various types of calcifications in the soft tissues of the body. Acta radiol 36, 217-233. 1951.
58. Drissi H, Zuscik M, Rosier R, O'Keefe R. Transcriptional regulation of chondrocyte maturation: potential involvement of transcription factors in OA pathogenesis. Mol Aspects Med 26, 169-179. 2005.
59. Rutges JP, Duit RA, Kummer JA, Oner FC, van Rijen MH, Verbout AJ et al. Hypertrophic differentiation and calcification during intervertebral disc degeneration. Osteoarthritis Cartilage 18, 1487-1495. 2010.
60. Wang H, Zhang J, Sub Q, Yang X. Altered gene expression in articular chondrocytes of Smad3ex8/ex8 mice, revealed by gene profiling using microarrays. J Genet Genomics 34, 698-708. 2007.
61. Yang X, Chen L, Xu X, Li C, Huang C, Deng CX. TGF-beta/Smad3 signals repress chondrocyte hypertrophic differentiation and are required for maintaining articular cartilage. J Cell Biol 153, 35-46. 2001.
62. Kamekura S, Kawasaki Y, Hoshi K, Shimoaka T, Chikuda H, Maruyama Z et al. Contribution of runt-related transcription factor 2 to the pathogenesis of osteoarthritis in mice after induction of knee joint instability. Arthritis & Rheumatism 54, 2462-2470. 2006.
63. Wang X, Manner PA, Horner A, Shum L, Tuan RS, Nuckolls GH. Regulation of MMP-13 expression by RUNX2 and FGF2 in osteoarthritic cartilage. Osteoarthritis Cartilage 12, 963-973. 2004.
64. Sato S, Kimura A, Ozdemir J, Asou Y, Miyazaki M, Jinno T et al. The distinct role of the Runx proteins in chondrocyte differentiation and intervertebral disc degeneration: findings in murine models and in human disease. Arthritis Rheum 58, 2764-2775. 2008.
65. Du HM, Zheng XH, Wang LY, Tang W, Liu L, Jing W et al. The osteogenic response of undifferentiated human adipose-derived stem cells under mechanical stimulation. Cells Tissues Organs 196, 313-324. 2012.
66. Yang X, Gong P, Lin Y, Zhang L, Yuan Q, Tan Z et al. Cyclic tensile stretch modulates osteogenic differentiation of adipose-derived stem cells via the BMP-2 pathway. Arch Med Sci 6, 152-159. 2010.
67. Ziros PG, Basdra EK, Papavassiliou AG. Runx2: of bone and stretch. Int J Biochem Cell Biol 40, 1659-1663. 2008.
68. Rutges J, Creemers LB, Dhert WJ, Milz S, Sakai D, Mochida J et al. Variations in gene and protein expression in human nucleus pulposus in comparison with annulus fibrosus and cartilage cells: potential associations with aging and degeneration. Osteoarthritis Cartilage 18, 416-423. 2010.
69. Mwale F, Roughley P, Antoniou J. Distinction between the extracellular matrix of the nucleus pulposus and hyaline cartilage: a requisite for tissue engineering of intervertebral disc. Eur.Cell Mater 8, 58-63. 2004.
70. Raj PP. Intervertebral disc: anatomy-physiology-pathophysiology-treatment. Pain Pract 8, 18-44. 2008.
71. Alini M, Eisenstein SM, Ito K, Little C, Kettler AA, Masuda K et al. Are animal models useful for studying human disc disorders/degeneration? Eur Spine J 17, 2-19. 2008.
72. Makarand V, Risbud MV, Shapiro IM. Notochordal Cells in the Adult Intervertebral Disc: New Perspective on an Old Question. Crit Rev Eukaryot Gene Expr 21, 29-41. 2011.
73. Smolders LA, Meij BP, Onis D, Riemers FM, Bergknut N, Wubbolts R et al. Gene expression profiling of early intervertebral disc degeneration reveals a down-regulation of canonical Wnt signaling and caveolin-1 expression: implications for development of regenerative strategies. Arthritis Res Ther 15, R23. 2013.

74. Choi KS, Cohn MJ, Harfe BD. Identification of nucleus pulposus precursor cells and notochordal remnants in the mouse: implications for disk degeneration and chordoma formation. Dev Dyn 237, 3953-3958. 2008.
75. Risbud MV, Schaer TP, Shapiro IM. Toward an understanding of the role of notochordal cells in the adult intervertebral disc: from discord to accord. Dev Dyn 239, 2141-2148. 2010.
76. Risbud MV, Guttapalli A, Tsai TT, Lee JY, Danielson KG, Vaccaro AR et al. Evidence for skeletal progenitor cells in the degenerate human intervertebral disc. Spine 32,2537-44. 2007.
77. Erwin WM, Islam D, Inman RD, Fehlings MG, Tsui FW. Notochordal cells protect nucleus pulposus cells from degradation and apoptosis: implications for the mechanisms of intervertebral disc degeneration. Arthritis Res Ther 13, R215. 2011.
78. Hunter CJ, Matyas JR, Duncan NA. The notochordal cell in the nucleus pulposus: a review in the context of tissue engineering. Tissue Eng 9, 667-677. 2003.
79. Cappello R, Bird JL, Pfeiffer D, Bayliss MT, Dudhia J. Notochordal cell produce and assemble extracellular matrix in a distinct manner, which may be responsible for the maintenance of healthy nucleus pulposus. Spine 31, 873-882. 2006.
80. Abbott RD, Purmessur D, Monsey RD, Iatridis JC. Regenerative potential of TGFB3 + Dex and notochordal cell conditioned media on degenerated human intervertebral disc cells. J Orthop Res 30, 482-488. 2012.
81. Purmessur D, Schek RM, Abbott RD, Ballif BA, Godburn KE, Iatridis JC. Notochordal conditioned media from tissue increases proteoglycan accumulation and promotes a healthy nucleus pulposus phenotype in human mesenchymal stem cells. Arthritis Res Ther 13, R81. 2011.
82. Moskowitz RW, Ziv I, Denko CW, Boja B, Jones PK, Adler JH. Spondylosis in sand rats: a model of intervertebral disc degeneration and hyperostosis. J Orthop Res 8, 401-411. 1990.
83. Bergknut N, Rutges JP, Kranenburg HJ, Smolders LA, Hagman R, Smidt HJ et al. The dog as an animal model for intervertebral disc degeneration? Spine 37, 351-358. 2012.
84. Hartman RA, Bell KM, Debski RE, Kang JD, Sowa GA. Novel ex-vivo mechanobiological intervertebral disc culture system. J Biomech 45, 382-385. 2012.
85. Paul CP, Zuiderbaan HA, Zandieh Doulabi B, van der Veen AJ, van de Ven PM, Smit TH et al. Simulated-physiological loading conditions preserve biological and mechanical properties of caprine lumbar intervertebral discs in ex vivo culture. PLoS One 7, e33147. 2012
86. Ponnappan RK, Markova DZ, Antonion PJ, Murray HB, Vaccaro AR, Shapiro IM et al. An organ culture system to model early degenerative changes of the intervertebral disc. Arthritis Res Ther 13, R171. 2011.
87. Chan SC, Gantenbein-Ritter B. Intervertebral disc regeneration or repair with biomaterials and stem cell therapy--feasible or fiction? Swiss Med Wkly 142, w13598. 2012.
88. Cheung KM, Karppinen J, Chan D, Ho DW, Song YQ, Sham P et al. Prevalence and pattern of lumbar magnetic resonance imaging changes in a population study of one thousand forty-three individuals. Spine (Phila Pa 1976) 34, 934-940. 2009.
89. Kjaer P, Leboeuf-Yde C, Korsholm L, Sorensen JS, Bendix T. Magnetic resonance imaging and low back pain in adults: a diagnostic imaging study of 40-year-old men and women. Spine (Phila Pa 1976) 30, 1173-1180. 2005.
90. MacGregor AJ, Andrew T, Sambrook PN, Spector TD. Structural, psychological, and genetic influences on low back and neck pain: a study of adult female twins. Arthritis Rheum 51, 160-167. 2004.
91. Williams FM, Sambrook PN. Neck and back pain and intervertebral disc degeneration: role of occupational factors. Best Pract Res Clin Rheumatol 25, 69-79. 2011.

92. Lawrence JS. Disc degneration; Its frequency and relation to symptoms. Ann rheum Dis 28, 121-138. 1969.
93. Haschtmann D, Stoyanov JV, Ettinger L, Nolte LP, Ferguson SJ. Establishment of a novel intervertebral disc/endplate culture model: analysis of an ex vivo in vitro whole-organ rabbit culture system. Spine 31, 2918-2925. 2006.
94. Wang D, Dong Q, Ngo K, Vo N. Development of an intervertebral disc organ culture model and its clinical significance. Zhonghua Yi Xue Za Zhi 91, 2511-2513. 2011.
95. Wegman F, Helm YV, Oner FC, Dhert WJ, Alblas J. Bone Morphogenetic Protein-2 Plasmid DNA as a Substitute for Bone Morphogenetic Protein-2 Protein in Bone Tissue Engineering. Tissue Eng Part A 23-24, 2686-92. 2013
96. Malda J, Visser J, Melchels FP, Jüngst T, Hennink WE, Dhert WJ et al. 25th anniversary article: engineering hydrogels for biofabrication. Adv Mater 25, 5011-5028. 2013.

SUMMARY

Samenvatting

In the **first chapter** the background and aims of this thesis are described. Low back pain has an annual incidence of 22-65% and the life time risk is 70-85%. Intervertebral disc (IVD) degeneration is assumed to be one of the most important causes for chronic low back pain. Current conservative and surgical treatment options for IVD related chronic low back pain yield far from optimal results and complications of surgical procedures can be devastating. Consequently, research on regenerative treatment strategies, focussing on restoring the biomechanical function of the degenerative disc, has greatly intensified. For the development of new treatment strategies for IVD degeneration, thorough understanding of the pathophysiology of the degenerative process is essential. Therefore, the main aim of this thesis is to contribute to a better understanding of the pathophysiology of IVD degeneration. The research described in this thesis consists of three phases. In the first phase we further elucidated the pathophysiology of IVD degeneration and identified new therapeutic targets. In the second phase we evaluated several animal models for IVD degeneration and developed a new histological grading system. In the last phase we investigated the possibility to stop or reverse IVD degeneration by the injection of enzyme inhibitors or growth factors in an animal model.

In **chapter 2** the presence and activity of several enzymes in healthy and degenerative IVD is described. IVD degeneration is associated with the increased expression of several matrix among which are metalloproteinases (MMPs), in particular MMP-2. However, little is known about the actual activity of this degenerative enzyme in IVDs and which mechanisms are involved in its activation. A major activation pathway involves complex formation with MMP-14 and a tissue inhibitor of metalloproteinases-2 (TIMP-2). In a series of 56 human IVDs, ranging from healthy to degenerative, we analysed whether MMP-2 activity was increased in different stages of IVD degeneration and to what extent activation was related to the production of MMP-14 and TIMP-2. MMP-2 activation and production were quantified by gelatin zymography. Immunohistochemical staining of MMP-14 and TIMP-2 was quantified with a video overlay-based system. A positive correlation was observed between the amount of active MMP-2 and pro-MMP-2 and degeneration grade. MMP-2 activity correlated positively with MMP-14 and less strongly with TIMP-2. Moreover, immunopositivity for MMP-14 correlated to degeneration grade. IVD degeneration was associated with the activity of MMP-2 and the correlation of its activation with MMP-14 production suggests that MMP-14 activates MMP-2 during degeneration. As MMP-14 is capable of activating several other enzymes that are also thought to be involved in IVD degeneration, it may be a key mediator of the degenerative process.

Nevertheless MMPs are not solely involved in pathological tissue degradation. MMPs also regulate connective tissue architecture and cell migration and are associated with several physiological processes. Although they are known to play a role in skeletal development, little is known about the role of MMPs in IVD development. In **chapter 3** the presence of several MMPs in different stages of fetal development is evaluated and compared to healthy IVDs. Sixteen fetal human lumbar spine segments were compared with five normal, non-fetal IVDs. Intensity and localization of immunohistochemical staining for MMP-1, -2, -3 and -14 were evaluated by three independent observers. MMP-2 production and activation was quantified by gelatin zymography. MMP-1 and -14 were abundantly present in the nucleus pulposus (NP) and notochordal (NC) cells of the fetal IVDs. In non-fetal

IVDs, MMP-1 and -14 staining was significantly less intense. MMP-2 staining in the NC and NP cells of the fetal IVD was moderate, but weak in the non-fetal IVD. Gelatin zymography showed a negative correlation of age with MMP-2 activity. MMP-14 immunostaining correlated positively with MMP-2 activity. For the first time, the presence of MMP-1, -2, -3 and -14 in the fetal human IVD is shown and the high levels of MMP-1, -2 and -14 suggest a role in the development of the IVD. Since these enzymes are involved in the development of the IVD, inhibition of degenerative enzymes, as part of a regenerative treatment strategy, should be done with caution.

Next to above mentioned catabolic process, nutrition is also an important factor in IVD degeneration. The IVD is dependent on nutrient provision through a cartilage layer with underlying subchondral bone. However, subchondral bone changes in IVD degeneration have never been quantified. Therefore, the subchondral bone changes at different stages of IVD degeneration were evaluated by micro-CT in **chapter 4.** Twenty-seven IVDs including the adjacent vertebral endplates were scanned. Per scan 12 standardized cylindrical volumes of interest (VOI) were selected. Six VOIs contained the bony endplate and trabeculae (endplate VOIs) and six accompanying VOIs only contained trabecular bone (vertebral VOIs). Bone volume as percentage of the total volume (BV/TV) of the VOI, trabecular thickness (TrTh) and connectivity density (CD) were determined. An increase in BV/TV and TrTh was found in endplate VOIs of IVDs with higher macroscopic degeneration score whereas these values remained stable or decreased in the vertebral VOIs. The increase in bone volume combined with the increase in TrTh in endplate VOIs strongly suggest that the subchondral endplate condenses to a more dense structure in degenerated IVDs. This may negatively influence the diffusion and nutrition of the IVD. The endplate differences between healthy and degenerative IVDs indicate an early association of subchondral endplate changes with IVD degeneration.

Subchondral bone changes are not the only bony changes found in IVD degeneration. In advanced stages of IVD degeneration calcifications of the annulus fibrosis (AF) and nucleus pulposus (NP) are commonly found. These calcifications could be the results of hypertrophic differentiation, a phenomenon characterized by the production of collagen type X, runt-related transcription factor 2 (Runx2), osteoprotegerin (OPG), alkaline phosphatase (ALP) and calcifications. In **chapter 5** we determined if hypertrophic differentiation also occurs in IVD degeneration. IVDs with different macroscopic degeneration grades were prepared for histology, extraction of NP and AF tissue (N= 50) and micro-CT (N= 27). The presence of collagen type X, OPG and Runx2 was determined by immunohistochemistry, and OPG levels were also determined by enzyme-linked immunosorbent assay (ELISA). The presence of calcifications was determined by micro-CT, von Kossa and Alizarin Red staining. Immunohistochemical staining for collagen type X, OPG, Runx2 were more intense in the NP of degenerative compared to healthy IVD samples. OPG levels correlated both significantly with degeneration grade and with the number of microscopic calcifications. The extent of calcifications on micro-CT also correlated with degeneration grade as it did with the von Kossa staining. ALP staining was only incidentally seen in the transition zone of more severe degenerated IVDs. This study demonstrates that hypertrophic differentiation occurs during IVD degeneration, as shown by an increase in OPG levels, the presence of ALP activity and increased immunopositivity of Runx2 and collagen type X.

Regardless of recent progress in the elucidation of IVD degeneration, the basic molecular characteristics that define a healthy human IVD are still largely unknown. Although earlier work in different animal species revealed distinct molecules that might be used as characteristic markers for IVD or specifically NP cells, the validity of these markers for the characterization of human IVD cells remains unknown. In **chapter 6** potential marker molecules were characterized with respect to their occurrence in human IVD cells. Gene expression levels of NP cells were compared with AF cells and articular cartilage (AC) cells, and potential correlations with aging were assessed. Higher mRNA levels of cytokeratin-19 (KRT19) and of neural cell adhesion molecule-1 were noted in NP cells compared to AF and AC cells. Compared to NP cells cytokeratin-18 expression was lower in AC cells, and alpha-2-macroglobulin and desmocollin-2 were lower in AF cells. Cartilage oligomeric matrix protein (COMP) and glypican-3 expression was higher in AF cells, while COMP, matrix gla protein (MGP), and pleiotrophin expression were higher in AC cells. Furthermore, an age-related decrease in KRT19 and increase in MGP expression were observed in NP cells. The age-dependent expression pattern of KRT19 was confirmed by immunohistochemistry, showing the most prominent KRT19 immunoreaction in the notochordal-like cells in juvenile NP, whereas MGP immunoreactivity was not restricted to juvenile NP cells and was found in all age groups. The gene expression of KRT19 has the potential to characterize healthy human NP cells. KRT19 protein expression was only detected in NP cells of donors younger than 54 years old. Identification of the IVD cell phenotype and Imitation of these unique characteristics of these cells is most likely essential for the restoration of the biomechanical properties of the IVD and consequently the success of regenerative medicine strategies.

Histology is an important outcome variable in basic science and pre-clinical studies for new regenerative medicine strategies for IVD degeneration. Nevertheless, an adequately validated histological classification for IVD degeneration is still lacking and the existing classifications are difficult to use for inexperienced observers. Therefore in **chapter 7** the validation of a histological classification for IVD degeneration was described. Moreover, the new classification was compared to the frequently used non-validated classification according Boos et. al. The new classification was applied to human IVD sections. The sections were scored twice by two independent inexperienced observers, twice by two experienced IVD researchers, and once by a pathologist. For comparison, the sections were also scored according to the classification described by Boos et al. Macroscopic grading according Thompson et al., glycosaminoglycan (GAG) content, and age were used for validation. The new classification had an excellent intra- and a good inter-observer reliability. Intra- and inter-observer reliability were comparable for experienced and inexperienced observers. Statistically significant correlations were found between the new classification, macroscopic score, GAG content in the NP, and age. The correlation coefficients of the Boos classification were all lower compared to the new classification. The new histological classification for IVD degeneration is a valid instrument for evaluating IVD degeneration in human IVD sections and is suitable for both inexperienced and experienced researchers. This classification could significantly contribute to standardization and hence research into mechanisms and treatment of IVD degeneration.

Besides standardized outcome parameters also appropriate animal models are required for effective development for new treatment strategies for IVD degeneration. In **Chapter 8** the characteristics of IVD degeneration in a rabbit model of mechanically induced IVD degeneration are described. IVDs of 24 NZW rabbits were compressed with an external loading device for 14, 18, and 56 days, including a sham group of 56 days follow-up. Disc height was measured by radiography and degeneration was histologically graded according the Boos score. The presence and activity of MMP-2 was determined by gelatin zymography. Significantly reduced disc height was found after 14 and 56 days in the compressed versus the non-compressed discs, but recovery of disc height 1 hour after in vivo release of compression was found in both cases. No differences in histological score were observed between the compressed and non-compressed discs. Growth plate closure was induced in both the compressed and sham compressed IVDs. Higher levels of active MMP-2 in the endplate region were found after 28 days of compression compared to the non-compressed and sham operated discs. Nevertheless, the limited degeneration in the current model suggests that this model may be more suitable for research into mechanisms of early disc degeneration than for the evaluation of new treatment strategies.

Many different animal models are used in IVD research. Similar to the model described in chapter 8, in most of these models IVD degeneration is induced manually or chemically rather than occurring spontaneously. In **chapter 9** it is investigated whether spontaneous IVD degeneration occurring in both chondrodystrophic dogs (CD) and nonchondrodystrophic dogs (NCD) can be used as a translational model for human IVD research. A total of 184 IVDs from 19 dogs of different breeds were used. The extent of IVD degeneration was evaluated by macroscopic grading, histopathology, GAG content, and MMP-2 activity. Canine data were compared with human IVD data acquired in this study. Gross pathology of the IVD in both dog types (CD and NCD) and humans showed many similarities, but the cartilaginous endplates were significantly thicker and the subchondral cortices significantly thinner in humans than in dogs. NC cells were still present in the IVDs of adult NCD but were not seen in the CD breeds or in humans. Signs of degeneration were seen in young dogs of CD breeds (< 1 year of age), whereas this was only seen in older dogs of NCD breeds (5–7 years of age). The relative GAG content and MMP-2 activity in canine IVDs were similar to those in humans: MMP-2 activity increased and GAG content decreased with increasing severity of IVD degeneration. In conclusion IVD degeneration appears to be similar in humans and dogs. Both CD and NCD breeds may therefore serve as models of spontaneous IVD degeneration for human research. However, as with all animal models, it is important to recognize interspecies differences and, moreover, the intraspecies differences between CD and NCD breeds to develop an optimal canine model of human IVD degeneration.

In **chapter 10** the final research project of this thesis is described. Injection of growth factors and inhibition of degenerative enzymes are two hypostasized regenerative treatment strategies for IVD degeneration. Therefore, the effect of the injection of BMP-7 (growth factor) and marimastat (enzyme inhibitor) on IVD degeneration was evaluated in a rabbit annular puncture model for IVD degeneration. In three different IVDs of 17 NWZ rabbits degeneration was induced by stabbing the AF with a 16G needle. After 6 weeks,

IVDs were injected with saline, BMP-7, marimastat or hydrogel. Animals were terminated at week 18, and the progression of IVD degeneration and/or IVD regeneration was evaluated using radiography, MRI, micro-CT, histology, morphologic appearance and by measuring GAG and DNA content of the NP. Moderate degeneration was seen in all IVDs, apart from the non-stabbed control group. No signs of regeneration could be detected in any of the IVDs. The rabbit annular puncture model is effective in producing moderate IVD degeneration, however no signs of IVD regeneration were found in the IVDs treated with BMP-7 or marimastat.

Some parts of the pathophysiology of IVD degeneration have been elucidated by this thesis, however more detailed knowledge regarding the pathophysiology of IVD degeneration is still required for the further development of new regenerative treatment strategies. A better understanding of the degenerative process will lead to more effective new therapies. However, before such a new treatment will become clinically available many hurdles have to be taken. These scientific challenges, future perspectives and ethical dilemmas are discussed in **chapter 11.**

In het **eerste hoofdstuk** wordt de achtergrond en de doelstelling van dit proefschrift beschreven. Lage rugpijn heeft een jaarlijkse incidentie van 22-65% en wereldwijd krijgt 70-85% van alle mensen rugklachten op enig moment in zijn of haar leven. Tussenwervelschijf (TWS) degeneratie wordt gezien als één van de belangrijkste oorzaken van chronische lage rugpijn. Huidige conservatieve en chirurgische behandelingen voor TWS gerelateerde chronische lage rugpijn hebben suboptimale resultaten en operatieve interventies kunnen gepaard gaan met ernstige complicaties. Het onderzoek naar regeneratieve behandelingsstrategieën, behandelingen gericht op herstel van de biomechanische functie van de degeneratieve TWS, is dan ook de laatste jaren sterk geïntensiveerd. Gedegen onderzoek naar de pathofysiologie van TWS-degeneratie is essentieel voor de ontwikkeling van nieuwe behandelingsstrategieën. Derhalve is het belangrijkste doel van dit proefschrift om bij te dragen aan beter begrip van de pathofysiologie van TWS-degeneratie. Het in dit proefschrift beschreven onderzoek bestaat uit drie afzonderlijke fasen. In de eerste fase hebben we de pathofysiologie van TWS-degeneratie onderzocht en zijn we op zoek gegaan naar nieuwe therapeutische targets. In de tweede fase hebben we verschillende diermodellen voor TWS-degeneratie geevalueerd en hebben we een nieuw histologisch scoringssysteem ontwikkeld. In de laatste fase hebben we onderzocht of het mogelijk is om TWS-degeneratie in een diermodel te behandelen met een injectie van enzymremmers of groeifactoren.

In **hoofdstuk 2** wordt de aanwezigheid en activiteit van verschillende enzymen in gezonde en degeneratieve TWS-en beschreven. TWS-degeneratie is geassocieerd met verhoogde expressie van verschillende degeneratieve enzymen, waaronder matrix metalloproteïnasen (MMPs) en in het bijzonder MMP-2. Er is echter weinig bekend over de werkelijke biologische activiteit van MMP-2 in TWS-en en welke mechanismen betrokken zijn bij de activering van dit enzym. Een belangrijke potentiele activatieroute betreft complexvorming met MMP-14 en tissue inhibitor of metalloproteinases 2 (TIMP-2). In een 56 TWS-en, werd MMP-2 activiteit in oplopende stadia van TWS-degeneratie bepaald en beoordeeld in hoeverre activering gerelateerd was aan de productie van MMP-14 en TIMP-2. MMP-2 activiteit en productie werd bepaald met gelatine zymografie. Immunohistochemische kleuring van MMP-14 en TIMP-2 werd gekwantificeerd met een video-overlay-systeem. Een positieve correlatie werd gezien tussen de hoeveelheid actief MMP-2 en pro-MMP-2 en de ernst van TWS-degeneratie. Daarnaast correleert MMP-2 activiteit positief met MMP-14 en ook met TIMP-2. Bovendien correleerde MMP-14 immunopositiviteit possitief met het degeneratie stadium. De hoge MMP-2 waarden in gedegenereerde TWS-en en de correlatie van MMP-2 activiteit met de aanwezigheid van MMP-14 suggereert een rol voor MMP-14 in de activatie van MMP-2 in TWS-degeneratie. Het feit dat MMP-14 ook verscheidene andere enzymen kan activeren die geassocieerd zijn met TWS-degeneratie impliceert dat MMP-14 een belangrijke mediator van het degeneratieve proces zou kunnen zijn.

Toch zijn MMPs niet alleen betrokken bij pathologische weefselafbraak. MMPs reguleren bindweefsel-architectuur en celmigratie en zijn geassocieerd met meerdere fysiologische processen. Hoewel ze bekend staan om hun rol in de ontwikkeling van het skelet, is er weinig bekend over de rol van deze enzymen in de ontwikkeling van de TWS. In **hoofdstuk 3** wordt de aanwezigheid van verschillende MMPs in diverse stadia van

de ontwikkeling van de foetus geëvalueerd en vergeleken met gezonde TWS-en. Zestien foetale menselijke lumbale TWS-en werden vergeleken met vijf normale, niet-foetale TWS-en. Intensiteit en lokalisatie van immunohistochemische kleuring voor MMP-1, -2, -3 en -14 werden beoordeeld door drie onafhankelijke onderzoekers. MMP-2 productie en activiteit werd gekwantificeerd met gelatine zymografie. MMP-1 en -14 waren overvloedig aanwezig in de nucleus pulposus (NP) en notochordaal (NC) cellen van de foetale TWS-en. In niet-foetale TWS-en was de MMP-1 en -14 kleuring aanzienlijk minder intens. MMP-2 kleuring in NC en NP cellen van foetale TWS-en was middelmatig, maar zwak in de niet-foetale TWS-en. Gelatine zymografie toonden een negatieve correlatie van leeftijd met MMP-2 activiteit. Immunohistochemische kleuring voor MMP-14 is positief gecorreleerd met MMP-2 activiteit. Dit onderzoek toont voor het eerst de aanwezigheid van MMP-1, -2, -3 en -14 in de foetale menselijke TWS aan en de hoge waardes van MMP-1, -2 en -14 suggereren een rol van deze enzymen in de ontwikkeling van de TWS. Aangezien deze enzymen ook betrokken zijn bij de ontwikkeling van de TWS dient remming van degeneratieve enzymen als onderdeel van een regeneratieve behandelingsstrategie zorgvuldig en gecontroleerd uitgevoerd te worden.

Naast het eerder genoemde degeneratieve proces, is nutritie ook een belangrijke factor in TWS-degeneratie. De TWS is voor zijn nutrientenvoorziening afhankelijk van diffusie van deze voedingstoffen door een laagje kraakbeen en het onderliggende subchondrale bot. Echter, subchondrale botveranderingen in TWS degeneratie zijn nog nooit gekwantificeerd. Daarom worden in **hoofdstuk 4** de subchondrale botveranderingen in verschillende stadia van TWS-degeneratie geëvalueerd met micro-CT. Zevenentwintig TWS-en inclusief de aangrenzende dek- en sluitplaten zijn gescand. Per scan werden 12 gestandaardiseerde cilindrische volumes of interest (VOI) geselecteerd. Zes VOI's bevatte de benige eindplaat en trabeculair bot (eindplaat VOI's) en zes begeleidende VOI's bevatten alleen trabeculair bot (wervellichaam VOI's). Botvolume als percentage van het totale volume (BV/TV) van de VOI en trabeculaire dikte (TrTh) werden bepaald. Een hogere BV/TV en TrTh werd gevonden in eindplaat VOI's van gedegenereerde TWS-en, deze waarden bleven stabiel of daalde in de wervellichaam VOI's. De toename van botvolume gecombineerd met de toename in TrTh in de eindplaat VOI suggeert dat de subchondrale eindplaat condenseert en een dichtere structuur krijgt in de gedegenereerde TWS. Dit kan een negatieve invloed hebben op de diffusie van nutrienten naar de TWS. De verschillen in de eindplaten van gezonde en mild gedegenereerde TWS-en suggereren dat eindplaatverdikking gerelateerd is aan vroege TWS-degeneratie.

Subchondrale botveranderingen zijn niet de enige ossale veranderingen in TWS-degeneratie. In gevorderde stadia van TWS-degeneratie worden verkalkingen van de annulus fibrosus (AF) en NP gevonden. Deze calcificaties zouden het resultaat kunnen zijn van hypertrofe differentiatie, een verschijnsel dat gekenmerkt wordt door de productie van collageen type X, runt-related transcription factor 2 (Runx2), osteoprotegerin (OPG), alkaline fosfatase (ALP) en calcificaties. In **hoofdstuk 5** is onderzocht of hypertrofe differentiatie ook voorkomt in TWS-degeneratie. Gezonde en gedegenereerde TWS-en werden bewerkt voor histologie, extractie van NP en AF weefsel (N = 50) en micro-CT (N = 27). De aanwezigheid van collageen type X, OPG en Runx2 werd bepaald door immunohistochemie en de hoeveelheid OPG werd tevens bepaald met enzym-

gekoppelde immunosorbent assay (ELISA). De aanwezigheid van calcificaties werd beoordeeld met micro-CT, von Kossa en Alizarinerood kleuringen. Immunohistochemische kleuring voor collageen type X, OPG, Runx2 waren meer intens in de NP van degeneratieve TWS-en dan in gezonde TWS-en. De hoeveelheid OPG correleerde significant met het degeneratie stadium en het aantal microscopische calcificaties in de TWS. Het aantal calcificaties op micro-CT correleerde ook met het degeneratie stadium evenals de von Kossa kleuring. ALP kleuring werd slechts incidenteel gezien in de overgangszone van AF naar NP in gevorderde stadia van TWS-degeneratie. Deze studie laat voor het eerst zien dat hypertrofe differentiatie voorkomt tijdens TWS-degeneratie.

Ondanks de recente toename van kennis over de TWS-en en de degeneratie hiervan, zijn de moleculaire kenmerken van de gezonde menselijke TWS nog grotendeels onbekend. Uit onderzoek in verschillende diersoorten blijkt dat meerdere moleculen potentieel gebruikt kunnen worden als markers voor TWS of specifiek NP cellen. Echter de toepasbaarheid van deze markers voor karakterisering van menselijke IVD cellen is nog niet onderzocht. In **hoofdstuk 6** werd geëvalueerd of elf potentiële markers aanwezig zijn in humane TWS cellen. Genexpressie niveaus van NP cellen werden vergeleken met AF en kraakbeen (AC) cellen en mogelijke correlaties met de leeftijd van de donoren werd beoordeeld. In vergelijking met AF en AC cellen werden er hogere mRNA levels van cytokeratine-19 (KRT19) en neural cell adhesion molecule-1 in de NP gevonden. Vergeleken met NP cellen was de cytokeratin-18 expressie lager in de AC cellen en alfa-2-macroglobuline en desmocollin-2 expressie was lager in de AF cellen. Cartilage oligomeric matrix protein (COMP) en glypican-3 expressie was hoger in AF cellen, terwijl COMP, matrix gla protein (MGP) en pleiotrophin expressie hoger was bij AC cellen. Bovendien werd een leeftijd-gerelateerde afname in KRT19 en toename van MGP expressie waargenomen in de NP cellen. Het leeftijd-gebonden expressie patroon van KRT19 werd bevestigd door middel van de immunohistochemie. De meest prominente KRT19 immuunreactie werd gezien in de notochordaal-achtige cellen in de juveniele NP, terwijl MGP immunoreactiviteit niet beperkt was tot NP cellen en gezien werd in alle leeftijdsgroepen. KRT19 eiwitexpressie werd daarentegen alleen gezien in de NP cellen van donoren jonger dan 54 jaar. Dit maakt KRT19 een potentiële marker voor NP cellen van niet gedegenereerde TWS-en. Identificatie van het TWS fenotype en simulatie van de unieke eigenschappen van deze cellen is waarschijnlijk essentieel voor het herstel van de biomechanische eigenschappen van de TWS en daarmee ook voor het succes van regeneratieve behandelingsstrategieën.

Histologie is een van de belangrijkste uitkomstparameter in basaal wetenschappelijk en pre-klinisch onderzoek naar nieuwe regeneratieve behandelingsstrategieën voor TWS-degeneratie. Desalniettemin is er nog geen adequaat gevalideerd histologisch classificatiesysteem voor TWS-degeneratie beschikbaar en de bestaande niet gevalideerde classificaties zijn moeilijk te gebruiken. Daarom wordt in **hoofdstuk 7** een nieuw en gevalideerd histologisch classificatie systeem voor TWS-degeneratie beschreven. Daarnaast is deze nieuwe classificatie vergeleken met de veel gebruikte niet-gevalideerde classificatie van Boos et. al. De nieuwe classificatie werd toegepast op humane TWS coupes. De coupes werden tweemaal gescoord door twee onafhankelijke onervaren onderzoekers en tweemaal door de twee ervaren TWS-onderzoekers en

eenmaal door een patholoog. Ter vergelijking werden de coupes ook volgens de Boos score beoordeeld door twee ervaren TWS-onderzoekers. De score werd gevalideerd aan de hand van macroscopische beoordeling, hoeveelheid Glycosaminoglycans (GAGs) en leeftijd van de donoren. De nieuwe classificatie had een uitstekende intra- en inter-observer reliability. Intra- en inter-observer reliability waren vergelijkbaar voor zowel ervaren als onervaren onderzoekers. Daarnaast werden er statistisch significante correlaties gevonden tussen de nieuwe classificatie, macroscopische score, hoeveelheid GAGs in de NP en leeftijd van de donoren. Voor de Boos classificatie waren alle correlatie coëfficiënten lager dan die van de nieuwe classificatie. De nieuwe histologische classificatie van TWS-degeneratie is een valide instrument voor het evalueren van TWS-degeneratie in humane TWS coupes en is geschikt voor zowel ervaren als onervaren onderzoekers. Deze classificatie kan een belangrijke bijdrage leveren aan de standaardisatie en daarmee de efficientie van onderzoek naar de pathofysiologie en behandeling van TWS-degeneratie.

Naast gestandaardiseerde uitkomstparameters zijn ook geschikte diermodellen nodig voor effectieve ontwikkeling van nieuwe behandelingsstrategieën voor TWS-degeneratie. In **hoofdstuk 8** worden de degeneratieve afwijkingen beschreven die werden geïnduceerd in een konijnenmodel voor TWS-degeneratie. TWS-en van 24 konijnen werden gecomprimeerd met een externe fixateur voor 14, 18 en 56 dagen, daarnaast was er een placebo groep met 56 dagen follow-up. TWS-hoogte werd gemeten op rontgenfoto's. Degeneratie werd histologisch gescoord volgens de Boos score en de aanwezigheid en activiteit van MMP-2 werd bepaald met gelatine zymografie. Significant verminderde TWS-hoogte werd gezien na 14 en 56 dagen compressie, maar de TWS-hoogte herstelde 1 uur na verwijderen van het frame in beide groepen. Er werd geen verschil in histologische score gezien tussen de gecomprimeerde en niet-gecomprimeerde TWS-en. Groeischijfsluiting werd geïnduceerd in de gecomprimeerde en de placebo TWS-en. Actief MMP-2 werd gevonden in de eindplaat regio van de TWS-en die 28 dagen gecomprimeerd werden. De beperkte degeneratie in het huidige model suggereert dat dit model meer geschikt is voor onderzoek naar de pathofysiologie van de vroege stadia van TWS-degeneratie dan voor evaluatie van nieuwe behandelingsstrategieën.

Op dit moment worden veel verschillende diermodellen gebruikt voor TWS-onderzoek. In de meeste van deze modellen wordt TWS-degeneratie mechanisch (hoofdstuk 8) of chemisch geïnduceerd en niet spontaan zoals bij mensen. In **hoofdstuk 9** wordt onderzocht of spontane TWS-degeneratie zoals wordt gezien in chondrodystrofisch (CD) en niet-chondrodystrofische honden (NCD), gebruikt kan worden als translationel model voor humane TWS-degeneratie. Hiervoor werden 184 TWS-en van 19 honden van verschillende rassen gebruikt. Het stadium van TWS-degeneratie werd beoordeeld op basis van macroscopische kenmerken, histologie, hoeveelheid GAGs, en MMP-2 activiteit. De resultaten van de TWS-en van honden werden vergeleken met humane TWS-en. Macroscopische beoordeling van TWS-en van CD en NCD honden vertoonde veel overeenkomsten met humane TWS-en, maar de kraakbeeneindplaten bij honden waren beduidend dikker dan bij mensen. Tevens is de subchondrale plaat bij de mens aanzienlijk dunner dan bij honden. NC cellen werden gezien in de NP van NCD honden, maar niet bij CD honden en volwassen mensen.

Tekenen van degeneratie werden gezien bij jonge CD honden (<1 jaar), terwijl bij NCD rassen dit alleen werd gezien bij oudere honden (5-7 jaar). De hoeveelheid GAGs en MMP-2-activiteit in TWS-en van honden was vergelijkbaar met die bij de mens. Concluderend, TWS- degeneratie is morfologisch, histologisch en biochemisch vergelijkbaar bij mensen en honden. Zowel CD als NCD honden kunnen gebruikt worden als model voor spontane TWS-degeneratie. Echter, onderscheid tussen CD en NCD rassen is essentieel voor de juiste interpretatie van de resultaten.

In **hoofdstuk 10** wordt het laatste onderzoeksproject van dit proefschrift beschreven. De injectie van groeifactoren en de remming van degeneratieve enzymen zijn twee gesuggereerde regeneratieve behandelingsstrategieën voor TWS-degeneratie. Daarom wordt het effect van een injectie met BMP-7 (groeifactor) of marimastat (enzymremmer) op TWS-degeneratie geëvalueerd in een konijnenmodel voor TWS-degeneratie. In drie verschillende TWS-en van 17 konijnen werd degeneratie geïnduceerd door middel van een punctie van de AF met een 16G naald. Na 6 weken werden de TWS-en geïnjecteerd met zoutoplossing (placebo), BMP-7, marimastat of een hydrogel. Dieren werden na 18 weken geëuthanaseerd en het stadium van TWS-degeneratie of regeneratie werd beoordeeld met rontgenfoto's, MRI, micro-CT, histologie, morfologische kenmerken en door het bepalen van de hoeveelheid GAGs en DNA in de NP. Matige degeneratie werd gezien bij alle TWS-en, behalve in de niet-gepuncteerde controlegroep. In geen van de behandelingsgroepen werden tekenen van regeneratie gevonden. Het onderzochte konijnenmodel is effectief gebleken in het induceren van matige TWS-degeneratie, er werden echter geen tekenen van regeneratie gevonden in de TWS-en die waren behandeld met BMP-7 of marimastat.

Hoewel sommige gedeelten van de pathofysiologie van TWS-degeneratie verder zijn uitgekristalliseerd door dit proefschrift, is er nog veel onbekend over dit proces. Meer gedetailleerde kennis over de pathofysiologie van TWS-degeneratie is essentieel voor de verdere ontwikkeling van nieuwe regeneratieve behandelingsstrategieën. Meer inzicht in het degeneratieve proces zal leiden tot nieuwe en effectievere therapieën. Echter, voordat dergelijke nieuwe behandelingen klinisch toepasbaar worden, moeten er nog veel vraagstukken opgelost worden. Deze wetenschappelijke uitdagingen, ethische dilemma's en toekomstperspectieven worden besproken in **hoofdstuk 11**.

ACKNOWLEDGEMENTS

Dankwoord

Geachte Prof. Dr. Dhert en Prof. Dr. Öner, beste Wouter en Cumhur, het is voor mij een grote eer dat ik bij jullie mag promoveren.

Beste Wouter, in 2005 zijn we samen met Laura en Cumhur aan het eerste tussenwervelschijf-project begonnen. Onder jouw leiding heeft dit geleid tot deze eerste humane tussenwevelschijf promotie, maar ook meerdere promoties van de faculteit diergeneeskunde, het BMM project IdiDas en zelfs een optreden van een van je postdocs bij De Wereld Leert Door. Ik heb erg veel bewondering voor hoe je de afgelopen jaren onze onderzoeksafdeling hebt getransformeerd tot een orthopaedisch research instituut. Naast de profesionele steun wil ik je ook graag bedanken voor alle persoonlijke steun die je Natasja en mij hebt gegeven.

Beste Cumhur, al sinds mijn eerste klinische stage in 2004 ben jij een van mijn begeleiders. Ik heb de afgelopen jaren erg veel van je geleerd. De eerste jaren vooral op wetenschappelijk gebied en later ook in de kliniek. Jouw enthousiasme en gedrevenheid hebben zeker een rol gespeeld in mijn keuze om me na mijn opleiding tot orthopeed verder in wervelchirurgie te verdiepen. Dank je voor al je hulp en steun bij mijn sollicitatie voor een Spine fellowship in Vancouver. Ik hoop de komende jaren nog veel op klinisch en wetenschappelijk vlak met je te kunnen samenwerken en de kans te krijgen om nog meer van je te leren.

Geachte Dr. Creemers, beste Laura. Na mijn eerste histologische kleuring tijdens de wetenschappelijk stage van mijn 6de jaar geneeskunde hebben we ons samen op het tussenwervelschijfonderzoek gestort. Als dagelijks begeleider hebben we samen vele projecten uitgevoerd, resultaten beoordeeld en weer nieuwe experimenten bedacht. Jij hebt me in die tijd de meeste van mijn laboratoriumvaardigheden bijgebracht en me geleerd mijn resultaten altijd kritisch te beoordelen. Bij het schrijven van dit proefschrift was jouw steun onmisbaar. Het begeleiden van een dyslectische promovendus moet je ongetwijfeld meerdere malen tot wanhoop hebben gedreven. Toch werden mijn meer rood dan zwart gekleurde manuscripten steevast teruggestuurd met louter constructieve feedback en handvaten om het stuk verder te verbeteren. Lieve Laura, super bedankt voor al je steun en geduld, ik ben super trost op dit eerste humane tussenwervelschijf proefschrift dat niet tot stand had kunnen komen zonder jouw begeleiding. Ik hoop dat er onder jouw begeleiding nog veel proefschriften mogen volgen.

Geachte Dr. Kummer, beste Alain. Jouw hulp is cruciaal geweest voor de studies met humane tussenwervelschijven. De destijds opgezette Biobank bood mij de unieke mogelijkheid om op grote schaal humane tussenwervelschijven te verzamelen voor mijn onderzoek. Daarnaast nodigde je me uit om deel te nemen aan alle besprekingen van je eigen onderzoeksgroep waar ik dankbaar gebruik van heb gemaakt. Het doet me goed dat we elkaar nog enkele malen per jaar spreken in ons “nieuwe thuis”, het St. Antonius. Alain, hartelijk dank voor je hulp, ook voor de leden van je onderzoeksgroep: Niels, Pieter, Razi, Robbert en Roel.

Geachte Prof. Dr. Verbout. Van u kreeg ik in 2001 mijn eerste college orthopaedie. Daarnaast was u ook betrokken bij mijn klinische stages en mijn promotie onderzoek. Ik heb altijd erg graag met u samengewerkt. Hartelijk dank voor uw ondersteuning tijdens mijn promotie onderzoek.

Geachte Prof. Dr. Castelein. U heeft me geleerd om mijn onderzoek altijd in het juiste klinische perspectief te zien. Uw feedback op mijn manuscripten omvatte altijd enkele suggesties die het artikel voor de clinicus interessanter en leesbaarder maakt. Hartelijk dank voor uw hulp.

Dear Dr. Bergknut, Dear Niklas. It was always a great pleasure to work with you! I really admire how your PhD project jump-started the veterinarian intervertebral disc research! Hopefully we can collaborate in future translational research as veterinarian neurosurgeon and human spine surgeon.

Dear Dr. Grad, Dear Sibylle. I think your work on the NP cell phenotype is a crucial step in the development of cell based regenerative treatment of IVD degeneration. I'm very proud on our fruitful collaboration and our two high impact publications.

Beste medewerkers van de afdeling Pathologie UMCU Utrecht. Er zijn binnen jullie afdeling zeer veel mensen die ik moet bedanken voor hun hulp bij het verwerken van de tussenwervelschijven en opslag daarvan in de Biobank. Graag wil ik Frank Bernhard en Aad de Ruiter in het bijzonder bedanken. Gedurende mijn onderzoeksjaren hadden we iedere dag om 8:15 even contact om te overleggen of er die dag tussenwervelschijven beschikbaar waren. Dankzij jullie hulp hebben we zo'n groot aantal tussenwervelschijven kunnen verzamelen, hartelijk dank voor jullie inzet.

Medewerkers van het Gemeenschappelijk Dierenlaboratorium Universiteit Utrecht. Anja, Hans, Hester, Jeroen en Nico, hartelijk dank voor jullie hulp.

Research laboratorium Orthopaedie UMCU. Yvonne en Mattie. Super bedankt voor jullie ondersteuning. Beste Mattie, waar zou het lab zijn zonder jou! Je bent voor mij onomstotelijk aan ons lab verbonden. Jouw kennis, vaardigheden en gezelligheid hebben zeker bijgedragen aan het succes van ons laboratorium.

Studenten geneeskunde en HBO laboratorium. Herma, Jasper, Karsten, Robin en Saskia. Ieder van jullie heeft op zijn eigen wijze bijgedragen aan mijn promotieonderzoek waarvoor ik jullie allemaal wil bedanken. Het doet me goed om te zien dat de meeste van jullie nog steeds binnen de orthopedie werkzaam zijn.

Mede-promovendi: Anneloes, Diederik, Diyar, Dirk-Jan, Fiona, Jan-Willem, Joris, Marijn, Michiel, Natalja, Roel, Ruth en Wouter. Ik heb met jullie teveel mooie momenten in het Stratenum, Q-gebouw, lab of op congres beleefd om hier te kunnen beschrijven. Jullie allemaal bedankt voor de geweldige onderzoeksjaren.

Sander Schilders, na het fantastische werk dat je met het proefschrift van Natasja verricht hebt was het niet meer dan logisch dat je ook mijn manuscript zou gaan ontwerpen. Door met je samen te werken heb ik nog meer respect voor je gekregen. Maar niet alleen professioneel, ook op persoonlijk vlak. Ik heb veel bewondering voor hoe jij en Lobke jullie gezin met 4 kinderen runnen. Jullie zijn een groot voorbeeld voor ons.

Lieve Dimfy, onze enige echte huisvriendin van de Rijnlaan, hartelijk dank voor je aanwijzingen ter verbetering van mijn proefschrift.

De mannen van het eerste uur. Aksel, Bas, Dennis, Kai, Lorenz, Paul, Richard, Sjoerd en Yuri. We kennen elkaar al weer meer dan 15 jaar en zijn al die jaren goede vrienden gebleven. Van middelbare-school-jongens zijn we stuk voor stuk uitgegroeid tot mannen, een groot aantal zelfs vaders en een enkeling ook echtgenoot. Ik ben er trots op dat ik jullie mijn vrienden mag noemen. Het was niet meer dan logisch dat een van jullie mijn paranimf zou worden. Ik heb voor de rust, betrouwbaarheid en organisatietalent van Lorenz gekozen, maar jullie zouden allemaal fantastische paranimfen zijn geweest.

Martijn Raijmakers, een betere zwager had ik me niet kunnen wensen. Bedankt voor al je hulp en heel veel geluk met Eva in jullie nieuwe huis.

Danielle Raijmakers, je zult deze tekst in je nieuwe thuisland Guatemala lezen. Ik heb heel veel bewondering voor de keuze die je afgelopen jaar gemaakt hebt. Tot in december!

Lieve Thea en Henrie Raijmakers, hartelijk dank voor al jullie steun de afgelopen jaren. Jullie zijn geweldige schoonouders!

Lambert Rutges, vanaf de start van mijn promotietraject wist ik dat jij mijn paranimf zou worden. Het voelt goed om mijn broer op deze dag aan mijn zijde te hebben. We hebben de afgelopen 32 jaar altijd een groot deel van elkaars leven uitgemaakt, ik hoop dat we dat ook de komende jaren zullen blijven doen.

Janny en Piet Rutges, lieve mama en papa. Jullie zijn er vanaf het eerste moment altijd voor mij geweest. Dank jullie wel voor alles. Ik ben trots jullie zoon te mogen zijn.

Allerliefste Tassie, super bedankt voor al je steun en hulp. You’re simply the best. Ik hou van je.

ABOUT THE AUTHOR

Joost Rutges was born on September 23, 1981 in Geertruidenberg, The Netherlands. In 1999 he graduated from secondary school (VWO, Dongemond College, Raamsdonkveer) and started to study medicine at the University of Utrecht, The Netherlands. During this time he started a research project on intervertebral disc degeneration at the Department of Orthopaedic surgery, University Medical Center in Utrecht (head: Prof. Dr. R.M. Castelein). Subsequently, he wrote a proposal for an Alexandre Suerman MD-PhD stipendium, a personal grant to stimulate scientific excellence among young medical doctors, which was granted by the University Medical Center in Utrecht. In 2005 he graduated from medical school and his stipendium allowed him to continue his research at the Department of Orthopaedics at the University Medical Center in Utrecht (Supervisors: Prof. Dr. F.C. Öner and Prof. Dr. W.J.A. Dhert, co-supervisor: Dr. L.B. Creemers). His research projects have resulted in several high-impact publications, presentation at (inter)national conferences, and this thesis.

In December 2008 he started his residency at the Department of Surgery at the St. Antonius Ziekenhuis in Nieuwegein, The Netherlands (head: Dr. P.M.N.Y.H. Go), as part of his orthopaedic training. He continued his training in December 2010 at the Department of Orthopaedic surgery at the St. Antonius Ziekenhuis, Nieuwegein, (head: Dr. M.R. Veen). As part of his training and to enhance his experience with trauma surgery, he worked for 3 months as a visiting resident at the Palmerston North Hospital, in Palmerston North, New Zealand (head: Mr. R. Lander). In December 2012 he continued his training at the University Medical Center Utrecht (head: Prof. Dr. D.B.F. Saris). He is currently working as a resident at the St. Antonius Ziekenhuis, Nieuwegein, (head: Dr. M.R. Veen) and is expected to complete his orthopaedic residency in December 2014. After his residency he will further specialize in spine surgery and is accepted as a fellow in spine surgery at the University of British Colombia, Vancouver, Canada (head: Dr. B. Kwon, MD, PhD).

Joost Rutges lives in Utrecht together with Natasja Raijmakers and their daughter Suze.